Application to Amend the Food Standards Code – Food Produced Using Gene Technology

OECD Unique Identifier - DP-Ø23211-2

DP23211 Maize

Submitting company:

Dow AgroSciences Australia Pty Ltd

Submitted by:

[redacted]

[redacted]

Regulatory and Stewardship Manager ANZ
Corteva Agriscience
Dow AgroSciences Australia Pty Ltd (ABN 24 003 771 659)
Level 9, 67 Albert Avenue
CHATSWOOD NSW 2067 Australia
Telephone [redacted]
Email [redacted]

March 2020

Summary

Corteva Agriscience is a publicly traded, global pure-play agriculture company that provides farmers around the world with the most complete portfolio in the industry - including a balanced and diverse mix of seed, crop protection and digital solutions focused on maximizing productivity to enhance yield and profitability. With some of the most recognized brands in agriculture and an industry-leading product and technology pipeline well positioned to drive growth, the company is committed to working with stakeholders throughout the food system as it fulfils its promise to enrich the lives of those who produce and those who consume, ensuring progress for generations to come. Corteva Agriscience became an independent public company on June 1, 2019 and was previously the Agriculture Division of DowDuPont. More information can be found at www.corteva.com.

Dow AgroSciences Australia, member of Corteva Agriscience group of companies, is submitting this application to FSANZ to vary the Code to approve uses of maize (*Zea mays L.*) event DP-Ø23211-2 (referred to as DP23211 maize), a new food produced using gene technology.

DP23211 maize was genetically modified to express DvSSJ1 double-stranded RNA (dsRNA) and the IPD072Aa protein, both for control of corn rootworm (CRW) pests, as well as the phosphinothricin acetyltransferase (PAT) protein for tolerance to glufosinate herbicide, and the phosphomannose isomerase (PMI) protein that was used as a selectable marker. The PAT and PMI proteins present in DP23211 maize are identical to the corresponding proteins found in a number of approved events across several different crops that are currently in commercial use.

This application presents information supporting the safety and nutritional comparability of DP23211 maize. The molecular characterisation analyses conducted on DP23211 maize demonstrated that the introduced genes are integrated at a single locus, stably inherited across multiple generations, and segregate according to Mendel's law of genetics. The toxicity and allergenicity potential of DvSSJ1 dsRNA and the IPD072Aa, PAT, and PMI proteins were evaluated and found unlikely to be toxic or allergenic to humans or animals. Based on the weight of evidence, consumption of DvSSJ1 dsRNA and the IPD072Aa, PAT, and PMI proteins is unlikely to cause an adverse effect on humans or animals. A compositional equivalence assessment demonstrated that the nutrient composition of DP23211 maize forage and grain is comparable to that of conventional maize, represented by non-genetically modified (non-GM) near-isoline maize and non-GM commercial maize.

Overall, data and information contained herein support the conclusion that DP23211 maize containing DvSSJ1 dsRNA and the IPD072Aa, PAT, and PMI proteins is as safe and nutritious as non-GM maize for food and feed uses.

Table of Contents

List of Tables

List of Figures

The Applicant

This application is submitted by:

Dow AgroSciences Australia Pty. Ltd.

Member of Corteva Agriscience group of companies

Level 9, 67 Albert Ave

Chatswood

NSW 2067

The primary contact is:

[redacted]

Regulatory and Stewardship Manager

Corteva Agriscience

Ph: [redacted]

Email: [redacted]

The Managing Director of Dow AgroSciences Australia Pty. Ltd. is:

[redacted]

Ph: [redacted]

Email: [redacted]

Checklist for General requirements

Check	Mandatory requirements
	A Form of application
✓	☐ *Application in English* ☐ *Executive Summary (separated from main application electronically)* ☐ *Relevant sections of Part 3 clearly identified* ☐ *Pages sequentially numbered* ☐ *Electronic copy (searchable)* ☐ *All references provided*
✓	B Applicant details
✓	C Purpose of the application
	D Justification for the application
✓	☐ *Regulatory impact information* ☐ *Impact on international trade*
✓	E Information to support the application ☐ *Data requirements*
	F Assessment procedure
✓	☐ *General* ☐ *Major* ☐ *Minor* ☐ *High level health claim variation*
	G Confidential commercial information
✓	☐ *CCI material separated from other application material* ☐ *Formal request including reasons* ☐ *Non-confidential summary provided*
	H Other confidential information
✓	☐ *Confidential material separated from other application material* ☐ *Formal request including reasons*
✓	I Exclusive Capturable Commercial Benefit ☐ *Justification provided*
	J International and other national standards
✓	☐ *International standards* ☐ *Other national standards*
✓	K Statutory Declaration
	L Checklist/s provided with application
✓	☐ *3.1.1 Checklist* ☐ *All page number references from application included* ☐ *Any other relevant checklists for Chapters 3.2–3.7*

Checklist for foods produced using gene technology (3.5.1)

Check	Mandatory requirements
	A.1 Nature and identity
	A.2 History of use of host and donor organisms
	A.3 Nature of genetic modification
	B.1 Characterisation and safety assessment
	B.2 New proteins
	B.3 Other (non-protein) new substances
	B.4 Novel herbicide metabolites in GM herbicide-tolerant plants
	B.5 Compositional analyses
	C Nutritional impact of GM food
	D Other information

Statutory Declaration

Statutory Declaration – Australia

The information provided in Parts 1 to 3 must be attested to by a statutory declaration in some suitable form along the following lines:

STATUTORY DECLARATION

Statutory Declarations Act 1959 [1]

I, [redacted] Regulatory and Stewardship Manager

make the following declaration under the *Statutory Declarations Act 1959*:

1. the information provided in this application fully sets out the matters required
2. the information provided in this application is true to the best of my knowledge and belief
3. no information has been withheld that might prejudice this application, to the best of my knowledge and belief

I understand that a person who intentionally makes a false statement in a statutory declaration is guilty of an offence under section 11 of the *Statutory Declarations Act 1959*, and I believe that the statements in this declaration are true in every particular.

[redacted]

[*Signature of person making the declaration*]

Declared at Chatswood on 4th of March 2020

Before me [redacted]

Legal Practitioner

[redacted]

General Information on the Application

1. **Purpose of the application**

Dow AgroSciences Australia Pty. Ltd., member of Corteva Agriscience group of companies (herein referred to as Corteva Agriscience), has developed DP23211 maize (OECD Unique Identifier DP-Ø23211-2), a new event that has been transformed with a single genetic construct expressing the DvSSJ1 dsRNA and the IPD072Aa, PAT, and PMI proteins.

As a result of this application, Corteva Agriscience seeks an amendment of Standard 1.5.2 by inserting: food which has been derived or developed from DP23211 maize, into column 1 of the Table to clause 2, after the last entry.

2. **Justification for the application**

a. **Need for the Proposed Change**

Corteva Agriscience is a member of Excellence Through Stewardship™ (ETS). Corteva Agriscience have developed the new maize line DP23211, which is being commercialized in accordance with the ETS Product Launch Stewardship Guidance and in compliance with Corteva polices regarding stewardship of those products. In line with these guidelines, Corteva's product launch process for launches of new products includes a longstanding process to evaluate export market information, value chain consultations, and regulatory functionality. Growers and end-users must take all steps within their control to follow appropriate stewardship requirements and confirm their buyer's acceptance of the grain or other material being purchased.

b. **Advantage of the Genetically Modified Food**

DP23211 maize was genetically modified to produce DvSSJ1 double-stranded ribonucleic acid (dsRNA) and the IPD072Aa protein for control of corn rootworm (CRW) pests, the phosphinothricin acetyltransferase (PAT) protein for tolerance to the herbicidal active ingredient glufosinate-ammonium, and the phosphomannose isomerase (PMI) protein that was used as a selectable marker.

Maize has multiple downstream uses for feed, fuel, and food that are significant for the global supply of this crop commodity. The introduction of insect-resistant and herbicide-tolerant DP23211 maize is intended to help growers keep pace with increasing maize demand globally. The United States is one of the world's largest maize producers and a leading exporter of maize, with approximately 89.1 million acres of maize planted in 2018 (USDA-NASS, 2018). One of the most serious pests of maize in the United States is Western corn rootworm (WCR; *Diabrotica virgifera virgifera*), with economic losses of greater than $1 billion annually from both management costs and yield loss (Metcalf, 1986; PHI, 2010; Shrestha et al., 2018).

WCR damage has historically been managed with crop rotation, broad-spectrum soil insecticides, and transgenic crops expressing crystalline (Cry) proteins, such as Cry3 and Cry34/35 classes of protein, developed from *Bacillus thuringiensis* (*Bt*). As adoption of *Bt* maize has increased, the selection pressure on target insects to develop resistance has become greater (Cullen et al., 2013). Insect resistance to transgenic traits can pose a threat to the long-term durability of *Bt* crops. As reduced performance of Cry3 and Cry34/35 proteins in maize has been reported in the scientific literature (Gassmann et al., 2016; Jakka et al., 2016), new modes of action (MOA) are important for maintaining sustainable and durable CRW management (Gassmann et al., 2016; Niu et al., 2017).

DP23211 maize was developed as a trait pyramid for CRW management, meaning that it contains two modes of action that are each individually active against the same target pest. DP23211 maize produces the Coleopteran-

active DvSSJ1 dsRNA and IPD072Aa protein and has been demonstrated to be efficacious against CRW pests including WCR. DP23211 maize diversifies the currently available *Bt* protein-based MOAs for CRW control through the combination of an RNA-mediated MOA with a new protein MOA. DP23211 maize provides farmers with an additional control option for CRW pests to protect maize grain yield.

c. Potential Impact on Trade

Corteva Agriscience have developed the new maize line DP23211, which is being commercialized in accordance with the ETS Product Launch Stewardship Guidance and in compliance with Corteva polices regarding stewardship of those products. In line with these guidelines, Corteva's product launch process for launches of new products includes a longstanding process to evaluate export market information, value chain consultations, and regulatory functionality. Growers and end-users must take all steps within their control to follow appropriate stewardship requirements and confirm their buyer's acceptance of the grain or other material being purchased.

d. Costs and Benefits for Industry, Consumers and Government

Corteva Agriscience acknowledges that the proposed amendment to the Standard will likely result in an exclusive capturable commercial benefit from the sale of seed in markets where DP23211 maize is cultivated being accrued to the parent company as defined in Section 8 of the *FSANZ Act*.

Most of the sweet corn consumed in Australia is grown domestically. Domestic production of corn in Australia and New Zealand is supplemented by import of a small amount of corn-based products usually frozen or canned, largely as high-fructose corn syrup, which is not currently manufactured in either Australia or New Zealand (www.grdc.com.au). Although not requiring a FSANZ approval for livestock feed, from time to time, mainly during periods of drought where local supply of feed grain is limited, maize is imported from the United States for use as stock feed, predominantly in the pig and poultry markets. This variation to the Standard permits the import and use of food derived or developed from DP23211 maize.

A. Technical information on the food produced using gene technology

A.1 Nature and identity of the genetical modified food

a. Description of the GM organisms, nature and purpose of the genetic modification

DP23211 maize was genetically modified to produce DvSSJ1 double-stranded ribonucleic acid (dsRNA) and the IPD072Aa protein for control of corn rootworm (CRW) pests, the phosphinothricin acetyltransferase (PAT) protein for tolerance to the herbicidal active ingredient glufosinate-ammonium, and the phosphomannose isomerase (PMI) protein that was used as a selectable marker.

The DvSSJ1 dsRNA produced in DP23211 maize is targeted to match a portion of the smooth septate junction protein 1 (*dvssj1*) gene from western corn rootworm (WCR, *Diabrotica virgifera virgifera*) to down-regulate expression of the DvSSJ1 protein in the mid-gut of WCR via RNA interference (RNAi). DP23211 maize produces DvSSJ1 dsRNA which, when ingested by WCR, results in suppression of the DvSSJ1 protein in the intestinal lining. Reduction in DvSSJ1 protein expression and the subsequent loss of formation of the gut epithelium barrier and cellular deformities result in WCR mortality (Hu et al., 2019).

The IPD072Aa protein, encoded by the *ipd072Aa* gene, confers control of CRW pests when expressed in plants by causing disruption of the midgut epithelium. The *ipd072Aa* gene was identified and cloned from a *Pseudomonas chlororaphis* strain that was cultured from a soil sample (Schellenberger et al., 2016).

The PAT protein, encoded by a maize-optimized version of the phosphinothricin acetyltransferase (*mo-pat*) gene from *Streptomyces viridochromogenes*, confers tolerance to the herbicidal active ingredient glufosinate-ammonium at current labeled rates by acetylating phosphinothricin, the active component of glufosinate-ammonium herbicide, to an inactive form. The PAT protein present in DP23211 maize is identical to the corresponding protein found in a number of approved events across several different crops that are currently in commercial use (CERA - ILSI Research Foundation, 2016; CERA, 2011; Hérouet et al., 2005).

The phosphomannose isomerase (PMI) protein is encoded by the *pmi* gene from *Escherichia coli*. The expressed PMI protein in plant tissue serves as a selectable marker during transformation which allows for tissue growth using mannose as the carbon source. The PMI protein present in DP23211 maize is identical to the corresponding protein found in a number of approved events across several different crops that are currently in commercial use (Negrotto et al., 2000).

b. GM Organism Identification

In accordance with OECD's "Guidance for the Designation of a Unique Identifier for Transgenic Plants", this event has an OECD identifier of DP-Ø23211-2, also referred to as DP23211.

c. Food Identity

Maize event DP23211 is at pre-commercialization stage and has not yet been assigned a commercial product name The introduced traits conferring control of corn rootworms and herbicide-tolerance in DP23211 maize are not intended to change any of the end-use characteristics of maize grain and the commercial introduction of maize hybrid containing event DP23211 is not anticipated to change the usage and consumption patterns of maize grain. It is anticipated that following commercialization, any food containing maize products may contain material derived from DP23211 maize.

d. Products containing the food or food ingredients.

Refer to the OECD Consensus Document on Compositional Considerations for New Varieties of Maize (*Zea mays*): Key Food and Feed Nutrients, Anti-nutrients and Secondary Plant Metabolites (2002), for the following aspects of the food uses of maize:

- Production of maize for food and feed
- Processing of maize
- Wet Milling
- Dry Milling
- Masa Production
- Feed Processing

The majority of grain and forage derived from maize is used for animal feeds. Less than 10% of maize grain is processed for human food products. Maize grain is also processed into industrial products, such as ethyl alcohol by fermentation and highly refined starch by wet-milling to produce starch and sweetener products. In addition to milling, maize germ can be processed to obtain maize oil.

Domestic production of maize in Australia (ca. 440,000t) and New Zealand is supplemented by import of a small amount of maize-based products, largely as high-fructose maize syrup, which is not currently manufactured in either Australia or New Zealand. Such products are processed into breakfast cereals, baking products, extruded confectionery and maize chips. Other maize products such as maize starch are also imported. This is used by the food industry for the manufacture of dessert mixes and canned foods (www.grdc.com.au).

A.2 History of use of the host and donor organisms

a. Donor Organism

***Pseudomonas chlororaphis*: donor of the *ipd072Aa* gene**

- Class: Gammaproteobacteria
- Order: Pseudomonadales
- Family: Pseudomonadaceae
- Genus: *Pseudomonas*
- Species: *P. chloroaphis*
- Strain: SS143D5

The *ipd072Aa* gene is derived from *Pseudomonas chlororaphis*, a rod-shaped, aerobic, Gram-negative bacterium that is ubiquitous in soil. *P. chlororaphis* has a history of safe use as a biopesticide in the United States and Europe and has not been shown to be pathogenic to plants, livestock, and humans (Anderson et al., 2018).

***Streptomyces viridochromogenes*: donor of the *mo-pat* gene**

- Class: Actinobacteria (high G+C Gram-positive bacteria)
- Order: Actinomycetales
- Family: Streptomycetaceae
- Genus: *Streptomyces*
- Species: *S. viridochromogenes*
- Strain: Tü494

Streptomyces. viridochromogenes is a Gram-positive, saprophytic, aerobic bacterium commonly found in soil. *S. viridochromogenes* is not considered pathogenic to humans or animals and is not known to be an allergen or toxin. *S. viridochromogenes* produces the tripeptide L-phosphinothricyl-L-alanyl-alanine (L-PPT), which was developed as a non-selective herbicide (OECD, 1999).

***Escherichia coli*: donor of the *pmi* gene**

- Class: Gammaproteobacteria
- Order: Enterobacteriales
- Family: Enterobacteriaceae
- Genus: *Escherichia*
- Species: *E. coli*
- Strain: K-12

Escherichia coli (*E. coli*) is a Gram-negative, anaerobic, rod-shaped bacterium. The strain *E. coli* K-12 is a strain which has been debilitated, does not normally colonize the human intestine and has a poor survival rate in the environment. *E. coli* K-12 has a history of safe use in human drug and specialty chemical production (US-EPA, 1997).

Please refer to Part C, section 4 and 5 of this dossier for information relating to the potential allergenicity and toxicity of the expressed protein.

b. Host Organism

Maize is extensively cultivated worldwide and has a long history of safe use. Maize grain and maize-derived products represent staple food and feed for a large portion of the global population (CFIA, 1994). No significant toxicity or allergenicity has been ascribed to any food or feed uses of maize, and maize has been described as a food that is likely to have low allergenicity (OECD, 2002). Maize is not included in the list of food allergy indications of the US Food and Drug Administration (FDA) (US-FDA, 2006).

Taxonomy

- Family name: *Poaceae* (Gramineae)
- Genus: *Zea*
- Species: *Z. mays L.*
- Subspecies: *Zea mays* ssp*. mays L*
- Common name: Maize; corn

Maize is a diploid species with a chromosome number of 2n = 2x = 20 and is a domesticated species of the tribe *Maydeae* and the grass family, *Poaceae*. The closest relatives to the genus *Zea* are grasses in the genus *Tripsacum* (OECD, 2003). Within the genus *Zea*, there are five species, including *Zea mays. Z. mays* contains four subspecies, including *Zea mays* ssp. *mays*, which is the only domesticated taxon (maize). The other three subspecies of *Z. mays* are called teosintes (OECD, 2003) including *huehuetenangensis, mexicana,* and *parviglumis*.

Morphology

Biology documents on unmodified maize have been published by the OECD (OECD, 2003). Maize is a tall annual grass consisting of a stalk with overlapping sheaths and broad leaves growing alternately around the stalk. Plants have one or more female flowers, consisting of silk on a thickened axis (cob), located midway on the stalk. Plants also have male flowers, consisting of the tassel at the top of the plant, which release pollen. Maize plants reproduce sexually, during which an individual silk must become pollinated, and fertilization must take place to produce one maize kernel. Kernels develop in 8 to 16 rows along the cob, which is surrounded by a layer of protective leaves called a husk (OECD, 2003).

Centre of Origin

The Meso-American region (middle South Mexico and Central America) is recognized as the centre of origin for maize (OECD, 2003).

Natural Habitat and Generation Time

Maize is grown over a wide range of climatic conditions and is well-suited for warm, temperate climates. The majority of maize is produced between latitudes 30 and 55 degrees, with a relatively small amount grown at latitudes higher than 47 degrees (Shaw, 1988). The greatest maize production occurs where the warmest month isotherms range between 21 °C and 27 °C and the freeze-free season lasts 120 to 180 days (Shaw, 1988). Survival and reproduction of maize are limited by extreme environmental conditions (heat stress, frost, drought, excessive rainfall, etc.) (Shaw, 1988). Maize is typically not cultivated in areas where the mean mid-summer temperature is < 19 ºC (66 ºF) or where the average night temperature falls much below 13 ºC (55 ºF). Maize yield is also susceptible both to excess water and low moisture stress. There is no upper limit of rainfall for growing maize, although excess rainfall will decrease yields (Shaw, 1988).

The maize life cycle ranges from as short as 10 weeks to as long as 48 weeks covering the period of seedling emergence to maturity (OECD, 2003; Shaw, 1988). The duration of the maize life cycle depends on the maize variety and environmental conditions in which it is grown (OECD, 2003).

Mode of Reproduction and Dispersal

Maize plants reproduce sexually with both male (tassels) and female (silk) reproductive organs present on each plant (monoecious species). Pollen, produced by the tassel, can pollinate silks from the same plant (self-fertilization) or can pollinate silks from neighbouring plants (cross fertilization). Both self-fertilization and cross-pollination are influenced by plant proximity, pollen dispersal, and pollen viability. Normally, approximately 95% of ovules are cross-pollinated from plants in the immediate vicinity, and 5% are self-pollinated (Sleper and Poehlman, 2006).

Wind-dispersal is the primary method by which pollen is carried to fertilize other maize plants (Galinat, 1988; Raynor *et al.*, 1972; Russell and Hallauer, 1980); however, viable maize pollen generally does not travel long distances (95-99% of maize pollen will be deposited within 30 meters of the source (Devos *et al.*, 2005; OECD, 2003). Insects such as bees, beetles, flies, and leafhoppers do enable pollen dispersal; however, the magnitude of that dispersal pathway is limited (Andersson and de Vicente, 2010).

Maize is highly domesticated, and the structure of the ear (cob and seeds enclosed in husk) limits seed dispersal from occurring naturally in the (Andersson and de Vicente, 2010; CFIA, 1994; OECD, 2003; Raybould *et al.*, 2012). Without human or animal aid, seed dispersal is limited to within a meter or so of the plant. Neither animal dispersal nor unintentional human dispersal distributes enough seed to be considered significant (Andersson and de Vicente, 2010).

Outcrossing Rate (Intra-Specific and Inter-Specific Crosses)/Gene Flow

Maize has a high outcrossing rate and can pollinate sexually compatible varieties (other cultivated maize hybrids, landraces, and teosinte) (OECD, 2003). However, gene flow in the environment is limited by environmental barriers (pollen viability, pollen dispersal, proximity and synchrony of flowering) (Andersson and de Vicente, 2010; CFIA, 1994; Luna *et al.*, 2001; Messeguer *et al.*, 2006) and genetic barriers (ability to outcross and produce fertile progeny) (OECD, 2003).

The risk of gene flow and introgression of transgenes from DP23211 maize into other varieties of cultivated maize is unlikely. This application seeks authorization of DP23211 maize for import for food and feed uses, and commercialization by Corteva Agriscience for cultivation of DP23211 in Australia is not currently planned.

Survival, Dormancy, and Weediness/Invasiveness

Maize is grown over a wide range of climatic conditions and is well-suited for warm, temperate climates (OECD, 2003). Survival and reproduction of maize are limited by extreme environmental conditions (heat stress, frost, drought, excessive rainfall, etc.) (Shaw, 1988). Populations of maize are unlikely to survive outside managed agricultural environments. Although plants may occasionally grow in uncultivated fields or occur as volunteers, maize generally does not sustain reproduction outside of cultivation (CFIA, 1994). Maize seeds are the only survival structures, and natural regeneration of maize from vegetative tissue is not known to occur.

Maize seeds show poor dormancy (CFIA, 1994) and generally only survive under favourable climatic conditions. Maize is an annual plant that lacks seed dormancy which limits survival from one growing season to the next (Andersson and de Vicente, 2010; CFIA, 1994).

Conventional maize is well established as having low weediness and invasiveness potential, is highly domesticated and unlikely to establish itself in self-sustaining populations outside of cultivation and is a poor competitor with native vegetation and lack of seed dormancy adds to its inability to establish sustainable feral populations (Raybould *et al.*, 2012). Additionally, maize has no history of weediness or invasiveness in either natural or managed agricultural systems (Raybould and Wilkinson, 2005).

Maize is a commonly cultivated crop around the world, and its biology and history of safe use demonstrate that the unmodified organism is safe for human and animal consumption.

A.3 The nature of the genetic modification

a. Transformation Method

DP23211 maize was created by site-specific integration (SSI) using two sequential transformation steps to (1) insert an integration site sequence (referred to as a "landing pad" sequence) at a specific location of the maize genome by microprojectile bombardment, and (2) insert the intended expression cassettes from the plasmid PHP74643 T-DNA region into the landing pad in the maize genome by *Agrobacterium*-mediated transformation [redacted] 2019). After each transformation step, the maize genome was characterized using a Next Generation Sequencing (NGS) method known as Southern-by-Sequencing (SbS™ technology, hereafter referred to as SbS) to ensure the intended insertion was present and there were no unintended plasmid-derived sequences present in the genome.

The landing pad was created by microprojectile bombardment of maize tissue with plasmid PHP56614 which contains the flippase recombination target sites, FRT1 and FRT87, and the maize genome-derived sequences, *zm*-SEQ9 and *zm*-SEQ8. The I-CreI endonuclease expressed by plasmid PHP56614 created a double-stranded DNA break at a specified location in the genome, after which homologous recombination between the maize genome and *zm*-SEQ9 and *zm*-SEQ8 inserted the landing pad into the maize genome. Two additional plasmids, PHP21139 and PHP31729, were included in this transformation to improve plant regeneration, but were not incorporated into the maize genome. After molecular characterisation, a line with the inserted landing pad and no unintended DNA insertions was selected and moved forward to the next step. Following *Agrobacterium*-mediated transformation with plasmid PHP74643, transfer of the intended expression cassettes from the plasmid PHP74643 T-DNA region into the SSI landing pad occurred via flippase-mediated recombination and exchange of the sequence between the FRT1 and FRT87 sites, resulting in the intended insertion containing the desired expression cassettes. Thus, the intended insertion in DP23211 maize comprises sequences from both PHP56614 and PHP74643 and includes the *pmi*, *mo-pat*, and *ipd072Aa* gene cassettes and the DvSSJ1 fragment cassette.

First Transformation Step: Insertion of PHP56614 T-DNA Landing Pad

The first transformation step utilized microprojectile co-bombardment with three plasmids to insert the landing pad sequence into the maize genome using an I-CreI endonuclease-mediated gene-editing process [redacted] 2019). The I-CreI protein binds to a defined DNA target location based on specific protein-DNA interaction (Daboussi et al., 2015). Three plasmids (PHP56614, PHP21139, and PHP31729) were used to deliver the various components needed for the recombination processes and improved plant regeneration (**Table 1**; **Figures 1** to **4**).

Following transformation, the I-*Cre*I (PHP56614), *zm-wus2* (PHP21139), and *zm-odp2* (PHP31729) genes are transiently expressed without integration into the maize genome. Expression of the I-CreI endonuclease produces a double-stranded break at a targeted location between the continuous, endogenous *zm*-SEQ9 and *zm*-SEQ8 sequences in the maize genome. These endogenous sequences are identical to the *zm*-SEQ9 and *zm*-SEQ8 sequences in plasmid PHP56614. The sequence homology between the target site (endogenous *zm*-SEQ9 and *zm*-SEQ8 sequences) and the plasmid (PHP56614 *zm*-SEQ9 and *zm*-SEQ8 sequences) allowed a native cellular mechanism known as homology-directed repair (HDR) to occur via crossovers between the *zm*-SEQ9 and *zm*-SEQ8 sequences in plasmid PHP56614 and the identical *zm*-SEQ9 and *zm*-SEQ8 sequences naturally present in the maize genome. Homologous recombination thus introduced the landing pad sequence located between the *zm*-SEQ9 and *zm*-SEQ8 sequences in the PHP56614 plasmid [consisting of the *ubi*ZM1 promoter including the 5' untranslated region (5' UTR) and intron, FRT1 recombination target site, *nptII* gene, *pin*II terminator, and FRT87

recombination target site] into the maize genome at the targeted location between the endogenous *zm*-SEQ9 and *zm*-SEQ8 sequences.

The transient expression of the WUS protein from plasmid PHP21139 and the ODP2 protein from plasmid PHP31729 allows for the improved regeneration of maize plants from the transformation process.

After transformation, regeneration of maize plants, and molecular characterization by SbS, a line with the landing pad and no unintended DNA sequence inserts was selected and advanced in the transformation process.

Table 1. Summary of Genetic Elements Used in Landing Pad Transformation and Presence in DP23211 Maize

Plasmid	Genetic Element	Description	Present in DP23211
PHP56614	*lox*P	Cre recombination site	No
	I-*Cre*I	Maize-optimized I-*Cre*I endonuclease gene from *Chlamydomonas reinhardtii* modified to target a specific maize genome location	No
	zm-SEQ9	Genomic recognition site for homology-directed repair (HDR)	Yes
	*ubi*ZM1	Promoter	Yes
	FRT1	Flippase recombination target site	Yes
	nptII	Neomycin phosphotransferase II gene	No
	FRT87	Flippase recombination target site	Yes
	zm-SEQ8	Genomic recognition site for HDR	Yes
PHP21139	*zm-wus2*	Developmental gene for regeneration	No
PHP31729	*zm-odp2*	Developmental gene for regeneration	No

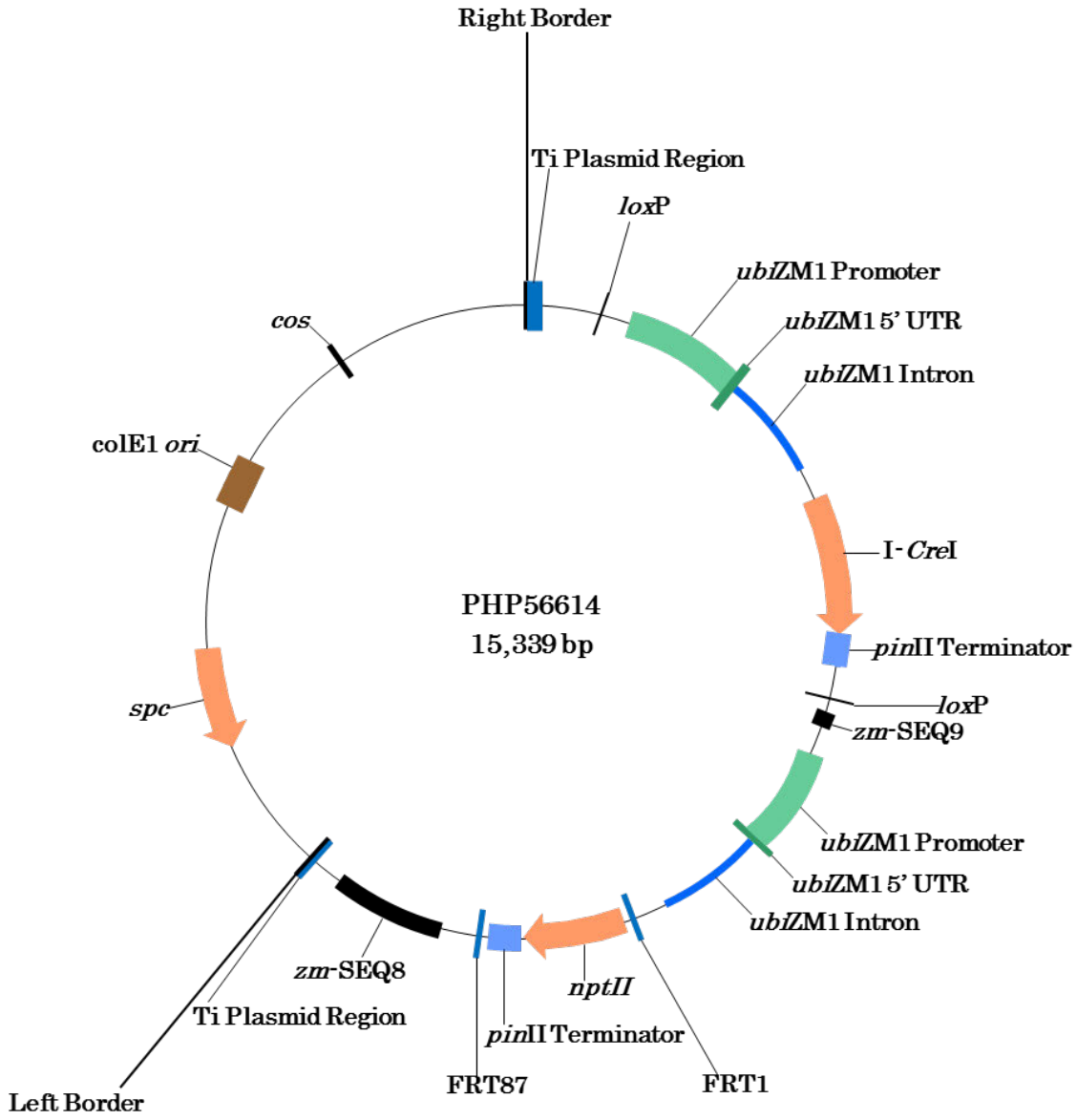

Figure 1. Schematic Diagram of Plasmid PHP56614

Schematic diagram of the plasmid PHP56614 containing the I-*Cre*I and *nptII* gene cassettes, along with the *zm*-SEQ9, *zm*-SEQ8, FRT1, and FRT87 elements. The plasmid size is 15,339 bp. The region between *zm*-SEQ9 and *zm*-SEQ8 formed the SSI landing pad in the maize genome. The region between FRT1 and FRT87 was replaced by SSI with the intended *pmi*, *mo-pat*, DvSSJ1, and *ipd072Aa* cassettes from the PHP74643 T-DNA (**Figure 6**) that is flanked by the same sites.

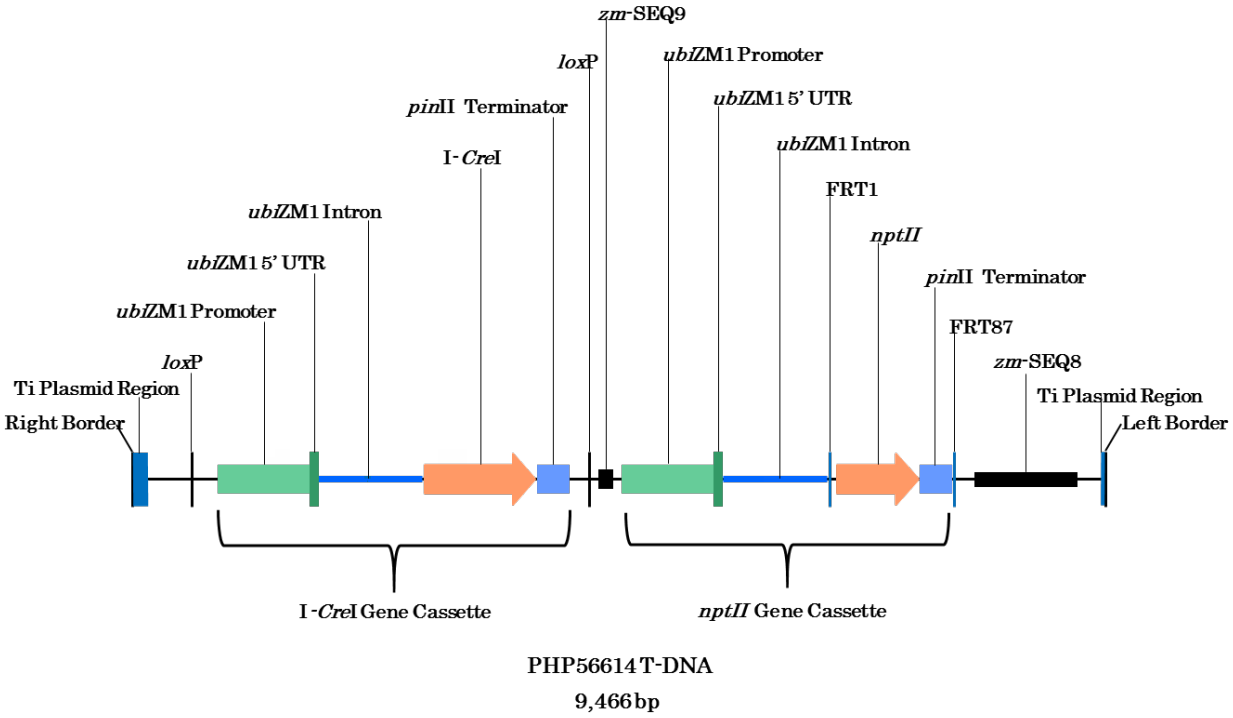

Figure 2. Schematic Diagram of the T-DNA Region from Plasmid PHP56614

Schematic diagram of the T-DNA region from plasmid PHP56614 containing the I-*Cre*I and *nptII* gene cassettes. The size of the T-DNA is 9,466 bp.

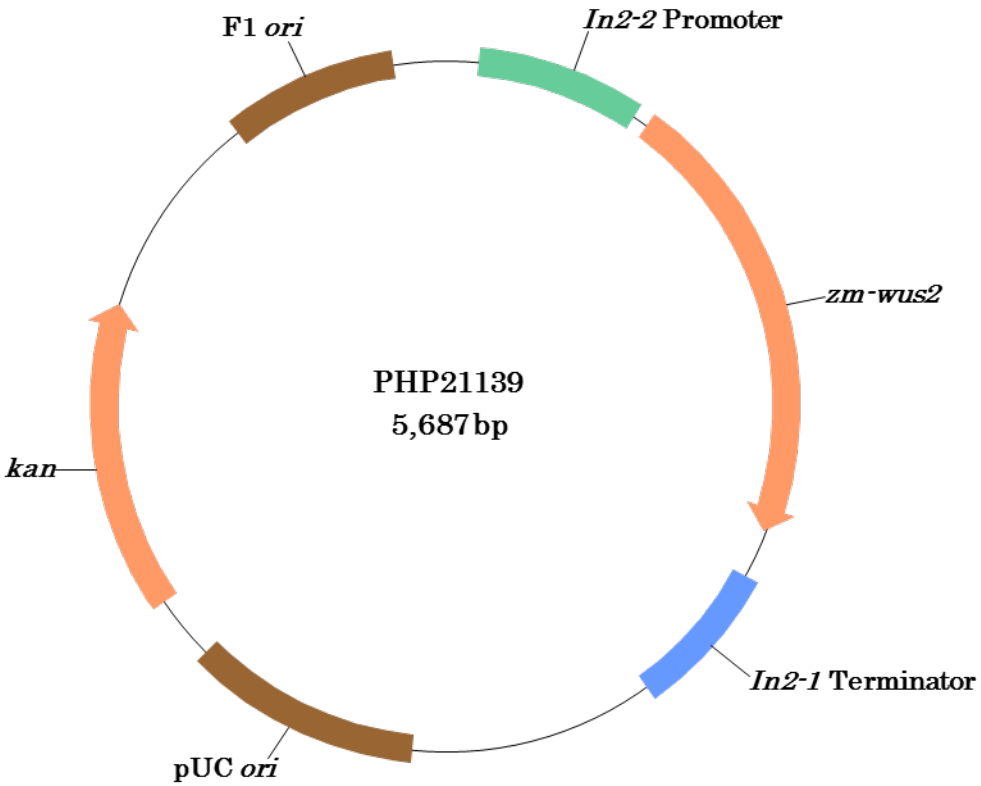

Figure 3. Schematic Diagram of Plasmid PHP21139

Schematic diagram of plasmid PHP21139 containing the *zm-wus2* gene cassette. The plasmid size is 5,687 bp. PHP21139 was used to enhance transformation and plant regeneration but was not incorporated into the maize genome.

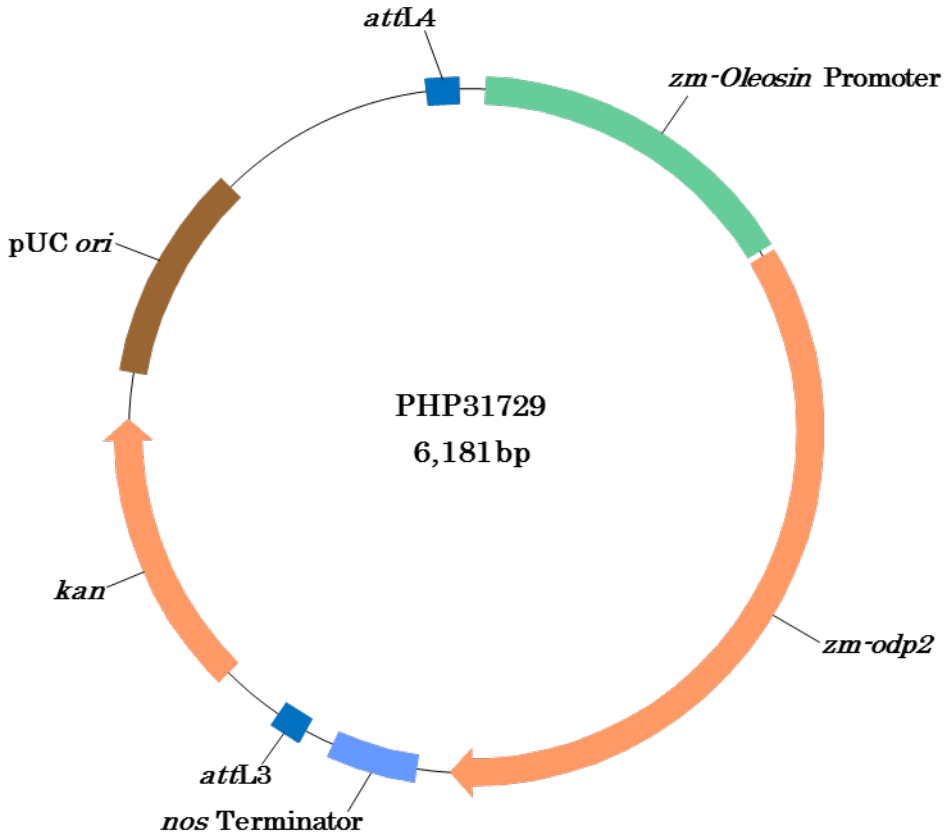

Figure 4. Schematic Diagram of Plasmid PHP31729

Schematic diagram of plasmid PHP31729 containing the *zm-odp2* gene cassette. The plasmid size is 6,181 bp. PHP31729 was used to enhance transformation and plant regeneration but was not incorporated into the maize genome.

Second Transformation Step: Site-Specific Integration of Expression Cassettes of PHP74643 T-DNA

The second transformation step used to create DP23211 maize utilized *Agrobacterium*-mediated transformation with plasmid PHP74643 (**Figure 5**) to transport the PHP74643 T-DNA (**Figure 6**) into the plant cell nucleus; however, the T-DNA did not integrate into the genome [redacted] 2019). Rather, the FLP recombinase encoded in the T-DNA (outside of the FRT1 and FRT87 sites) exchanged the *nptII* cassette for the intended trait gene cassettes (*pmi*, *pat*, and *ipd072Aa* gene cassettes and the DvSSJ1 fragment cassette) to result in the intended insertion of DP23211 maize (**Figure 7**).

Following transformation, the *zm-wus2*, *zm-odp2*, *mo-Flp*, and *DsRed2* genes are transiently expressed without integration into the DP23211 maize genome. Expression of the WUS and ODP2 proteins allows for improved regeneration of maize plants from the transformation process, and the DsRed2 protein provides visual evidence to detect the undesired integration of the T-DNA in the genome. **Table 2** lists the relevant genetic elements within the PHP74643 T-DNA and indicates whether they are present in the final DP23211 event.

Table 2. Summary of Genetic Elements in PHP74643 T-DNA and Presence in DP23211 Maize

Genetic Element	Description	Present in DP23211
Right Border	T-DNA right border	No
zm-wus2	Developmental gene for regeneration	No
zm-odp2	Developmental gene for regeneration	No
mo-Flp	Maize-optimized flippase recombinase gene	No
DsRed2	Red fluorescent protein gene	No
FRT1	Flippase recombination target site	Yes
pmi	Phosphomannose isomerase gene	Yes
mo-pat	Maize-optimized phosphinothricin acetyltransferase gene	Yes
*lox*P	Cre recombination site	Yes
DvSSJ1 Fragment	Fragment of the smooth septate junction protein 1 (*dvssj1*) gene from western corn rootworm (*Diabrotica virgifera virgifera*)	Yes
ipd072Aa	Insect protection protein gene	Yes
FRT87	Flippase recombination target site	Yes
Left Border	T-DNA left border	No

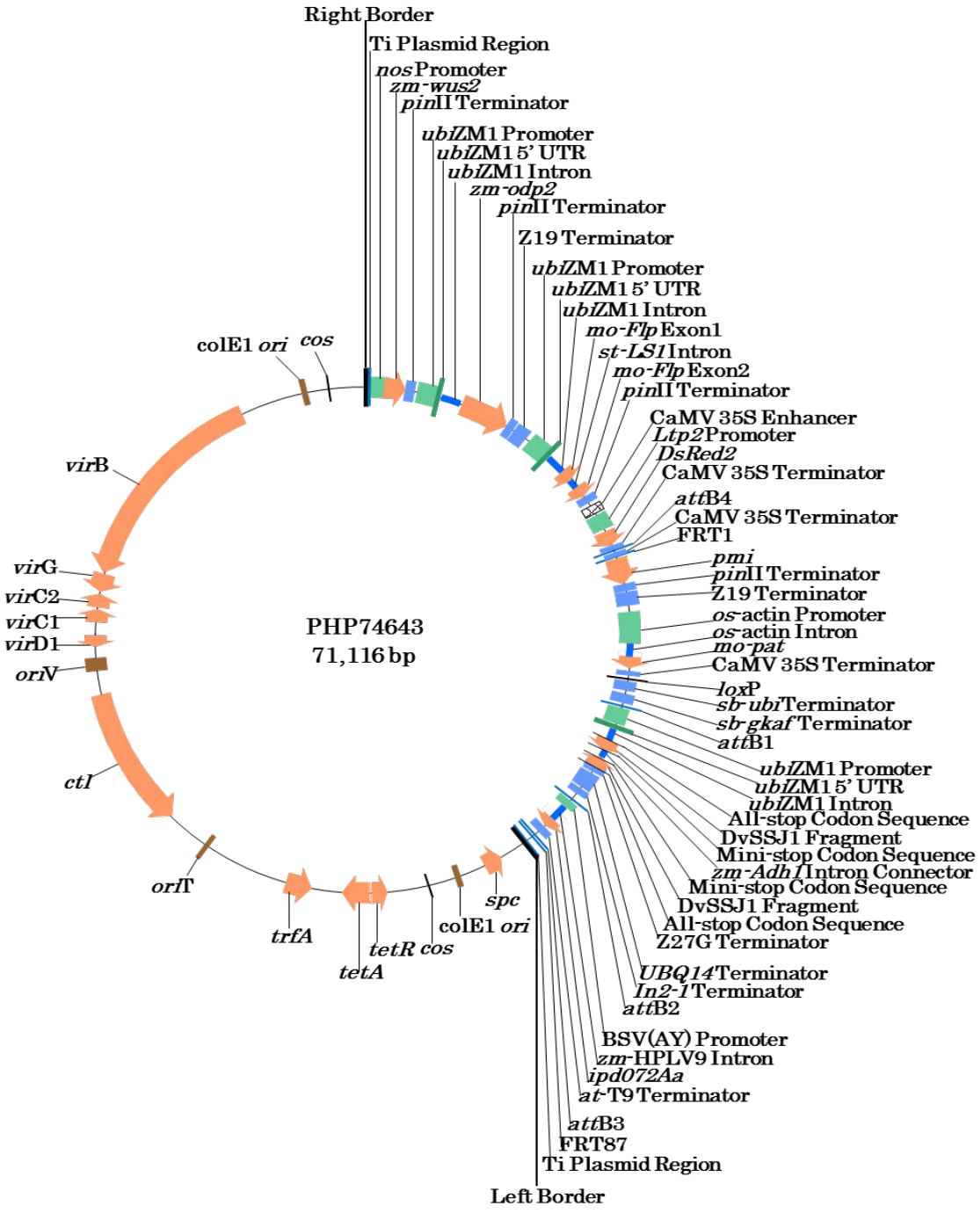

Figure 5. Schematic Diagram of Plasmid PHP74643

Schematic diagram of plasmid PHP74643 containing the DvSSJ1 fragment cassette and the *pmi*, *mo-pat*, and *ipd072Aa* gene cassettes intended for incorporation into the maize genome and the *zm-wus2*, *zm-odp2*, *mo-Flp*, and *DsRed2* gene cassettes not intended for incorporation into the maize genome. The size of plasmid PHP74643 is 71,116 bp.

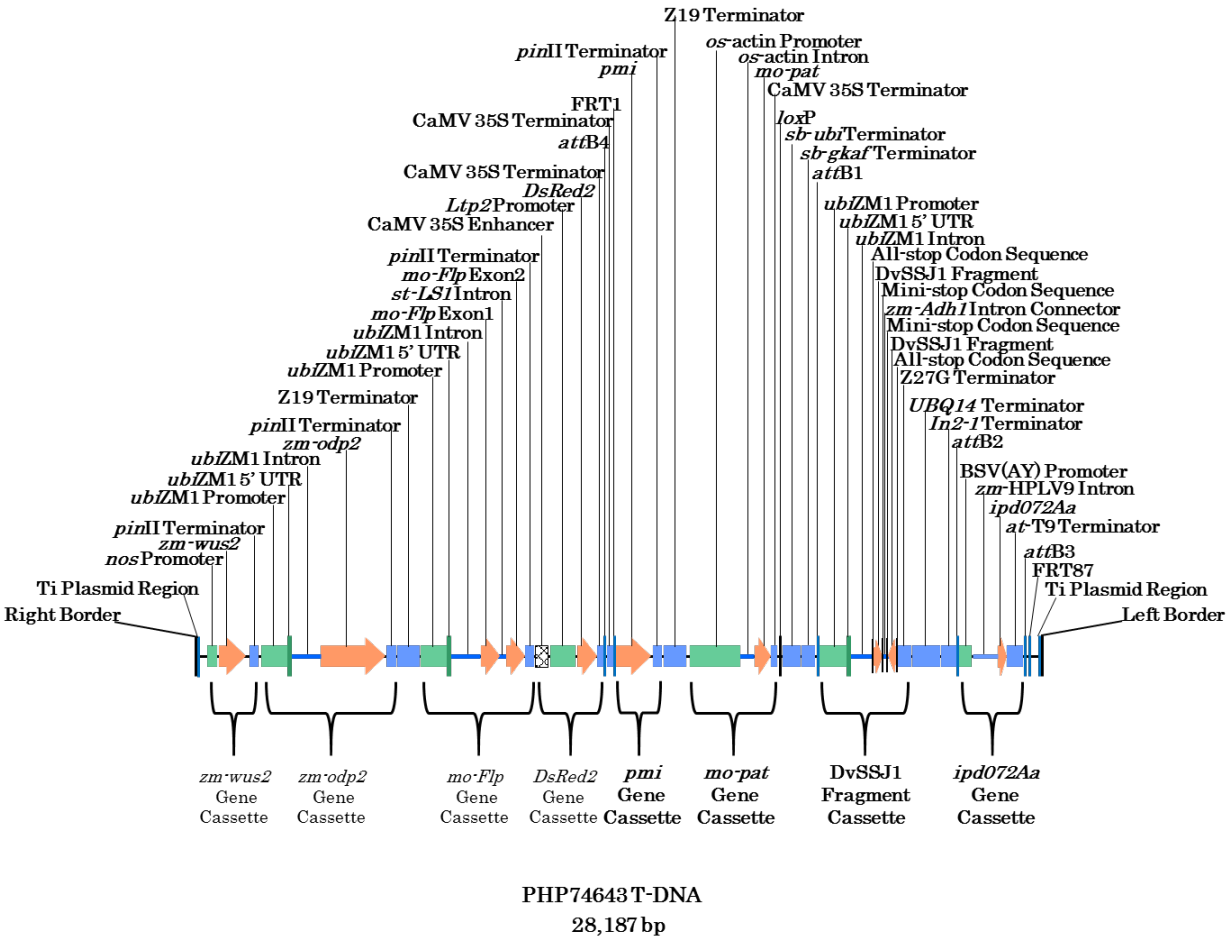

Figure 6. Schematic Diagram of the T-DNA Region from Plasmid PHP74643

Schematic diagram of the T-DNA region of plasmid PHP74643 indicating the DvSSJ1 fragment cassette and the *pmi*, *mo-pat*, and *ipd072Aa* gene cassettes intended for incorporation into the maize genome and the *zm-wus2*, *zm-odp2*, *mo-Flp*, and *DsRed2* gene cassettes not intended for incorporation into the maize genome. The size of the T-DNA is 28,187 bp.

The T-DNA of plasmid PHP74643 contains a total of eight cassettes, four of which are present in the intended insertion (DvSSJ1 fragment cassette and the *ipd072Aa*, *pat*, and *pmi* gene cassettes; Figure 7), and the remaining four cassettes (*zm-wus2*, *zm-odp2*, *mo-Flp*, and *DsRed2* genes) are transiently expressed without integration into the maize genome. Further description of the cassettes included in the T-DNA of plasmid PHP74643 is provided below. The PHP74643 T-DNA also contains two Flp recombinase target sequences, FRT1 and FRT87 sites (Proteau et al., 1986; Tao et al., 2007, respectively), as well as one *lox*P (Dale and Ow, 1990) and four *att*B recombination sites (Cheo et al., 2004; Hartley et al., 2000; Katzen, 2007). Summaries of the genetic elements within plasmid PHP74643 and the T-DNA region of plasmid PDP74643 are provided in Tables 3 and 4, respectively, [redacted] 2018).

- The *zm-wus2* gene cassette contains the maize *Wuschel2* (*wus2*) gene (Mayer et al., 1998) encoding the WUS protein. The expressed WUS protein enhances tissue regeneration during transformation (Lowe et al., 2016). The WUS protein is 302 amino acids in length and has a molecular weight of approximately 31 kDa. Expression of the *wus2* gene is controlled by the promoter from the *Agrobacterium tumefaciens* Ti

plasmid nopaline synthase (*nos*) gene (Depicker et al., 1982), in conjunction with the presence of the terminator region from the potato (*Solanum tuberosum*) proteinase inhibitor II (*pin*II) gene (An et al., 1989; Keil et al., 1986).

- The *zm-odp2* gene cassette contains the maize ovule development protein 2 (*odp2*) gene (GenBank accession XM008676474) encoding the ODP2 protein. The expressed ODP2 protein enhances the regeneration of maize plants from tissue culture after transformation (Gordon-Kamm *et al.*, 2013). The ODP2 protein is 710 amino acids in length and has a molecular weight of approximately 74 kDa. Expression of the *odp2* gene is controlled by the promoter region from the maize ubiquitin gene 1 (*ubi*ZM1) including the 5' untranslated region (5' UTR) and intron (Christensen et al., 1992). The terminator for the *odp2* gene is a second copy of the *pin*II terminator. An additional terminator is present between the second and third cassettes: the terminator region from the maize 19-kDa zein (Z19) gene (GenBank accession KX247647; Dong et al., 2016). This additional terminator element is intended to prevent any potential transcriptional interference with the downstream cassettes. Transcriptional interference is defined as the transcriptional suppression of one gene on another when both are in close proximity (Shearwin et al., 2005). The placement of one or multiple transcriptional terminators between gene cassettes has been shown to reduce the occurrence of transcriptional interference (Greger et al., 1998).

- The *mo-Flp* gene cassette contains maize-optimized exon 1 and exon 2 of the flippase (*Flp*) gene (Dymecki, 1996) from *Saccharomyces cerevisiae,* separated by an intron region from the potato *LS1* (*st-LS1*) gene (Eckes et al., 1986). The expressed FLP protein facilitates site-specific recombination during transformation. The FLP protein is 423 amino acids in length and has a molecular weight of approximately 49 kDa. Expression of the *mo-Flp* gene is controlled by a second copy of the *ubi*ZM1 promoter, the 5' UTR and intron, in conjunction with a third copy of the *pin*II terminator.

- The *DsRed2* gene cassette contains a modified red fluorescent protein (*DsRed2*) gene from *Discosoma sp.* (Wasson-Blader, 2001), in which an internal *Bst*E II restriction site was removed from the original *DsRed2* gene without altering the amino acid sequence of the expressed protein. The tissue-specific expression of the DsRed2 protein in the aleurone layer of the maize seed produces a red coloration in seeds that contain the DNA insertion, allowing for differentiation during seed sorting. The DsRed2 protein is 225 amino acids in length and has a molecular weight of approximately 26 kDa. Expression of the *DsRed2* gene is controlled by the 35S enhancer region from the cauliflower mosaic virus genome (CaMV 35S enhancer) (Franck et al., 1980; Kay et al., 1987) and the promoter region from the barley (*Hordeum vulgare*) lipid transfer protein (*Ltp2*) gene (Kalla et al., 1994) which provides aleurone-specific transcription of the *DsRed2* gene. The terminator for the *DsRed2* gene is the 35S terminator region from the cauliflower mosaic virus genome (CaMV 35S terminator) (Franck et al., 1980; Guilley et al., 1982). An additional copy of the CaMV 35S terminator present between the fourth and fifth cassettes is intended to prevent transcriptional interference between cassettes.

- The *pmi* gene cassette contains the phosphomannose isomerase (*pmi*) gene from *Escherichia coli* (Negrotto et al., 2000). The expressed PMI protein in plant tissue serves as a selectable marker during transformation which allows for tissue growth using mannose as the carbon source. The PMI protein is 391 amino acids in length and has a molecular weight of approximately 43 kDa. As present in the T-DNA region of PHP74643, the *pmi* gene lacks a promoter, but its location next to the flippase recombination target site, FRT1, allows post-recombination expression by an appropriately-placed promoter. The terminator for the *pmi* gene is a fourth copy of the *pin*II terminator. An additional Z19 terminator present between the fifth and sixth

cassettes is intended to prevent transcriptional interference between cassettes.

- The *mo-pat* gene cassette contains a maize-optimized version of the phosphinothricin acetyltransferase gene (*mo-pat*) from *Streptomyces viridochromogenes* (Wohlleben et al., 1988) encoding the PAT protein. The expressed PAT protein confers tolerance to phosphinothricin. The PAT protein is 183 amino acids in length and has a molecular weight of approximately 21 kDa. Expression of the *mo-pat* gene is controlled by the promoter and intron region of the rice (*Oryza sativa*) actin (*os*-actin) gene (GenBank accession CP018159; GenBank accession EU155408.1), in conjunction with a third copy of the CaMV35S terminator. Two additional terminators are present between the sixth and seventh cassettes to prevent transcriptional interference: the terminator regions from the sorghum *(Sorghum bicolor*) ubiquitin (*sb-ubi*) gene (Phytozome gene ID Sobic.004G049900.1) and γ-kafarin (*sb-gkaf*) gene (de Freitas et al., 1994), respectively.

- The DvSSJ1 fragment cassette is expressed as a transcript to form an inverted repeat configuration that contains two RNA fragments of the smooth septate junction protein 1 (*dvssj1*) gene matching WCR (Hu et al., 2016) separated by an intron connector sequence derived from the intron 1 region of the maize alcohol dehydrogenase (*zm-Adh1*) gene (Dennis et al., 1984). Each of the two DvSSJ1 fragments is flanked by stop codon sequences designed to terminate translation through the site. The transcription product of this cassette, DvSSJ1 dsRNA, is intended to downregulate the expression of the DvSSJ1 protein in the mid-gut of WCR via RNAi. Expression of the DvSSJ1 fragment is controlled by a third copy of the *ubi*ZM1 promoter, the 5' UTR, and intron, in conjunction with the terminator region from the maize W64 line 27-kDa gamma zein (Z27G) gene (Das et al., 1991; Liu et al., 2016). Two additional terminators are present between the between the DvSSJ1 fragment cassette and the *ipd072Aa* gene cassette to prevent transcriptional interference: the terminator region from the *Arabidopsis thaliana* ubiquitin 14 (*UBQ14*) gene (Callis et al., 1995) and the terminator region from the maize *In2-1* gene (Hershey and Stoner, 1991).

- The *ipd072Aa* gene cassette contains the insecticidal protein gene, *ipd072Aa*, from *Pseudomonas chlororaphis* (Schellenberger et al., 2016). The expressed IPD072Aa protein in plants is effective against certain coleopteran pests by causing disruption of the midgut epithelium. The IPD072Aa protein is 86 amino acids in length and has a molecular weight of approximately 10 kDa. Expression of the *ipd072Aa* gene is controlled by the promoter region from the banana streak virus of acuminata Yunnan strain (BSV [AY]) (GenBank accession DQ092436.1; Zhuang et al., 2011) and the intron region from the maize ortholog of a rice (*Oryza sativa*) hypothetical protein (*zm*-HPLV9), in conjunction with the terminator region from the *Arabidopsis thaliana at*-T9 gene (GenBank accession NM_001202984; Salanoubat et al., 2000).

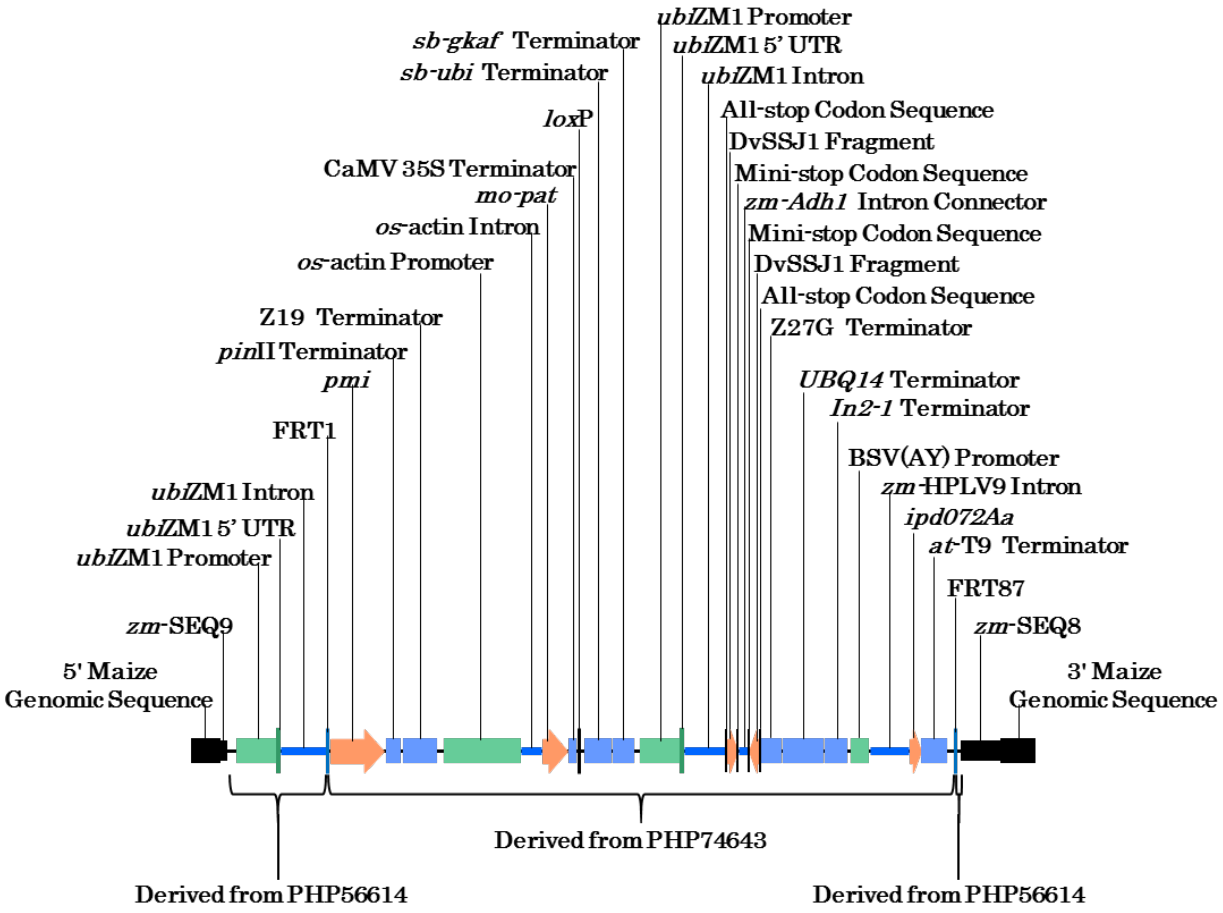

Figure 7. Schematic Diagram of the Intended DP23211 Insertion

Schematic diagram of the insertion intended to be present (bracketed regions) in the DP23211 maize genome following SSI at the FRT1 and FRT87 sites. The size of the intended insertion is 16,176 bp and it includes sequences from PHP74643 (**Figure 6**) and PHP56614 (**Figure 2**). The flanking maize genomic regions are represented by horizontal black bars. Although *zm*-SEQ9 and *zm*-SEQ8 are present in PHP56614, they are derived from the maize genome and appear in their natural context in the chromosome, so are considered to be parts of the flanking maize genome and are not included in the intended insertion.

Table 3. Description of the Genetic Elements in Plasmid PHP74643

Region	Location on Plasmid (bp to bp)	Genetic Element	Size (bp)	Description
T-DNA	1 – 28,187		28,187	See **Table 4** for information on the elements in this region
Plasmid Construct	28,188 – 53,071	Includes Elements Below	24,884	DNA from various sources for plasmid construction and plasmid replication
	29,363 – 30,151 (complementary)	*spc*	789	Spectinomycin resistance gene from bacteria (Fling et al., 1985)
	31,274 – 31,643 (complementary)	colE1 *ori*	370	Origin of replication region from *Escherichia coli* (Tomizawa et al., 1977)
	32,737 – 32,750	*cos*	14	Cohesive ends from lambda bacteriophage DNA (Komari et al., 1996)
	34,455 – 35,105 (complementary)	*tetR*	651	Tetracycline resistance regulation gene from bacteria (Komari et al., 1996)
	35,211 – 36,410	*tetA*	1,200	Tetracycline resistance gene from bacteria (Komari et al., 1996)
	37,683 – 38,831 (complementary)	*trfA*	1,149	Trans-acting replication gene from bacteria (Komari et al., 1996)
	42,613 – 42,979 (complementary)	*ori*T	367	Origin of transfer region from bacteria (Komari et al., 1996)
	44,596 – 50,866 (complementary)	*Ctl*	6,271	Central control operon region from bacteria (Komari et al., 1996)
	51,874 – 52,584 (complementary)	*ori*V	711	Origin of replication region from bacteria (Komari et al., 1996)
Ti Plasmid Backbone	53,072 – 67,888	Includes Elements Below	14,817	Virulence (*vir*) gene region and intergenic regions from Ti plasmid of *Agrobacterium tumefaciens* (Komari et al., 1996)
	53,385 – 53,828 (complementary)	*vir*D1	444	Virulence gene from *Agrobacterium tumefaciens* important for T-DNA insertion into genome
	54,097 – 54791	*vir*C1	695	Virulence gene from Agrobacterium tumefaciens important for T-DNA insertion into genome
	54,794 – 55,402	*vir*C2	609	Virulence gene from Agrobacterium tumefaciens important for T-DNA insertion into genome
	55,513 – 56,316 (complementary)	*vir*G	804	Virulence gene from Agrobacterium tumefaciens important for T-DNA insertion into genome
	56,448 – 65,883 (complementary)	*vir*B	9,436	Virulence operon region from Agrobacterium tumefaciens important for T-DNA insertion into genome
Plasmid Construct	67,889 – 71,116	Includes Elements Below	3,228	DNA from various sources for plasmid construction and plasmid replication
	68,184 – 68,553 (complementary)	colE1 *ori*	370	Origin of replication region from Escherichia coli (Tomizawa et al., 1977)
	69,647 – 69,660	*cos*	14	Cohesive ends from lambda bacteriophage DNA (Komari et al., 1996)

Table 4. Description of the Genetic Elements in the T-DNA Region from Plasmid PHP74643

Gene Cassette	Location on T-DNA (bp to bp)	Genetic Element	Size (bp)	Description
	1 – 25	Right Border (RB)	25	T-DNA Right Border from the *Agrobacterium tumefaciens* Ti plasmid (Komari et al., 1996)
	26 – 75	Ti Plasmid Region	50	Sequence from the *Agrobacterium tumefaciens* Ti plasmid (Komari et al., 1996)
	76 – 406	Intervening Sequence	331	DNA sequence used for cloning
zm-wus2 gene cassette	407 – 728	*nos* Promoter	322	Promoter region from the *Agrobacterium tumefaciens* Ti plasmid nopaline synthase gene (Depicker et al., 1982)
	729 – 781	Intervening Sequence	53	DNA sequence used for cloning
	782 – 1690	*zm-wus2*	909	*Wuschel 2* gene from *Zea mays* (Lowe et al., 2016; Mayer et al., 1998)
	1,691 – 1,802	Intervening Sequence	112	DNA sequence used for cloning
	1,803 – 2,113	*pin*II Terminator	311	Terminator region from the *Solanum tuberosum* (potato) proteinase inhibitor II gene (An et al., 1989; Keil et al., 1986)
	2,114 – 2,175	Intervening Sequence	62	DNA sequence used for cloning
zm-odp2 gene cassette	2,176 – 3,075	*ubi*ZM1 Promoter	900	Promoter region from the *Zea mays* ubiquitin gene 1 (Christensen et al., 1992)
	3,076 – 3,158	*ubi*ZM1 5' UTR	83	5' untranslated region from the *Zea mays* ubiquitin gene 1 (Christensen et al., 1992)
	3,159 – 4,171	*ubi*ZM1 Intron	1,013	Intron region from the *Zea mays* ubiquitin gene 1 (Christensen et al., 1992)
	4,172 – 4,189	Intervening Sequence	18	DNA sequence used for cloning
	4,190 – 6,322	*zm-odp2*	2,133	Ovule development protein 2 gene from *Zea mays* (Gordon-Kamm *et al.*, 2013; GenBank accession XM008676474)
	6,323 – 6,390	Intervening Sequence	68	DNA sequence used for cloning
	6,391 – 6,701	*pin*II Terminator	311	Terminator region from the *Solanum tuberosum* (potato) proteinase inhibitor II gene (An et al., 1989; Keil et al., 1986)
	6,702 – 6,717	Intervening Sequence	16	DNA sequence used for cloning

Table 4. Description of the Genetic Elements in the T-DNA Region from Plasmid PHP74643 (continued)

Gene Cassette	Location on T-DNA (bp to bp)	Genetic Element	Size (bp)	Description
	6,718 – 7,459	Z19 Terminator	742	Terminator region from the *Zea mays* 19-kDa zein gene (GenBank accession KX247647; Dong et al., 2016)
	7,460 – 7,480	Intervening Sequence	21	DNA sequence used for cloning
mo-Flp gene cassette	7,481 – 8,380	*ubi*ZM1 Promoter	900	Promoter region from the *Zea mays* ubiquitin gene 1 (Christensen et al., 1992)
	8,381 – 8,463	*ubi*ZM1 5' UTR	83	5' untranslated region from the *Zea mays* ubiquitin gene 1 (Christensen et al., 1992)
	8,464 – 9,476	*ubi*ZM1 Intron	1,013	Intron region from the *Zea mays* ubiquitin gene 1 (Christensen et al., 1992)
	9,477 – 9,506	Intervening Sequence	30	DNA sequence used for cloning
	9,507 – 10,140	*mo-Flp* Exon1	634	Maize-optimized exon 1 of the flippase gene from *Saccharomyces cerevisiae* (Dymecki, 1996)
	10,141 – 10,329	*st-LS1* Intron	189	Intron region from the *Solanum tuberosum* (potato) *LS1* gene (Eckes et al., 1986)
	10,330 – 10,967	*mo-Flp* Exon2	638	Maize-optimized exon 2 of the flippase gene from *Saccharomyces cerevisiae* (Dymecki, 1996)
	10,968 – 10,972	Intervening Sequence	5	DNA sequence used for cloning
	10,973 – 11,283	*pin*II Terminator	311	Terminator region from the *Solanum tuberosum* (potato) proteinase inhibitor II gene (An et al., 1989; Keil et al., 1986)
	11,284 – 11,296	Intervening Sequence	13	DNA sequence used for cloning
DsRed2 gene cassette	11,297 – 11,771	CaMV 35S Enhancer	475	35S enhancer region from the cauliflower mosaic virus genome (Franck et al., 1980; Kay et al., 1987)
	11,772 – 11,804	Intervening Sequence	33	DNA sequence used for cloning
	11,805 – 12,650	*Ltp2* Promoter	846	Promoter region from the *Hordeum vulgare* (barley) aleurone-specific lipid transfer protein gene (Kalla et al., 1994)
	12,651 – 12,694	Intervening Sequence	44	DNA sequence used for cloning
	12,695 – 13,372	*DsRed2*	678	Modified red fluorescent protein gene from *Discosoma sp.* (Wasson-Blader, 2001) with internal *Bst*E II restriction site removed

Table 4. Description of the Genetic Elements in the T-DNA Region from Plasmid PHP74643 (continued)

Gene Cassette	Location on T-DNA (bp to bp)	Genetic Element	Size (bp)	Description
DsRed2 gene cassette (cont)	13,373 – 13,376	Intervening Sequence	4	DNA sequence used for cloning
	13,377 – 13,570	CaMV 35S Terminator	194	35S terminator region from the cauliflower mosaic virus genome (Franck et al., 1980; Guilley et al., 1982)
	13,571 – 13,596	Intervening Sequence	26	DNA sequence used for cloning
	13,597 – 13,617	*att*B4	21	Bacteriophage lambda integrase recombination site (Cheo et al., 2004)
	13,618 – 13,696	Intervening Sequence	79	DNA sequence used for cloning
	13,697 – 13,890	CaMV 35S Terminator	194	35S terminator region from the cauliflower mosaic virus genome (Franck et al., 1980; Guilley et al., 1982)
	13,891 – 13,905	Intervening Sequence	15	DNA sequence used for cloning
	13,906 – 13,953	FRT1	48	Flippase recombination target site from *Saccharomyces cerevisiae* (Proteau et al., 1986)
	13,954 – 13,971	Intervening Sequence	18	DNA sequence used for cloning
pmi gene cassette	13,972 – 15,187	*pmi*	1,216	Phosphomannose isomerase gene from *Escherichia coli* including 5' and 3' untranslated regions (UTR) (Negrotto et al., 2000) as described below: 5' UTR at bp 13,972-13,975 (4 bp long) Coding sequence at bp 13,976-15,151 (1,176 bp long) 3' UTR at bp 15,152-15,187 (36 bp long)
	15,188 – 15,197	Intervening Sequence	10	DNA sequence used for cloning
	15,198 – 15,508	*pin*II Terminator	311	Terminator region from the *Solanum tuberosum* (potato) proteinase inhibitor II gene (An et al., 1989; Keil et al., 1986)
	15,509 – 15,518	Intervening Sequence	10	DNA sequence used for cloning
	15,519 – 16,260	Z19 Terminator	742	Terminator region from the *Zea mays* 19-kDa zein gene (GenBank accession KX247647; Dong et al., 2016)

Table 4. Description of the Genetic Elements in the T-DNA Region from Plasmid PHP74643 (continued)

Gene Cassette	Location on T-DNA (bp to bp)	Genetic Element	Size (bp)	Description
	16,261 – 16,463	Intervening Sequence	203	DNA sequence used for cloning
mo-pat gene cassette	16,464 – 18,145	*os*-actin Promoter	1,682	Promoter region from the *Oryza sativa* (rice) actin gene (GenBank accession CP018159; GenBank accession EU155408.1)
	18,146 – 18,614	*os*-actin Intron	469	Intron region from the *Oryza sativa* (rice) actin gene (GenBank accession CP018159; GenBank accession EU155408.1)
	18,615 – 18,629	Intervening Sequence	15	DNA sequence used for cloning
	18,630 – 19,181	*mo-pat*	552	Maize-optimized phosphinothricin acetyltransferase gene from *Streptomyces viridochromogenes* (Wohlleben et al., 1988)
	19,182 – 19,199	Intervening Sequence	18	DNA sequence used for cloning
	19,200 – 19,393	CaMV 35S Terminator	194	35S terminator region from the cauliflower mosaic virus genome (Franck et al., 1980; Guilley et al., 1982)
	19,394 – 19,414	Intervening Sequence	21	DNA sequence used for cloning
	19,415 – 19,448	*lox*P	34	Bacteriophage P1 recombination site recognized by Cre recombinase (Dale and Ow, 1990)
	19,449 – 19,544	Intervening Sequence	96	DNA sequence used for cloning
	19,545 – 20,128	*sb-ubi* Terminator	584	Terminator region from the *Sorghum bicolor* (sorghum) ubiquitin gene (Phytozome gene ID Sobic.004G049900.1)
	20,129 – 20,169	Intervening Sequence	41	DNA sequence used for cloning
	20,170 – 20,633	*sb-gkaf* Terminator	464	Terminator region from the *Sorghum bicolor* (sorghum) γ-kafarin gene (de Freitas et al., 1994)
	20,634 – 20,666	Intervening Sequence	33	DNA sequence used for cloning
	20,667 – 20,690	*att*B1	24	Bacteriophage lambda integrase recombination site from the Invitrogen Gateway® cloning system (Hartley et al., 2000; Katzen, 2007)

Table 4. Description of the Genetic Elements in the T-DNA Region from Plasmid PHP74643 (continued)

Gene Cassette	Location on T-DNA (bp to bp)	Genetic Element	Size (bp)	Description
	20,691 – 20,777	Intervening Sequence	87	DNA sequence used for cloning
DvSSJ1 fragment cassette	20,778 – 21,677	*ubi*ZM1 Promoter	900	Promoter region from the *Zea mays* ubiquitin gene 1 (Christensen et al., 1992)
	21,678 – 21,760	*ubi*ZM1 5' UTR	83	5' untranslated region from the *Zea mays* ubiquitin gene 1 (Christensen et al., 1992)
	21,761 – 22,773	*ubi*ZM1 Intron	1,013	Intron region from the *Zea mays* ubiquitin gene 1 (Christensen et al., 1992)
	22,774 – 22,798	Intervening Sequence	25	DNA sequence used for cloning
	22,799 – 22,812	All-stop Codon Sequence	14	DNA sequence containing stop codons to terminate translation in all six reading frames through the site
	22,813 – 23,022	DvSSJ1 Fragment	210	Fragment of the smooth septate junction protein 1 gene from *Diabrotica virgifera* (Western corn rootworm; Hu et al., 2016)
	23,023 – 23,030	Mini-stop Codon Sequence	8	DNA sequence containing stop codons to terminate translation in designated reading frames through the site
	23,031 – 23,041	Intervening Sequence	11	DNA sequence used for cloning
	23,042 – 23,147	*zm-Adh1* Intron Connector	106	Connector sequence derived from the intron 1 region of the *Zea mays* alcohol dehydrogenase gene (Dennis et al., 1984)
	23,148 – 23,156	Intervening Sequence	9	DNA sequence used for cloning
	23,157 – 23,164 (complementary)	Mini-stop Codon Sequence	8	DNA sequence containing stop codons to terminate translation in designated reading frames through the site
	23,165 – 23,374 (complementary)	DvSSJ1 Fragment	210	Fragment of the smooth septate junction protein 1 gene from *Diabrotica virgifera* (Western corn rootworm; Hu et al., 2016)
	23,375 – 23,388 (complementary)	All-stop Codon Sequence	14	DNA sequence containing stop codons to terminate translation in all six reading frames through the site
	23,389 – 23,408	Intervening Sequence	20	DNA sequence used for cloning
	23,409 – 23,888	Z27G Terminator	480	Terminator region from the *Zea mays* W64 line 27-kDa gamma zein gene (Das et al., 1991; Liu et al., 2016)

Table 4. Description of the Genetic Elements in the T-DNA Region from Plasmid PHP74643 (continued)

Gene Cassette	Location on T-DNA (bp to bp)	Genetic Element	Size (bp)	Description
	23,889 – 23,894	Intervening Sequence	6	DNA sequence used for cloning
	23,895 – 24,796	*UBQ14* Terminator	902	Terminator region from the *Arabidopsis thaliana* ubiquitin 14 gene (Callis et al., 1995)
	24,797 – 24,802	Intervening Sequence	6	DNA sequence used for cloning
	24,803 – 25,296	*In2-1* Terminator	494	Terminator region from the *Zea mays In2-1* gene (Hershey and Stoner, 1991)
	25,297 – 25,353	Intervening Sequence	57	DNA sequence used for cloning
	25,354 – 25,377	*att*B2	24	Bacteriophage lambda integrase recombination site from the Invitrogen Gateway® cloning System (Hartley et al., 2000; Katzen, 2007)
	25,378 – 25,414	Intervening Sequence	37	DNA sequence used for cloning
ipd072Aa gene cassette	25,415 – 25,828	BSV(AY) Promoter	414	Promoter region from the banana streak virus (acuminata Yunnan strain) genome (GenBank accession DQ092436.1; Zhuang et al., 2011)
	25,829 – 25,847	Intervening Sequence	19	DNA sequence used for cloning
	25,848 – 26,703	*zm*-HPLV9 Intron	856	Intron region from the *Zea mays* predicted calmodulin 5 gene (Phytozome gene ID Zm00008a029682)
	26,704 – 26,712	Intervening Sequence	9	DNA sequence used for cloning
	26,713 – 26,973	*ipd072Aa*	261	Insecticidal protein gene from *Pseudomonas chlororaphis* (Schellenberger et al., 2016)
	26,974 – 26,979	Intervening Sequence	6	DNA sequence used for cloning
	26,980 – 27,552	*at*-T9 Terminator	573	Terminator region from an *Arabidopsis thaliana* putative gene of the mannose-binding protein superfamily (GenBank accession NM_001202984; Salanoubat et al., 2000)
	27,553 – 27,591	Intervening Sequence	39	DNA sequence used for cloning
	27,592 – 27,612 (complementary)	*att*B3	21	Bacteriophage lambda integrase recombination site (Cheo et al., 2004)
	27,613 – 27,733	Intervening Sequence	121	DNA sequence used for cloning

Table 4. Description of the Genetic Elements in the T-DNA Region from Plasmid PHP74643 (continued)

Gene Cassette	Location on T-DNA (bp to bp)	Genetic Element	Size (bp)	Description
	27,734 – 27,781	FRT87	48	Modified Flippase recombination target site derived from *Saccharomyces cerevisiae* (Tao et al., 2007)
	27,782 – 28,112	Intervening Sequence	331	DNA sequence used for cloning
	28,113 – 28,162	Ti Plasmid Region	50	Sequence from the *Agrobacterium tumefaciens* Ti plasmid (Komari et al., 1996)
	28,163 – 28,187	Left Border (LB)	25	T-DNA Left Border from the *Agrobacterium tumefaciens* Ti plasmid (Komari et al., 1996)

Selection of Maize Event DP23211

Plants that were regenerated from transformation and tissue culture (designated T0 plants) were selected for further characterisation. Refer to **Figure 8** for a schematic overview of the transformation and event development process for DP23211 maize.

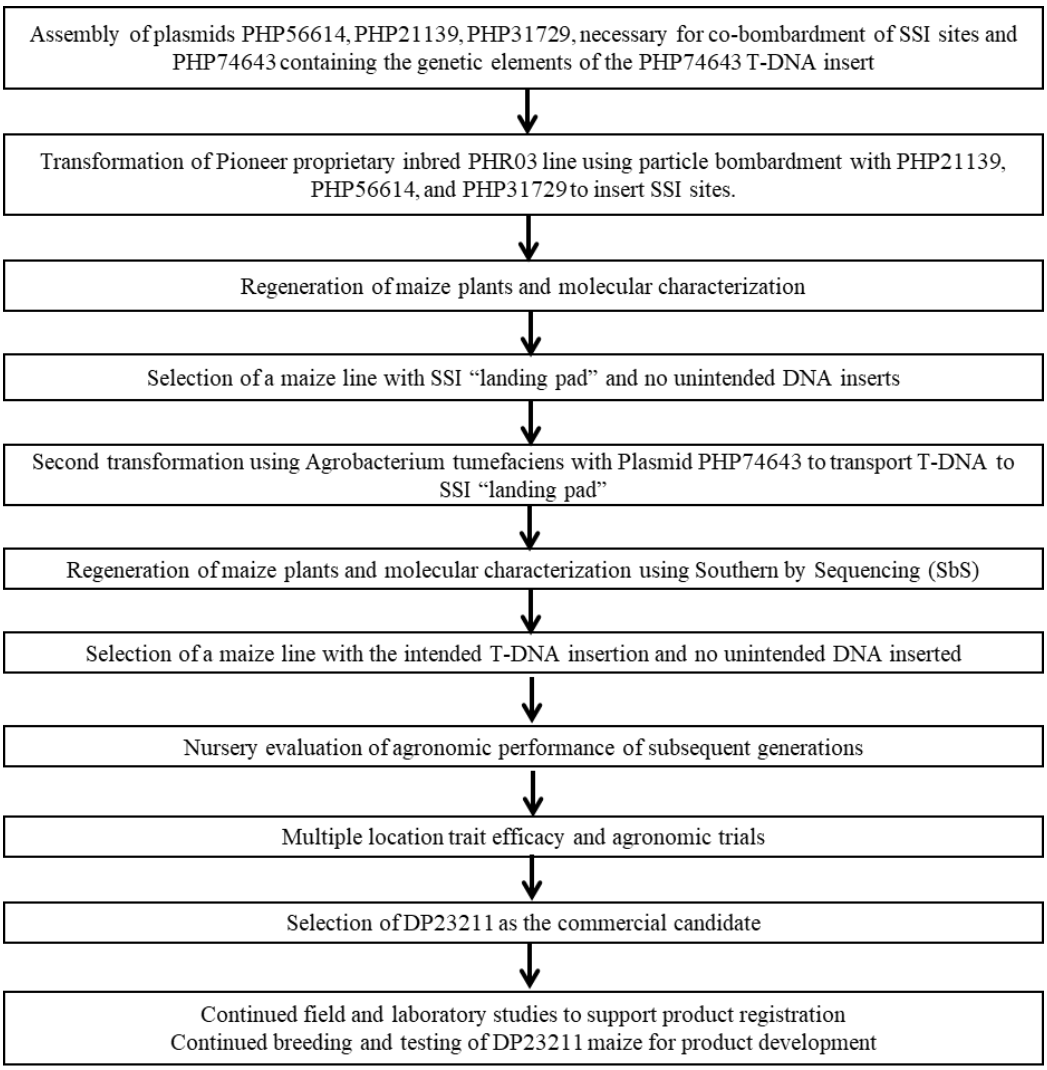

Figure 8. Event Development Process of DP23211 Maize

Breeding Method

The subsequent breeding of DP23211 maize proceeded as indicated in **Figure 9** to produce specific generations for the characterisation and assessments conducted, as well as for the development of commercial maize lines. **Table 5** provides the generations used for each characterisation study.

Figure 9. Breeding Diagram for DP23211 Maize and Generations Used for Analysis

Table 5. Generations and Comparators Used for Analysis of DP23211 Maize

Analysis	Seed Generation(s) Used	Comparators
Copy Number, Intactness, and Backbone by SbS	T1	PHR03
Intactness and Stability by Southern Blot	T1, T2, T3, T4, T5	PHR03
Mendelian Inheritance	BC1F1 (PH1V5T), BC1F1 (PH2SRH) BC2F1 (PH1V5T), T1, T5,	N/A
Composition and Expression Analysis	F1	PHEJW/PHR03

Bacteria used for manipulation

A lab strain of *Agrobacterium tumefaciens* (strain AGL1) was used for all vector manipulations and for amplification of the plasmid DNA (PHP74643) that was used for the transformation.

Gene Construct and Vectors

Please refer to **Table 3** for a description of the genetic elements of the Plasmid PHP74643; **Figure 5** for the map of Plasmid PHP74643; **Table 4** for the description of the genetic elements in T-DNA Region of Plasmid PHP74643; and **Figure 6** for the T-DNA region maps from Plasmid PHP74643.

b. Molecular Characterisation

Molecular characterisation of DP23211 maize plants was conducted using Southern-by-Sequencing (SbS™ technology) to determine the number of insertions within the plant genome, insertion intactness, and to confirm the absence of plasmid backbone and other unintended sequences. Southern blot analysis was performed to confirm stable genetic inheritance of the inserted DvSSJ1 fragment cassette and *ipd072Aa*, *pmi*, and *mo-pat* gene cassettes. Segregation analysis was conducted for five generations of DP23211 maize to confirm stable Mendelian inheritance.

Based on the SbS analysis described below, it was determined that a single, intact copy of the intended DNA (**Figure 7**) was inserted into the genome of DP23211 maize and that no plasmid backbone sequences or other unintended insertions were present in the genome. In addition, Southern blot analysis across five breeding generations confirmed the stable genetic inheritance of the DNA insertion in DP23211 maize. Segregation analysis across five breeding generations confirmed a stable Mendelian inheritance pattern.

Southern-by-Sequencing (SbS) Analysis to Determine Copy Number, Insertion Intactness, and Confirm the Absence of Vector Backbone Sequences

SbS analysis utilizes probe-based sequence capture, Next Generation Sequencing (NGS) techniques, and bioinformatics procedures to capture, sequence, and identify inserted DNA within the maize genome. By compiling a large number of unique sequencing reads and mapping them against the transformation plasmid and control maize genome, unique junctions due to inserted DNA are identified in the bioinformatics analysis and used to determine the number of insertions within the plant genome, verify insertion intactness, and confirm the absence of plasmid backbone sequences.

The SbS technique (**Figure 10**) utilizes capture probes homologous to the transformation plasmid to isolate genomic DNA that hybridizes to the probe sequences (Zastrow-Hayes et al., 2015). Captured DNA is then sequenced using a Next Generation Sequencing (NGS) procedure and the results are analyzed using bioinformatics tools. During the analysis, junction reads are identified as those sequence reads where part of the read shows exact homology to the plasmid DNA sequence while the rest of the read does not match the contiguous plasmid. Junctions may occur between inserted DNA and genomic DNA, or between insertions of two plasmid-derived DNA sequences that are not contiguous in the transformation plasmid. Multiple sequence reads are generated for each junction and are compiled into a consensus sequence for the junction. By compiling a large number of unique sequencing reads and comparing them to the transformation plasmid and control maize genome, unique junctions due to inserted DNA are identified. A unique junction is defined as one in which the plasmid-derived sequence and the adjacent sequence are the same across multiple reads, although the overall length of the multiple reads for that junction will vary due to the sequencing process. The number of unique junctions is related to the number of plasmid insertions present in the maize genome (for example, a single T-DNA insertion is expected to have two unique junctions). Detection of additional unique junctions beyond the two expected for a single insertion would indicate the presence of rearrangements or additional insertions derived from plasmid DNA. Absence of any junctions indicates there are no detectable insertions within the maize genome.

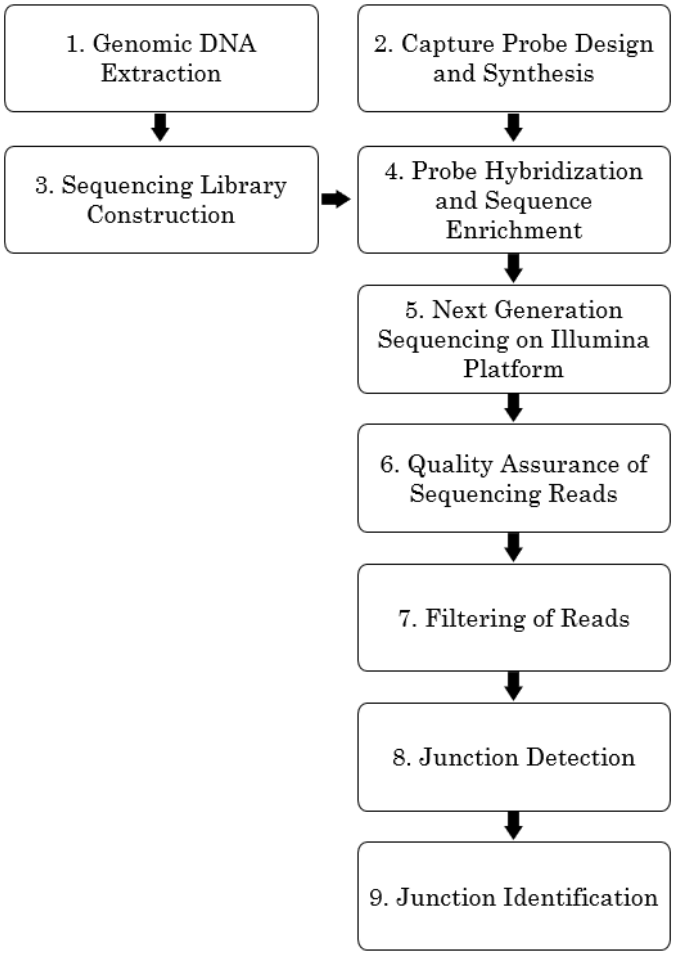

Figure 10. Southern by Sequencing (SbS) Process Flow Diagram

The T1 generation of DP23211 maize was analysed by SbS, using full-coverage probes comprising the entire sequences of the trait plasmid PHP74643, the landing pad plasmid PHP56614, and the helper plasmids PHP21139 and PHP31729, to determine the insertion copy number and intactness and to confirm the absence of plasmid backbone sequences or unintended plasmid integration [redacted] 2019). SbS was also performed on non-GM near-isoline PHR03 maize as a control, and on positive control samples of each plasmid to confirm that the assay could reliably detect plasmid fragments spiked into control maize genomic DNA at a level equivalent to one copy of plasmid per genome copy. Based on the results obtained in this study, a schematic diagram of the DP23211 insertion was developed and is provided in **Figure 11.**

Several genetic elements in the positive control plasmids are derived from maize and thus the homologous elements in the PHR03 maize genome will be captured by the full-coverage probes used in the SbS analysis. These endogenous elements (*zm-wus2*, *ubi*ZM1 promoter, 5' UTR, and intron, *zm-odp2*, Z19 terminator, *zm-Adh1* intron connector, Z27G terminator, *In2-1* terminator, *zm*-HPLV9 intron, *zm*-SEQ9, *zm*-SEQ8, *In2-2* promoter, and *zm-Oleosin* promoter; **Table 6, Figures 1-7**) will have sequencing reads in the SbS results due to the homologous elements in the PHR03 maize genome. However, if no junctions are detected, these sequencing reads only indicate the presence of the endogenous elements in their normal context of the maize genome and are not from inserted DNA.

SbS analysis results for the control maize are shown in **Figure 12** and the positive control samples are presented in **Figure 13**. Example SbS results for one positive plant from the DP23211 T1 generation are presented in **Figure 14**. The SbS results for the remaining 9 plants tested are presented in **Appendix A.**

Sequencing reads were detected in the PHR03 control maize (**Figure 12**); however, coverage above background level (35x) was obtained only for the genetic elements derived from the maize genome. These sequence reads were due to capture and sequencing of these genetic elements in their normal context within the PHR03 control maize genome. Variation in coverage of the endogenous elements is due to sequence variations between the PHR03 control maize and the maize varieties from which the genetic elements in the four plasmids were derived. No junctions were detected between plasmid sequences and the maize genome, indicating that there are no plasmid DNA insertions in the control maize, and the sequence reads were solely due to the endogenous genetic elements present in the PHR03 control maize genome.

SbS analysis of the positive control samples containing spiked-in plasmid DNA resulted in sequence coverage across the entire length of each plasmid (**Figure 13**), indicating that the SbS assay utilizing the full-coverage probe library is sensitive enough to detect PHP74643, PHP56614, PHP21139, or PHP31729 sequences at a concentration equivalent to one copy of plasmid per copy of the maize genome. No junctions were detected between plasmid and genomic sequences, indicating that the sequence reads were due to either the spiked-in plasmid or the endogenous maize genetic elements that were detected in the control maize.

SbS analysis of the T1 generation of DP23211 maize resulted in three plants that contained the intended insertion (**Table 7, Figure 14** and **Appendix A Figures A8** and **A9**). Each of these plants contained two unique genome-insertion junctions, one at each end of the intended insertion, that were identical across the three plants. The 5' junction starts with bp 1 of the intended insertion, derived from PHP56614 and PHP74643 (**Figure 7**), and the insertion ends with the 3' junction at bp 16,176 of the intended insertion. The number of sequence reads at the 5' and 3' junctions is provided in **Table 7.** There were no other junctions between PHP74643, PHP56614, PHP21139, or PHP31729 plasmid sequences and the maize genome detected in the plants, indicating that there are no additional plasmid-derived insertions present in DP23211 maize. Alignment of the reads from the three positive plants (**Table 7, Figure 14,** and **Appendix A Figures A8** and **A9**) to the four plasmid maps (**Figures 1, 3, 4, and 5**) shows coverage of the genetic elements found in the intended insertion, along with coverage of the endogenous elements in the plasmids that were not incorporated into the insertion (*zm-wus2*, *zm-odp2*, *In2-2* promoter, *zm-Oleosin* promoter, *zm*-SEQ9, and *zm*-SEQ8). Reads also aligned to the *pin*II terminator elements present outside of the intended insertion regions in PHP56614 and PHP74643 although these elements were not incorporated into the insertion. The NGS reads that aligned to these copies of the *pin*II terminator are from fragments containing the *pin*II terminator in the *pmi* cassette of the intended insertion; however, the reads from this single copy align to all copies of the *pin*II terminator in the plasmid maps. Similarly, reads aligned to the CaMV 35S terminator elements in the *DsRed2* cassette of PHP74643 due to the presence of an identical element in the *mo-pat* cassette of the intended insertion, and reads aligned to a portion of PHP31729 containing a Gateway™ *att* site element that matches a corresponding *att* site in the intended insertion.

There were no unexpected junctions between non-contiguous regions of the intended insertion identified, indicating that there are no rearrangements or truncations in the inserted DNA. Furthermore, there were no junctions between maize genome sequences and the backbone sequence of any of the plasmids involved in the production of DP23211 maize, demonstrating that no plasmid backbone sequences were incorporated into DP23211 maize.

Each of the seven DP23211 maize plants from the T1 generation that were determined to be negative for the DP23211 insertion yielded sequencing reads (**Table 7** and **Appendix A Figures A1** to **A7**) that matched the reads in the control maize, indicating the reads were due to endogenous maize sequences. There were no junctions between plasmid sequences and the maize genome detected in these plants, indicating that these plants did not contain any insertions derived from PHP74643, PHP56614, PHP21139, or PHP31729.

SbS analysis of the T1 generation of DP23211 maize demonstrated that DP23211 maize contains a single, intact copy of the intended insertion, derived from PHP56614 and the PHP74643 T-DNA, and that no additional insertions or plasmid backbone sequences are present in the DP23211 maize genome.

Additional details regarding analytical methods for SbS analysis are provided in **Appendix A.**

Table 6. Maize Endogenous Elements in Plasmids and DP23211 Insertion

Number[a]	Name of Endogenous Element[b]	Present in Plasmid(s) or Insertion
1	*zm-wus2*	PHP21139, PHP74643
2	*ubi*ZM1 promoter, 5' UTR, and intron	PHP56614, PHP74643, DP23211 insertion
3	*zm-odp2*	PHP31729, PHP74643
4	Z19 terminator	PHP74643, DP23211 insertion
5	*zm-Adh1* intron connector	PHP74643, DP23211 insertion
6	Z27G terminator	PHP74643, DP23211 insertion
7	*In2-1* terminator	PHP21139, PHP74643, DP23211 insertion
8	*zm*-HPLV9 intron	PHP74643, DP23211 insertion
9	*zm*-SEQ9[c]	PHP56614
10	*zm*-SEQ8[c]	PHP56614
11	*In2-2* promoter	PHP21139
12	*zm-Oleosin* promoter	PHP31729

[a] The numbers indicating endogenous genetic elements are shown as circled numbers found below linear construct maps in **Figures 12-14** and **Appendix A Figures A1 to A9.**

[b]As shown in the plasmid and T-DNA maps in **Figures 1,3,5,6** and the intended insertion map in **Figure 7**.

[c]As *zm*-SEQ9 and *zm*-SEQ8 are found in their native context in the genomic flanking regions, they are considered part of the flanking regions and not part of the DP23211 insertion.

Table 7. DP23211 Maize and Control Maize SbS Junction Reads

Sample Description	Supporting Reads at 5′ Junction[a]	Unique Reads at 5′ Junction[b]	Supporting Reads at 3′ Junction[c]	Unique Reads at 3′ Junction[d]	DP23211 Insertion
DP23211 Maize Plant ID 343210845	96	39	37	22	+
DP23211 Maize Plant ID 343210846	0	0	0	0	-
DP23211 Maize Plant ID 343210847	0	0	0	0	-
DP23211 Maize Plant ID 343210848	0	0	0	0	-
DP23211 Maize Plant ID 343210849	0	0	0	0	-
DP23211 Maize Plant ID 343210850	0	0	0	0	-
DP23211 Maize Plant ID 343210851	0	0	0	0	-
DP23211 Maize Plant ID 343210852	0	0	0	0	-
DP23211 Maize Plant ID 343210853	137	44	38	23	+
DP23211 Maize Plant ID 343210854	85	33	56	29	+
Control Maize	0	0	0	0	-
PHP21139 Positive Control	0	0	0	0	-
PHP31729 Positive Control	0	0	0	0	-
PHP56614 Positive Control	0	0	0	0	-
PHP74643 Positive Control	0	0	0	0	-

[a] Total number of sequence reads across the 5′ junction of the DP23211 insertion.

[b] Unique sequence reads establishing the location of the 5′ genomic junction of the DP23211 insertion (**Figure 11**). Multiple identical NGS supporting reads are condensed into each unique read.

[c] Total number of sequence reads across the 3′ junction of the DP23211 insertion.

[d] Unique sequence reads establishing the location of the 3′ genomic junction of the DP23211 insertion (**Figure 11**). Multiple identical NGS supporting reads are condensed into each unique read.

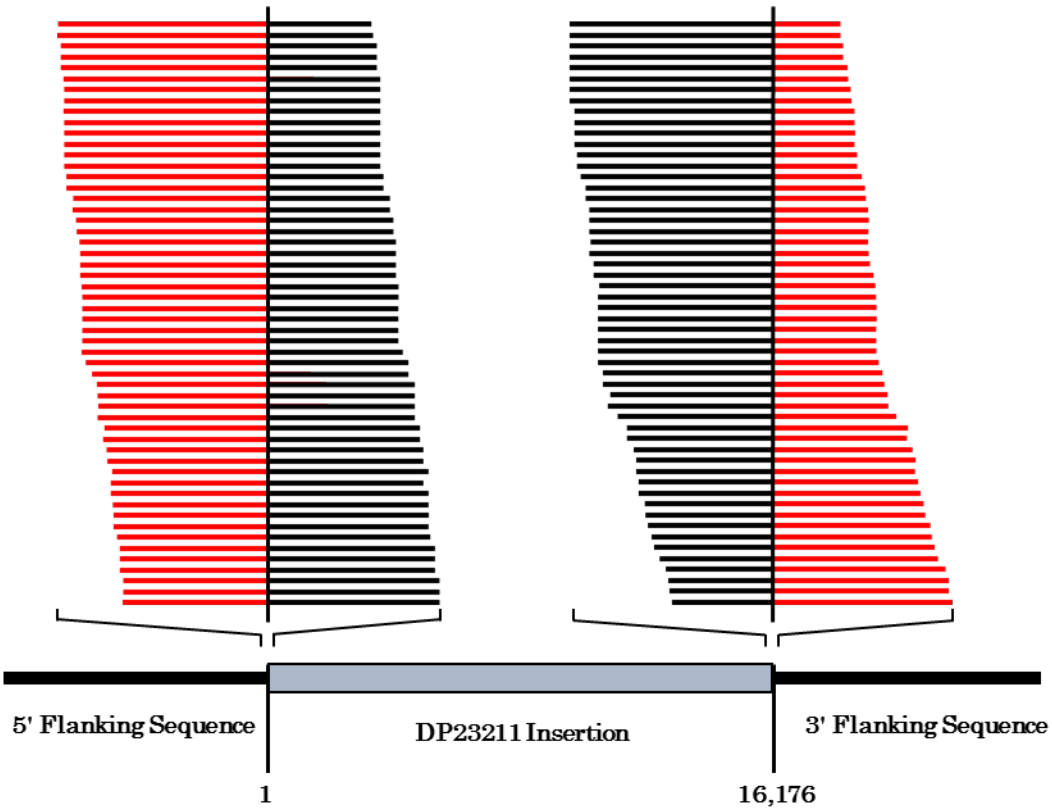

Figure 11. Map of the Insertion in DP23211 Maize

Schematic map of the DNA insertion in DP23211 maize based on the SbS analysis described. The flanking maize genomic regions, including *zm*-SEQ9 and *zm*-SEQ8, are indicated in the map by black bars. A single, intact copy of the intended insertion, derived from PHP56614 and PHP74643 and shown by the gray box, is integrated into the DP23211 maize genome. Vertical lines show the locations of the two-unique genome-insertion junctions. The numbers below the map indicate the bp location of the junction nucleotide in reference to the sequence of the intended insertion (**Figure 7**). Representative individual sequencing reads across the junctions are shown as stacked lines above each junction (not to scale); red indicates genomic flanking sequence and black indicates inserted DNA sequence within each read.

A. Alignment to Intended Insertion

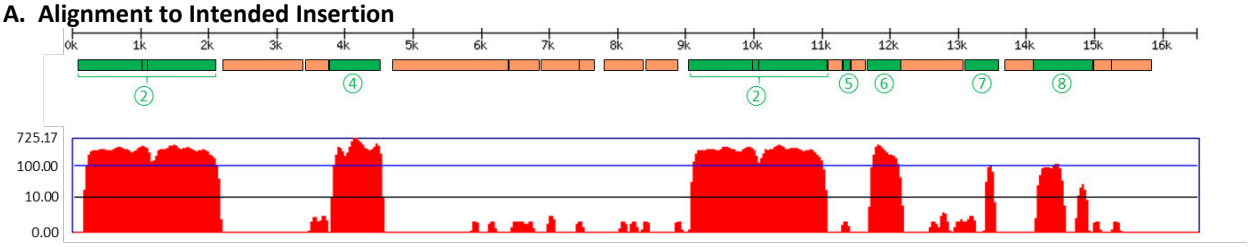

B. Alignment to PHP74643

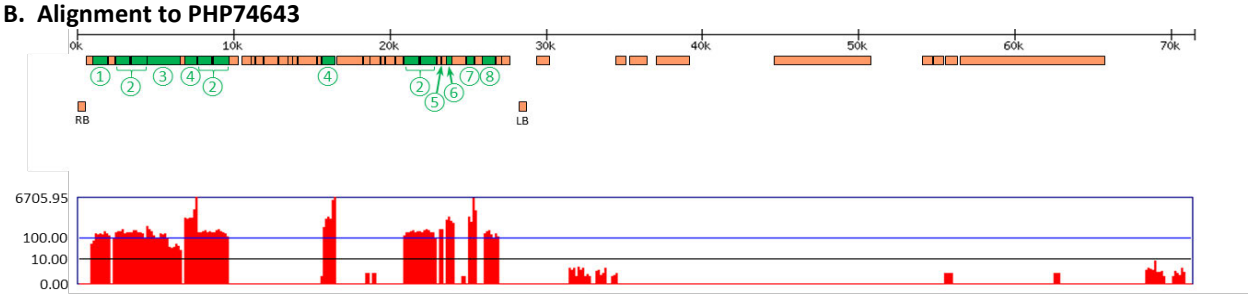

C. Alignment to PHP56614

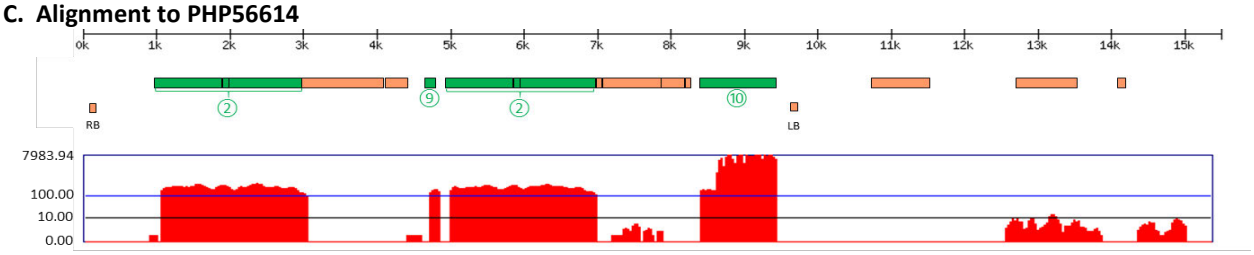

D. Alignment to PHP21139

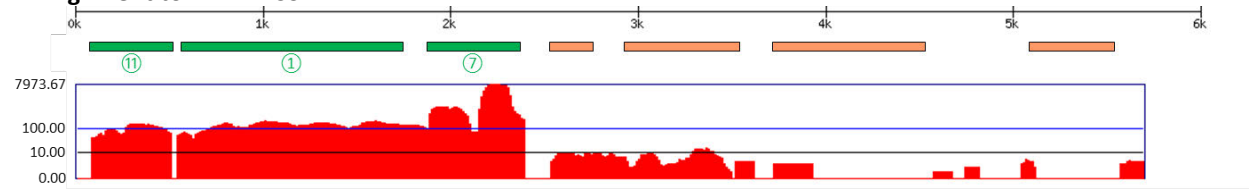

E. Alignment to PHP31729

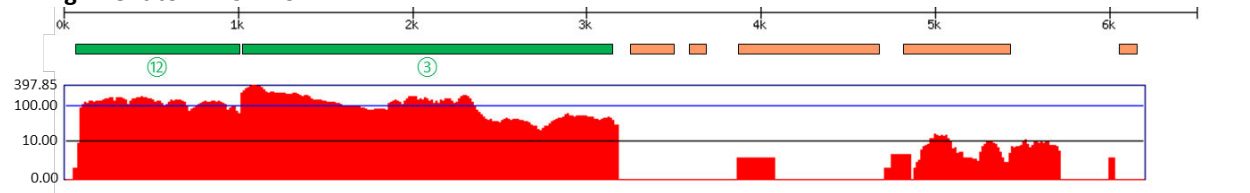

Figure 12. SbS Results for Control Maize

The red coverage graph shows the number of individual NGS reads aligned at each point on the intended insertion or construct using a logarithmic scale. Green bars above the coverage graph indicate endogenous genetic elements in each plasmid derived from the maize genome (identified by numbers, **Table 6**), while tan bars indicate genetic elements derived from other sources. The absence of any junctions between plasmid and genomic sequences indicates that there are no insertions or plasmid backbone sequence present in the PHR03 control maize. **A)** SbS results for PHR03 control maize aligned against the intended insertion (16,176 bp; **Figure 7**). Coverage above background level (35x) was obtained only for regions derived from maize endogenous elements. Variation in coverage of the endogenous elements is due to some sequence variation between the control maize and the source of the corresponding genetic elements. As no junctions were detected between plasmid sequences and the maize genome, there are no DNA insertions identified in the PHR03 control maize, and the sequence reads are solely due to the endogenous elements present in the PHR03 genome. **B)** SbS results aligned against the

plasmid PHP74643 sequence (71,116 bp; **Figure 5**). Coverage was obtained only for the endogenous elements. **C)** SbS results aligned against the plasmid PHP56614 sequence (15,339 bp; **Figure 1**). Coverage was obtained only for the endogenous elements. **D)** SbS results aligned against the plasmid PHP21139 sequence (5,687 bp; **Figure 3**). Coverage was obtained only for the endogenous elements. **E)** SbS results aligned against the plasmid PHP31729 sequence (6,181 bp; **Figure 4**). Coverage was obtained only for the endogenous elements.

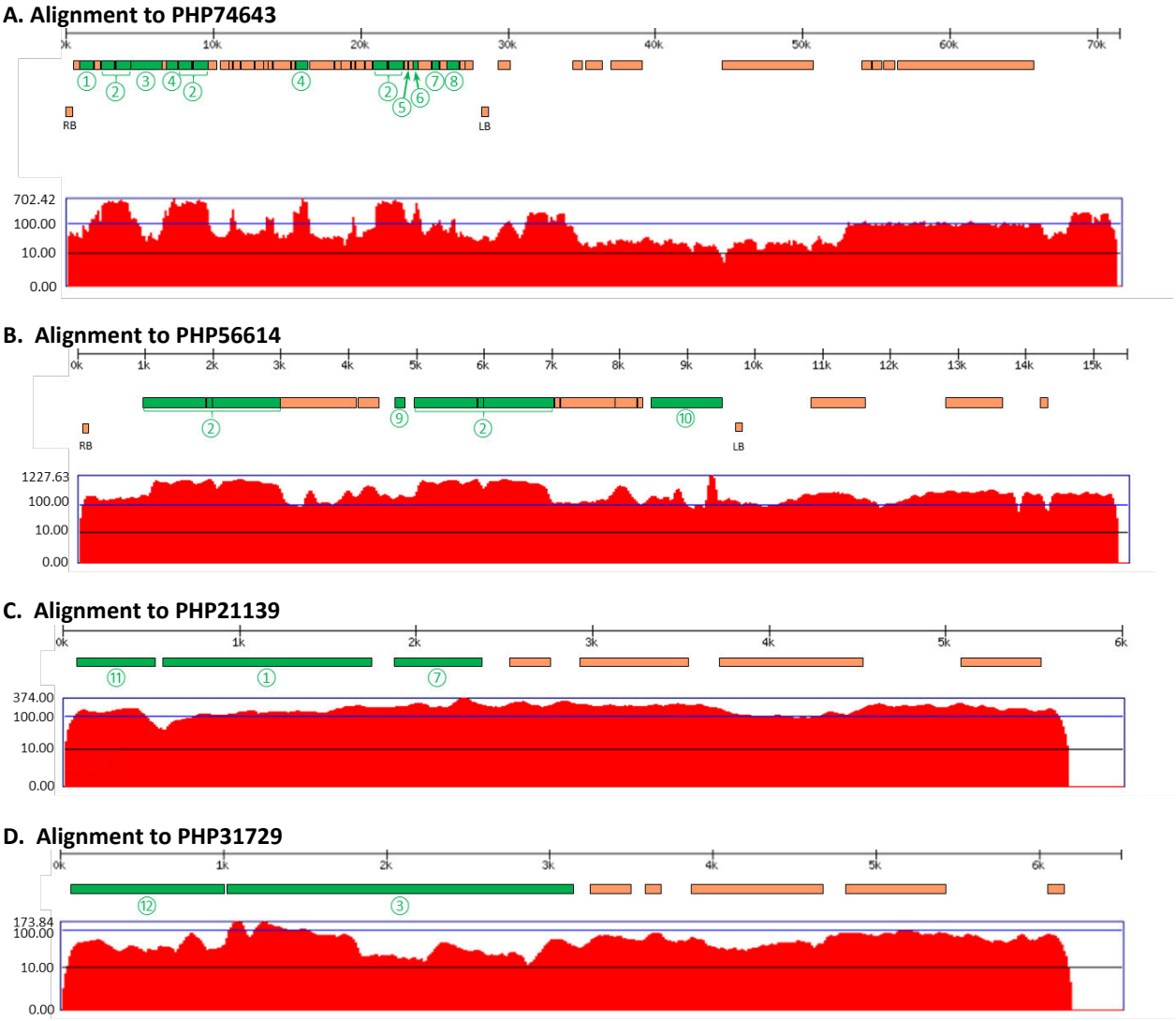

Figure 13. SbS Results for Positive Control Samples

The positive control sample consisted of control maize DNA spiked with each plasmid at a level corresponding to one copy of plasmid per copy of the maize genome. The red coverage graph shows the number of individual NGS reads aligned at each point on the intended insertion or construct using a logarithmic scale. Green bars above the coverage graph indicate endogenous genetic elements in the plasmid derived from the maize genome (identified by numbers, **Table 6**), while tan bars indicate genetic elements derived from other sources. **A)** SbS results of the PHP74643 positive control sample aligned against PHP74643 (71,116 bp; **Figure 7**). Coverage was obtained across the full length of the plasmid, indicating successful capture of PHP74643 sequences by the SbS probe library. **B)** SbS results of the PHP56614 positive control sample aligned against PHP56614 (15,339 bp; **Figure 1**). Coverage was obtained across the full length of the plasmid, indicating successful capture of PHP56614 sequences by the SbS probe library. **C)** SbS results of the PHP21139 positive control sample aligned against PHP21139 (5,687 bp; **Figure 3**). Coverage was obtained across the full length of the plasmid, indicating successful capture of PHP21139 sequences by the SbS probe library. **D)** SbS results of the PHP31729 positive control sample aligned against PHP31729 (6,181 bp; **Figure 4**). Coverage was obtained across the full length of the plasmid, indicating successful capture of PHP31729 sequences by the SbS probe library.

A. Alignment to Intended Insertion

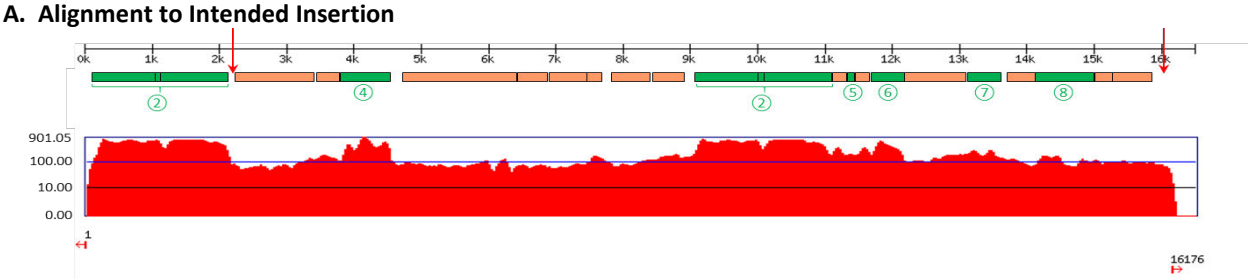

B. Alignment to PHP74643

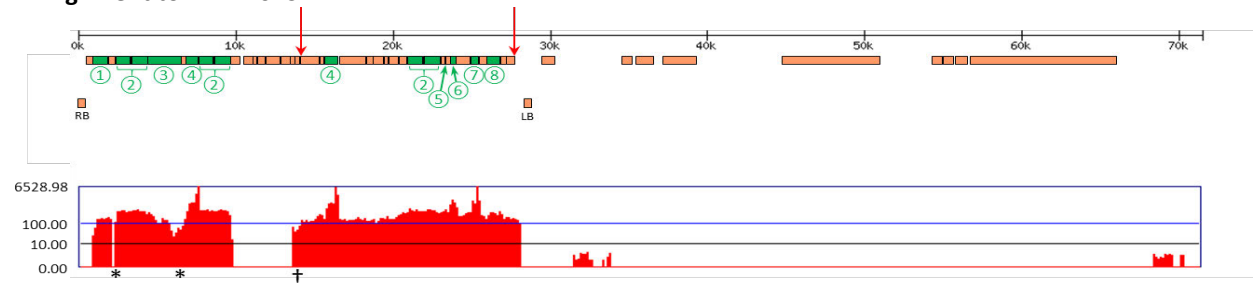

C. Alignment to PHP56614

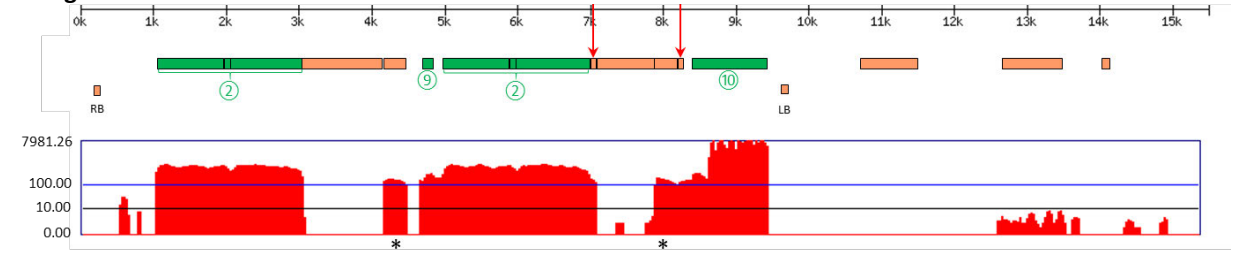

D. Alignment to PHP21139

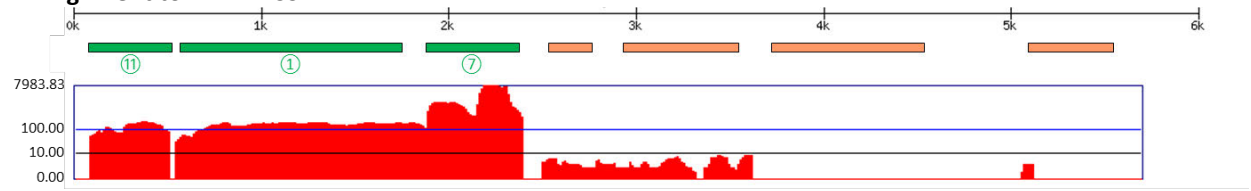

E. Alignment to PHP31729

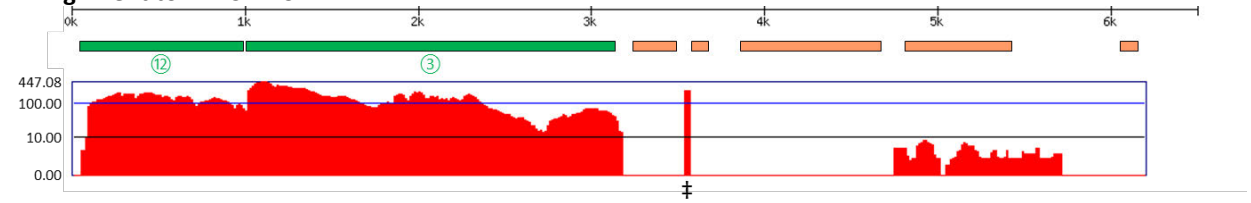

Figure 14. SbS Results for DP23211 Maize (Plant ID 343210845)

The red coverage graph shows the number of individual NGS reads aligned at each point on the intended insertion or construct using a logarithmic scale. Green bars above the coverage graph indicate endogenous genetic elements in each plasmid derived from the maize genome (identified by numbers, **Table 6**), while tan bars indicate genetic elements derived from other sources. FRT sites are indicated by red arrows. **A)** SbS results aligned against the intended insertion (16,176 bp; **Figure 7**), indicating that this plant contains the intended insertion. Arrows below the graph indicate the two plasmid-to-genome sequence junctions identified by SbS; the numbers above the arrows refer to the bp location of the junction relative to the intended insertion (**Figure 7**). The presence of only two junctions demonstrates the presence of a single insertion in the DP23211 maize genome. **B)** SbS results aligned against the plasmid PHP74643 sequence (71,116 bp; **Figure 5**). Coverage was obtained for the elements

between FRT1 and FRT87 transferred into DP23211 maize (region between the red arrows at top of graph). Coverage was also obtained for the endogenous elements in the region from approximately 1k to 10k that were not transferred into the DP23211 maize genome, and to the *pin*II terminator (*) and CaMV35S terminator (†) elements outside of the FRT sites due to alignment of reads derived from identical elements in the final insertion to all copies of these elements in PHP74643. **C)** SbS results aligned against the plasmid PHP56614 sequence (15,339 bp; **Figure 1**). Coverage was obtained for *zm*-SEQ9, *zm*-SEQ8, the elements found in the intended insertion (between *zm*-SEQ9 to FRT1 and between FRT87 to *zm*-SEQ8), and for the endogenous elements not in the intended insertion (the *ubi*ZM1 promoter, 5' UTR, and intron in the I-*Cre*I cassette), along with the *pin*II terminator elements (*) in PHP56614 due to alignment of reads derived from the *pin*II terminator in the *pmi* cassette of the intended insertion to the two copies of this element in PHP56614. **D)** SbS results aligned against the plasmid PHP21139 sequence (5,687 bp; **Figure 3**). Coverage was obtained only for the endogenous elements. **E)** SbS results aligned against the plasmid PHP31729 sequence (6,181 bp; **Figure 4**). Coverage was obtained for the endogenous elements and for a small segment of an *att* recombination site that matches an *att* site found in the intended insertion (‡). The absence of any junctions other than to the intended insertion indicates that there are no additional insertions or backbone sequence present in DP23211 maize.

Breeding Process

Please refer to **Figure 9.** Breeding Diagram for DP23211 Maize and Generations Used for Analysis for a schematic overview of the transformation and event development process for DP23211 maize. The subsequent breeding of DP23211 maize proceeded as indicated in **Figure 8**. Event Development Process of DP23211 Maize to produce specific generations for the characterisation and assessments conducted, as well as for the development of commercial lines.

c. Stability of Genetic Changes

Southern Analysis to Determine Stable Genetic Inheritance

Southern blot analysis was performed on five generations of DP23211 maize to evaluate the stability of the inserted DvSSJ1 fragment cassette and the *ipd072Aa*, *mo-pat*, and *pmi* gene cassettes across multiple generations [redacted]2019).

Restriction enzyme *Kpn* I (indicated in **Figures 15** and **16**) was selected to verify the stability of the DP23211 maize insertion across the five generations (T1, T2, T3, T4, and T5) of DP23211 maize plants. *Kpn* I was selected because there is a single *Kpn* I restriction site within the DP23211 maize insertion, which provides a means to uniquely identify the event, as additional sites would be in the adjacent flanking genomic DNA (**Figure 17**). Genomic DNA samples from the five generations of DP23211 maize and control maize plants were digested with *Kpn* I and hybridized with the *pmi, mo-pat* and *ipd072Aa* gene and DvSSJ1 fragment probes for Southern analysis. Hybridization patterns of these probes exhibited event-specific bands unique to the DP23211 maize insertion, and thus provided a means of verification that the genomic border regions of the DP23211 maize insertion were not changed across the five generations during breeding. Plasmid PHP74643 was added to control maize DNA, digested with *Kpn* I, and included on the blot to verify successful probe hybridization. The probes used for Southern hybridization are described in **Table 8** and shown in **Figure 16**.

Hybridization of the DvSSJ1 fragment and the *ipd072Aa* gene probes to *Kpn* I-digested genomic DNA resulted in a single band of approximately 21,000 bp in all five generations of DP23211 maize samples analyzed (**Table 9, Figures 18** and **19**, respectively). These results confirmed that the 3' border fragment, containing the DvSSJ1 fragment and *ipd072Aa* gene in the DP23211 maize insertion, is intact and stable across the five generations of DP23211 maize. The lanes containing plasmid DNA showed the expected band of 32,601 bp, confirming successful hybridization of the DvSSJ1 fragment and *ipd072Aa* gene probes.

Hybridization of the *mo-pat* and *pmi* probes to *Kpn* I-digested genomic DNA resulted in a consistent band of approximately 10,000 bp in all five generations of DP23211 maize (**Table 9, Figures 20** and **21**, respectively). These results confirmed that the 5' border fragment, containing the *mo-pat* and *pmi* genes in the DP23211 maize insertion, is intact and stable across the five generations of DP23211 maize. The lanes containing plasmid DNA showed the expected band of 6,794 bp, confirming successful hybridization of the *mo-pat* and *pmi* gene probes.

The presence of equivalent bands from hybridization with the DvSSJ1 fragment and *ipd072Aa*, *mo-pat*, and *pmi* gene probes within all five generations analyzed confirms that the inserted DNA in DP23211 maize is stable and equivalent across multiple generations during the breeding process.

Additional details regarding analytical methods for Southern analysis are provided in **Appendix B**.

Table 8. Description of DNA Probes Used for Southern Hybridization

Genetic Element/ Probe Name	Probe Length bp	Position on PHP74643 T-DNA (bp to bp)[a]
pmi gene[b]	569	13,964 to 14,532
	660	14,502 to 15,161
mo-pat gene	582	18,611 to 19,192
DvSSJ1 fragment	236	22,789 to 23,024
ipd072Aa gene	264	26,712 to 26,975

[a]: The probe position is based on the PHP74643 T-DNA map (Figure16).

[b]: This probe comprises two fragments that are combined in a single hybridization solution.

Table 9. Predicted and Observed Hybridization Bands on Southern Blots; Kpn I Digest

Probe Name	Predicted and Observed Fragment Size from Plasmid PHP74643 (bp)	Predicted Fragment Size from Intended Insertion Map of DP23211 Maize (bp)	Observed Fragment Size in DP23211 Maize[a] (bp)	Figure
DvSSJ1 fragment	32,601	>8,475	~21,000	Figure18
ipd072Aa gene	32,601	>8,475	~21,000	Figure19
mo-pat gene	6,794	>8,877	~10,000	Figure20
pmi gene	6,794	>8,877	~10,000	Figure21

[a]: Observed fragment sizes are approximated from the DIG-labeled DNA Molecular Weight Marker III and VII fragments on the Southern blots. Due to inability to determine the exact sizes on the blot, all approximated values are rounded to the nearest 100 bp.

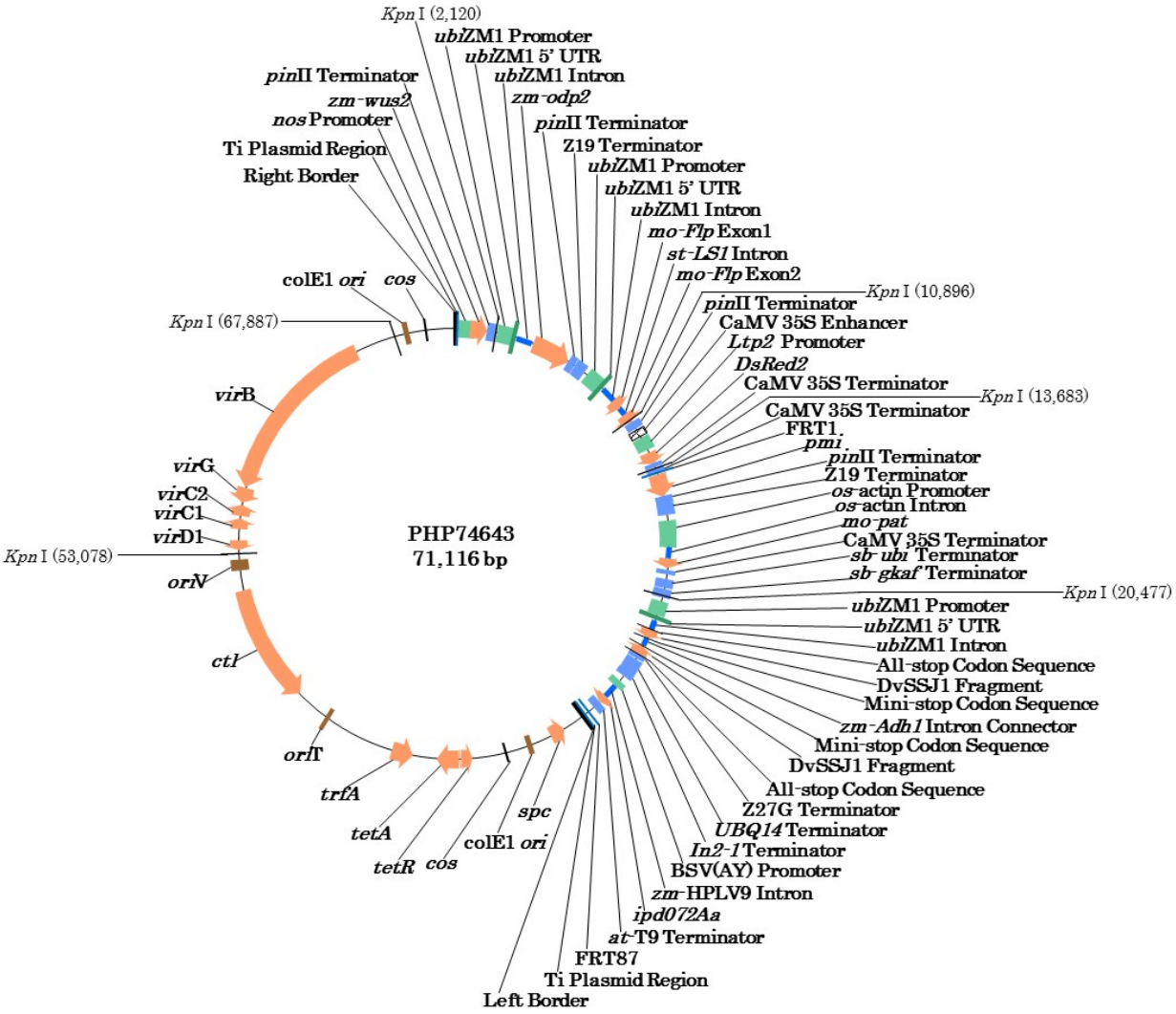

Figure 15. Map of Plasmid PHP74643 for Southern Analysis

Plasmid map of PHP74643 indicating *Kpn* I restriction enzyme sites with base pair positions. Right and Left Borders flank the T-DNA (**Figure 16**) that was transferred into the plant cell during transformation. The plasmid size is 71,116 bp.

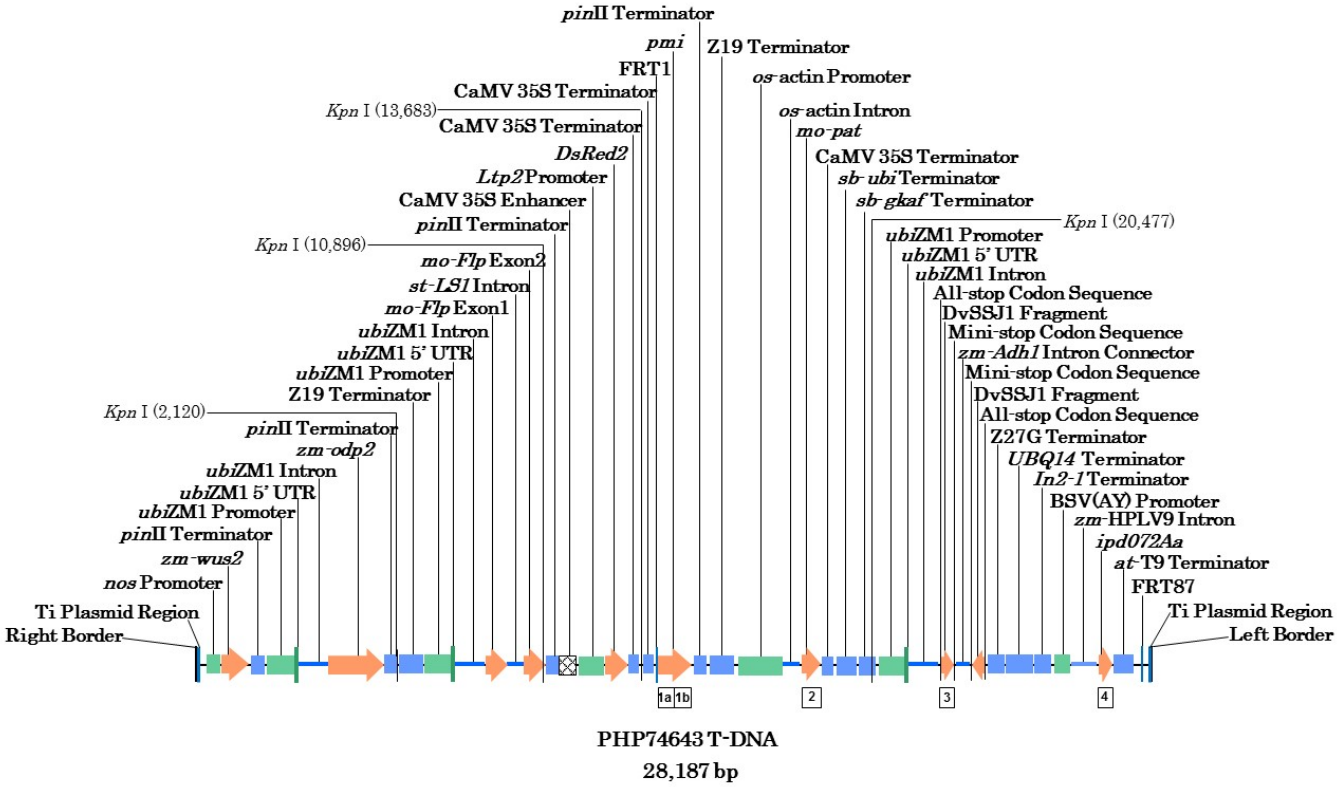

Number	Probe Name
1a and 1b	*pmi* gene
2	*mo-pat* gene
3	DvSSJ1 fragment
4	*ipd072Aa* gene

Figure 16. Map of PHP74643 T-DNA for Southern Analysis

Map of PHP74643 T-DNA indicating the *Kpn* I restriction enzyme sites, the *pmi*, *mo-pat*, and *ipd072Aa* gene cassettes and the DvSSJ1 fragment cassette located between the FRT1 and FRT87 sites and intended for insertion into the landing pad (**Figure 17**), and the *zm-wus2, zm-odp2, mo-Flp,* and *DsRed2* gene cassettes outside the FRT1 and FRT87 sites. The T-DNA region size is 28,187 bp. The portion of the T-DNA between the FRT1 and FRT87 sites is incorporated in the final DNA insertion (**Figure 17**). The locations of the Southern blot probes are shown by the boxes below the map.

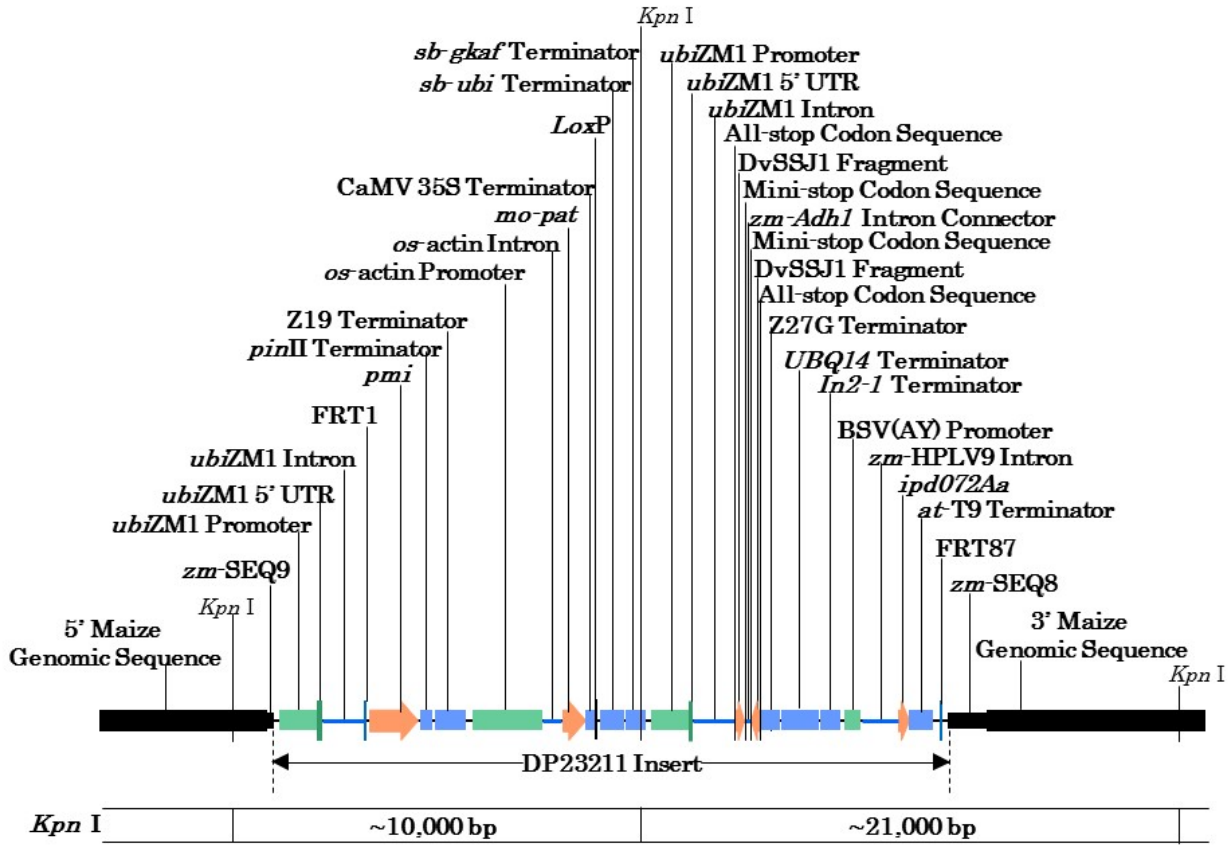

Figure 17. Map of Insertion in DP23211 Maize for Southern Analysis

Map of the final DNA insertion in the DP23211 maize genome following SSI integration of the gene cassettes from the PHP74643 T-DNA (**Figure 16).** The DP23211 maize DNA insertion comprises sequences from two sources: the parts of the landing pad outside the FRT1 and FRT87 sites and the sequences from the PHP74643 plasmid surrounded by the FRT1 and FRT87 sites (with *pmi*, *mo-pat*, and *ipd072Aa* gene cassettes and the DvSSJ1 fragment cassette). The flanking maize genomic DNA is represented by the horizontal black rectangular bars. *Kpn* I restriction sites are indicated with the sizes of observed fragments on Southern blots shown below the map in base pairs (bp). The locations of restriction enzyme sites in the flanking maize genomic DNA are not to scale.

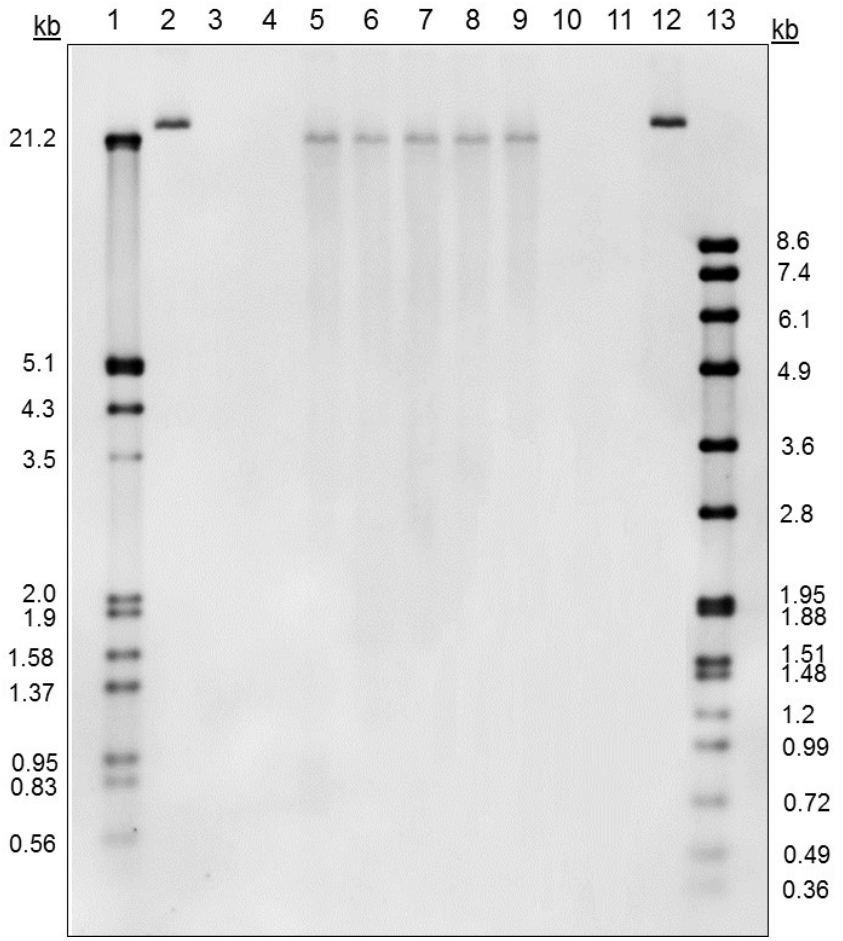

Lane	Sample
1	DIG-labeled DNA marker III
2	1 copy of PHP74643 + PHR03 control maize
3	PHR03 control maize
4	Blank
5	DP23211 maize T1 generation
6	DP23211 maize T2 generation
7	DP23211 maize T3 generation

Lane	Sample
8	DP23211 maize T4 generation
9	DP23211 maize T5 generation
10	Blank
11	PHR03 control maize
12	1 copy of PHP74643 + PHR03 control maize
13	DIG-labeled DNA marker VII

Figure 18. Southern Blot Analysis of DP23211 Maize; *Kpn* I Digest with DvSSJ1 Fragment Probe

Genomic DNA isolated from leaf tissues of DP23211 maize from T1, T2, T3, T4, and T5 generations, and PHR03 control maize plants, was digested with *Kpn* I and hybridized to the DvSSJ1 fragment probe. Approximately 10 µg of genomic DNA was digested and loaded per lane. Positive control lanes include PHP74643 plasmid DNA at approximately one gene copy number and 10 µg of control maize DNA. Sizes of the DIG-labeled DNA Molecular Weight Marker III and VII are indicated adjacent to the blot image in kilobases (kb).

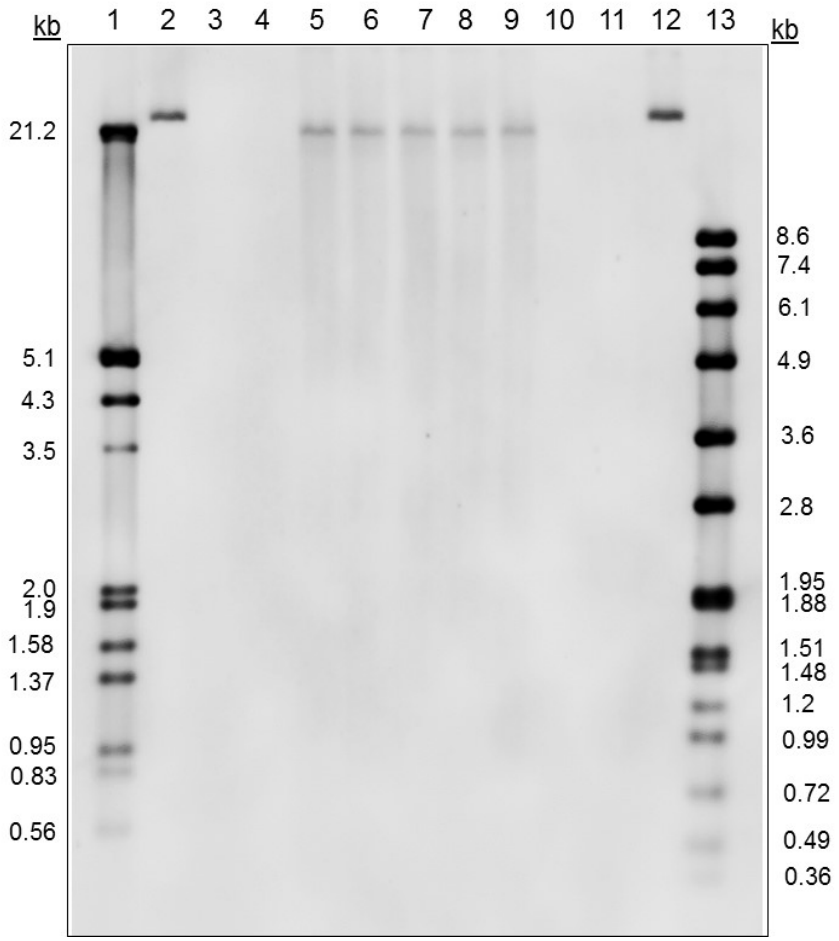

Lane	Sample
1	DIG-labeled DNA marker III
2	1 copy of PHP74643 + PHR03 control maize
3	PHR03 control maize
4	Blank
5	DP23211 maize T1 generation
6	DP23211 maize T2 generation
7	DP23211 maize T3 generation

Lane	Sample
8	DP23211 maize T4 generation
9	DP23211 maize T5 generation
10	Blank
11	PHR03 control maize
12	1 copy of PHP74643 + PHR03 control maize
13	DIG-labeled DNA marker VII

Figure 19. Southern Blot Analysis of DP23211 Maize; *Kpn* I Digest with *ipd072Aa* Gene Probe

Genomic DNA isolated from leaf tissues of DP23211 maize from T1, T2, T3, T4, and T5 generations, and PHR03 control maize plants, was digested with *Kpn* I and hybridized to the *ipd072Aa* gene probe. Approximately 10 µg of genomic DNA was digested and loaded per lane. Positive control lanes include PHP74643 plasmid DNA at approximately one gene copy number and 10 µg of control maize DNA. Sizes of the DIG-labeled DNA Molecular Weight Marker III and VII are indicated adjacent to the blot image in kilobases (kb).

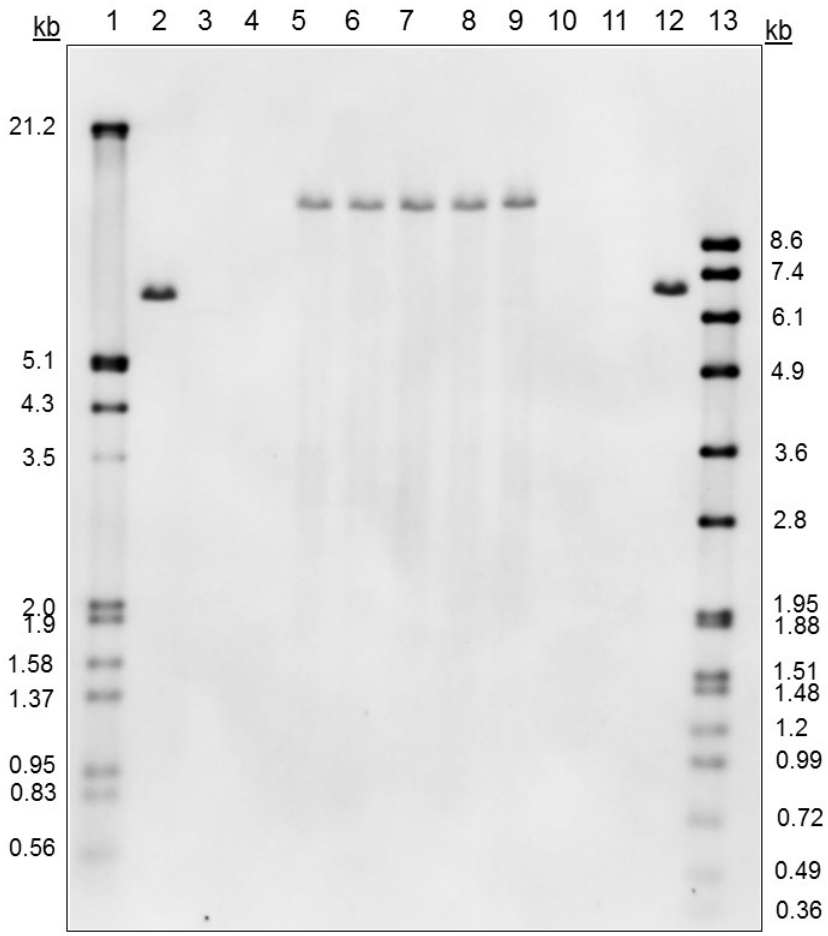

Lane	Sample
1	DIG-labeled DNA marker III
2	1 copy of PHP74643 + PHR03 control maize
3	PHR03 control maize
4	Blank
5	DP23211 maize T1 generation
6	DP23211 maize T2 generation
7	DP23211 maize T3 generation

Lane	Sample
8	DP23211 maize T4 generation
9	DP23211 maize T5 generation
10	Blank
11	PHR03 control maize
12	1 copy of PHP74643 + PHR03 control maize
13	DIG-labeled DNA marker VII

Figure 20. Southern Blot Analysis of DP23211 Maize; *Kpn* I Digest with *mo-pat* Gene Probe

Genomic DNA isolated from leaf tissues of DP23211 maize from T1, T2, T3, T4, and T5 generations, and PHR03 control maize plants, was digested with *Kpn* I and hybridized to the *mo-pat* gene probe. Approximately 10 µg of genomic DNA was digested and loaded per lane. Positive control lanes include PHP74643 plasmid DNA at approximately one gene copy number and 10 µg of control maize DNA. Sizes of the DIG-labeled DNA Molecular Weight Marker III and VII are indicated adjacent to the blot image in kilobases (kb).

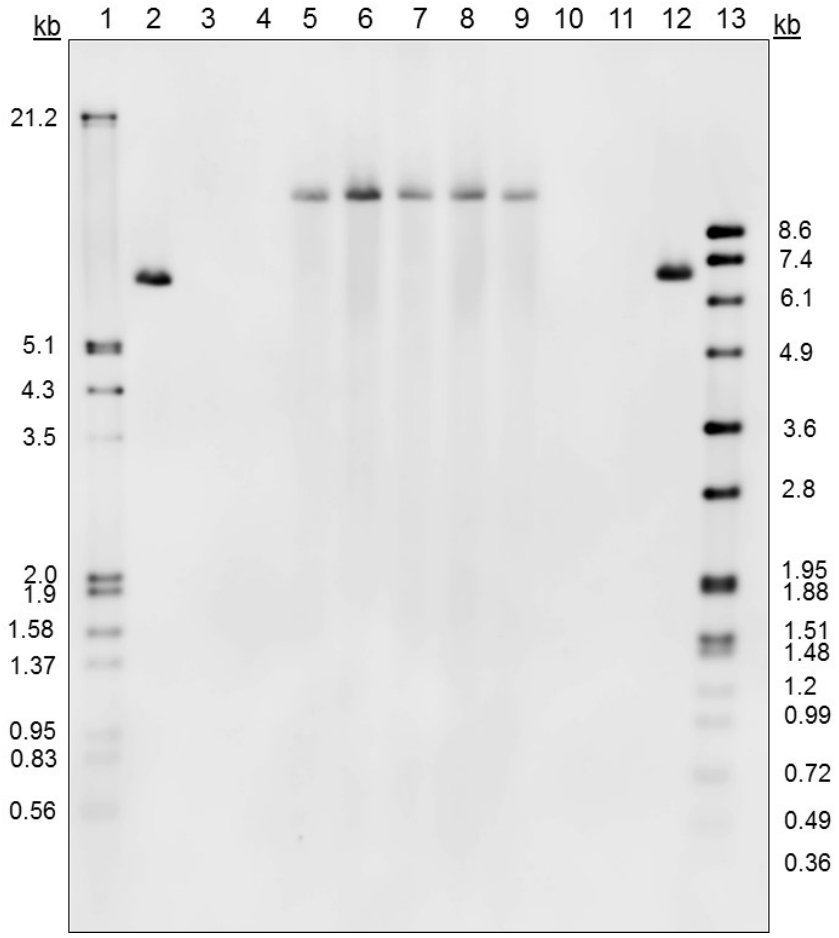

Lane	Sample
1	DIG-labeled DNA marker III
2	1 copy of PHP74643 + PHR03 control maize
3	PHR03 control maize
4	Blank
5	DP23211 maize T1 generation
6	DP23211 maize T2 generation
7	DP23211 maize T3 generation

Lane	Sample
8	DP23211 maize T4 generation
9	DP23211 maize T5 generation
10	Blank
11	PHR03 control maize
12	1 copy of PHP74643 + PHR03 control maize
13	DIG-labeled DNA marker VII

Figure 21. Southern Blot Analysis of DP23211 Maize; *Kpn* I Digest with *pmi* Gene Probe

Genomic DNA isolated from leaf tissues of DP23211 maize from T1, T2, T3, T4, and T5 generations, and PHR03 control maize plants, was digested with *Kpn* I and hybridized to the *pmi* gene probe. Approximately 10 µg of genomic DNA was digested and loaded per lane. Positive control lanes include PHP74643 plasmid DNA at approximately one gene copy number and 10 µg of control maize DNA. Sizes of the DIG-labeled DNA Molecular Weight Marker III and VII are indicated adjacent to the blot image in kilobases (kb).

Multi-Generation Segregation Analysis

Segregation analysis was performed on five generations of DP23211 maize to confirm the Mendelian inheritance pattern of the inserted DNA during the breeding process [redacted] 2018). The observed inheritance pattern predicts the segregation of these genes and/or traits as a single unit and as a single genetic locus throughout the commercial breeding process. A total of 100 maize plants from each generation of DP23211 maize (BC1F1 generation in genetic backgrounds PH1V5T and PH2SRH, and the BC2F1, T1, and T5 generations) were analyzed using genotypic and phenotypic analyses. The selected maize generations represent a range of different crossing, backcrossing, and selfing points in a typical maize breeding program.

The genotypic analyses utilized a quantitative polymerase chain reaction (qPCR) assay to confirm the presence or absence of the DP23211 insertion, DvSSJ1 fragments, and the *ipd072Aa*, *mo-pat,* and *pmi* genes in DP23211 maize leaf samples. In addition, endpoint PCR analysis was conducted to confirm the presence or absence of the following genetic elements or genetic element junctions from plasmid PHP74643: *STOPS2-UBI1, AT-T9-STOPS3, ATTB2-S2-BSV*. The phenotypic analysis utilized a visual herbicide injury evaluation to confirm the presence or absence of tolerance to glufosinate-ammonium for each individual plant. The individual results for each plant were compared to the qPCR results to verify co-segregation of genotype with phenotype.

A chi-square statistical test (at the 0.05 significance level) was conducted for the qPCR results of the segregating generations of DP23211 maize to compare the observed segregation ratios to the expected segregation ratios of 1:1 for the T1, BC1F1 and BC2F1 generations. A chi-square test was not performed for the T5 generation of DP23211 maize as all plants were identified as positive (i.e., not segregating) as expected for a homozygous generation.

A summary of segregation results for DP23211 maize is provided in **Table 10**. For each individual plant, all genotypic results (i.e., PCR results) matched the corresponding phenotypic result (i.e., herbicide tolerance result). No statistically significant differences were found between the observed and expected segregation ratios for each of the four segregating generations of DP23211 maize.

The results of the multi-generation segregation analysis demonstrated that the inserted DNA in DP23211 maize segregated together and in accordance with Mendelian rules of inheritance for a single genetic locus, indicating stable integration of the insert into the maize genome and a stable genetic inheritance pattern across breeding generations.

Additional details regarding analytical methods for the multi-generation segregation analysis are provided in **Appendix C**.

Table 10. Summary of Genotypic and Phenotypic Segregation Results for Five Generations of DP23211 Maize

Generation	Expected Segregation Ratio	Observed Segregation[a]			Statistical Analysis	
	(Positive:Negative)	Positive	Negative	Total	Chi-Square[b]	P-Value
BC1F1 (in genetic background PH1V5T)	1:1	46	54	100	0.64	0.4237
BC1F1 (in genetic background PH2SRH)	1:1	50	50	100	0.00	1.0000
BC2F1	1:1	50	50	100	0.00	1.0000
T1	1:1	52	48	100	0.16	0.6892
T5	Homozygous	100	0	100	--	--

[a] Genotypic analyses were conducted for each plant to confirm the presence or absence of event DP-Ø23211-2, DvSSJ1 fragments, *ipd072Aa* gene, *mo-pat* gene, and *pmi* gene, as well as the presence or absence of the following genetic elements or genetic element junctions from plasmid PHP74643: *STOPS2-UBI1, AT-T9-STOPS3, ATTB2-S2-BSV*. Phenotypic analysis was conducted for each plant to confirm the presence or absence of a glufosinate-tolerant phenotype. All genotypic results matched the corresponding phenotypic result for each plant analyzed.

[b] Degrees of freedom = 1. A Chi-Square value greater than 3.84 (P-value less than 0.05) would indicate a significant difference.

Nucleotide Sequencing of the Introduced DNA and Genomic Flanking Regions - Please refer to Attachment 2, Confidential Commercial Information.

Open Reading Frame Analysis of the Insert/Border Junctions

Assessing potentially-expressed peptides within an insertion or crossing the boundary between an insertion and its genomic borders for similarity to known and putative allergens and toxins is a critical part of the weight-of-evidence approach used to evaluate the safety of genetically-modified plant products (Codex Alimentarius Commission, 2003). Here, a bioinformatics assessment of potentially-expressed peptides (*i.e.*, translations of open reading frames [ORFs]) was conducted following established international criteria (Codex Alimentarius Commission, 2003; FAO/WHO, 2001a). All potentially-expressed peptides of length ≥ 30 amino acids that are within the DP23211 insertion or that cross the boundary between the insertion and its genomic borders were identified and evaluated [redacted] 2019b). From this study ([redacted] 2019b), the following observations and conclusions were made:

- Seventy-six potentially-expressed peptides were identified.
- E-value thresholds for the searches against the allergen and toxin databases were set to 10e-4
- No alignments were returned between a potentially-expressed peptide and any protein sequence in the COMPARE allergen database.
- Frame DP23211_9, corresponding to the intended protein PMI, produced an eight-contiguous amino acid match to an allergen in the COMPARE allergen database. Comprehensive analysis of this match demonstrates that no risk of allergenic cross-reactivity exists.
- No alignments were returned between a potentially-expressed peptide and any protein sequence in the internal toxin database. Therefore, no toxicity concerns arose from the bioinformatics assessment of the potentially-expressed peptides.

Collectively, these data indicate that there is no allergenicity or toxicity concern regarding the potentially expressed peptides in DP23211 maize.

Safety evaluations of PMI protein have been previously disclosed by the developer (Syngenta Biotechnology, Inc.) (FSANZ Application 1001). Using the same bioinformatic parameters, an updated *in silico* analysis was conducted on the PMI amino acid sequence to search for any similarity with known allergens. A full-length sequence search using FASTA identified no significant sequence alignments with known or putative allergens. A search for exact matches of eight of more contiguous amino acid residues revealed a single match with α-parvalbumin from frog

(*Rana* species CH-2001). This match was also reported in previous assessments. To investigate this match in greater detail, immunological testing was undertaken using serum IgE antibody screening. Serum from a single individual with demonstrated IgE-mediated allergy to this specific α-parvalbumin from *Rana* species, did not react with any portion of PMI. Based on the updated bioinformatic analysis, there is no indication that PMI shares structural similarity with known or putative protein allergens that would raise concerns about potential allergenicity.

These data indicate that it is unlikely that any of the identified translated ORFs at the DP23211 maize insertion site result in allergenicity concerns. None of the putative ORFs at the DP23211 maize insertion site returned alignments from the search against an internal toxin database, indicating that it is unlikely that any of the putative ORFs at the DP23211 maize insertion site result in human or animal toxicity.

Event-Specific Detection Methodology - Please refer to **Attachment 2**, Confidential Commercial Information.

The event-specific quantitative real-time PCR method for DP23211 maize was developed and validated to measure the relative content of DP23211 maize to total maize DNA utilizing standard curves for both the taxon-specific High Mobility Group (HMG) and DP23211 maize assays [redacted] 2019). The relative content of the DP23211 maize was determined using the ratio between the mean copy number of the DP23211 maize insertion event compared to the haploid maize genome. The testing results of the event-specific quantitative real-time PCR method for DP23211 maize demonstrates that this method fulfils the internationally accepted minimum performance requirements for analytical methods of GMO testing.

Conclusions on the Molecular Characterisation of DP23211 Maize

SbS, Southern blot, multi-generation segregation, and translated ORFs bioinformatics analyses were conducted to characterize the DNA insertion in DP23211 maize.

SbS analysis confirmed that DP23211 maize contains a single, intact copy of the intended insertion, and that the intactness of the insertion was maintained. SbS analysis results also showed no additional insertions or plasmid backbone sequences were inserted into DP23211 maize. Southern blot analysis of five generations of DP23211 maize confirmed that the inserted DNA in DP23211 maize is stable and equivalent across multiple generations during the breeding process.

Segregation analysis confirmed that the inserted DNA segregated as a single locus according to Mendelian rules of inheritance across five generations of DP23211 maize, and the stability of the insertion and of the herbicide tolerance phenotype was demonstrated in these populations. Bioinformatic analyses support the conclusion that there are no allergenicity or toxicity concerns regarding the putative translated ORFs at the DP23211 insertion site.

Sanger sequencing analyses determined the inserted DNA sequences that produce the intended insertion and the flanking genomic border regions in DP23211 maize. The total length of sequence determined in DP23211 maize is 19,865 base pairs (bp), comprised of 1,488 bp of the 5' flanking genomic border sequence, 2,201 bp of the 3' flanking genomic border sequence, and 16,176 base pairs (bp) of inserted DNA (consisting, from the 5' end to the 3' end, of 2,201 bp from plasmid PHP56614, 13,828 bp from plasmid PHP74643, and another 147 bp from plasmid PHP56614).

Together, these analyses confirmed a single, intact, copy of the intended insertion, with no plasmid backbone sequences or other unintended sequences, is present in the DP23211 maize genome, and that it is unlikely that the putative ORFs at the DP23211 maize insertion site result in allergenicity or toxicity concerns.

B. Characterisation and safety assessment of the new substance

B.1 Characterisation and safety assessment of new substances

DvSSJ1 dsRNA

Plants engineered to contain novel RNAi technology have been evaluated using the same global regulatory framework as other genetically modified plants, most commonly those that express novel transgenic protein(s). The regulatory framework was developed based on recommendations and guidelines from scientific and regulatory authorities (Chassy et al., 2004; Codex Alimentarius Commission, 2008; EFSA, 2011; FAO/WHO, 1996; FAO/WHO, 2000; FAO/WHO, 2001b; Jonas et al., 1996; OECD, 1993; US-FDA, 1992; WHO, 1995). Safety assessment of GM plants is designed to evaluate the impact of intended effects of the genetic modification, as well as the impact of unintended effects that may result from the transformation process or the activity of the introduced trait. This assessment is comparative in nature, relies principally on the comparison of response variables in the GM crop with those of a conventional, non-GM counterpart with a history of safe use, and typically includes a compositional assessment and molecular characterisation. A tiered approach is applied for safety assessment of expressed trait products, which includes evaluations of history of safe use, mode of action and specificity, bioinformatics analyses, expression and intake assessments, and other measures of the potential for systemic exposure. In cases where specific hazards are identified that cannot otherwise be mitigated, specific toxicology studies may be conducted to inform the safety assessment. Application of the comparative assessment paradigm for evaluation of novel GM plants has proven effective over time, as commercialized GM crops have a well-established history of safe use and have not been associated with adverse effects in humans or animals based on their consumption as food and feed (Delaney et al., 2018; Flachowsky and Reuter, 2017; Sánchez and Parrott, 2017; Van Eenennaam and Young, 2014).

Recent investigations have considered the applicability of the current safety assessment framework to the evaluation of plants containing one or more dsRNA traits. The conclusions of regulatory authorities, academic scientists and industry professionals support that the existing regulatory framework as appropriate for plants containing RNAi technology, except that bioinformatics assessments for similarity to protein toxins or known allergens are not relevant due to the absence of novel protein expression (FSANZ, 2013; Parrott et al., 2010; Petrick et al., 2013; Sherman et al., 2015). Therefore, this historically-accepted and robust approach was applied to the safety assessment of DvSSJ1 dsRNA expressed in DP23211 maize [redacted], 2019)

History of Safe Consumption of RNA

The ubiquity and conservation of nucleic acids in the molecular biology of virtually all living organisms ensures that nearly every bite of food consumed by humans and animals contains RNA and DNA. Nucleic acids have always been present in human and animal food and feed, and their consumption has not been associated with adverse health effects (FSANZ, 2013; US-EPA, 2001; US-FDA, 1992). RNA-mediated gene silencing (e.g. RNAi) is similarly conserved across eukaryotic species, including plants, fungi and animals (Pickford and Cogoni, 2003). Reports of the detection of endogenous RNAi in plants and animals, including those used as food and feed, are plentiful in the peer-reviewed literature (Ambros, 2004; Della Vedova *et al.*, 2005; Frizzi and Huang, 2010; Hou *et al.*, 2017; Kusaba, 2004; Senda *et al.*, 2012; Tuteja *et al.*, 2004; Wagner *et al.*, 2015). These reports demonstrate a history of safe consumption of dsRNA in food and feed. Some investigators have identified RNA sequences, including long dsRNA in commonly consumed plants (Ivashuta et al., 2009; Jensen et al., 2013) and animals (Dever et al., 2015)

with sequence complementarity to human and other animal genes, and without evidence of biologic activity or adverse effects, further supporting their history of safe consumption.

Knowledge and experience with the specificity and selectivity of RNAi has increased its utility in the development of agricultural biotechnology, with applications for insect control (Baum et al., 2007; Baum and Roberts, 2014), viral and fungal pathogen resistance (McLoughlin et al., 2018; Pence et al., 2016), nutritional alterations (Buhr et al., 2002; Stoutjesdijk et al., 2002; Tran et al., 2017), and alterations to improve processing and shelf-life stability or delay ripening (Krieger et al., 2008; Sheehy et al., 1988; Waltz, 2015). According to the International Service for the Acquisition of Agri-Biotech Applications, RNAi-based events have been approved in many jurisdictions for food, feed, or cultivation in multiple crops including: alfalfa, apple, bean, maize, papaya, potato, plum, soybean, squash, and tomato (ISAAA, 2019).

DvSSJ1 dsRNA Mode of Action and Molecular Target

The safety assessment of DvSSJ1 dsRNA begins with an understanding of its functional activity and molecular target as the DvSSJ1 dsRNA is sequence-specific to a portion of the smooth septate junction protein 1 (*dvssj1*) gene from WCR (*Diabrotica virgifera virgifera)*. Smooth septate junctions are occluding junctions comprising a network of proteins that physically connect adjacent cells. These junctions are found in insect midgut epithelial cells and are unique to arthropods, and have identified roles in intestinal barrier function and paracellular transport in the renal system (Furuse and Izumi, 2017; Hu et al., 2016). The *dvssj1* gene identified in WCR is an ortholog of the snakeskin (*ssk*) gene, originally identified in the *Drosophila* midgut, and its protein product is a critical component of the SSJ protein complex (Hu et al., 2016; Yanagihashi et al., 2012). Relative *dvssj1* mRNA expression is highest in WCR neonates, and *dvssj1* mRNA and protein localize to the midgut. When ingested by the WCR, plant-derived DvSSJ1 dsRNA is processed into 21 nucleotide (21-nt) small interfering RNAs (siRNAs) which downregulates *dvssj1* mRNA and decreases translation of DvSSJ1 protein. Loss of DvSSJ1 protein in the WCR midgut disrupts the SSJ protein complex, leading to loss of barrier integrity, growth inhibition and larval mortality (Hu et al., 2019).

DvSSJ1 dsRNA Spectrum of Activity and Species Specificity

The spectrum of activity of the DvSSJ1 dsRNA was assessed in feeding bioassays with ten species from four families of Coleoptera (Chrysomelidae, Tenebrionidae, Coccinellidae, and Staphylinidae), and four species from four families of Lepidoptera (Crambidae, Tortricidae, Nymphalidae, and Noctuidae) (Boeckman, 2019, in preparation). An *in silico* comparative bioinformatics approach was used to assess how conserved the *ssj1* gene sequence is across different organisms with varied evolutionary distance from WCR. The sequence of the *ssj1* homologs of twenty species, representing four families within the order Coleoptera, four families within the order Lepidoptera, and two additional non-target organisms were compared to a 210-base pair (210-bp) sequence from the *dvssj1* gene (referred to as 210-bp *dvssj1* sequence) to determine the percent similarity, number of single nucleotide polymorphisms (SNPs), and the number of 21-nt matches (Boeckman, 2019, in preparation; [redacted] 2019).

Western corn rootworm was the most sensitive species tested in the feeding bioassay, with a median LC_{50} of 36 ppb. Of the other species evaluated, only southern corn rootworm (SCR; *Diabrotica undecimpunctata*) was observed to have decreased survival at a dietary concentration of 100 ppb. There were no adverse effects observed with any other coleopteran and lepidopteran species tested at concentrations up to 1 ppm, which represented dietary concentrations approximately 28-fold higher than the median LC_{50} for WCR under normal

conditions in the agroecosystem under normal conditions in the agroecosystem (Boeckman, 2019, in preparation). The results of the feeding bioassays were consistent with the results of the *in-silico* analyses. The closest genomic sequence match (percent identity to the 210-bp *dvssj1* sequence) was the *ssj1* homologous gene from WCR, which as intended had a 100% sequence match, 0 SNPs, and 190 21-nt matches. The *ssj1* homologous gene from the closely related species, northern corn rootworm (NCR; *Diabrotica barberi*), shared 97.1% identity with the 210-bp *dvssj1* sequence, with 6 SNPs and 135 21-nt matches. The *ssj1* homologous gene from SCR shared 92.9% identity with the 210-bp *dvssj1* sequence, with 15 SNPs and 79 21-nt matches. The *ssj1* homologous genes from all of the non-*Diabrotica* species analyzed had lower percent identity (60-78%) with the 210-bp *dvssj1* sequence, a higher number of SNPs (47-84), and zero 21-nt matches [redacted] 2019).

An additional *in silico* approach was used to evaluate the species-specificity of DvSSJ1 dsRNA and investigate the potential for off-target effects in humans, livestock, and companion animals. The DvSSJ1 dsRNA sense and anti-sense fragment sequences were parsed into all possible sequentially-overlapping 21-nt siRNA subsequences, and each resultant sequence was compared to similarly-parsed sequentially-overlapping 21-nt sequences from the transcriptomes of humans, chickens, pigs, cattle, sheep, goats, turkeys, salmon, dogs and cats. These analyses did not yield any exact 21-nt matches between the sense or anti-sense DvSSJ1 dsRNA fragment sequences and any human or animal transcript, and did not indicate a potential for off-target effects ([redacted] 2018; [redacted] 2019a).

Mammalian Barriers to Exposure to DvSSJ1 dsRNA Consumed in Food and Feed

The physical, chemical, enzymatic and molecular barriers to exposure and activity of dietary dsRNAs ingested by humans and other mammals have been well-described in the context of agricultural biotechnology and the safety assessment of crops containing RNAi technology (FSANZ, 2013; Sherman et al., 2015; US-EPA, 2016). In the absence of identified and well-characterized mammalian transporters, the gut epithelium and vascular endothelium form a physical barrier to the uptake of hydrophilic macromolecules like dsRNAs and siRNAs. The low pH in the stomach and nucleases present in saliva and the lumen of the GI tract degrade free RNAs, thus reducing the potential for systemic exposure. Any dsRNA that could potentially cross the gut lumen and enter the systemic circulation would encounter additional nucleases in blood, resulting in further degradation, and would likely be rapidly cleared via glomerular filtration in the kidneys. Further, for any small amount of dsRNA (such as DvSSJ1 dsRNA) that could potentially persist in systemic circulation to exert a biological effect, it would need to cross additional hydrophobic cellular membranes to penetrate cells of tissue parenchyma, escape endosomal capture and lysosomal degradation, accumulate in cytosol at sufficient cellular concentrations to impact gene regulation, and have a molecular target with which to interact (Sherman et al., 2015).

The function of these well-defined barriers is exemplified by published information resulting from pharmaceutical industry efforts to improve systemic exposure to oligonucleotide-based therapeutics via the oral route (Forbes and Peppas, 2012; Lorenzer et al., 2015; O'Neill et al., 2011). Current efforts to increase stability and target-site trafficking of oligonucleotide-based biotherapeutics include: chemical modifications (Geary et al., 2015; Shukla et al., 2010); macromolecular complexes, carriers, and conjugates (Loretz et al., 2006; Moroz et al., 2016a); encapsulation (Moroz et al., 2016b); association with functional nanoparticles (Liu et al., 2019; Rabanel et al., 2012); and the use of permeability enhancers (Sánchez-Navarro et al., 2016), often in combination. In consideration of potential oral exposure to dsRNA, it was recently demonstrated that repeated oral administration of dsRNA, or a pool of 21-nt siRNAs, specifically targeted to the murine ortholog of the vacuolar ATPase (*vATPase*) did not result in toxicologically-relevant or adverse effects in mice at high dose levels of 64 mg/kg BW/day (dsRNA) and 48 mg/kg BW/day (siRNA pool) (Petrick et al., 2015). Additionally, gene expression analysis did not reveal evidence of vATPase gene suppression in tissues from the gastrointestinal tract, liver, kidneys, brain or bone.

These described barriers to exposure and activity of ingested dsRNAs are anticipated to prevent or significantly reduce human and animal exposure to DvSSJ1 dsRNA from consumption of foods or feed containing DP23211 maize.

Potential for Systemic Exposure to Ingested DvSSJ1 dsRNA in Vertebrates

The presence of dsRNA in conventional crops and vegetables commonly consumed in food and feed has been described (Jensen et al., 2013). The DvSSJ1 dsRNA expressed in DP23211 maize is not anticipated to behave differently when ingested by humans or other animals. However, the potential for transfer and activity of ingested dsRNA or other small RNAs to humans and animals from food and feed has resulted in several published reports describing the detection of exogenous sequences in various body fluids (Chen et al., 2016; Han and Luan, 2015; Link et al., 2019). Some investigators have also reported functional impacts on gene expression (Baier et al., 2014; Mlotshwa et al., 2015; Wang et al., 2017) occasionally associated with differences in health-based outcomes in animal models (Zhang et al., 2012). Other investigators have reported contradictory results that do not support significant dietary exposure to small RNAs from food or feed (Micó et al., 2016; Snow et al., 2013; Witwer et al., 2013). In some cases, data purporting to demonstrate cross-kingdom transfer and functional activity of small RNAs were not reproducible (Auerbach et al., 2016; Dickinson et al., 2013). Several reports of cross-kingdom transfer and biologic activity were recently reviewed during a United States Environmental Protection Agency (EPA) Scientific Advisory Panel (SAP) evaluating scientific issues impacting the human health and ecological risk assessments of plant-incorporated pesticide products containing RNAi technology (US-EPA, 2016). The panel concluded that the studies describing cross-kingdom transfer contained a number of experimental insufficiencies including: lack of appropriate controls, absence of sufficient data to support health-based conclusions, extrapolation of low-abundance targets detected *in vivo* to experimental effects of high-concentration exposures observed *in vitro* (Witwer and Halushka, 2016), and failure to consider stoichiometric estimates of target abundance and strength of siRNA-target interactions in the facilitation of canonical regulatory functions (Snow et al., 2013). Additionally, the panel noted that improvements in analytical methods are required to address identified concerns with sensitivity and specificity related to the potential for environmental contamination or the presence of artifacts in biological samples (Lusk, 2014; Witwer, 2015; Witwer and Halushka, 2016). Questions about the validation of analytical methods (sensitivity, specificity and reproducibility) for reliable detection and quantification of small RNAs continue to challenge investigators, and have been highlighted as a significant hurdle which must be overcome (Chan and Snow, 2017; Kang et al., 2017; Witwer and Halushka, 2016; Witwer and Zhang, 2017). Despite these methodologic and analytical challenges, and irrespective of the previously described arthropod-specific nature of the gene target and specificity of activity limited to the *Diabrotica* species within the Chrysomelidae family, the potential for systemic exposure of humans and animals to DvSSJ1 dsRNA from ingestion of foods and feed containing DP23211 maize cannot be definitively excluded; therefore, an assessment of human dietary exposure was conducted.

Human Dietary Exposure Assessment of DvSSJ1 dsRNA in DP23211 Maize

A dietary exposure assessment was conducted for DvSSJ1 dsRNA in DP202216 maize using the Dietary Exposure Evaluation Model – Food Commodity Intake Database (DEEM™ - FCID), Version 4.02 (DEEM/FCID, 2018) and mean concentrations of DvSSJ1 dsRNA in DP23211 maize grain (0.00413mg/kg) [redacted] 2019). While the consumption and recipe data that form the basis of the DEEM™ - FCID model are derived from a U.S. survey, the data are applicable to other populations with similar dietary consumption patterns such as New Zealand

(WHO-GEMS, 2019) and includes estimates for a wide range of subpopulations. Specifically, WHO-GEMS took data from 179 countries and clustered them into 17 diets based on statistical similarities between dietary patterns. The US and New Zealand are in the same country cluster (G10) which has higher estimated daily intakes of maize than country cluster (G07) which contains Australia (DEEM/FCID, 2018; WHO-GEMS, 2019). Maize consumption is defined as maize, raw (including glucose & dextrose & isoglucose; flour; oil; beer; germ; and starch - GC 0645).

Conservative total replacement scenarios were utilized for both acute and chronic exposures, assuming that maize in each foodstuff was derived from DP23211 maize grain. It was assumed that no degradation of dsRNA occurred during processing or cooking of corn flour, corn-flour-baby food, corn meal, corn meal-baby food and corn bran foodstuff categories. The estimated mean annual consumption of DvSSJ1 dsRNA varied from <1 to 2 ng/kg BW/day for all population subgroups, with the highest consumption of 2 ng/kg BW/day estimated for 'Hispanics' and children from 1 to 12 years of age. The range of estimated intakes for 95th percentile consumption of DvSSJ1 dsRNA was 4 to 12 ng/kg BW/day, with the highest estimate of 12 ng/kg BW/day calculated for children 1 to 5 years of age.

To put these estimates into appropriate context, it is important to reconsider their reliance on the assumption that all DvSSJ1 dsRNA remains intact and is systemically available following ingestion, an unlikely scenario based on the previously described barriers to exposure. As a component of current research regarding cross-kingdom transfer of small RNAs, several investigators have concluded it is highly unlikely that diet-derived small RNAs would accumulate in cells with sufficient copy numbers or at molar concentrations sufficient to impact canonical gene expression (Chan and Snow, 2017; Kang et al., 2017; Sherman et al., 2015; Snow et al., 2013; US-EPA, 2016; Witwer et al., 2013). This methodology can be adapted to evaluation of DvSSJ1 dsRNA using the conservative assumptions presented in Sherman et al. (2015) that a minimum 100 copies/cell are required for canonical target gene suppression, and that there are 10^{13} cells in the average human body. Considering a 70-kg human, the highest estimate of potential intake of DvSSJ1 dsRNA is 840 ng/day (12 ng DvSSJ1 dsRNA/kg BW/day x 70 kg BW) and equivalent to approximately $1.9x10^{12}$ molecules of DvSSJ1 dsRNA [840 ng DvSSJ1 dsRNA/day x 266 kDa (g/mol) DvSSJ1dsRNA x $6.022x10^{23}$ molecules/mol DvSSJ1 dsRNA], which represents less than one copy/cell ($1.9x10^{12}$ molecules DvSSJ1 dsRNA / $1x10^{13}$ cells/human).

These exposure estimates can also be considered within the framework of the Threshold of Toxicological Concern (TTC), a valid method used to assess substances of unknown toxicity found in food (Kroes et al., 2005). Under this framework, the conservative DvSSJ1 dsRNA exposure estimates for humans and all animal species are orders of magnitude below the value of 1.5 µg/kg BW/day. This value represents the TTC intake level below which substances with chemical structures that do not permit an assumption of safety, or that may suggest significant toxicity or reactivity (Cramer Class III) are not anticipated to result in increased risk of adverse effects over a lifetime of exposure from consumption in food (EFSA Scientific Committee et al., 2019).

Conclusions on the Safety of DvSSJ1 dsRNA in DP23211 Maize

The overall weight of evidence supports the conclusion that consumption of DvSSJ1 dsRNA by humans and animals in foods and feeds containing DP23211 maize is not expected to result in negative health effects in humans and animals. Nucleic acids, including dsRNA, are normal components of human and animal diets, and have a history of safe consumption in food and feed. The molecular target of DvSSJ1 dsRNA is arthropod-specific, has not been described in vertebrates, and has been shown to be specific to the *Diabrotica* species within the Chrysomelidae family of Coleoptera. Additionally, bioinformatic sequence comparisons of DvSSJ1 dsRNA 21-nt siRNAs to mammalian, avian and fish transcriptomes indicate no 21-nt siRNA exact matches. Conservative estimates

demonstrate low potential exposures to DvSSJ1 dsRNA for humans in food and animals in feed that are unlikely to result in cellular concentrations that could impact gene regulation, if a molecular target existed. Further, the well-characterized physical, enzymatic, biochemical and molecular barriers to exposure of ingested small RNAs will further reduce potential exposure to DvSSJ1 dsRNA consumed in food and feed from DP23211 maize. Collectively, the information presented herein indicates that consumption of DvSSJ1 dsRNA in food or feed containing DP23211 maize is not expected to present a hazard to human or animal health, therefore supporting the overall safety assessment of DP23211 maize.

Please refer to section B.2 below for the safety assessment of IPD072Aa, PAT and PMI protein.

B.2 New Proteins

a. IPD072Aa Protein

Amino Acid Sequence

The deduced amino acid sequence from the translation of the *ipd072Aa* gene is 86 amino acids in length and has a molecular weight of approximately 10 kDa **(Figure 22; [redacted] 2018)**.

1 MGITVTNNSS NPIEVAINHW GSDGDTSFFS VGNGKQETWD RSDSRGFVLS

51 LKKNGAQHPY YVQASSKIEV DNNAVKDQGR LIEPLS*

Figure 22. Deduced Amino Acid Sequence of the IPD072Aa Protein
The deduced amino acid sequence from the translation of the *ipd072Aa* gene from plasmid PHP74643. The asterisk (*) indicates the translational stop codon. The full-length protein is 86 amino acids in length and has a molecular weight of approximately 10 kDa.

Function and Activity of the IPD072Aa Protein

The IPD072Aa protein, encoded by the *ipd072Aa* gene, confers control of certain coleopteran pests when expressed in plants by causing disruption of the midgut epithelium. The *ipd072Aa* gene was identified and cloned from a *Pseudomonas chlororaphis* strain that was cultured from a soil sample (Schellenberger et al., 2016).

Equivalence of IPD072Aa Protein Derived from DP23211 Maize and Microbial Systems

The IPD072Aa protein was partially purified from DP23211 maize whole plant tissue using ammonium sulfate precipitation and immuno-affinity chromatography.

In order to have sufficient amounts of purified IPD072Aa protein for the multiple studies required to assess its safety, IPD072Aa protein was expressed in an *Escherichia coli* protein expression system as a fusion protein with an N-terminal histidine tag. The microbially derived protein was purified using nickel affinity chromatography, and the histidine tag was cleaved with immobilized trypsin and then removed using nickel affinity chromatography (Carlson *et al.*, 2019).

The equivalence in biochemical characteristics between the microbially derived IPD072Aa protein and the DP23211 maize-expressed IPD072Aa protein was characterized using sodium dodecyl sulfate polyacrylamide gel electrophoresis (SDS-PAGE) analysis, western blot analysis, peptide mapping by mass spectrometry, N-terminal amino acid sequencing, and glycoprotein analysis. The results demonstrated that the IPD072Aa protein derived from DP23211 maize is of the expected molecular weight, immunoreactivity, amino acid sequence, and showed a lack of glycosylation [redacted] 2019a). The microbially derived IPD072Aa protein was demonstrated to be equivalent to the DP23211 maize-derived IPD072Aa protein for use in safety testing [redacted] 2016; [redacted] 2017).

SDS-PAGE Analysis

Samples of IPD072Aa protein purified from DP23211 maize whole plant tissue and microbially derived IPD072Aa protein purified from a microbial expression system were analysed separately by SDS-PAGE. As expected, all IPD072Aa protein samples migrated as a predominant band consistent with the expected molecular weight of approximately 10 kDa (Carlson *et al.*, 2019), as shown in **Figure 23**.

Additional details regarding SDS-PAGE analytical methods are provided in **Appendix D.**

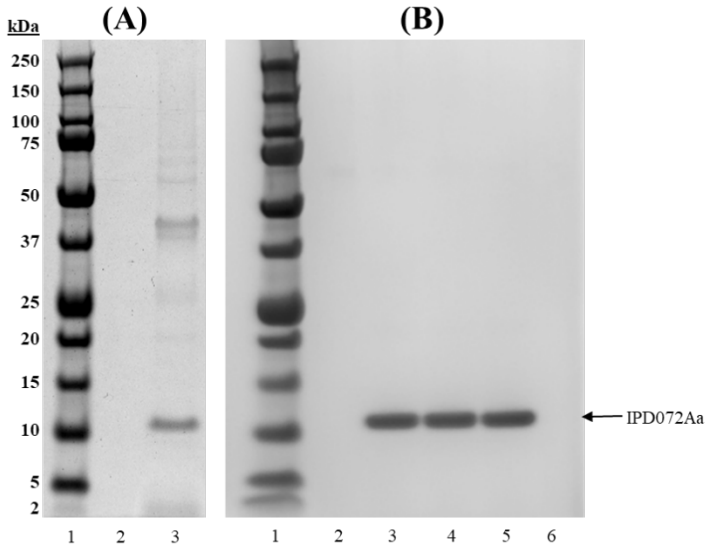

Panel	Lane	Sample Identification
A	1	Pre-stained Protein Molecular Weight Marker
	2	1X LDS Sample Buffer Blank
	3	DP23211 Maize-Derived IPD072Aa Protein
B	1	Pre-stained Protein Molecular Weight Marker
	2	1X LDS Sample Buffer Blank
	3	Microbially Derived IPD072Aa Protein (1 µg)
	4	Microbially Derived IPD072Aa Protein (1 µg)
	5	Microbially Derived IPD072Aa Protein (1 µg)
	6	1X LDS Sample Buffer Blank

Note: kilodalton (kDa), microgram (µg). Molecular weight markers were included to provide a visual estimate that migration was within the expected range of the predicted molecular weight.

Figure 23. SDS-PAGE Analysis of IPD072Aa Protein

Western Blot Analysis

Samples of IPD072Aa protein purified from DP23211 maize whole plant tissue and IPD072Aa protein purified from a microbial expression system were analysed separately by Western blot. As expected, all IPD072Aa protein samples were immunoreactive to an IPD072Aa polyclonal antibody and visible as a predominant band consistent with the expected molecular weight of approximately 10 kDa (Carlson *et al.*, 2019), as shown in **Figure 24**.

Additional details regarding Western blot analytical methods are provided in **Appendix D**.

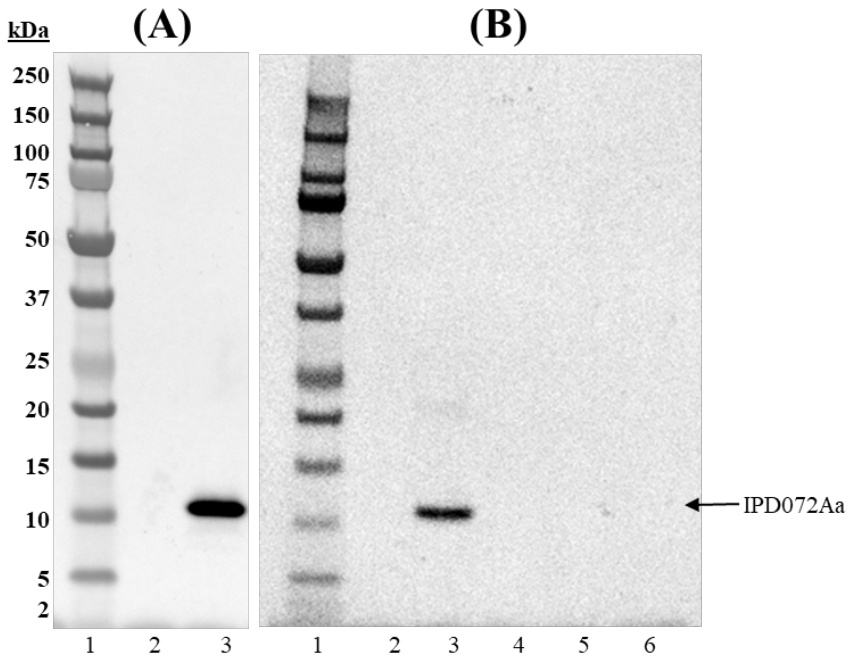

Panel	Lane	Sample Identification
A	1	Pre-stained Protein Molecular Weight Marker
	2	1X LDS Sample Buffer Blank
	3	DP23211 Maize-Derived IPD072Aa Protein
B	1	Pre-stained Protein Molecular Weight Marker
	2	1X LDS Sample Buffer Blank
	3	Microbially Derived IPD072Aa Protein (5 ng)
	4	1X LDS Sample Buffer Blank
	5	1X LDS Sample Buffer Blank
	6	1X LDS Sample Buffer Blank

Note: kilodalton (kDa), nanogram (ng). Molecular weight markers were included to provide a visual estimate that migration was within the expected range of the predicted molecular weight.

Figure 24. Western Blot Analysis of IPD072Aa Protein

Mass Spectrometry Peptide Mapping Analysis

Samples of IPD072Aa protein purified from DP23211 maize whole plant tissue and IPD072Aa protein purified from a microbial expression system were analysed separately by SDS-PAGE. Protein bands were stained with Coomassie stain reagent, and the band containing IPD072Aa protein was excised for each sample.

The excised IPD072Aa protein bands derived from DP23211 maize were digested with trypsin and chymotrypsin. Digested samples were analyzed using liquid chromatography-mass spectrometry (LC-MS). The mass data was used to search and match the peptides from the expected IPD072Aa protein sequence. The identified matched peptides account for 65% (56/86) of the expected IPD072Aa amino acid sequence (**Tables 11** to **13** and **Figure 25**).

The microbially derived IPD072Aa protein bands were digested with chymotrypsin. Digested samples were analyzed using matrix assisted laser desorption/ionization-time of flight (MALDI-TOF) mass spectrometry (MS). For some digested peptides, MALDI tandem mass spectrometry (MALDI MS/MS) was performed for peptide fragmentation analysis (i.e., partial sequencing). The MS and MS/MS spectra were combined, and the data was used to search and match the peptides from the expected IPD072Aa protein sequence. The identified matched peptides account for 100% of the expected IPD072Aa amino acid sequence (Carlson *et al.*, 2019), as shown in **Table 14** and **Figure 26**.

Additional details regarding peptide mapping analytical methods are provided in **Appendix D**.

Table 11. Combined Sequence Coverage of Identified Tryptic and Chymotryptic Peptides of DP23211 Maize-Derived IPD072Aa Protein Using LC-MS Analysis

Protease	% Coverage	Combined % Coverage
Trypsin	53	65
Chymotrypsin	20	

Table 12. Tryptic Peptides of DP23211 Maize-Derived IPD072Aa Protein Identified Using LC-MS Analysis

Matched Residue Position	Experimental Mass[a]	Theoretical Mass[b]	Identified Peptide Sequence
36-41	833.3607	833.3668	QETWDR
46-52	762.4591	762.4640	GFVLSLK
54-67	1548.7241	1548.7321	NGAQHPYYVQASSK
68-76	1000.5124	1000.5189	IEVDNNAVK
68-80	1456.7226	1456.7270	IEVDNNAVKDQGR
81-86	670.3866	670.3901	LIEPLS

[a] The experimental mass is the uncharged mass calculated from the mass to charge ratio of the observed ion.

[b] The theoretical mass is the *in silico* generated mass that matches closest to the experimental mass.

Table 13. Chymotryptic Peptides of DP23211 Maize-Derived IPD072Aa Protein Identified Using LC-MS Analysis

Matched Residue Position	Experimental Mass[a]	Theoretical Mass[b]	Identified Peptide Sequence
30-39	1104.5143	1104.5200	SVGNGKQETW
40-47	938.4152	938.4206	DRSDSRGF

[a] The experimental mass is the uncharged mass calculated from the mass to charge ratio of the observed ion.

[b] The theoretical mass is the *in silico* generated mass that matches closest to the experimental mass.

1 MGITVTNNSS NPIEVAINHW GSDGDTSFFS VGNGKQETWD RSDSRGFVLS

51 LKKNGAQHPY YVQASSKIEV DNNAVKDQGR LIEPLS

Gray shading	Gray-shaded type indicates DP23211 maize-derived IPD072Aa peptides identified using LC-MS analysis.
Amino acid residue abbreviations	alanine (A), aspartic acid (D), glutamic acid (E), phenylalanine (F), glycine (G), histidine (H), isoleucine (I), lysine (K), leucine (L), methionine (M), asparagine (N), proline (P), glutamine (Q), arginine (R), serine (S), threonine (T), tryptophan (W), tyrosine (Y), and valine (V).

Figure 25. Amino Acid Sequence of DP23211 Maize-Derived IPD072Aa Protein Indicating Tryptic and Chymotryptic Peptides Identified Using LC-MS Analysis

Table 14. Chymotryptic Peptides of Microbially Derived IPD072Aa Protein Identified Using MALDI-MS Analysis

IPD072Aa Amino Acid Residue Position	IPD072Aa Theoretical Peptide Mass [M+H]	IPD072Aa Observed Peptide Mass [M+H] (input)	Identified Peptide Sequence
1 - 30	3247.47	3247.33	HMGITVTNNSSNPIEVAINHWGSDGDTSFF
31 - 40	1105.52	1105.51	SVGNGKQETW
31 - 48	2025.93	2025.91	SVGNGKQETWDRSDSRGF
31 - 50	2238.08	2238.05	SVGNGKQETWDRSDSRGFVL
41 - 48	939.42	939.42	DRSDSRGF
41 - 50	1151.57	1151.56	DRSDSRGFVL
49 - 61	1454.80	1454.79	VLSLKKNGAQHPY
51 - 61	1242.65	1242.64	SLKKNGAQHPY
62 - 87	2873.49	2873.46	YVQASSKIEVDNNAVKDQGRLIEPLS

Note: alanine (A), arginine (R), asparagine (N), aspartic acid (D), glutamic acid (E), glutamine (Q), glycine (G), histidine (H), isoleucine (I), leucine (L), lysine (K), methionine (M), phenylalanine (F), proline (P), serine (S), threonine (T), tryptophan (W), tyrosine (Y), and valine (V).

HMGITVTNNSSNPIEVAINHWGSDGDTSFFSVGNGKQETWDRSDSRGFVLSLKKNGAQHPYYVQ
ASSKIEVDNNAVKDQGRLIEPLS

Gray shading	Gray-shaded type indicates microbially derived IPD072Aa peptides identified using MALDI-MS analysis.
Amino acid residue abbreviations	alanine (A), aspartic acid (D), glutamic acid (E), phenylalanine (F), glycine (G), histidine (H), isoleucine (I), lysine (K), leucine (L), methionine (M), asparagine (N), proline (P), glutamine (Q), arginine (R), serine (S), threonine (T), tryptophan (W), tyrosine (Y), and valine (V).

Figure 26. Amino Acid Sequence of Microbially Derived IPD072Aa Protein Indicating Chymotryptic Peptides Identified Using MALDI-MS Analysis

N-Terminal Amino Acid Sequence Analysis

Two samples of IPD072Aa protein purified from DP23211 maize whole plant tissue were analysed by SDS-PAGE followed by electrophoretic transfer to polyvinylidene difluoride (PVDF) membrane. Protein bands were stained using GelCode Blue stain reagent, and the band containing IPD072Aa protein was excised for each sample. Both bands were analysed as a single sample using Edman sequencing to determine the N-terminal amino acid sequence. The analysis obtained a primary sequence (GITVTNNSSN) matching amino acid residues 2-11 of the deduced IPD072Aa protein sequence (**Table 15**), indicating the N-terminal methionine was absent as expected (Dummitt et al., 2003; Sherman et al., 1985).

Samples of IPD072Aa protein purified from a microbial expression system were directly analysed using Edman sequencing to determine the N-terminal amino acid sequence. The analysis obtained the same primary sequence (HMGITVTNNS), matching amino acid residues 1-10 of the expected sequence of the microbially derived IPD072Aa protein (Carlson *et al.*, 2019).

Additional details regarding N-terminal amino acid sequencing analytical methods are provided in **Appendix D**.

Table 15. N-Terminal Amino Acid Sequence Analysis of IPD072Aa Protein

Description		Amino Acid Sequence
DP23211 Maize-Derived IPD072Aa Protein	Theoretical Sequence	M – G – I – T – V – T – N – N – S – S – N
	Observed Sequence	G – I – T – V – T – N – N – S – S – N
Microbially Derived IPD072Aa Protein	Theoretical Sequence	H – M – G – I – T – V – T – N – N – S
	Observed Sequence (Tox Lot PCF-0037-AP)	H – M – G – I – T – V – T – N – N – S
	Observed Sequence (Tox Lot PCF-0040)	H – M – G – I – T – V – T – N – N – S

Note: The N-terminal methionine in the detected primary sequence for DP23211 maize-derived IPD072Aa protein was absent as expected. Asparagine (N), glycine (G), histidine (H), isoleucine (I), methionine (M), serine (S), threonine (T), and valine (V).

Glycoprotein Analysis

Samples of IPD072Aa protein purified from DP23211 maize whole plant tissue and IPD072Aa protein purified from a microbial expression system were analysed separately by SDS-PAGE ([redacted], 2016; [redacted] 2017; [redacted] 2019a). Each gel also included a positive control (horseradish peroxidase) and negative control (soybean trypsin inhibitor). The gels were then stained using a Pierce Glycoprotein Staining Kit to visualize any glycoproteins. The gels were imaged and then stained with GelCode Blue stain reagent to visualize all protein bands.

Glycosylation was not detected for any of the IPD072Aa protein samples (**Figures 27** and **28**). The horseradish peroxidase positive control was clearly visible as a stained band. The soybean trypsin inhibitor negative control was not stained by the glycoprotein stain.

Additional details regarding glycoprotein analytical methods are provided in **Appendix D**.

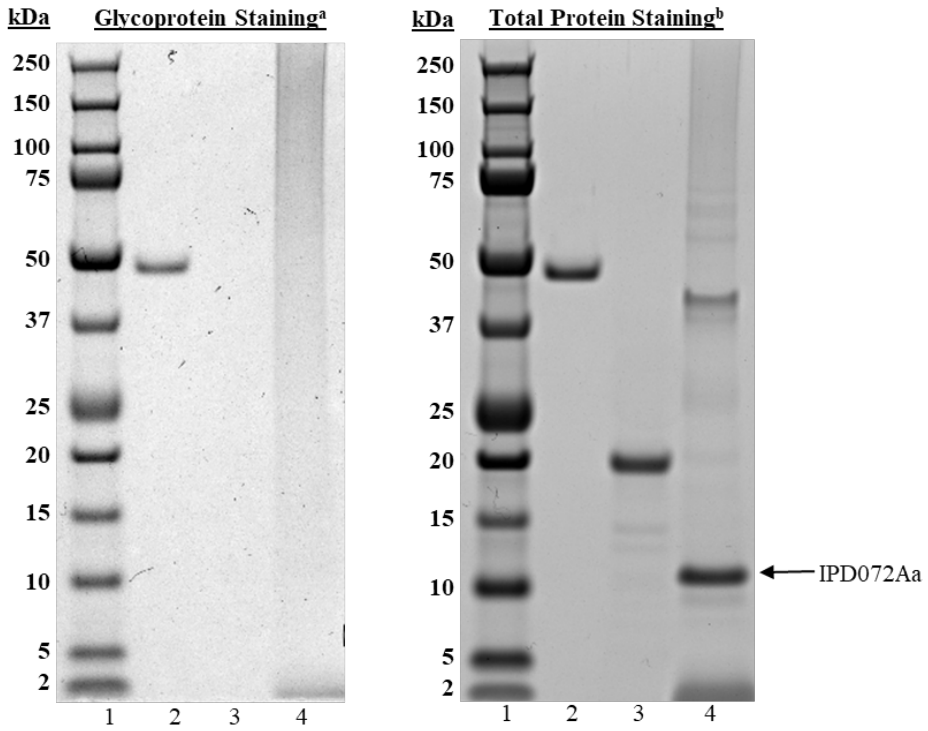

Lane	Sample Identification
1	Pre-stained Protein Molecular Weight Marker[c]
2	Positive Control: Horseradish Peroxidase (1.0 µg)
3	Negative Control: Soybean Trypsin Inhibitor (1.0 µg)
4	DP23211 Maize-Derived IPD072Aa Protein

Note: kilodalton (kDa), microgram (µg).

[a] Gel was stained with glycoprotein staining reagent.

[b] Gel was stained with glycoprotein staining reagent followed by staining with Coomassie Blue Reagent for total proteins.

[c] Molecular weight markers were included to provide a visual estimate that migration was within the expected range of the predicted molecular weight.

Figure 27. Glycosylation Analysis of DP23211 Maize-Derived IPD072Aa Protein

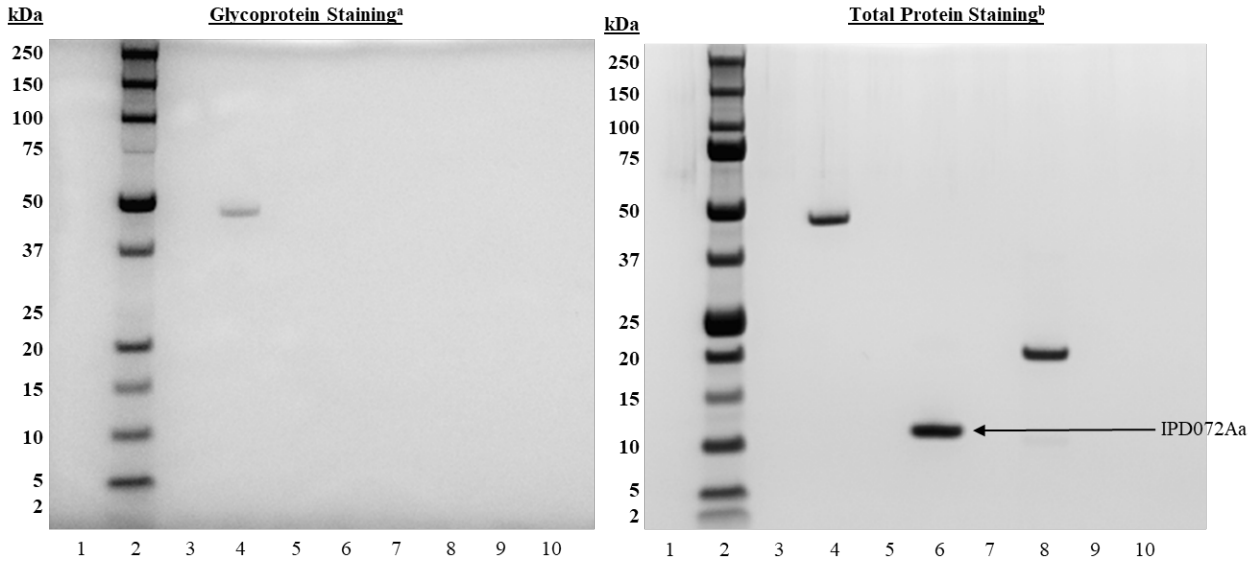

Lane	Sample Identification
1	1X LDS Sample Buffer Blank
2	Pre-stained Protein Molecular Weight Marker[c]
3	1X LDS Sample Buffer Blank
4	Positive Control: Horseradish Peroxidase (1 µg)
5	1X LDS Sample Buffer Blank
6	Microbially Derived IPD072Aa Protein (1 µg)
7	1X LDS Sample Buffer Blank
8	Negative Control: Soybean Trypsin Inhibitor (1 µg)
9	1X LDS Sample Buffer Blank
10	1X LDS Sample Buffer Blank

Note: kilodalton (kDa), microgram (µg).

[a] Gel was stained with glycoprotein staining reagent.

[b] Gel was stained with glycoprotein staining reagent followed by staining with Coomassie Blue Reagent for total proteins.

[c] Molecular weight markers were included to provide a visual estimate that migration was within the expected range of the predicted molecular weight.

Figure 28. Glycosylation Analysis of Microbially Derived IPD072Aa Protein

Allergenicity and Toxicity Analyses of the IPD072Aa Protein

A weight-of-evidence approach was applied to determine the allergenic and toxic potential of the IPD072Aa protein expressed in DP23211 maize, including an assessment of the following: the history of safe use of the source organism, a bioinformatic comparison of the amino acid sequence of IPD072Aa protein to known or putative allergenic and toxic proteins, evaluation of the stability of the IPD072Aa protein using *in vitro* gastric and intestinal digestion models, determination of the glycosylation status of the IPD072Aa protein, an evaluation of the heat lability of IPD072Aa protein via a sensitive insect bioassay, and an evaluation of acute toxicity in mice following oral exposure to IPD072Aa protein. A summary of the safety assessment for IPD072Aa protein was published by Carlson *et al.* (2019).

IPD072Aa Protein Source and History of Safe Use

The *ipd072Aa* gene that encodes the IPD072Aza protein was identified and cloned from a *Pseudomonas chlororaphis* strain that was isolated from a soil sample (Schellenberger et al., 2016). *Pseudomonas chlororaphis* is a rod-shaped, aerobic, Gram-negative bacterium that is ubiquitous in soil, has a history of safe use in agriculture and in food and feed crops, and is not known to be allergenic, toxic, or pathogenic to humans, animals, or livestock (Anderson et al., 2018).

Bioinformatic Analysis of Homology to Known or Putative Allergens

Assessing newly expressed proteins for potential cross-reactivity with known or putative allergens is an important part of the weight-of-evidence approach used to evaluate the safety of these proteins in genetically-modified plant products (Codex Alimentarius Commission, 2003). In this study, a bioinformatic assessment of the IPD072Aa protein sequence for potential cross-reactivity with known or putative allergens was conducted according to relevant guidelines (Codex Alimentarius Commission, 2003; FAO/WHO, 2001a).

Two separate searches for the IPD072Aa protein sequence were performed using the Comprehensive Protein Allergen Resource (COMPARE) 2019 database (January 2019) available at http://comparedatabase.org. [redacted], 2019a). This peer-reviewed database is a collaborative effort of the Health and Environmental Sciences Institute (HESI) Protein Allergens, Toxins, and Bioinformatics (PATB) Committee and is comprised of 2,081 sequences. The first search used the IPD072Aa protein sequence as the query in a FASTA v35.4.4 (Pearson and Lipman, 1988) search against the allergen sequences. The search was conducted using default parameters, except the *E*-score threshold was set to 10^{-4}. An *E*-score threshold of 10^{-4} has been shown to be an appropriate value for allergenicity searches (Mirsky *et al.*, 2013). The generated alignments were examined to identify any that are a length of 80 or greater and possess a sequence identity of ≥ 35%. The second search used an in-house Perl script (runLinearEpitopeScreen.pl) to identify any contiguous 8-residue identical matches between the IPD072Aa protein sequence and the allergen sequences.

Results of the search of the IPD072Aa protein sequence against the COMPARE database of known and putative allergen sequences found no alignments that were a length of 80 or greater with a sequence identity of ≥ 35%. No contiguous 8-residue matches between the IPD072Aa protein sequence and the allergen sequences were identified in the second search. Taken together, these data indicate that no allergenicity concern was identified from the bioinformatics assessment of the IPD072Aa protein.

Thermolability Analysis

Thermal stability of the IPD072Aa protein was characterized by determining the biological activity of heat-treated IPD072Aa protein incorporated in an artificial diet fed to western corn rootworm (WCR; *Diabrotica virgifera virgifera*) [redacted] 2018). Purified IPD072Aa protein was incubated at various temperatures for approximately 30 minutes before incorporation into the artificial diet. WCR larvae were exposed via oral ingestion to the diets in a 7-day bioassay. A positive control diet containing unheated IPD072Aa protein and a bioassay control diet containing water were included in the bioassay to verify assay performance. After seven days, statistical analyses were conducted to evaluate WCR mortality of the heat-treated test groups relative to the unheated test group.

The results demonstrated that IPD072Aa protein autoclaved for approximately 30 minutes at a targeted temperature of 121 °C and 20 psi was inactive against WCR when incorporated in an artificial insect diet (**Table 16**).

Additional details regarding thermolability analytical methods are provided in **Appendix D**.

Table 16. Biological Activity of Heat-Treated IPD072Aa Protein in Artificial Diet Fed to Western Corn Rootworm

Treatment	Treatment Description	Test Dosing Solution Incubation Condition	Total Number of Observations[a]	Total Number of Dead Organisms	Mortality (%)	Fisher's Exact Test P-Value
1	Bioassay Control Diet	NA	29	8	27.6	--
2	Test Diet	Unheated	22	20	90.9	--
3	Test Diet	25 °C	29	26	89.7	1.0000
4	Test Diet	50 °C	26	23	88.5	1.0000
5	Test Diet	60 °C	28	24	85.7	0.6825
6	Test Diet	95 °C	24	20	83.3	0.6672
7	Test Diet	121 °C (autoclaved)	29	4	13.8	<0.0001[b]

Note: Test diets contained a targeted concentration of 50 ng IPD072Aa protein per mg diet wet weight. Not applicable (NA); the bioassay control diet was not incubated.

[a] Organisms counted as missing during the bioassay, or wells containing more than one organism, were not included in the total number of observations for a given treatment.

[b] A statistically significant difference (P-value < 0.05) was observed in comparison to Treatment 2.

Digestibility Analysis with Simulated Gastric Fluid

Simulated gastric fluid (SGF) containing pepsin at pH ~1.2 was used to assess the susceptibility of the IPD072Aa protein to proteolytic digestion by pepsin *in vitro* [redacted] 2018b). IPD072Aa protein was incubated in SGF for 0, 0.5, 1, 2, 5, 10, 20, 30, and 60 minutes. A positive control (bovine serum albumin) and a negative control (β-lactoglobulin) were included in the assay and were incubated in SGF for 0, 1, and 60 minutes. After incubation in SGF, the samples were analyzed by SDS-PAGE. Coomassie-based stain or western blot was used to detect protein bands.

A summary of the SGF results is provided in **Table 17**. The IPD072Aa protein was rapidly digested (within 0.5 minutes) in SGF as demonstrated by both SDS-PAGE and western blot analysis (**Figures** 29 and 30, respectively). The bovine serum albumin control substance disappeared rapidly (less than one minute) in SGF and the β-lactoglobulin control persisted through the 60-minute time course, verifying that the assay performed as expected.

Additional details regarding SGF analytical methods are provided in **Appendix D**.

Table 17. Summary of IPD072Aa Protein In Vitro Pepsin Resistance Assay Results

Protein	Approximate Molecular Weight (kDa)	Digestion Time Determined by SDS-PAGE (minutes)	Digestion Time Determined by Western Blot (minutes)
IPD072Aa Protein	10	≤ 0.5	≤ 0.5
Bovine Serum Albumin (positive control)	66	≤ 1	NA
β-Lactoglobulin (negative control)	18	> 60	NA

Note: Kilodalton (kDa), sodium dodecyl sulfate polyacrylamide gel electrophoresis (SDS-PAGE), and not applicable (NA).

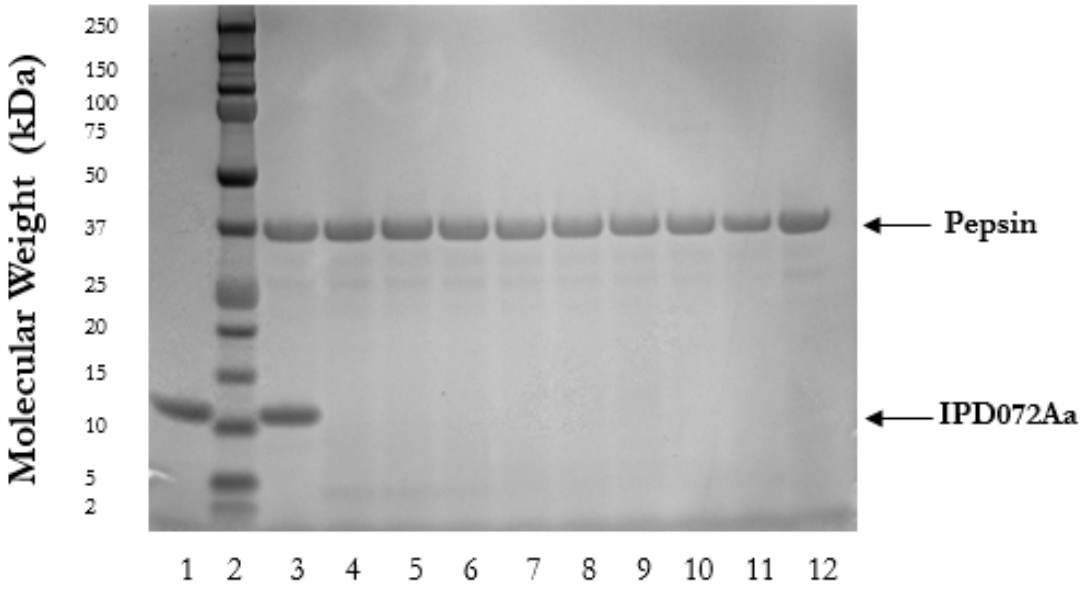

Lane	Sample Descriptions
1	IPD072Aa protein in water, time 0
2	Pre-stained protein molecular weight marker
3	IPD072Aa protein in SGF, time 0
4	IPD072Aa protein in SGF, 0.5 minutes
5	IPD072Aa protein in SGF, 1 minute
6	IPD072Aa protein in SGF, 2 minutes
7	IPD072Aa protein in SGF, 5 minutes
8	IPD072Aa protein in SGF, 10 minutes
9	IPD072Aa protein in SGF, 20 minutes
10	IPD072Aa protein in SGF, 30 minutes
11	IPD072Aa protein in SGF, 60 minutes
12	SGF control, 60 minutes

Figure 29. SDS-PAGE Analysis of IPD072Aa Protein in Simulated Gastric Fluid Digestion Time-Course

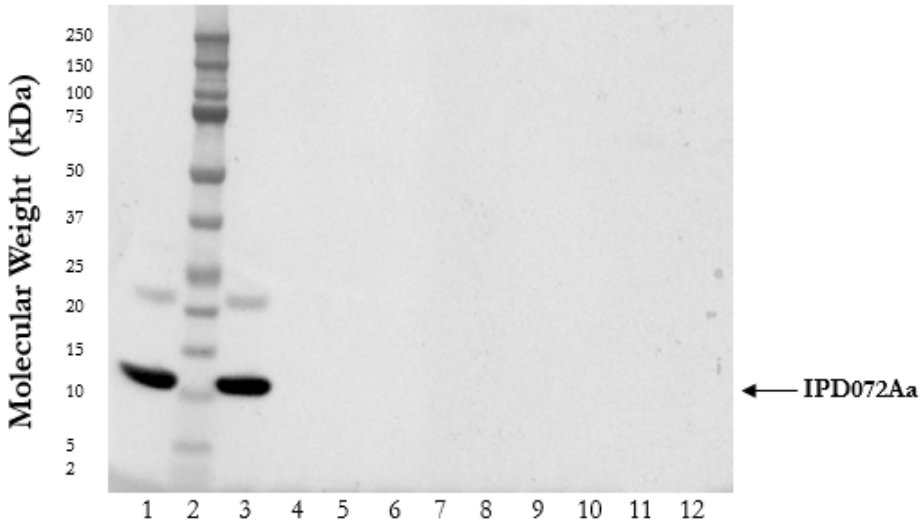

Lane	Sample Descriptions
1	IPD072Aa protein in water, time 0
2	Pre-stained protein molecular weight marker
3	IPD072Aa protein in SGF, time 0
4	IPD072Aa protein in SGF, 0.5 minutes
5	IPD072Aa protein in SGF, 1 minute
6	IPD072Aa protein in SGF, 2 minutes
7	IPD072Aa protein in SGF, 5 minutes
8	IPD072Aa protein in SGF, 10 minutes
9	IPD072Aa protein in SGF, 20 minutes
10	IPD072Aa protein in SGF, 30 minutes
11	IPD072Aa protein in SGF, 60 minutes
12	SGF control, 60 minutes

Note: Kilodalton (kDa), simulated gastric fluid (SGF), and sodium dodecyl sulfate polyacrylamide gel electrophoresis (SDS-PAGE).

Figure 30. Western Blot Analysis of IPD072Aa Protein in Simulated Gastric Fluid Digestion Time-Course

Digestibility Analysis with Simulated Intestinal Fluid

Simulated intestinal fluid (SIF) containing pancreatin at ~pH 7.5 was used to assess the susceptibility of the IPD072Aa protein to proteolytic digestion by pancreatin *in vitro* [redacted] 2018a). IPD072Aa protein was incubated in SIF for 0, 0.5, 1, 2, 5, 10, 20, 30, and 60 minutes. Two control proteins (bovine serum albumin and β-lactoglobulin) were included in the assay and were incubated in SIF for 0, 1, and 60 minutes. After incubation in SIF, the samples were analyzed by SDS-PAGE. Coomassie-based stain or western blot was used to detect protein bands.

A summary of the SIF assay results is provided in **Table 18**. The IPD072Aa protein was digested in SIF within 20 minutes as demonstrated by both SDS-PAGE and western blot analysis (**Figures 31** and **32**, respectively). The β-lactoglobulin control substance disappeared rapidly (less than one minute) in SIF and the bovine serum albumin control persisted through the 60-minute time course, verifying that the assay performed as expected.

Additional details regarding SIF analytical methods are provided in **Appendix D**.

Table 18. Summary of IPD072Aa Protein In Vitro Pancreatin Resistance Assay Results

Protein	Approximate Molecular Weight (kDa)	Digestion Time Determined by SDS-PAGE (minutes)	Digestion Time Determined by Western Blot (minutes)
IPD072Aa Protein	10	≤ 20	≤ 20
Bovine Serum Albumin (control)	66	> 60	NA
β-Lactoglobulin (control)	18	≤ 1	NA

Note: Kilodalton (kDa), sodium dodecyl sulfate polyacrylamide gel electrophoresis (SDS-PAGE), not applicable (NA).

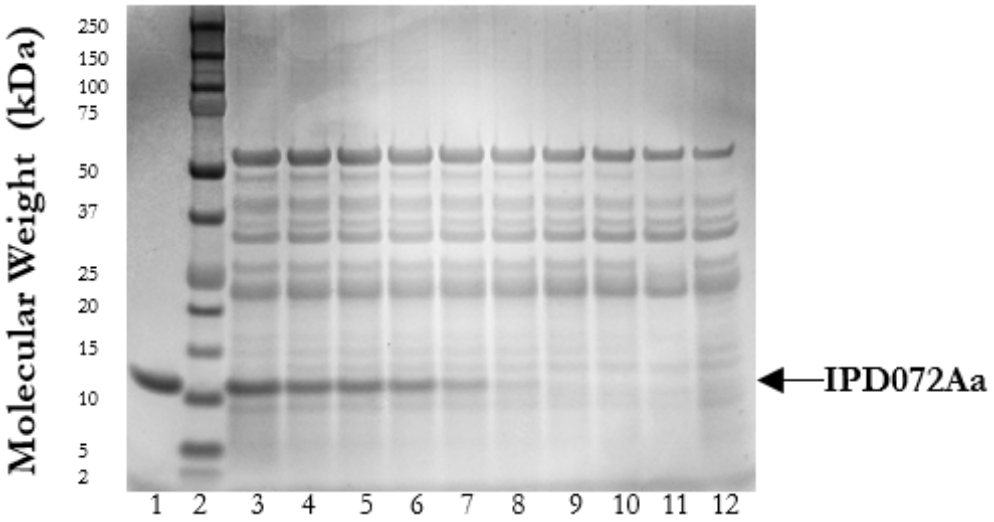

Lane	Sample Descriptions
1	IPD072Aa protein in water, time 0
2	Pre-stained protein molecular weight marker
3	IPD072Aa protein in SIF, time 0
4	IPD072Aa protein in SIF, 0.5 minutes
5	IPD072Aa protein in SIF, 1 minute
6	IPD072Aa protein in SIF, 2 minutes
7	IPD072Aa protein in SIF, 5 minutes
8	IPD072Aa protein in SIF, 10 minutes
9	IPD072Aa protein in SIF, 20 minutes
10	IPD072Aa protein in SIF, 30 minutes
11	IPD072Aa protein in SIF, 60 minutes
12	SIF control, 60 minutes

Note: Kilodalton (kDa), simulated intestinal fluid (SIF), and sodium dodecyl sulfate polyacrylamide gel electrophoresis (SDS-PAGE).

Figure 31. SDS-PAGE Analysis of IPD072Aa Protein in Simulated Intestinal Fluid Digestion Time-Course

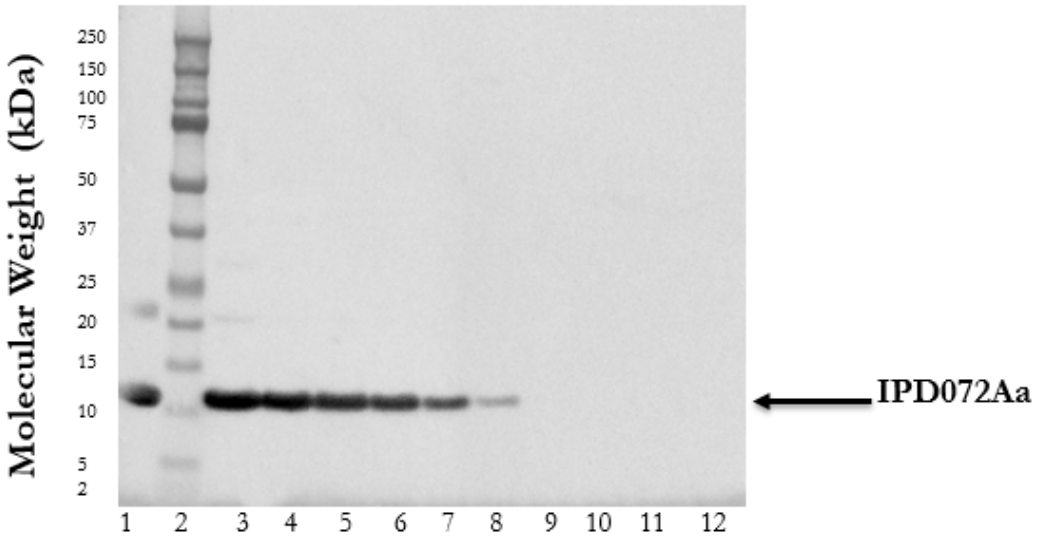

Lane	Sample Descriptions
1	IPD072Aa protein in water, time 0
2	Pre-stained protein molecular weight marker
3	IPD072Aa protein in SIF, time 0
4	IPD072Aa protein in SIF, 0.5 minutes
5	IPD072Aa protein in SIF, 1 minute
6	IPD072Aa protein in SIF, 2 minutes
7	IPD072Aa protein in SIF, 5 minutes
8	IPD072Aa protein in SIF, 10 minutes
9	IPD072Aa protein in SIF, 20 minutes
10	IPD072Aa protein in SIF, 30 minutes
11	IPD072Aa protein in SIF, 60 minutes
12	SIF control, 60 minutes

Note: Kilodalton (kDa), simulated intestinal fluid (SIF), and sodium dodecyl sulfate polyacrylamide gel electrophoresis (SDS-PAGE).

Figure 32. Western Blot Analysis of IPD072Aa Protein in Simulated Intestinal Fluid Digestion Time-Course

Glycoprotein Analysis

As stated previously in Section 6.c., the results from glycoprotein staining analysis confirmed the absence of glycosylation for IPD072Aa protein isolated and purified from DP23211 maize tissue ([redacted] 2016; [redacted] 2017; [redacted] 2019a).

Bioinformatic Analysis of Homology to Known or Putative Toxins

Assessing newly expressed proteins for potential toxicity is an important part of the weight-of-evidence approach used to evaluate the safety of these proteins in genetically modified plant products (Codex Alimentarius Commission, 2003). The potential toxicity of the IPD072Aa protein was assessed by comparison of its sequence to the sequences in an internal toxin database [redacted] 2019c). The internal toxin database is a subset of sequences found in UniProtKB/Swiss-Prot (https://www.uniprot.org/). To produce the internal toxin database,

the proteins in UniProtKB/Swiss-Prot are filtered for molecular function by keywords that could imply toxicity or adverse health effects (e.g., toxin, hemagglutinin, vasoactive, etc.). The internal toxin database is updated annually. The search between the IPD072Aa protein sequence and protein sequences in the internal toxin database was conducted with BLASTP using default parameters, except that low complexity filtering was turned off, the *E*-value threshold was set to 10^{-4}, and unlimited alignments were returned.

No alignments with an *E*-value ≤ 10^{-4} were returned between the IPD072Aa protein sequence and any protein sequence in the internal toxin database. These data indicate that no toxicity concern was identified from the bioinformatics assessment of the IPD072Aa protein.

Evaluation of the Acute Toxicity of IPD072Aa Protein

A study was conducted to evaluate the acute toxicity of the test substance, IPD072Aa protein, in groups of 6 male and 6 female Crl:CD1(ICR) mice following oral exposure at a dose of 2000 mg/kg [redacted] 2016). IPD072Aa protein and Bovine Serum Albumin (BSA) protein were each reconstituted in deionized water. A vehicle control, BSA control and IPD072Aa test substance formulations were administered orally by gavage. The mice were fasted prior to and throughout the dosing procedure.

Body weights were evaluated on test days 1 (prefast and shortly prior to dose administration), 2, 3, 5, 8, and 15. Clinical signs were evaluated before and after dosing on test day 1 and daily thereafter. On test day 15, all mice were euthanized and given a gross pathological examination.

All animals survived to scheduled euthanasia. There were no clinical abnormalities or overall (test day 1-15) losses in body weight among any of the animals tested. No gross lesions were present at necropsy.

Under the conditions of this study, intragastric exposure of IPD072Aa protein to male and female mice at 2000 mg/kg did not result in mortality or other evidence of acute oral toxicity, based on evaluation of body weight, clinical signs, and gross pathology. Therefore, the LD_{50} of IPD072Aa protein was determined to be greater than 2000 mg/kg.

Conclusions on the Safety of IPD072Aa Protein in DP23211 Maize

In conclusion, protein characterisation results via SDS-PAGE, western blot, peptide mapping, N-terminal amino acid sequence, and glycoprotein analysis have demonstrated that the IPD072Aa protein derived from DP23211 maize is of the expected molecular weight, immunoreactivity, amino acid sequence, and showed a lack of glycosylation. Microbially derived IPD072Aa protein was demonstrated to be equivalent to the DP23211 maize-derived IPD072Aa protein for use in safety testing.

The allergenic potential of the IPD072Aa protein was evaluated by assessing the IPD072Aa protein source organism and history of safe use; a bioinformatic comparison of the amino acid sequence of the IPD072Aa protein with known or putative protein allergen sequences; evaluation of the stability of the IPD072Aa protein using *in vitro* gastric and intestinal digestion models; determination of the IPD072Aa protein glycosylation status; and evaluation of the heat lability of the IPD072Aa protein using a sensitive insect bioassay. The toxicity potential of the IPD072Aa protein was evaluated by an acute toxicity study in mice and a bioinformatic comparison of the IPD072Aa amino acid sequence to known and putative protein toxins.

The results showed that the IPD072Aa protein is digested in SGF and SIF digestion analyses. The IPD072Aa protein autoclaved for approximately 30 minutes at 121 °C was inactive against WCR when incorporated in an artificial diet. The bioinformatic comparisons of the IPD072Aa protein sequence to known and putative allergen and toxin sequences showed that the IPD072Aa protein is unlikely to be allergenic or toxic for humans or animals. The acute oral toxicity assessment determined the LD_{50} of IPD072Aa protein to be greater than 2000 mg/kg. These data support the conclusion that the IPD072Aa protein in DP23211 maize is as safe as conventional maize for the food and feed supply.

Based on this weight of evidence, consumption of the IPD072Aa protein is unlikely to cause an adverse effect on humans or animals.

b. PAT

Amino Acid Sequence

The gene encoding the PAT protein in DP23211 maize, referred to as the *mo-pat* gene, was isolated from *Streptomyces viridochromogenes* with codon-optimization for expression in maize. The deduced amino acid sequence from the translation of the *mo-pat* gene is identical to the deduced amino acid sequence from the translation of the *pat* gene. The PAT protein encoded by the *pat* and *mo-pat* genes is 183 amino acids in length and has a molecular weight of approximately 21 kDa (**Figure 33; [redacted] 2018**).

```
PAT(pat)       1 MSPERRPVEI RPATAADMAA VCDIVNHYIE TSTVNFRTEP QTPQEWIDDL
PAT(mo-pat)    1 MSPERRPVEI RPATAADMAA VCDIVNHYIE TSTVNFRTEP QTPQEWIDDL

PAT(pat)      51 ERLQDRYPWL VAEVEGVVAG IAYAGPWKAR NAYDWTVEST VYVSHRHQRL
PAT(mo-pat)   51 ERLQDRYPWL VAEVEGVVAG IAYAGPWKAR NAYDWTVEST VYVSHRHQRL

PAT(pat)     101 GLGSTLYTHL LKSMEAQGFK SVVAVIGLPN DPSVRLHEAL GYTARGTLRA
PAT(mo-pat)  101 GLGSTLYTHL LKSMEAQGFK SVVAVIGLPN DPSVRLHEAL GYTARGTLRA

PAT(pat)     151 AGYKHGGWHD VGFWQRDFEL PAPPRPVRPV TQI*
PAT(mo-pat)  151 AGYKHGGWHD VGFWQRDFEL PAPPRPVRPV TQI*
```

Figure 33. Alignment of the Deduced Amino Acid Sequence of PAT Protein Encoded by *pat* and *mo-pat* Genes
Deduced amino acid sequence alignment, where PAT (*pat*) represents the deduced amino acid sequence from the translation of the *pat* gene that is found in a number of authorized events across several different crops that are currently in commercial use (Hérouet et al., 2005; USDA-APHIS, 2001; USDA-APHIS, 2005; USDA-APHIS, 2013). The PAT (*mo-pat*) sequence represents the deduced amino acid sequence from translation of the *mo-pat* gene. The asterisk (*) indicates the translational stop codon.

As shown in **Figure 33**, the deduced amino acid sequence from translation of the *mo-pat* gene is identical to that of the already-deregulated PAT protein from translation of the *pat* gene, for which safety has been confirmed (Hérouet et al., 2005) in a number of approved events across several different crops that are currently in commercial use.

Characterisation of the PAT Protein Derived from DP23211 Maize

The DP23211 maize-expressed PAT protein was characterized using SDS-PAGE analysis, western blot analysis, peptide mapping by mass spectrometry, N-terminal amino acid sequencing, and glycoprotein analysis [redacted] 2019b). The results demonstrated that the PAT protein derived from DP23211 maize is of the expected molecular weight, immunoreactivity, amino acid sequence, and showed a lack of glycosylation.

SDS-PAGE Analysis

Samples of PAT protein purified from DP23211 maize whole plant tissue were analyzed by SDS-PAGE. As expected, all PAT protein samples migrated as a predominant band consistent with the expected molecular weight of approximately 21 kDa (**Figure 34**).

Additional details regarding SDS-PAGE analytical methods are provided in **Appendix E**.

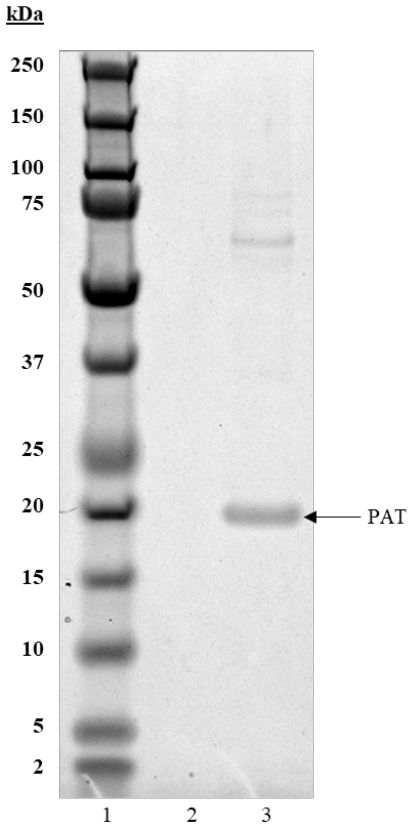

Lane	Sample Identification
1	Pre-stained Protein Molecular Weight Marker[a]
2	1X LDS Sample Buffer Blank
3	DP23211 Maize-Derived PAT Protein

Note: kilodalton (kDa).

[a] Molecular weight markers were included to provide a visual estimate that migration was within the expected range of the predicted molecular weight.

Figure 34. SDS-PAGE Analysis of DP23211 Maize-Derived PAT Protein

Western Blot Analysis

Samples of PAT protein purified from DP23211 maize whole plant tissue were analysed by Western blot. As expected, all PAT protein samples were immunoreactive to a PAT monoclonal antibody and visible as a predominant band consistent with the expected molecular weight of approximately 21 kDa (**Figure 35**).

Additional details regarding Western blot analytical methods are provided in **Appendix E.**

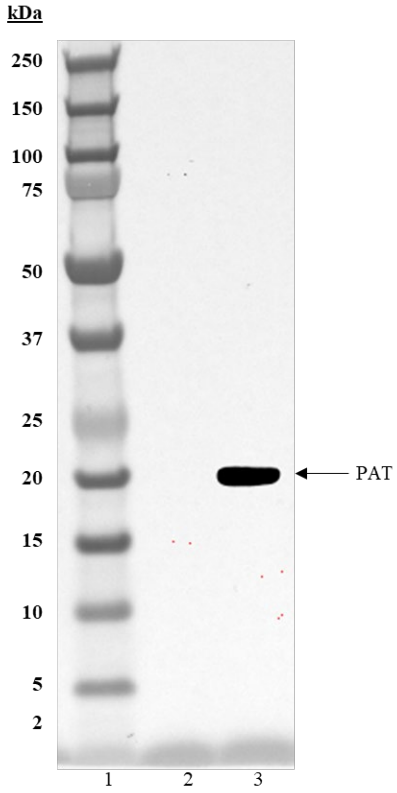

Lane	Sample Identification
1	Pre-stained Protein Molecular Weight Marker[a]
2	1X LDS Sample Buffer Blank
3	DP23211 Maize-Derived PAT Protein

Note: kilodalton (kDa).

[a] Molecular weight markers were included to provide a visual estimate that migration was within the expected range of the predicted molecular weight.

Figure 35. Western Blot Analysis of PAT Protein

LC-MS Peptide Mapping Analysis

Two samples of PAT protein purified from DP23211 maize whole plant tissue were analysed by SDS-PAGE. Protein bands were stained with Coomassie stain reagent, and the band containing PAT protein was excised for each sample. The DP23211 maize-derived excised PAT protein bands were digested with trypsin and chymotrypsin. Digested samples were analyzed using LC-MS, and an MS/MS ion search was used to match the detected peaks to peptides from the expected PAT protein sequence.

The analysis identified a total of 173 unique peptides from the trypsin- and chymotrypsin-derived PAT protein derived from DP23211 maize, representing 95% of the deduced PAT protein sequence containing 183 amino acids (**Tables 19** to **21** and **Figure 36**).

Additional details regarding peptide mapping analytical methods are provided in **Appendix E**.

Table 19. Combined Sequence Coverage of Identified Tryptic and Chymotryptic Peptides of DP23211 Maize-Derived PAT Protein Using LC-MS Analysis

Protease	% Coverage	Combined % Coverage
Trypsin	77	95
Chymotrypsin	91	

Table 20. Identified Tryptic Peptides of DP23211 Maize-Derived PAT Protein Using LC-MS Analysis

Matched Residue Position	Experimental Mass[a]	Theoretical Mass[b]	Identified Peptide Sequence
6–37	3615.7594	3615.7926	RPVEIRPATAADMAAVCDIVNHYIETSTVNFR
38–52	1855.8440	1855.8588	TEPQTPQEWIDDLER
38–56	2368.1132	2368.1295	TEPQTPQEWIDDLERLQDR
81–96	1925.8734	1925.8908	NAYDWTVESTVYVSHR
100–112	1414.8078	1414.8184	LGLGSTLYTHLLK
113–120	896.4005	896.4062	SMEAQGFK
121–135	1521.8415	1521.8515	SVVAVIGLPNDPSVR
136–145	1129.5787	1129.5880	LHEALGYTAR
155–166	1480.6633	1480.6749	HGGWHDVGFWQR
167–183	1931.0481	1931.0629	DFELPAPPRPVRPVTQI

[a] The experimental mass is the uncharged mass calculated from the mass to charge ratio of the observed ion.

[b] The theoretical mass is the *in silico* generated mass that matches closest to the experimental mass.

Table 21. Identified Chymotryptic Peptides of DP23211 Maize-Derived PAT Protein Using LC-MS Analysis

2–28	3037.4683	3037.4862	SPERRPVEIRPATAADMAAVCDIVNHY
2–36	3928.9026	3928.9200	SPERRPVEIRPATAADMAAVCDIVNHYIETSTVNF
37–46	1270.5835	1270.5942	RTEPQTPQEW
37–53	2125.0306	2125.0440	RTEPQTPQEWIDDLERL
47–53	872.4542	872.4603	IDDLERL
47–59	1717.8286	1717.8424	IDDLERLQDRYPW
54–59	863.3866	863.3926	QDRYPW
60–73	1388.7452	1388.7551	LVAEVEGVVAGIAY
78–83	721.3817	721.3871	KARNAY
78–85	1022.4838	1022.4933	KARNAYDW
78–92	1801.8474	1801.8635	KARNAYDWTVESTVY
84–92	1098.4808	1098.4870	DWTVESTVY
93–100	1031.5674	1031.5737	VSHRHQRL
107–111	645.3448	645.3486	YTHLL
108–119	1360.6716	1360.6809	THLLKSMEAQGF
111–119	1009.4812	1009.4902	LKSMEAQGF
112–119	896.3991	896.4062	KSMEAQGF
120–136	1763.0176	1763.0305	KSVVAVIGLPNDPSVRL
120–140	2213.2354	2213.2532	KSVVAVIGLPNDPSVRLHEAL
120–142	2433.3209	2433.3380	KSVVAVIGLPNDPSVRLHEALGY
137–142	688.3129	688.3180	HEALGY
143–148	617.3456	617.3497	TARGTL
154–163	1138.5250	1138.5309	KHGGWHDVGF
154–164	1324.6017	1324.6102	KHGGWHDVGFW
159–164	759.3286	759.3340	HDVGFW
165–183	2215.2038	2215.2226	QRDFELPAPPRPVRPVTQI
169–183	1668.9516	1668.9675	ELPAPPRPVRPVTQI

[a] The experimental mass is the uncharged mass calculated from the mass to charge ratio of the observed ion.

[b] The theoretical mass is the *in silico* generated mass that matches closest to the experimental mass.

```
  1 MSPERRPVEI RPATAADMAA VCDIVNHYIE TSTVNFRTEP QTPQEWIDDL
 51 ERLQDRYPWL VAEVEGVVAG IAYAGPWKAR NAYDWTVEST VYVSHRHQRL
101 GLGSTLYTHL LKSMEAQGFK SVVAVIGLPN DPSVRLHEAL GYTARGTLRA
151 AGYKHGGWHD VGFWQRDFEL PAPPRPVRPV TQI
```

Gray shading	Gray-shaded type indicates DP23211 maize-derived PAT peptides identified using LC-MS analysis.
Amino acid residue abbreviations	alanine (A), aspartic acid (D), glutamic acid (E), phenylalanine (F), glycine (G), histidine (H), isoleucine (I), lysine (K), leucine (L), methionine (M), asparagine (N), proline (P), glutamine (Q), arginine (R), serine (S), threonine (T), tryptophan (W), tyrosine (Y), and valine (V).

Figure 36. Identified Tryptic and Chymotryptic Peptide Amino Acid Sequence of DP23211 Maize-Derived PAT Protein Using LC-MS Analysis

N-Terminal Amino Acid Sequence Analysis

PAT protein purified from DP23211 maize whole plant tissue was analysed by SDS-PAGE followed by electrophoretic transfer to polyvinylidene difluoride (PVDF) membrane. Protein bands were stained using GelCode Blue stain reagent, and the band containing IPD072Aa protein was excised. The excised band was analysed using Edman sequencing to determine the N-terminal amino acid sequence. The analysis obtained a primary sequence (SPERRPVEIR) matching amino acid residues 2-11 of the deduced PAT protein sequence (**Table 22**), indicating the N-terminal methionine was absent as expected (Dummitt et al., 2003; Sherman et al., 1985).

Additional details regarding N-terminal amino acid sequencing analytical methods are provided in **Appendix E**.

Table 22. N-Terminal Amino Acid Sequence Analysis of DP23211 Maize-Derived PAT Protein

Theoretical PAT Sequence	M – S – P – E – R – R – P – V – E – I – R
Detected Primary Sequence	S – P – E – R – R – P – V – E – I – R

Note: The N-terminal methionine in the detected primary sequence for DP23211 maize-derived PAT protein was absent as expected.

Note: glutamic acid (E), isoleucine (I), methionine (M), proline (P), arginine (R), serine (S), and valine (V).

Glycosylation Analysis

Samples of PAT protein purified from DP23211 maize whole plant tissue were analysed by SDS-PAGE. Each gel also included a positive control (horseradish peroxidase) and negative control (soybean trypsin inhibitor). The gels were stained using a Pierce Glycoprotein Staining Kit to visualize any glycoproteins. The gels were imaged and then stained with GelCode Blue stain reagent to visualize all protein bands.

Glycosylation was not detected for the PAT protein (**Figure 37**). The horseradish peroxidase positive control was stained and clearly visible as a magenta-colored band. The soybean trypsin inhibitor negative control was not stained by the glycoprotein stain.

Additional details regarding glycosylation analytical methods are provided in **Appendix E**.

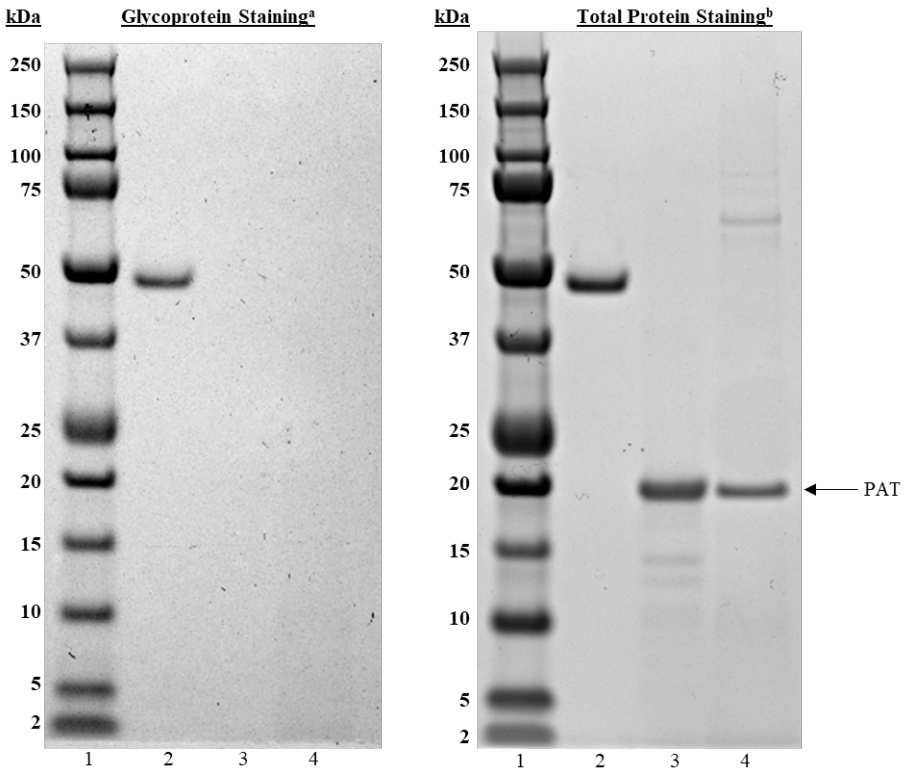

Lane	Sample Identification
1	Pre-stained Protein Molecular Weight Marker[c]
2	Positive Control: Horseradish Peroxidase (1.0 µg)
3	Negative Control: Soybean Trypsin Inhibitor (1.0 µg)
4	DP23211 Maize-Derived PAT Protein

Note: kilodalton (kDa), microgram (µg).

[a] Gel was stained with glycoprotein staining reagent.

[b] Gel was stained with glycoprotein staining reagent followed by staining with Coomassie Blue Reagent for total proteins.

[c] Molecular weight markers were included to provide a visual estimate that migration was within the expected range of the predicted molecular weight.

Figure 37. Glycosylation Analysis of DP23211 Maize-Derived PAT Protein

Mode of Action of PAT Protein

The mode of action of the PAT protein has been previously characterized and described (CERA, 2011; Hérouet et al., 2005). The PAT protein confers tolerance to the herbicidal active ingredient glufosinate-ammonium, the active ingredient in phosphinothricin herbicides. Glufosinate chemically resembles the amino acid glutamate and acts to inhibit an enzyme called glutamine synthetase, which is involved in the synthesis of glutamine. Glutamine synthetase is also involved in ammonia detoxification. Due to its similarity to glutamate, glufosinate blocks the activity of glutamine synthetase, resulting in reduced glutamine levels and a corresponding increase in concentrations of ammonia in plant tissues, leading to cell membrane disruption and cessation of photosynthesis resulting in plant death. The PAT protein confers tolerance to glufosinate-ammonium herbicides by acetylating phosphinothricin, an isomer of glufosinate-ammonium, thus detoxifying the herbicide (CERA, 2011; Hérouet et al., 2005).

Allergenicity and Toxicity Analyses of the PAT Protein

The PAT protein has been risk-assessed in multiple previously authorized maize events and is unlikely to present significant risks to the environment, human, or animal health (CERA - ILSI Research Foundation, 2016; CERA, 2011; Hérouet et al., 2005). Authorizations for GM plants that express the PAT protein have been issued in 7 species of plants and total over 450 authorized uses, including authorizations for food and feed use by regulatory authorities in 20 different countries and/or regions (ILSI, 2016).

There is a considerable body of public information supporting the safety of the PAT protein, including bioinformatic analyses, evaluation of the stability of the PAT protein using *in vitro* gastric and intestinal digestion models, heat lability analysis, and an evaluation of acute toxicity in mice following oral exposure to PAT protein (CERA - ILSI Research Foundation, 2016; Hérouet et al., 2005). These previous assessments are relevant for the assessment of PAT protein expressed in DP23211 maize.

A weight-of-evidence approach was applied to determine the allergenic and toxic potential of the PAT protein expressed in DP23211 maize, including an assessment of the following: the source and history of safe use of PAT protein, a bioinformatic comparison of the amino acid sequence of PAT protein to known or putative toxins and protein allergen sequences, and glycoprotein analysis. Updated bioinformatic and glycoprotein analyses support the original conclusions that the PAT protein is unlikely to be an allergen or toxin. These data support the conclusion that the PAT protein in DP23211 maize is safe for the food and feed supply.

PAT Protein Source and History of Safe Use

The *mo-pat* coding sequence was originally isolated from *Streptomyces viridochromogenes* followed by codon optimization for expression in maize. *S. viridochromogenes* is a common soil bacterium that is not considered pathogenic to humans or animals (OECD, 1999).

Bioinformatic Analysis of PAT Protein Homology to Known or Putative Allergens

Assessing newly expressed proteins for potential cross-reactivity with known or putative allergens is a critical part of the weight-of-evidence approach used to evaluate the safety of these proteins in genetically-modified plant products (Codex Alimentarius Commission, 2003). In this study, a bioinformatic assessment of the PAT protein sequence for potential cross-reactivity with known or putative allergens was conducted according to relevant guidelines (Codex Alimentarius Commission, 2003; FAO/WHO, 2001a).

Two separate searches for the PAT protein sequence were performed using the Comprehensive Protein Allergen Resource (COMPARE) 2019 database (January 2019) available at http://comparedatabase.org [redacted] 2019b). This peer-reviewed database is a collaborative effort of the Health and Environmental Sciences Institute (HESI) Protein Allergens, Toxins, and Bioinformatics (PATB) Committee and is comprised of 2,081 sequences. The first search used the PAT protein sequence as the query in a FASTA v35.4.4 (Pearson and Lipman, 1988) search against the allergen sequences. The search was conducted using default parameters, except the *E*-score threshold was set to 10^{-4}. An *E*-score threshold of 10^{-4} has been shown to be an appropriate value for allergenicity searches (Mirsky *et al.*, 2013). The generated alignments were examined to identify any that are a length of 80 or greater and possess a sequence identity of ≥ 35%. The second search used an in-house Perl script

(runLinearEpitopeScreen.pl) to identify any contiguous 8-residue identical matches between the PAT protein sequence and the allergen sequences.

Results of the search of the PAT protein sequence against the COMPARE database of known and putative allergen sequences found no alignments that were a length of 80 or greater with a sequence identity of ≥ 35%. No contiguous 8-residue matches between the PAT protein sequence and the allergen sequences were identified in the second search. Taken together, these data indicate that no allergenicity concern was identified from the bioinformatics assessment of the PAT protein.

Bioinformatic Analysis of PAT Protein Homology to Known or Putative Toxins

Assessing newly expressed proteins for potential toxicity is a critical part of the weight-of-evidence approach used to evaluate the safety of these proteins in genetically modified plant products (Codex Alimentarius Commission, 2003). The potential toxicity of the IPD072Aa protein was assessed by comparison of its sequence to the sequences in an internal toxin database ([redacted] 2019). The internal toxin database is a subset of sequences found in UniProtKB/Swiss-Prot (https://www.uniprot.org/). To produce the internal toxin database, the proteins in UniProtKB/Swiss-Prot are filtered for molecular function by keywords that could imply toxicity or adverse health effects (e.g., toxin, hemagglutinin, vasoactive, etc.). The internal toxin database is updated annually. The search between the PAT protein sequence and protein sequences in the internal toxin database was conducted with BLASTP using default parameters, except that low complexity filtering was turned off, the *E*-value threshold was set to 10^{-4}, and unlimited alignments were returned.

No alignments with an *E*-value ≤ 10^{-4} were returned between the PAT protein sequence and any protein sequence in the internal toxin database. These data indicate that no toxicity concern was identified from the bioinformatics assessment of the PAT protein.

Glycosylation Analysis

As stated previously in below, the results from glycoprotein staining analysis confirmed the absence of glycosylation for PAT protein isolated and purified from DP23211 maize tissue ([redacted] 2019b).

Safety of PAT Protein Determined in Risk Assessments for Previously-Authorized GM Events

The PAT protein encoded by the *mo-pat* gene in DP23211 maize is identical to the PAT protein encoded by the *pat* gene that is found in a number of authorized GM events across several different crops that are currently in commercial use (CERA - ILSI Research Foundation, 2016; Hérouet et al., 2005). Maize containing the PAT protein has been commercially grown in the United States since 1996. The PAT protein has been previously risk-assessed for potential allergenicity and toxicity by numerous regulatory agencies, and is unlikely to present significant risks to the environment, human, or animal health (CERA - ILSI Research Foundation, 2016; CERA, 2011; Hérouet et al., 2005). These previous assessments of PAT protein are also relevant for the assessment of PAT protein in DP23211 maize.

PAT protein safety has been reviewed and authorized for food and feed use by regulatory authorities in 20 different countries and/or regions. In total there are about 460 regulatory approvals in these countries, representing 7 species of plants and more than 110 transformation events (ILSI, 2016). PAT protein safety data has

been provided has been reviewed by FSANZ, resulting in authorizations of PAT protein in numerous currently commercially available crops.

In addition, there is a considerable body of public information supporting the safety of the PAT protein, including but not limited to the following:

- No homology to known allergens or toxins (Hérouet et al., 2005)
- The PAT protein was tested for heat lability at temperatures of 60, 75, and 90 °C for periods of 10, 30, and 60 minutes. The resulting proteins were analyzed by SDS-PAGE. The PAT protein remained detectable by SDS-PAGE, i.e., no protein degradation, at all temperatures and time points tested. These results corroborated the results obtained by Wehrmann et al. (1996) showing that the PAT protein was completely heat inactivated after 10 minutes at 50 °C or higher temperatures despite the fact that the protein was not degraded. The results from the heat lability assessments support that the PAT protein is unstable at high temperatures and will be inactivated by many of the processes involved in food or animal processing (Hérouet et al., 2005).
- The PAT protein has been shown to degrade to non-detectable levels within 5 seconds after digestion in SGF containing pepsin or SIF containing pancreatin (Hérouet et al., 2005; OECD, 1999).
- Glycoprotein staining analysis confirmed the absence of glycosylation for PAT protein (Hérouet et al., 2005)
- The PAT protein was evaluated for acute oral toxicity in mice, and the dose tested was 6,000 mg of test material per kg body weight. When adjusted for purity of the test material (84% pure or 0.84 mg PAT/mg powder), the dose was 5,000 mg PAT protein per kg body weight. During the two-week observation period, mortality and/or clinical or behavioral signs of pathology as well as body weights were recorded. Gross necropsies were conducted at the end of the study. The results showed no mortality occurred during the course of the study. Additionally, no adverse clinical signs were observed during the study and no adverse findings were noted at necropsy. Therefore, the acute oral LD_{50} for the PAT protein in mice could not be determined and is estimated to be higher than 5,000 mg PAT per kg body weight [redacted] 2000).

Conclusions on the Safety of PAT Protein in DP23211 Maize

The amino acid sequence of the PAT protein present in DP23211 maize was demonstrated to be identical to the corresponding protein found in a number of authorized GM events across several different crops that are currently in commercial use. Protein characterisation results via SDS-PAGE, western blot, peptide mapping, N-terminal amino acid sequence, and glycoprotein analysis have demonstrated that the PAT protein derived from DP23211 maize is of the expected molecular weight, immunoreactivity, amino acid sequence, and showed a lack of glycosylation.

The PAT protein has been risk-assessed in previously authorized maize events and is unlikely to present significant risks to the environment, human, or animal health. Previous assessments of this protein included bioinformatic analyses, heat lability, digestibility, glycosylation, and acute protein toxicity studies. These previous assessments are relevant for the assessment of DP23211 maize. Updated bioinformatics comparisons of the PAT protein

sequence to known or putative allergen and toxin sequences support the original conclusions that the PAT protein is unlikely to be allergenic or toxic to humans or animals. These data support the conclusion that the PAT protein in DP23211 maize is as safe as conventional maize for the food and feed supply.

Based on this weight of evidence, consumption of the PAT protein is unlikely to cause an adverse effect on humans or animals.

c. PMI Protein

Amino Acid Sequence

The gene encoding the PMI protein in DP23211 maize, referred to as the *pmi* gene, was isolated from *Escherichia coli.* PMI served as a selectable marker during transformation which allowed for tissue growth using mannose as the carbon source. The deduced amino acid sequence from translation of the *pmi* gene is 391 amino acids in length and has a molecular weight of approximately 43 kDa (**Figure 38; [redacted] 2018**).

```
  1   MQKLINSVQN YAWGSKTALT ELYGMENPSS QPMAELWMGA HPKSSSRVQN
 51   AAGDIVSLRD VIESDKSTLL GEAVAKRFGE LPFLFKVLCA AQPLSIQVHP
101   NKHNSEIGFA KENAAGIPMD AAERNYKDPN HKPELVFALT PFLAMNAFRE
151   FSEIVSLLQP VAGAHPAIAH FLQQPDAERL SELFASLLNM QGEEKSRALA
201   ILKSALDSQQ GEPWQTIRLI SEFYPEDSGL FSPLLLNVVK LNPGEAMFLF
251   AETPHAYLQG VALEVMANSD NVLRAGLTPK YIDIPELVAN VKFEAKPANQ
301   LLTQPVKQGA ELDFPIPVDD FAFSLHDLSD KETTISQQSA AILFCVEGDA
351   TLWKGSQQLQ LKPGESAFIA ANESPVTVKG HGRLARVYNK L*
```

Figure 38. Deduced Amino Acid Sequence of the PMI Protein
The deduced amino acid sequence from the translation of the *pmi* gene from plasmid PHP74643. The asterisk (*) indicates the translational stop codon. The full-length protein is 391 amino acids in length and has a molecular weight of approximately 43 kDa.

Function and Activity of the PMI Protein

The mode of action of PMI has been previously characterized and described (Negrotto et al., 2000; Privalle, 2002; Reed et al., 2001; Weisser et al., 1996). PMI is widely present in nature and is expressed in fungi, insects, plants, and mammals (Slein, 1950; US-EPA, 2004). The United States EPA has granted an exemption from the requirement of a tolerance for the PMI protein as an inert ingredient in plants (US-EPA, 2004). The PMI protein catalyzes the reversible interconversion between mannose-6-phosphate and fructose-6-phosphate. Mannose is phosphorylated by hexokinase to mannose-6-phosphate and in the presence of PMI enters the glycolytic pathway after isomerization to fructose 6-phosphate. In the absence of PMI, mannose-6-phosphate accumulates in the plant cells and inhibits glycolysis; additionally, high levels of mannose can lead to other impacts on photosynthesis and ATP production (Negrotto et al., 2000; Privalle, 2002). However, in the presence of PMI, plant cells may survive on media containing mannose as a carbon source, thus allowing PMI to be utilized as a selectable marker (Negrotto et al., 2000; Reed et al., 2001).

Characterisation of the PMI Protein Derived from DP23211 Maize

The DP23211 maize-expressed PMI protein was characterized using SDS-PAGE analysis, western blot analysis, peptide mapping by mass spectrometry, N-terminal amino acid sequencing, and glycoprotein analysis ([redacted] 2019). The results demonstrated that the PMI protein derived from DP23211 maize is of the expected molecular weight, immunoreactivity, amino acid sequence, and showed a lack of glycosylation.

SDS-PAGE Analysis

Samples of PMI protein purified from DP23211 maize whole plant tissue were analyzed by SDS-PAGE. As expected, all PMI protein samples migrated as a predominant band consistent with the expected molecular weight of approximately 43 kDa (**Figure 39**).

Additional details regarding SDS-PAGE analytical methods are provided in **Appendix F**.

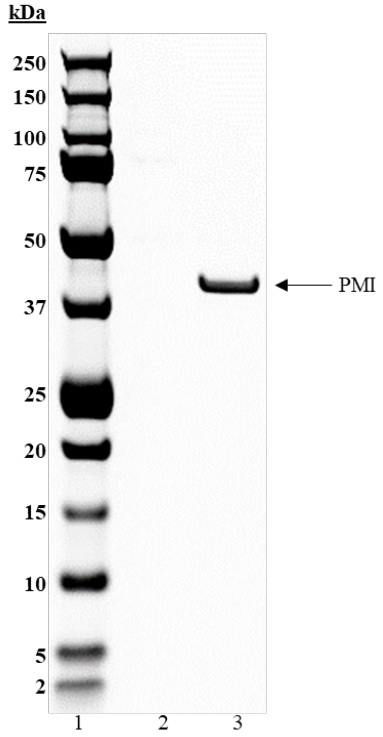

Lane	Sample Identification
1	Pre-stained Protein Molecular Weight Marker[a]
2	1X LDS Sample Buffer Blank
3	DP23211 Maize-Derived PMI Protein

Note: kilodalton (kDa).

[a] Molecular weight markers were included to provide a visual estimate that migration was within the expected range of the predicted molecular weight.

Figure 39. SDS-PAGE Analysis of DP23211 Maize-Derived PMI Protein

Western Blot Analysis

Samples of PMI protein purified from DP23211 maize whole plant tissue were analysed by Western blot. As expected, all PMI protein samples were immunoreactive to a PMI monoclonal antibody and visible as a predominant band consistent with the expected molecular weight of approximately 43 kDa (**Figure 40**).

Additional details regarding western blot analytical methods are provided in **Appendix F**.

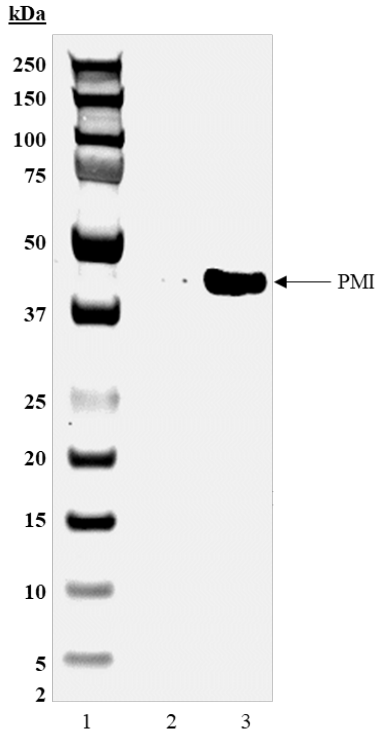

Lane	Sample Identification
1	Pre-stained Protein Molecular Weight Marker[a]
2	1X LDS Sample Buffer Blank
3	DP23211 Maize-Derived PMI Protein

Note: kilodalton (kDa).

[a] Molecular weight markers were included to provide a visual estimate that migration was within the expected range of the predicted molecular weight.

Figure 40. Western Blot Analysis of DP23211 Maize-Derived PMI Protein

LC-MS Peptide Mapping and N-Terminal Amino Acid Sequencing Analyses

Two samples of PMI protein purified from DP23211 maize whole plant tissue were analysed by SDS-PAGE. Protein bands were stained with Coomassie stain reagent, and the band containing PMI protein was excised for each sample. The DP23211 maize-derived excised PMI protein bands were digested with trypsin and chymotrypsin. Digested samples were analyzed using LC-MS, and an MS/MS ion search was used to match the detected peaks to peptides from the expected PMI protein sequence.

The analysis identified a total of 346 unique peptides from the trypsin- and chymotrypsin-derived PMI protein derived from DP23211 maize, representing 88% of the deduced PMI protein sequence containing 391 amino acids (**Tables 23** to **25** and **Figure 41**). The N-terminal peptide was identified as MQKLINSVQNY from the chymotryptic digestion and the sequence matched amino acid residues 1-11 of the expected protein sequence (**Figure 42**). The results indicated the N-terminal methionine residue of the protein was acetylated.

Additional details regarding peptide mapping and N-terminal amino acid sequencing analytical methods are provided in **Appendix F**.

Table 23. Combined Sequence Coverage of Identified Tryptic and Chymotryptic Peptides of DP23211 Maize-Derived PMI Protein Using LC-MS Analysis

Protease	% Coverage	Combined % Coverage
Trypsin	52	88
Chymotrypsin	68	

Table 24. Identified Tryptic Peptides of DP23211 Maize-Derived PMI Protein Using LC-MS Analysis

Matched Residue Position	Experimental Mass[a]	Theoretical Mass[b]	Identified Peptide Sequence
4–16	1478.7461	1478.7518	LINSVQNYAWGSK
17–43	2988.3849	2988.3819	TALTELYGMENPSSQPMAELWMGAHPK
48–59	1241.6656	1241.6728	VQNAAGDIVSLR
48–66	2028.0412	2028.0487	VQNAAGDIVSLRDVIESDK
60–66	804.3812	804.3865	DVIESDK
60–76	1773.926	1773.9360	DVIESDKSTLLGEAVAK
67–76	987.5541	987.5600	STLLGEAVAK
77–86	1252.6911	1252.6968	RFGELPFLFK
78–86	1096.5882	1096.5957	FGELPFLFK
87–102	1773.9469	1773.9560	VLCAAQPLSIQVHPNK
103–111	1001.4864	1001.4930	HNSEIGFAK
112–124	1343.6072	1343.6139	ENAAGIPMDAAER
180–195	1807.8989	1807.9026	LSELFASLLNMQGEEK
198–203	627.427	627.4319	ALAILK
204–218	1714.8196	1714.8275	SALDSQQGEPWQTIR
281–292	1372.7543	1372.7602	YIDIPELVANVK
293–307	1682.926	1682.9355	FEAKPANQLLTQPVK
355–379	2598.3459	2598.3653	GSQQLQLKPGESAFIAANESPVTVK

[a] The experimental mass is the uncharged mass calculated from the mass to charge ratio of the observed ion.

[b] The theoretical mass is the *in silico* generated mass that matches closest to the experimental mass.

Table 25. Identified Chymotryptic Peptides of DP23211 Maize-Derived PMI Protein Using LC-MS Analysis

Matched Residue Position	Experimental Mass[a]	Theoretical Mass[b]	Identified Peptide Sequence
1–11	1378.6872	1378.6915	MQKLINSVQNY+ Acetyl (Protein N-term)
5–11	836.3979	836.4028	INSVQNY
14–23	1081.5597	1081.5655	GSKTALTELY
24–37	1575.6651	1575.6697	GMENPSSQPMAELW
86–94	998.5526	998.5583	KVLCAAQPL
89–94	658.3073	658.3108	CAAQPL
95–126	3507.6818	3507.6953	SIQVHPNKHNSEIGFAKENAAGIPMDAAERNY
110–126	1819.8459	1819.8522	AKENAAGIPMDAAERNY
127–137	1322.6929	1322.6983	KDPNHKPELVF
143–148	665.3189	665.3207	LAMNAF
143–151	1097.526	1097.5277	LAMNAFREF
152–171	2056.1043	2056.1105	SEIVSLLQPVAGAHPAIAHF
158–171	1427.7612	1427.7674	LQPVAGAHPAIAHF
185–199	1645.8387	1645.8457	ASLLNMQGEEKSRAL
189–199	1261.6004	1261.6084	NMQGEEKSRAL
200–214	1641.831	1641.8362	AILKSALDSQQGEPW
203–214	1344.6274	1344.6310	KSALDSQQGEPW
237–248	1317.6698	1317.6751	NVVKLNPGEAMF
249–257	1047.4969	1047.5025	LFAETPHAY
250–257	934.4132	934.4185	FAETPHAY
251–257	787.3462	787.3501	AETPHAY
258–273	1671.8471	1671.8502	LQGVALEVMANSDNVL
259–273	1558.764	1558.7661	QGVALEVMANSDNVL
264–273	1090.4913	1090.4965	EVMANSDNVL
303–323	2333.157	2333.1580	TQPVKQGAELDFPIPVDDFAF
324–343	2156.0912	2156.0961	SLHDLSDKETTISQQSAAIL
344–353	1196.5122	1196.5172	FCVEGDATLW
345–353	1049.4431	1049.4488	CVEGDATLW
354–368	1616.8449	1616.8522	KGSQQLQLKPGESAF
360–368	975.4969	975.5025	QLKPGESAF
369–384	1647.8966	1647.9056	IAANESPVTVKGHGRL
369–388	2137.1677	2137.1756	IAANESPVTVKGHGRLARVY

[a] The experimental mass is the uncharged mass calculated from the mass to charge ratio of the observed ion.

[b] The theoretical mass is the *in silico* generated mass that matches closest to the experimental mass.

```
  1 MQKLINSVQN YAWGSKTALT ELYGMENPSS QPMAELWMGA HPKSSSRVQN
 51 AAGDIVSLRD VIESDKSTLL GEAVAKRFGE LPFLFKVLCA AQPLSIQVHP
101 NKHNSEIGFA KENAAGIPMD AAERNYKDPN HKPELVFALT PFLAMNAFRE
151 FSEIVSLLQP VAGAHPAIAH FLQQPDAERL SELFASLLNM QGEEKSRALA
201 ILKSALDSQQ GEPWQTIRLI SEFYPEDSGL FSPLLLNVVK LNPGEAMFLF
251 AETPHAYLQG VALEVMANSD NVLRAGLTPK YIDIPELVAN VKFEAKPANQ
301 LLTQPVKQGA ELDFPIPVDD FAFSLHDLSD KETTISQQSA AILFCVEGDA
351 TLWKGSQQLQ LKPGESAFIA ANESPVTVKG HGRLARVYNK L
```

Gray shading	Gray-shadedd type indicates maize-derived PMI peptides identified using LC-MS analysis.
Amino acid residue abbreviations	alanine (A), cysteine (C), aspartic acid (D), glutamic acid (E), phenylalanine (F), glycine (G), histidine (H), isoleucine (I), lysine (K), leucine (L), methionine (M), asparagine (N), proline (P), glutamine (Q), arginine (R), serine (S), threonine (T), tryptophan (W), tyrosine (Y), and valine (V).

Figure 41. Identified Tryptic and Chymotryptic Peptide Amino Acid Sequence of DP23211 Maize-Derived PMI Protein Using LC-MS Analysis

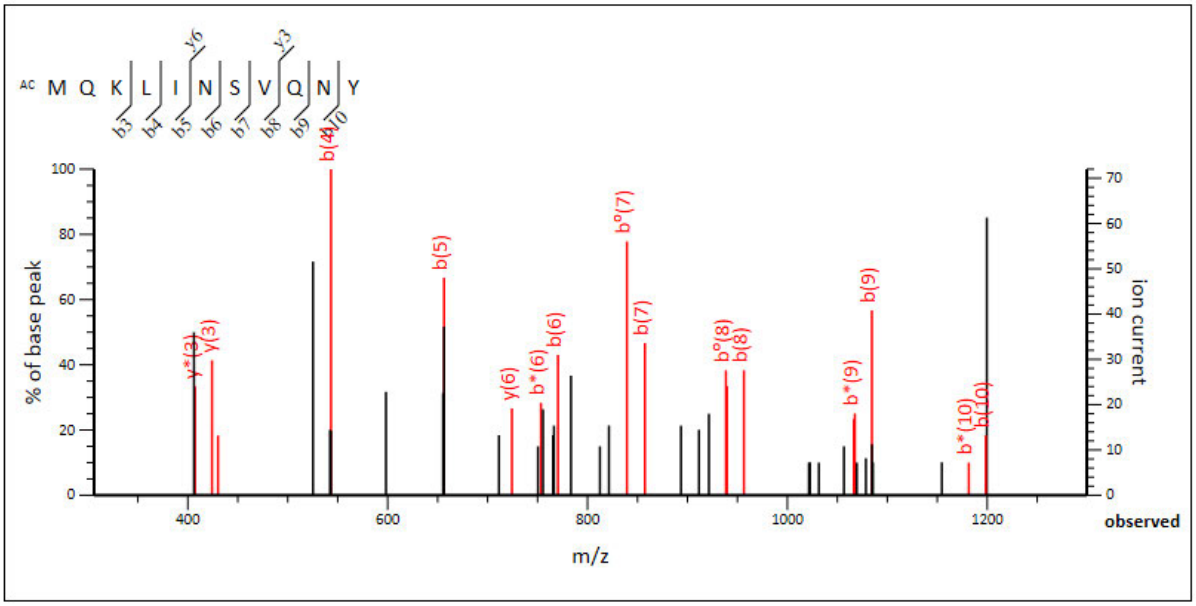

Note: The N-terminal peptide was identified as MQKLINSVQNY from the chymotryptic digestion of the DP23211 maize-derived PMI protein by LC-MS analysis. The N-terminal methionine residue of the protein was acetylated (Ac). The mass spectrometry data show the mass to charge ratio (m/z) versus the intensity of the observed peptide fragment ions. The peptides were fragmented at the amide bond yielding b- and y-ions. Peaks labeled "b" or "y" represent ions where the charge is retained on the N-terminus or C-terminus, respectively. The number after the b- or y-ion corresponds to the peptide fragmentation site.

Figure 42. Identified N-Terminal Peptide Amino Acid Sequence with Acetylated Methionine of DP23211 Maize-Derived PMI Protein Using LC-MS Analysis

Glycosylation Analysis

Samples of PMI protein purified from DP23211 maize whole plant tissue were analysed by SDS-PAGE. Each gel also included a positive control (horseradish peroxidase) and negative control (soybean trypsin inhibitor). The gels were stained using a Pierce Glycoprotein Staining Kit to visualize any glycoproteins. The gels were imaged and then stained with GelCode Blue stain reagent to visualize all protein bands.

Glycosylation was not detected for the PMI protein (**Figure 43**). The horseradish peroxidase positive control was stained and clearly visible as a magenta-colored band. The soybean trypsin inhibitor negative control was not stained by the glycoprotein stain.

Additional details regarding glycosylation analytical methods are provided in **Appendix F**.

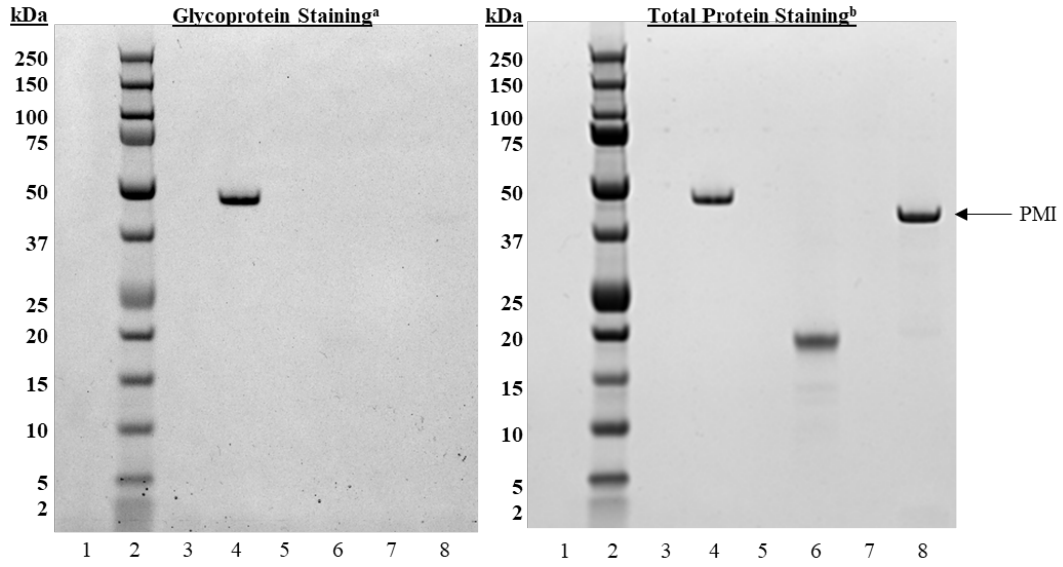

Lane	Sample Identification
1	1X LDS Sample Buffer Blank
2	Pre-stained Protein Molecular Weight Marker[c]
3	1X LDS Sample Buffer Blank
4	Horseradish Peroxidase (1.0 µg)
5	1X LDS Sample Buffer Blank
6	Soybean Trypsin Inhibitor (1.0 µg)
7	1X LDS Sample Buffer Blank
8	DP23211 Maize-Derived PMI Protein

Note: kilodalton (kDa), microgram (µg).

[a] Gel was stained with glycoprotein staining reagent.

[b] Gel was stained with glycoprotein staining reagent followed by staining with Coomassie Blue Reagent for total proteins.

[c] Molecular weight markers were included to provide a visual estimate that migration was within the expected range of the predicted molecular weight.

Figure 43. Glycosylation Analysis of DP23211 Maize-Derived PMI Protein

Allergenicity and Toxicity Analyses of the PMI Protein

The phosphomannose isomerase (PMI) protein has been previously assessed in Australia as part of the authorization for event 5307 (FSANZ Application 1001) and Corteva Agriscience references the PMI protein data and study reports previously submitted by Syngenta to FSANZ as part of these regulatory approvals (see enclosed Letter of Authorization to Refer to Regulatory Data provided by Syngenta).

The PMI protein has been risk-assessed in previously authorized maize events and has been determined to be unlikely to be a potential allergen or toxin to humans and animals. Previous assessments of this protein included heat lability, digestibility, glycosylation, and acute protein toxicity studies and are relevant for the assessment of DP23211 maize (USDA-APHIS, 2011). Updated bioinformatic analyses support the original conclusions that the PMI protein is unlikely to be an allergen or toxin. These data support the conclusion that the PMI protein in DP23211 maize is safe for the food and feed supply.

Bioinformatic Analysis of PMI Protein Homology to Known or Putative Allergens

Please find below a summary outlining the bioinformatics analyses, derived from the study report [redacted] 2019a), provided by Syngenta Biotechnology, Inc.

Using the same bioinformatic parameters, an updated in silico analysis was conducted on the PMI amino acid sequence to search for any similarity with known allergens. A full-length sequence search using FASTA identified no significant sequence alignments with known or putative allergens. A search for exact matches of eight of more contiguous amino acid residues revealed a single match with α-parvalbumin from frog (Rana species CH-2001). This match was also reported in previous assessments. To investigate this match in greater detail, immunological testing was undertaken using serum IgE antibody screening. Serum from a single individual with demonstrated IgE-mediated allergy to this specific α-parvalbumin from Rana species, did not react with any portion of PMI. Based on the updated bioinformatic analysis, there is no indication that PMI shares structural similarity with known or putative protein allergens that would raise concerns about potential allergenicity.

Bioinformatic Analysis of PMI Protein Homology to Known or Putative Toxins

The summary below is based on information of the study [redacted] 2019b) provided by Syngenta Biotechnology, Inc.The NCBI Entrez® Protein Database search identified 1000 sequences with potentially significant similarity to the PMI amino acid sequence (i.e., *E*-values less than 1×10^{-5}). All 1000 of these sequences were grouped into categories and then grouped by the source organism for each set of sequences. Of the 1000 sequences, all were identified as PMI or related proteins. The *E*-values for alignments between these sequences and the PMI amino acid sequence were all 0, indicating that all aligning sequences were also PMI proteins.

There were no alignments between the PMI amino acid sequence and any proteins in the Syngenta toxin database with significant sequence similarity (*E*-value < 1×10^{-5}). Five alignments below the upper reportable *E*-value (*E*-value < 10) were observed. The most similar alignment with a protein from the database had an *E*-value of 2.07901. This *E*-value is greater than the significance threshold *E*-value of 1×10^{-5} and indicates that the alignment is unlikely to be of biological relevance.

An assessment of the PMI amino acid sequence using a comprehensive similarity search of a non-redundant NCBI Entrez® Protein Database and a toxin-specific database created from the NCBI Entrez® Protein listing (2019)

supports the conclusion that the PMI amino acid sequence shows no biologically relevant similarity to any known or putative toxins.

Conclusions on the Safety of PMI Protein in DP23211 Maize

Protein characterisation results via SDS-PAGE, western blot, peptide mapping, N-terminal amino acid sequence, and glycoprotein analysis have demonstrated that the PMI protein derived from DP23211 maize is of the expected molecular weight, immunoreactivity, amino acid sequence, and showed a lack of glycosylation.

The PMI protein has been risk-assessed in previously authorized maize events and is unlikely to present significant risks to the environment, human, or animal health. Previous assessments of this protein included bioinformatic analyses, heat lability, digestibility, glycosylation, and acute protein toxicity studies. These previous assessments are relevant for the assessment of DP23211 maize. Updated bioinformatics comparisons of the PMI protein sequence to known or putative allergen and toxin sequences support the original conclusions that the PMI protein is unlikely to be allergenic or toxic to humans or animals. These data support the conclusion that the PMI protein in DP23211 maize is as safe as conventional maize for the food and feed supply.

Based on this weight of evidence, consumption of the PMI protein is unlikely to cause an adverse effect on humans or animals.

B.5 Compositional analyses of the food produced

a. Trait Expression Assessment

The concentration levels of DvSSJ1 dsRNA and the IPD072Aa, PAT, and PMI proteins were evaluated in DP23211 maize [redacted] 2019a; [redacted] 2019c).

Tissue samples were collected during the 2018 growing season at six sites in commercial maize-growing regions of the United States and Canada. A randomized complete block design with four blocks was utilized at each site. The following tissue samples were collected: root (V6, V9, R1, R4, and R6 growth stages), leaf (V9, R1, R4, and R6 growth stages), pollen (R1 growth stage), forage (R4 growth stage), whole plant (R1 and R6 growth stages), and grain (R6 growth stage). Concentrations of DvSSJ1 dsRNA were determined using a QuantiGene Plex Assay and concentrations of the IPD072Aa, PAT, and PMI proteins were determined using quantitative enzyme-linked immunosorbent assays (ELISAs). All assays were internally validated to demonstrate method suitability.

Concentration results (means, ranges, and standard deviations) are summarized across sites in **Tables 26** to **29** for DvSSJ1 dsRNA, IPD072Aa protein, PAT protein, and PMI protein, respectively. Individual sample results below the LLOQ were assigned a value equal to half of the LLOQ for calculation purposes.

Additional details regarding analytical methods and calculations for trait expression analysis are provided in **Appendix G**.

Table 26. Across-Sites Summary of DvSSJ1 dsRNA Concentrations in DP23211 Maize

Tissue (Growth Stage)	µg DvSSJ1 dsRNA/g Tissue Fresh Weight				Number of Samples <LLOQ/ Number of Samples Reported	µg DvSSJ1 dsRNA/g Tissue Dry Weight		
	Mean	Range	Standard Deviation	Sample LLOQ[a]		Mean	Range	Standard Deviation
DP23211 Maize								
Root (V6)	5.91×10^{-3}	3.73×10^{-3} - 8.77×10^{-3}	1.46×10^{-3}	5.55×10^{-5}	0/24	5.13×10^{-2}	2.22×10^{-2} - 9.44×10^{-2}	2.08×10^{-2}
Root (V9)	4.51×10^{-3}	2.44×10^{-3} - 7.05×10^{-3}	1.27×10^{-3}	5.55×10^{-5}	0/24	3.74×10^{-2}	1.95×10^{-2} - 8.70×10^{-2}	1.48×10^{-2}
Root (R1)	4.08×10^{-3}	2.42×10^{-3} - 6.28×10^{-3}	1.07×10^{-3}	5.55×10^{-5}	0/24	2.91×10^{-2}	1.52×10^{-2} - 5.85×10^{-2}	1.00×10^{-2}
Root (R4)	2.88×10^{-3}	1.34×10^{-3} - 4.51×10^{-3}	8.36×10^{-4}	5.55×10^{-5}	0/24	1.84×10^{-2}	7.77×10^{-3} - 3.56×10^{-2}	6.69×10^{-3}
Root (R6)	1.84×10^{-3}	1.90×10^{-4} - 4.76×10^{-3}	1.34×10^{-3}	5.55×10^{-5}	0/24	1.15×10^{-2}	1.50×10^{-3} - 3.57×10^{-2}	8.31×10^{-3}
Leaf (V9)	1.33×10^{-2}	6.59×10^{-3} - 2.90×10^{-2}	4.84×10^{-3}	2.52×10^{-4}	0/24	5.92×10^{-2}	3.43×10^{-2} - 9.85×10^{-2}	1.34×10^{-2}
Leaf (R1)	1.30×10^{-2}	5.61×10^{-3} - 2.84×10^{-2}	5.13×10^{-3}	2.52×10^{-4}	0/24	4.97×10^{-2}	2.35×10^{-2} - 9.67×10^{-2}	1.79×10^{-2}
Leaf (R4)	2.25×10^{-2}	9.80×10^{-3} - 3.79×10^{-2}	6.95×10^{-3}	2.52×10^{-4}	0/24	6.46×10^{-2}	2.43×10^{-2} - 1.13×10^{-1}	2.32×10^{-2}
Leaf (R6)	8.10×10^{-3}	1.77×10^{-3} - 2.67×10^{-2}	6.64×10^{-3}	2.52×10^{-4}	0/24	1.32×10^{-2}	2.40×10^{-3} - 3.31×10^{-2}	1.05×10^{-2}
Pollen (R1)	5.59×10^{-4}	3.30×10^{-4} - 9.60×10^{-4}	1.27×10^{-4}	2.64×10^{-4}	0/24	9.87×10^{-4}	5.61×10^{-4} - 2.02×10^{-3}	3.09×10^{-4}
Forage (R4)	5.15×10^{-3}	2.64×10^{-3} - 1.77×10^{-2}	3.31×10^{-3}	7.97×10^{-5}	0/24	1.90×10^{-2}	9.77×10^{-3} - 5.65×10^{-2}	1.07×10^{-2}
Whole Plant (R1)	3.64×10^{-3}	2.23×10^{-3} - 6.41×10^{-3}	9.24×10^{-4}	6.85×10^{-5}	0/24	2.19×10^{-2}	1.27×10^{-2} - 3.59×10^{-2}	5.10×10^{-3}
Whole Plant (R6)	4.13×10^{-3}	1.53×10^{-3} - 1.20×10^{-2}	2.45×10^{-3}	6.85×10^{-5}	0/22	1.08×10^{-2}	4.59×10^{-3} - 2.99×10^{-2}	5.40×10^{-3}
Grain (R6)	3.22×10^{-3}	1.02×10^{-3} - 7.27×10^{-3}	1.61×10^{-3}	6.94×10^{-5}	0/24	4.13×10^{-3} [b]	1.22×10^{-3} - 1.09×10^{-2}	2.36×10^{-3}

Note: Growth stages are adapted from Abendroth et al. (2011).

[a] Lower limit of quantification (LLOQ) in µg/g tissue fresh weight.

[b] One sample from the respective tissue/growth stage was not included in the dry weight mean because fresh weight : dry weight ratio could not be calculated due to insufficient sample weight after lyophilization.

Table 27. Across-Sites Summary of IPD072Aa Protein Concentrations in DP23211 Maize

Tissue (Growth Stage)	ng IPD072Aa/mg Tissue Dry Weight				Number of Samples <LLOQ/ Number of Samples Reported
	Mean	Range	Standard Deviation	Sample LLOQ	
DP23211 Maize					
Root (V6)	25	4.2 - 60	16	0.11	0/24
Root (V9)	19	3.6 - 84	23	0.11	0/24
Root (R1)	21	7.5 - 51	8.8	0.11	0/24
Root (R4)	24	6.6 - 42	8.5	0.11	0/24
Root (R6)	31	0.93 - 72	21	0.11	0/24
Leaf (V9)	13	2.8 - 39	11	0.054	0/24
Leaf (R1)	16	5.5 - 33	7.6	0.054	0/24
Leaf (R4)	10	5.8 - 15	2.5	0.054	0/24
Leaf (R6)	1.6[a]	<0.054 - 10	2.5[a]	0.054	1/24
Pollen (R1)	0.65	0.14 - 1.3	0.38	0.11	0/24
Whole Plant (R1)	7.9	2.4 - 14	2.3	0.018	0/24
Whole Plant (R6)	11	1.7 - 24	7.5	0.018	0/24
Forage (R4)	16	6.0 - 28	7.2	0.018	0/24
Grain (R6)	2.1	0.51 - 4.8	1.2	0.027	0/24

Note: Growth stages (Abendroth et al., 2011). Lower limit of quantification (LLOQ) in ng/mg tissue dry weight. [a] Some, but not all, sample results were below the LLOQ. A value equal to half the LLOQ value was assigned to those samples to calculate the mean and standard deviation.

Table 28. Across-Sites Summary of PAT Protein Concentrations in DP23211 Maize

Tissue (Growth Stage)	ng PAT/mg Tissue Dry Weight				Number of Samples <LLOQ/ Number of Samples Reported
	Mean	Range	Standard Deviation	Sample LLOQ	
DP23211 Maize					
Root (V6)	7.7	2.2 - 11	2.6	0.054	0/24
Root (V9)	4.5	2.4 - 7.8	1.4	0.054	0/24
Root (R1)	3.5	1.6 - 5.1	0.93	0.054	0/24
Root (R4)	1.6	0.66 - 3.9	1.0	0.054	0/24
Root (R6)	0.65[a]	<0.054 - 2.3	0.65[a]	0.054	4/24
Leaf (V9)	7.6	4.0 - 11	1.9	0.11	0/24
Leaf (R1)	7.8	5.3 - 13	1.5	0.11	0/24
Leaf (R4)	3.6	2.3 - 6.6	1.2	0.11	0/24
Leaf (R6)	<0.11	<0.11	ND	0.11	24/24
Pollen (R1)	58	47 - 85	13	0.22	0/24
Whole Plant (R1)	9.2	6.2 - 14	2.0	0.036	0/24
Whole Plant (R6)	1.1[a]	<0.036 - 4.0	1.2[a]	0.036	2/24
Forage (R4)	8.2	4.8 - 11	1.7	0.036	0/24
Grain (R6)	5.1	2.5 - 8.1	1.6	0.054	0/24

Note: Growth stages (Abendroth et al., 2011). Lower limit of quantification (LLOQ) in ng/mg tissue dry weight. Not determined (ND); all samples were below the LLOQ.

[a] Some, but not all, sample results were below the LLOQ. A value equal to half the LLOQ value was assigned to those samples to calculate the mean and standard deviation.

Table 29. Across-Sites Summary of PMI Protein Concentrations in DP23211 Maize

Tissue (Growth Stage)	ng PMI/mg Tissue Dry Weight				Number of Samples <LLOQ/ Number of Samples Reported
	Mean	Range	Standard Deviation	Sample LLOQ	
DP23211 Maize					
Root (V6)	12	5.7 - 21	4.4	0.27	0/24
Root (V9)	6.5	3.3 - 11	2.2	0.27	0/24
Root (R1)	5.3	2.7 - 11	1.9	0.27	0/24
Root (R4)	3.7	2.1 - 5.4	0.96	0.27	0/24
Root (R6)	2.6[a]	<0.27 - 5.7	1.6[a]	0.27	3/24
Leaf (V9)	11	6.6 - 20	3.4	0.54	0/24
Leaf (R1)	12	7.2 - 19	2.7	0.54	0/24
Leaf (R4)	29	17 - 43	6.7	0.54	0/24
Leaf (R6)	0.30[a]	<0.54 - 0.66	0.097[a]	0.54	22/24
Pollen (R1)	33	28 - 43	4.4	1.1	0/24
Whole Plant (R1)	8.9	7.0 - 12	1.4	1.8	0/24
Whole Plant (R6)	3.6[a]	<1.8 - 8.8	2.2[a]	1.8	7/24
Forage (R4)	9.4	6.2 - 17	2.3	1.8	0/24
Grain (R6)	4.3	2.3 - 6.3	1.1	0.27	0/24

Note: Growth stages (Abendroth et al., 2011). Lower limit of quantification (LLOQ) in ng/mg tissue dry weight.

[a] Some, but not all, sample results were below the LLOQ. A value equal to half the LLOQ value was assigned to those samples to calculate the mean and standard deviation.

b. Nutrient Composition Assessment

An assessment of the compositional equivalence of a GM product compared to that of a conventional non-GM comparator with a history of safe use in food and feed is an important part of the weight-of-evidence approach used to evaluate the safety of genetically modified plant products (Codex Alimentarius Commission, 2008; OECD, 1993). Compositional assessments of DP23211 maize were evaluated in comparison to concurrently grown non-GM, near-isoline maize (referred to as control maize) to identify statistical differences, and subsequently were evaluated in the context of natural variation established from multiple sources of non-GM, commercial maize data [redacted] 2019b).

Forage (R4 growth stage) and grain (R6 growth stage) samples were collected during the 2018 growing season at eight sites in commercial maize-growing regions of the United States and Canada. A randomized complete block design with four blocks was utilized at each site. Each block included DP23211 maize, non-GM near-isoline control maize, and four non-GM commercial maize reference lines.

The samples were assessed for key nutritional components. Proximates, fibers, and minerals were assessed in the forage samples (9 analytes total), and the grain sample assessment included proximates, fibers, fatty acids, amino acids, minerals, vitamins, secondary metabolites, and anti-nutrients analytes (70 analytes total). The analytes included in the compositional assessment were selected based on the OECD consensus document on compositional considerations for new varieties of maize (OECD, 2002). Procedures and methods for nutrient composition analyses of maize forage and grain were conducted in accordance with the requirements for the U.S. EPA Good Laboratory Practice (GLP) Standards, 40 CFR Part 160. The analytical procedures used were validated methods, with the majority based on methods published by AOAC International, AACC (American Association of Cereal Chemists), and AOCS (American Oil Chemists' Society).

Statistical analyses were conducted to evaluate and compare the nutrient composition of DP23211 maize and the control maize. A total of 69 analytes were analyzed using mixed model analysis. Three analytes did not meet criteria for sufficient quantities of observations above the LLOQ and therefore Fisher's exact test was performed instead of mixed model analysis. No statistical analysis was conducted on the remaining 7 analytes as all data values were below the LLOQ. For a given analyte in the mixed model analysis, if a statistical difference (P-value < 0.05) was observed between DP23211 maize and the control maize but the False Discovery Rate (FDR) adjusted P-value was non-significant, it was concluded that the difference was likely a false positive. Additionally, three reference ranges representing the non-GM maize population with a history of safe use (i.e., tolerance interval, literature range, and in-study reference range) were utilized to evaluate statistical differences in the context of natural variation. If the measured values of DP23211 maize for that analyte fell within at least one of the reference ranges, then this analyte would be considered comparable to conventional maize.

The outcome of the nutrient composition assessment is provided in **Table 30**. Nutrient composition analysis results are provided in **Tables 31** to **41**. No statistically significant differences were observed between DP23211 maize and the control maize for 66 of the 72 analytes that went through across-site analysis via either mixed model analysis or Fisher's exact test. All individual values for these analytes were within the tolerance interval, literature range, and/or in-study reference range, indicating DP23211 maize is within the range of natural variation for these analytes and the statistical differences are not biologically meaningful.

The results of the nutrient composition assessment demonstrated that nutrient composition of forage and grain derived from DP23211 maize was comparable to that of conventional maize represented by non-GM near-isoline control maize and non-GM commercial maize.

Additional details regarding methods for nutrient composition and statistical analyses are provided in **Appendix H**.

Table 30. Outcome of the Nutrient Composition Assessment for DP23211 Maize

Subgroup	No Statistical Difference Identified	Statistical Difference Identified					Not Included in Statistical Analysis (All Data Values Below the Lower Limit of Quantification)
		All Data Values Within Tolerance Interval	One or More Data Values Outside Tolerance Interval, or Tolerance Interval Not Available			Adjusted P-Value<0.05	
			All Data Values Within Literature Range	One or More Data Values Outside Literature Range, or Literature Range Not Available			
				All Data Values Within Reference Data Range	One or More Data Values Outside Reference Data Range, or Reference Data Range Not Available		
Forage (R4 Growth Stage)							
Proximate, Fiber, and Mineral Composition	Crude Protein Crude Fat Crude Fiber ADF NDF Ash Carbohydrates Calcium Phosphorus	--	--	--	--	--	--
Grain (R6 Growth Stage)							
Proximate and Fiber Composition	Total Dietary Fiber Crude Protein Crude Fat Crude Fiber ADF NDF Ash Carbohydrates	--	--	--	--	--	--
Fatty Acid Composition	Lauric Acid (C12:0) Palmitic Acid (C16:0) Palmitoleic Acid (C16:1) Heptadecanoic Acid (C17:0) Stearic Acid (C18:0) Linoleic Acid (C18:2) α-Linolenic Acid (C18:3) Eicosadienoic Acid (C20:2) Behenic Acid (C22:0) Lignoceric Acid (C24:0)	Oleic Acid (C18:1) Arachidic Acid (C20:0) Eicosenoic Acid (C20:1)	--	--	--	--	Myristic Acid (C14:0) Heptadecenoic Acid (C17:1) Erucic Acid (C22:1)

Table 30. Outcome of Nutrient Composition Assessment Across Sites (continued)

Subgroup	No Statistical Difference Identified	Statistical Difference Identified					Not Included in Statistical Analysis (All Data Values Below the Lower Limit of Quantification)
		All Data Values Within Tolerance Interval	One or More Data Values Outside Tolerance Interval, or Tolerance Interval Not Available			Adjusted P-Value<0.05	
			All Data Values Within Literature Range	One or More Data Values Outside Literature Range, or Literature Range Not Available			
				All Data Values Within Reference Data Range	One or More Data Values Outside Reference Data Range, or Reference Data Range Not Available		
Grain (R6 Growth Stage)							
Amino Acid Composition	Alanine Arginine Aspartic Acid Cystine Glutamic Acid Glycine Histidine Isoleucine Leucine Lysine Methionine Phenylalanine Proline Serine Threonine Tryptophan Tyrosine Valine	--	--	--	--	--	--
Mineral Composition	Calcium Copper Iron Magnesium Manganese Phosphorus Potassium Sodium Zinc	--	--	--	--	--	--

Table 30. Outcome of Nutrient Composition Assessment Across Sites (continued)

Subgroup	No Statistical Difference Identified	Statistical Difference Identified					Not Included in Statistical Analysis (All Data Values Below the Lower Limit of Quantification)
		All Data Values Within Tolerance Interval	One or More Data Values Outside Tolerance Interval, or Tolerance Interval Not Available			Adjusted P-Value<0.05	
			All Data Values Within Literature Range	One or More Data Values Outside Literature Range, or Literature Range Not Available			
				All Data Values Within Reference Data Range	One or More Data Values Outside Reference Data Range, or Reference Data Range Not Available		
Grain (R6 Growth Stage)							
Vitamin Composition	β-Carotene Vitamin B1 (Thiamine) Vitamin B3 (Niacin) Vitamin B5 (Pantothenic Acid) Vitamin B9 (Folic Acid) γ-Tocopherol Total Tocopherols	α-Tocopherol	Vitamin B6 (Pyridoxine)	--	--	--	Vitamin B2 (Riboflavin) β-Tocopherol δ-Tocopherol
Secondary Metabolite and Anti-Nutrient Composition	Ferulic Acid Inositol Phytic Acid Raffinose Trypsin Inhibitor	*p*-Coumaric Acid	--	--	--	--	Furfural

Note: Growth stages (Abendroth et al. 2011).

Proximates, Fiber, and Minerals in DP23211 Maize Forage

Proximates, fiber, and minerals were analyzed in forage derived from DP23211 maize and control maize. Results are shown in **Table 31**. No statistically significant differences (P-value < 0.05) were observed between DP23211 maize and control maize.

The results of the analysis of proximates, fiber, and minerals in maize forage demonstrate that DP23211 maize is comparable to conventional maize represented by non-GM near-isoline control maize and non-GM commercial maize.

Table 31. Proximates, Fiber, and Minerals Results for DP23211 Maize Forage

Analyte	Reported Statistics	Control Maize	DP23211 Maize	Tolerance Interval	Literature Range	Reference Data Range
	Mean	7.71	7.78			
	Range	5.53 - 9.94	3.94 - 10.3			
Crude Protein	Confidence Interval	6.75 - 8.67	6.82 - 8.73	3.44 - 12.4	2.37 - 16.32	4.79 - 10.5
	Adjusted P-Value	--	0.944			
	P-Value	--	0.725			
	Mean	4.14	3.93			
	Range	2.88 - 6.02	2.73 - 5.38			
Crude Fat	Confidence Interval	3.66 - 4.62	3.45 - 4.41	0.784 - 6.17	ND - 6.755	2.42 - 6.27
	Adjusted P-Value	--	0.833			
	P-Value	--	0.234			
	Mean	25.0	25.4			
	Range	17.6 - 32.5	18.4 - 33.9			
Crude Fiber	Confidence Interval	22.7 - 27.3	23.1 - 27.7	14.1 - 30.8	12.5 - 42	13.9 - 32.2
	Adjusted P-Value	--	0.911			
	P-Value	--	0.585			
	Mean	32.5	32.6			
	Range	23.3 - 42.0	23.6 - 43.1			
ADF	Confidence Interval	29.9 - 35.0	30.1 - 35.1	15.4 - 39.6	5.13 - 47.39	18.9 - 41.5
	Adjusted P-Value	--	0.999			
	P-Value	--	0.869			
	Mean	50.2	51.3			
	Range	42.0 - 64.3	41.9 - 60.7			
NDF	Confidence Interval	47.3 - 53.3	48.4 - 54.4	28.1 - 63.7	18.30 - 67.80	29.7 - 61.5
	Adjusted P-Value	--	0.911			
	P-Value	--	0.366			
	Mean	5.08	4.86			
	Range	2.46 - 7.83	3.19 - 7.74			
Ash	Confidence Interval	4.38 - 5.77	4.16 - 5.55	2.39 - 9.40	0.66 - 13.20	2.61 - 7.57
	Adjusted P-Value	--	0.796			
	P-Value	--	0.208			
	Mean	83.0	83.6			
	Range	77.9 - 87.0	77.3 - 91.2			
Carbohydrates	Confidence Interval	81.2 - 84.8	81.8 - 85.4	76.9 - 91.6	73.3 - 92.9	76.9 - 89.4
	Adjusted P-Value	--	0.796			
	P-Value	--	0.206			
	Mean	0.273	0.249			
	Range	0.170 - 0.422	0.139 - 0.438			
Calcium	Confidence Interval	0.233 - 0.314	0.209 - 0.289	0.0736 - 0.531	0.04 - 0.58	0.110 - 0.434
	Adjusted P-Value	--	0.550			
	P-Value	--	0.0739			
	Mean	0.237	0.246			
	Range	0.114 - 0.361	0.144 - 0.375			
Phosphorus	Confidence Interval	0.203 - 0.272	0.211 - 0.281	0.0844 - 0.428	0.07 - 0.55	0.159 - 0.371
	Adjusted P-Value	--	0.911			
	P-Value	--	0.516			

Note: Proximates, fiber, and minerals unit of measure is % dry weight. Not detectable (ND); one or more assay values in the published literature references were below the lower limit of quantification (LLOQ) and were not quantified.

Proximates and Fiber in DP23211 Maize Grain

Proximates and fiber were analyzed in grain derived from DP23211 maize and near-isoline control maize. Results are shown in **Table 32**. No statistically significant differences (P-value < 0.05) were observed between DP23211 maize and control maize.

The results of the analysis of proximates and fiber in maize grain demonstrate that DP23211 maize is comparable to conventional maize represented by non-GM near-isoline control maize and non-GM commercial maize.

Table 32. Proximates and Fiber Results for DP23211 Maize Grain

Analyte	Reported Statistics	Control Maize	DP23211 Maize	Tolerance Interval	Literature Range	Reference Data Range
Total Dietary Fiber	Mean	9.71	9.43			
	Range	8.19 - 11.7	7.67 - 12.0			
	Confidence Interval	9.18 - 10.2	8.89 - 9.96	3.15 - 21.8	5.78 - 35.31	4.44 - 13.4
	Adjusted P-Value	--	0.833			
	P-Value	--	0.260			
Crude Protein	Mean	10.6	10.6			
	Range	8.44 - 12.0	7.94 - 11.7			
	Confidence Interval	9.98 - 11.3	9.98 - 11.3	6.66 - 13.3	5.72 - 17.26	6.95 - 11.3
	Adjusted P-Value	--	0.999			
	P-Value	--	0.999			
Crude Fat	Mean	4.25	4.22			
	Range	3.63 - 4.87	3.48 - 4.94			
	Confidence Interval	4.09 - 4.42	4.05 - 4.39	2.34 - 5.90	1.363 - 7.830	3.66 - 5.41
	Adjusted P-Value	--	0.911			
	P-Value	--	0.495			
Crude Fiber	Mean	2.43	2.50			
	Range	1.97 - 2.71	2.13 - 3.02			
	Confidence Interval	2.28 - 2.58	2.35 - 2.65	1.57 - 3.61	0.49 - 5.5	2.02 - 3.14
	Adjusted P-Value	--	0.667			
	P-Value	--	0.155			
ADF	Mean	4.22	4.27			
	Range	3.22 - 4.84	3.04 - 5.16			
	Confidence Interval	3.92 - 4.53	3.96 - 4.57	2.64 - 6.24	1.41 - 11.34	3.20 - 5.69
	Adjusted P-Value	--	0.911			
	P-Value	--	0.637			
NDF	Mean	10.5	10.4			
	Range	8.12 - 12.8	8.18 - 13.4			
	Confidence Interval	9.73 - 11.3	9.60 - 11.2	7.49 - 18.6	4.28 - 24.3	8.15 - 13.3
	Adjusted P-Value	--	0.911			
	P-Value	--	0.526			
Ash	Mean	1.37	1.40			
	Range	1.24 - 1.49	1.24 - 1.54			
	Confidence Interval	1.33 - 1.41	1.36 - 1.44	1.01 - 1.87	0.616 - 6.282	1.04 - 1.49
	Adjusted P-Value	--	0.667			
	P-Value	--	0.150			
Carbohydrates	Mean	83.7	83.7			
	Range	82.4 - 85.9	82.6 - 86.1			
	Confidence Interval	83.1 - 84.4	83.1 - 84.3	80.5 - 88.5	77.4 - 89.7	82.9 - 87.6
	Adjusted P-Value	--	0.999			
	P-Value	--	0.932			

Note: Proximates and fiber unit of measure is % dry weight.

Fatty Acids in DP23211 Maize Grain

Fatty acids were analyzed in grain derived from DP23211 maize and near-isoline control maize. Results are shown in **Tables 33** and **34**.

A statistically significant difference (P-value < 0.05) was observed between DP23211 maize and control maize for three fatty acids: oleic acid (C18:1), arachidic acid (C20:0), and eicosenoic acid (C20:1). All individual values were within the respective tolerance interval, indicating DP23211 maize is within the range of natural variation for these analytes and the statistical differences are not biologically meaningful. The non-significant FDR-adjusted P-values indicate that these differences were likely false positives.

The results of the analysis of fatty acids in maize grain demonstrate that DP23211 maize is comparable to conventional maize represented by non-GM near-isoline control maize and non-GM commercial maize.

Table 33. Fatty Acid Results for DP23211 Maize Grain

Analyte	Reported Statistics	Control Maize	DP23211 Maize	Tolerance Interval	Literature Range	Reference Data Range
Lauric Acid (C12:0)	Mean	0.101	0.0899	0 - 0.209[r]	ND - 0.698	0.0360 - 0.271
	Range	0.0439 - 0.300	0.0432 - 0.311			
	Confidence Interval	NA	NA			
	Adjusted P-Value	--	NA			
	P-Value	--	NA			
Myristic Acid (C14:0)	Mean	<LLOQ[a]	<LLOQ[a]	0 - 0.267[r]	ND - 0.288	<LLOQ[a]
	Range	<LLOQ[a]	<LLOQ[a]			
	Confidence Interval	NA	NA			
	Adjusted P-Value	--	NA			
	P-Value	--	NA			
Palmitic Acid (C16:0)	Mean	13.5	13.5	9.33 - 24.7	6.81 - 39.0	11.1 - 18.0
	Range	13.1 - 13.9	13.0 - 14.0			
	Confidence Interval	13.3 - 13.7	13.3 - 13.6			
	Adjusted P-Value	--	0.985			
	P-Value	--	0.800			
Palmitoleic Acid (C16:1)	Mean	0.118	0.115	0 - 0.445	ND - 0.67	0.0562 - 0.195
	Range	0.0543 - 0.127	0.0514 - 0.149			
	Confidence Interval	0.114 - 0.122	0.111 - 0.119			
	Adjusted P-Value	--	0.833			
	P-Value	--	0.251			
Heptadecanoic Acid (C17:0)	Mean	0.0734	0.0822	0 - 0.236	ND - 0.203	0.0382 - 0.141
	Range	0.0454 - 0.105	0.0459 - 0.117			
	Confidence Interval	NA	NA			
	Adjusted P-Value	--	NA			
	P-Value	--	NA			
Heptadecenoic Acid (C17:1)	Mean	<LLOQ[a]	<LLOQ[a]	0 - 0.135[r]	ND - 0.131	<LLOQ[a]
	Range	<LLOQ[a]	<LLOQ[a]			
	Confidence Interval	NA	NA			
	Adjusted P-Value	--	NA			
	P-Value	--	NA			
Stearic Acid (C18:0)	Mean	1.73	1.76	1.31 - 3.83	ND - 4.9	1.60 - 2.33
	Range	1.58 - 1.94	1.60 - 2.02			
	Confidence Interval	1.64 - 1.82	1.68 - 1.85			
	Adjusted P-Value	--	0.550			
	P-Value	--	0.0583			
Oleic Acid (C18:1)	Mean	21.5	21.1	17.3 - 38.6	16.38 - 42.81	20.0 - 32.8
	Range	20.7 - 22.3	20.2 - 22.1			
	Confidence Interval	21.1 - 21.8	20.8 - 21.5			
	Adjusted P-Value	--	0.264			
	P-Value	--	0.00765[*]			
Linoleic Acid (C18:2)	Mean	60.1	60.4	30.7 - 65.5	13.1 - 67.68	49.8 - 62.6
	Range	58.6 - 60.8	59.0 - 61.5			
	Confidence Interval	59.7 - 60.4	60.0 - 60.7			
	Adjusted P-Value	--	0.550			
	P-Value	--	0.0698			
α-Linolenic Acid (C18:3)	Mean	1.70	1.70	0 - 1.90	ND - 2.33	1.35 - 2.02
	Range	1.54 - 1.84	1.47 - 1.94			
	Confidence Interval	1.64 - 1.76	1.65 - 1.76			
	Adjusted P-Value	--	0.999			
	P-Value	--	0.962			

Table 33. Fatty Acid Results for DP23211 Maize Grain (continued)

Analyte	Reported Statistics	Control Maize	DP23211 Maize	Tolerance Interval	Literature Range	Reference Data Range
Arachidic Acid (C20:0)	Mean	0.361	0.367			
	Range	0.332 - 0.399	0.337 - 0.399			
	Confidence Interval	0.348 - 0.373	0.355 - 0.379	0.295 - 0.872	0.267 - 1.2	0.328 - 0.539
	Adjusted P-Value	--	0.454			
	P-Value	--	0.0395*			
Eicosenoic Acid (C20:1)	Mean	0.306	0.313			
	Range	0.266 - 0.334	0.290 - 0.331			
	Confidence Interval	0.300 - 0.311	0.308 - 0.319	0 - 0.614	ND - 1.952	0.233 - 0.425
	Adjusted P-Value	--	0.377			
	P-Value	--	0.0245*			
Eicosadienoic Acid (C20:2)	Mean	<LLOQ[a]	0.0519			
	Range	<LLOQ[a]	0.0407 - 0.110			
	Confidence Interval	NA	NA	0 - 0.825[r]	ND - 2.551	0.0339 - 0.185
	Adjusted P-Value	--	NA			
	P-Value	--	NA			
Behenic Acid (C22:0)	Mean	0.191	0.178			
	Range	0.0951 - 0.227	0.0912 - 0.247			
	Confidence Interval	0.172 - 0.206	0.157 - 0.195	0 - 0.423	ND - 0.5	0.100 - 0.298
	Adjusted P-Value	--	0.658			
	P-Value	--	0.115			
Lignoceric Acid (C24:0)	Mean	0.278	0.279			
	Range	0.244 - 0.311	0.250 - 0.354			
	Confidence Interval	0.269 - 0.287	0.270 - 0.289	0 - 0.639	ND - 0.91	0.252 - 0.501
	Adjusted P-Value	--	0.911			
	P-Value	--	0.646			

Note: Fatty acids unit of measure is % total fatty acids. Fatty acids analyte erucic acid (C22:1) was not statistically analyzed because all sample values in the current study and in historical commercial reference lines were below the lower limit of quantification (LLOQ). This analyte was excluded from the report table. NA (not applicable): mixed model analysis was not performed or confidence interval was not determined. ND (not detectable): one or more assay values in the published literature references were below the lower limit of quantification (LLOQ) and were not quantified.

[a] < LLOQ, all fatty acid sample values in the current study were below the assay LLOQ. Statistical analysis was not performed for those analytes.

[r] A historical reference data range was provided as tolerance interval was not calculated since the data did not meet the assumptions of any tolerance interval calculation method.

* A statistically significant difference (P-Value <0.05) was observed.

Table 34. Number of Fatty Acid Sample Values Below the Lower Limit of Quantification for DP23211 Maize Grain

Analyte	Number of Samples Below the LLOQ		Fisher's Exact Test P-Value
	Control Maize (n=32)	DP23211 Maize (n=32)	
Lauric Acid (C12:0)	22	23	1.00
Myristic Acid (C14:0)	32	32	--
Palmitoleic Acid (C16:1)[a]	2	4	--
Heptadecanoic Acid (C17:0)	17	13	0.453
Heptadecenoic Acid (C17:1)	32	32	--
Eicosadienoic Acid (C20:2)	32	31	1.00
Behenic Acid (C22:0)[a]	9	14	--

Note: Fatty acids analyte erucic acid (C22:1) was not statistically analyzed because all sample values in the current study and in historical commercial reference lines were below the lower limit of quantification (LLOQ). This analyte was excluded from the report table.

[a] This analyte had <50% below-LLOQ sample values in both maize lines and was subjected to the mixed model analyses.

Amino Acids in DP23211 Maize Grain

Amino acids were analyzed in grain derived from DP23211 maize and near-isoline control maize. Results are shown in **Table 35**. No statistically significant differences (P-value < 0.05) were observed between DP23211 maize and control maize.

The results of the analysis of amino acids in maize grain demonstrate that DP23211 maize is comparable to conventional maize represented by non-GM near-isoline control maize and non-GM commercial maize.

Table 35. Amino Acid Results for DP23211 Maize Grain

Analyte	Reported Statistics	Control Maize	DP23211 Maize	Tolerance Interval	Literature Range	Reference Data Range
Alanine	Mean	0.812	0.818	0.457 - 1.07	0.40 - 1.48	0.505 - 0.889
	Range	0.601 - 0.929	0.565 - 0.929			
	Confidence Interval	0.755 - 0.869	0.761 - 0.875			
	Adjusted P-Value	--	0.911			
	P-Value	--	0.644			
Arginine	Mean	0.455	0.453	0.302 - 0.598	0.12 - 0.71	0.356 - 0.486
	Range	0.388 - 0.500	0.378 - 0.500			
	Confidence Interval	0.433 - 0.477	0.431 - 0.475			
	Adjusted P-Value	--	0.944			
	P-Value	--	0.722			
Aspartic Acid	Mean	0.683	0.689	0.414 - 0.901	0.30 - 1.21	0.475 - 0.730
	Range	0.538 - 0.756	0.522 - 0.764			
	Confidence Interval	0.643 - 0.723	0.649 - 0.729			
	Adjusted P-Value	--	0.911			
	P-Value	--	0.430			
Cystine	Mean	0.220	0.224	0.132 - 0.295	0.12 - 0.51	0.114 - 0.276
	Range	0.160 - 0.288	0.110 - 0.301			
	Confidence Interval	0.197 - 0.244	0.200 - 0.248			
	Adjusted P-Value	--	0.911			
	P-Value	--	0.499			
Glutamic Acid	Mean	2.12	2.14	1.11 - 2.76	0.83 - 3.54	1.25 - 2.32
	Range	1.55 - 2.45	1.45 - 2.43			
	Confidence Interval	1.96 - 2.28	1.98 - 2.30			
	Adjusted P-Value	--	0.911			
	P-Value	--	0.600			
Glycine	Mean	0.391	0.389	0.285 - 0.485	0.184 - 0.685	0.304 - 0.423
	Range	0.345 - 0.423	0.317 - 0.428			
	Confidence Interval	0.373 - 0.410	0.370 - 0.407			
	Adjusted P-Value	--	0.911			
	P-Value	--	0.647			
Histidine	Mean	0.317	0.315	0.190 - 0.380	0.14 - 0.46	0.202 - 0.325
	Range	0.270 - 0.360	0.238 - 0.351			
	Confidence Interval	0.299 - 0.335	0.297 - 0.333			
	Adjusted P-Value	--	0.944			
	P-Value	--	0.714			
Isoleucine	Mean	0.376	0.382	0.213 - 0.498	0.18 - 0.69	0.235 - 0.404
	Range	0.287 - 0.428	0.271 - 0.432			
	Confidence Interval	0.351 - 0.402	0.356 - 0.407			
	Adjusted P-Value	--	0.911			
	P-Value	--	0.458			
Leucine	Mean	1.41	1.43	0.694 - 1.85	0.60 - 2.49	0.759 - 1.53
	Range	1.03 - 1.67	0.923 - 1.63			
	Confidence Interval	1.30 - 1.52	1.32 - 1.53			
	Adjusted P-Value	--	0.911			
	P-Value	--	0.599			
Lysine	Mean	0.309	0.306	0.178 - 0.396	0.129 - 0.668	0.254 - 0.346
	Range	0.258 - 0.352	0.276 - 0.354			
	Confidence Interval	0.296 - 0.321	0.293 - 0.318			
	Adjusted P-Value	--	0.911			
	P-Value	--	0.420			

Table 35. Amino Acid Results for DP23211 Maize Grain (continued)

Analyte	Reported Statistics	Control Maize	DP23211 Maize	Tolerance Interval	Literature Range	Reference Data Range
Methionine	Mean	0.206	0.213	0.120 - 0.328	0.10 - 0.47	0.0934 - 0.268
	Range	0.163 - 0.253	0.110 - 0.264			
	Confidence Interval	0.181 - 0.231	0.188 - 0.238			
	Adjusted P-Value	--	0.658			
	P-Value	--	0.107			
Phenylalanine	Mean	0.572	0.570	0.303 - 0.736	0.24 - 0.93	0.318 - 0.590
	Range	0.449 - 0.674	0.374 - 0.648			
	Confidence Interval	0.528 - 0.615	0.526 - 0.614			
	Adjusted P-Value	--	0.999			
	P-Value	--	0.917			
Proline	Mean	1.04	1.04	0.557 - 1.26	0.46 - 1.75	0.641 - 1.07
	Range	0.804 - 1.19	0.735 - 1.16			
	Confidence Interval	0.972 - 1.11	0.972 - 1.11			
	Adjusted P-Value	--	0.999			
	P-Value	--	0.984			
Serine	Mean	0.540	0.545	0.307 - 0.685	0.15 - 0.91	0.348 - 0.572
	Range	0.434 - 0.614	0.395 - 0.603			
	Confidence Interval	0.508 - 0.573	0.512 - 0.577			
	Adjusted P-Value	--	0.911			
	P-Value	--	0.592			
Threonine	Mean	0.393	0.396	0.245 - 0.491	0.17 - 0.67	0.270 - 0.410
	Range	0.331 - 0.434	0.305 - 0.427			
	Confidence Interval	0.373 - 0.412	0.376 - 0.415			
	Adjusted P-Value	--	0.911			
	P-Value	--	0.546			
Tryptophan	Mean	0.0650	0.0668	0.0376 - 0.0991	0.027 - 0.215	0.0512 - 0.0843
	Range	0.0490 - 0.0791	0.0528 - 0.0877			
	Confidence Interval	0.0612 - 0.0688	0.0630 - 0.0706			
	Adjusted P-Value	--	0.658			
	P-Value	--	0.134			
Tyrosine	Mean	0.312	0.311	0.170 - 0.557	0.10 - 0.73	0.192 - 0.359
	Range	0.252 - 0.396	0.214 - 0.367			
	Confidence Interval	0.287 - 0.337	0.286 - 0.336			
	Adjusted P-Value	--	0.999			
	P-Value	--	0.891			
Valine	Mean	0.482	0.489	0.307 - 0.629	0.21 - 0.86	0.329 - 0.513
	Range	0.386 - 0.536	0.367 - 0.542			
	Confidence Interval	0.454 - 0.511	0.460 - 0.517			
	Adjusted P-Value	--	0.911			
	P-Value	--	0.390			

Note: Amino acids unit of measure is % dry weight.

Minerals in DP23211 Maize Grain

Minerals were analyzed in grain derived from DP23211 maize and near-isoline control maize. Results are shown in **Tables 36** and **37**. No statistically significant differences (P-value < 0.05) were observed between DP23211 maize and control maize.

The results of the analysis of minerals in maize grain demonstrate that DP23211 maize is comparable to conventional maize represented by non-GM near-isoline control maize and non-GM commercial maize.

Table 36. Mineral Results for DP23211 Maize Grain

Analyte	Reported Statistics	Control Maize	DP23211 Maize	Tolerance Interval	Literature Range	Reference Data Range
Calcium	Mean	0.00361	0.00346	0.00167 - 0.00872	ND - 0.101	0.00215 - 0.00650
	Range	0.00245 - 0.00538	0.00231 - 0.00496			
	Confidence Interval	0.00316 - 0.00406	0.00301 - 0.00391			
	Adjusted P-Value	--	0.550			
	P-Value	--	0.0798			
Copper	Mean	0.0000904	0.0000903	<0.0000625[a] - 0.000411	ND - 0.0021	<0.0000625[a] - 0.000194
	Range	<0.0000625[a] - 0.000134	<0.0000625[a] - 0.000130			
	Confidence Interval	0.0000684 - 0.000112	0.0000683 - 0.000112			
	Adjusted P-Value	--	0.999			
	P-Value	--	0.981			
Iron	Mean	0.00176	0.00176	0.00123 - 0.00308	0.0000712 - 0.0191	0.000955 - 0.00245
	Range	0.00139 - 0.00222	0.00121 - 0.00239			
	Confidence Interval	0.00157 - 0.00194	0.00157 - 0.00195			
	Adjusted P-Value	--	0.999			
	P-Value	--	0.958			
Magnesium	Mean	0.132	0.132	0.0809 - 0.159	0.0035 - 1.000	0.0858 - 0.133
	Range	0.117 - 0.142	0.117 - 0.148			
	Confidence Interval	0.127 - 0.136	0.127 - 0.136			
	Adjusted P-Value	--	0.999			
	P-Value	--	0.843			
Manganese	Mean	0.000747	0.000740	0.000327 - 0.00123	0.0000312 - 0.0054	0.000359 - 0.000870
	Range	0.000466 - 0.00101	0.000361 - 0.000979			
	Confidence Interval	0.000625 - 0.000868	0.000619 - 0.000861			
	Adjusted P-Value	--	0.914			
	P-Value	--	0.663			
Phosphorus	Mean	0.359	0.357	0.207 - 0.415	0.010 - 0.750	0.264 - 0.373
	Range	0.331 - 0.403	0.325 - 0.400			
	Confidence Interval	0.350 - 0.368	0.349 - 0.366			
	Adjusted P-Value	--	0.911			
	P-Value	--	0.617			
Potassium	Mean	0.354	0.355	0.255 - 0.534	0.020 - 0.720	0.306 - 0.486
	Range	0.311 - 0.441	0.313 - 0.429			
	Confidence Interval	0.339 - 0.368	0.341 - 0.369			
	Adjusted P-Value	--	0.963			
	P-Value	--	0.754			
Sodium	Mean	0.000491	0.000414	<LLOQ[a] - 0.0151	ND - 0.150	<0.0000625[a] - 0.00953
	Range	<0.0000625[a] - 0.00596	<0.0000625[a] - 0.00518			
	Confidence Interval	0.000217 - 0.00111	0.000183 - 0.000938			
	Adjusted P-Value	--	0.911			
	P-Value	--	0.622			
Zinc	Mean	0.00208	0.00208	0.00140 - 0.00347	0.0000283 - 0.0043	0.00132 - 0.00312
	Range	0.00152 - 0.00264	0.00154 - 0.00266			
	Confidence Interval	0.00187 - 0.00229	0.00187 - 0.00229			
	Adjusted P-Value	--	0.999			
	P-Value	--	0.956			

Note: Minerals unit of measure is % dry weight. Not detectable (ND): one or more assay values in the published literature references were below the LLOQ and were not quantified.

[a] < LLOQ (where a numerical number for LLOQ value is reported, e.g. <0.0000625 for Sodium), one or more mineral sample values were below the assay LLOQ.

Table 37. Number of Mineral Sample Values Below the Lower Limit of Quantification for DP23211 Maize Grain

Analyte	Number of Samples Below the LLOQ	
	Control Maize (n=32)	DP23211 Maize (n=32)
Copper[a]	5	6
Sodium[a]	4	4

[a] This analyte had <50% below-LLOQ sample values in both maize lines and was subjected to the mixed model analyses.

Vitamins in DP23211 Maize Grain

Vitamins were analyzed in grain derived from DP23211 maize and near-isoline control maize. Results are shown in **Tables 38** and **39**.

A statistically significant difference (P-value < 0.05) was observed between DP23211 maize and control maize for two vitamins (vitamin B6 and α-tocopherol). All individual values for α-tocopherol were within the tolerance interval. For vitamin B6 (pyridoxine), all values were within the literature range. As all values for these two analytes were within at least one of the reference ranges, DP23211 maize is within the range of normal variation for these analytes and the statistical differences are not biologically meaningful. Additionally, the non-significant FDR-adjusted P-value indicates that these differences were likely false positives.

The results of the analysis of vitamins in maize grain demonstrate that DP23211 maize is comparable to conventional maize represented by non-GM near-isoline control maize and non-GM commercial maize.

Table 38. Vitamin Results for DP23211 Maize Grain

Analyte	Reported Statistics	Control Maize	DP23211 Maize	Tolerance Interval	Literature Range	Reference Data Range
β-Carotene	Mean	0.283	0.302	0.0330 - 4.24	0.3 - 5.4	0.0996 - 1.71
	Range	0.111 - 0.475	0.171 - 0.531			
	Confidence Interval	0.209 - 0.357	0.228 - 0.376			
	Adjusted P-Value	--	0.658			
	P-Value	--	0.126			
Vitamin B1 (Thiamine)	Mean	2.43	2.42	1.74 - 5.38	ND - 40.00	1.58 - 2.91
	Range	1.85 - 2.80	1.95 - 2.91			
	Confidence Interval	2.33 - 2.53	2.32 - 2.52			
	Adjusted P-Value	--	0.999			
	P-Value	--	0.835			
Vitamin B2 (Riboflavin)	Mean	<0.900[a]	<0.900[a]	<0.900[a] - 2.27[r]	ND - 7.35	<0.900[a]
	Range	<0.900[a]	<0.900[a]			
	Confidence Interval	NA	NA			
	Adjusted P-Value	--	NA			
	P-Value	--	NA			
Vitamin B3 (Niacin)	Mean	13.0	13.1	7.85 - 32.5	ND - 70	9.29 - 18.0
	Range	10.9 - 17.9	10.6 - 17.7			
	Confidence Interval	12.2 - 13.7	12.3 - 13.9			
	Adjusted P-Value	--	0.911			
	P-Value	--	0.555			
Vitamin B5 (Pantothenic Acid)	Mean	5.46	5.50	2.42 - 7.53	3.01 - 14	4.56 - 6.95
	Range	3.46 - 6.57	4.56 - 6.22			
	Confidence Interval	5.09 - 5.83	5.13 - 5.87			
	Adjusted P-Value	--	0.911			
	P-Value	--	0.318			
Vitamin B6 (Pyridoxine)	Mean	2.99	2.76	1.61 - 8.88	ND - 12.14	1.62 - 5.26
	Range	2.00 - 4.65	1.40 - 4.09			
	Confidence Interval	2.63 - 3.35	2.40 - 3.12			
	Adjusted P-Value	--	0.377			
	P-Value	--	0.0273*			
Vitamin B9 (Folic Acid)	Mean	1.17	1.27	0.323 - 2.44	ND - 3.50	0.280 - 3.63
	Range	0.400 - 2.20	0.322 - 2.08			
	Confidence Interval	0.939 - 1.41	1.04 - 1.51			
	Adjusted P-Value	--	0.911			
	P-Value	--	0.526			
α-Tocopherol	Mean	3.37	3.00	0 - 23.5	ND - 68.67	<0.500[a] - 19.3
	Range	<0.500[a] - 7.22	<0.500[a] - 7.39			
	Confidence Interval	1.80 - 4.93	1.43 - 4.56			
	Adjusted P-Value	--	0.377			
	P-Value	--	0.0243*			
β-Tocopherol	Mean	<0.500[a]	<0.500[a]	<0.500[a] - 1.10[r]	ND - 19.80	<0.500[a] - 0.863
	Range	<0.500[a]	<0.500[a]			
	Confidence Interval	NA	NA			
	Adjusted P-Value	--	NA			
	P-Value	--	NA			
γ-Tocopherol	Mean	10.8	10.6	0 - 44.8	ND - 58.61	2.19 - 31.2
	Range	<1.00[a] - 17.8	<1.00[a] - 19.5			
	Confidence Interval	7.08 - 14.5	6.92 - 14.3			
	Adjusted P-Value	--	0.964			
	P-Value	--	0.769			

Table 38. Vitamin Results for DP23211 Maize Grain continued

Analyte	Reported Statistics	Control Maize	DP23211 Maize	Tolerance Interval	Literature Range	Reference Data Range
	Mean	<0.500[a]	<0.500[a]			
	Range	<0.500[a]	<0.500[a]			
δ-Tocopherol	Confidence Interval	NA	NA	<0.500[a] - 2.61[r]	ND - 14.61	<0.500[a] - 1.68
	Adjusted P-Value	--	NA			
	P-Value	--	NA			
	Mean	14.6	14.1			
	Range	<2.50[a] - 24.3	<2.50[a] - 26.3			
Total Tocopherols	Confidence Interval	9.47 - 19.8	8.95 - 19.3	0 - 59.1	ND - 89.91	4.56 - 40.7
	Adjusted P-Value	--	0.911			
	P-Value	--	0.425			

Note: Vitamins unit of measure is mg/kg dry weight. Not detectable (ND): one or more assay values in the published literature references were below the LLOQ and were not quantified. Not applicable (NA): mixed model analysis was not performed or confidence interval was not determined.

[a] < LLOQ (where a numerical number for LLOQ value is reported, e.g. <0.900 for vitamin B2), one or more vitamin sample values were below the assay LLOQ.

[r] Historical reference data range was provided as tolerance interval was not calculated since the data did not meet the assumptions of any tolerance interval calculation method.

[*] A statistically significant difference (P-Value < 0.05) was observed.

Table 39. Number of Vitamin Sample Values Below the Lower Limit of Quantification for DP23211 Maize Grain

Analyte	Number of Samples Below the LLOQ	
	Control Maize (n=32)	DP23211 Maize (n=32)
Vitamin B2 (Riboflavin)	32	32
α-Tocopherol[a]	4	4
β-Tocopherol	32	32
γ-Tocopherol[a]	1	1
δ-Tocopherol	32	32
Total Tocopherols[a]	1	1

[a] This analyte had <50% below-LLOQ sample values in both maize lines and was subjected to the mixed model analyses.

Secondary Metabolites and Anti-Nutrients in DP23211 Maize Grain

Secondary metabolites and anti-nutrients were analyzed in grain derived from DP23211 maize and near-isoline control maize. Results are shown in **Tables 40** and **41**.

A statistically significant difference (P-value < 0.05) was observed between DP23211 maize and control maize for one analyte (*p*-coumaric acid); however, all individual values were within the tolerance interval, indicating DP23211 maize is within the range of natural variation for this analyte and the statistical difference is not biologically meaningful. The non-significant FDR-adjusted P-value indicates that this difference was likely a false positive.

The results of the analysis of secondary metabolites and anti-nutrients in maize grain demonstrate that DP23211 maize is comparable to conventional maize represented by non-GM near-isoline control maize and non-GM commercial maize.

Table 40. Secondary Metabolite and Anti-Nutrient Results for DP23211 Maize Grain

Analyte	Reported Statistics	Control Maize	DP23211 Maize	Tolerance Interval	Literature Range	Reference Data Range
p-Coumaric Acid	Mean	0.0218	0.0198	0.00742 - 0.0492	ND - 0.08	0.0132 - 0.0403
	Range	0.0161 - 0.0298	0.0159 - 0.0294			
	Confidence Interval	0.0199 - 0.0236	0.0179 - 0.0217			
	Adjusted P-Value	--	0.168			
	P-Value	--	0.00244*			
Ferulic Acid	Mean	0.233	0.236	0.123 - 0.349	0.02 - 0.44	0.164 - 0.298
	Range	0.185 - 0.284	0.199 - 0.306			
	Confidence Interval	0.219 - 0.247	0.222 - 0.250			
	Adjusted P-Value	--	0.911			
	P-Value	--	0.491			
Furfural	Mean	<0.000100[a]	<0.000100[a]	<0.0000500[a]	ND	<0.000100[a]
	Range	<0.000100[a]	<0.000100[a]			
	Confidence Interval	NA	NA			
	Adjusted P-Value	--	NA			
	P-Value	--	NA			
Inositol	Mean	0.0257	0.0264	0.00966 - 0.0548	0.00613 - 0.257	0.0157 - 0.0450
	Range	0.0180 - 0.0433	0.0181 - 0.0371			
	Confidence Interval	0.0224 - 0.0291	0.0230 - 0.0297			
	Adjusted P-Value	--	0.911			
	P-Value	--	0.312			
Phytic Acid	Mean	1.08	1.08	0.493 - 1.33	ND - 1.940	0.696 - 1.21
	Range	0.891 - 1.34	0.853 - 1.38			
	Confidence Interval	1.02 - 1.14	1.02 - 1.14			
	Adjusted P-Value	--	0.999			
	P-Value	--	0.931			
Raffinose	Mean	0.135	0.126	0 - 0.396	ND - 0.466	<0.0800[a] - 0.339
	Range	<0.0800[a] - 0.264	<0.0800[a] - 0.239			
	Confidence Interval	0.0847 - 0.186	0.0755 - 0.177			
	Adjusted P-Value	--	0.833			
	P-Value	--	0.266			
Trypsin Inhibitor (TIU/mg DW)	Mean	2.50	2.54	1.03 - 9.18	ND - 8.42	1.64 - 3.21
	Range	2.16 - 3.23	1.98 - 3.38			
	Confidence Interval	2.28 - 2.73	2.31 - 2.76			
	Adjusted P-Value	--	0.911			
	P-Value	--	0.341			

Note: Secondary metabolites and anti-nutrients unit of measure is % dry weight or as indicated. Trypsin inhibitors unit of measure is trypsin inhibitor units per milligram dry weight (TIU/mg DW). Not detectable (ND): one or more assay values in the published literature references were below the lower limit of quantification (LLOQ) and were not quantified. Not applicable (NA): mixed model analysis was not performed or confidence interval was not determined

[a] < LLOQ, one or more sample values were below the assay LLOQ.

* A statistically significant difference (P-Value < 0.05) was observed.

Table 41. Number of Secondary Metabolite and Anti-Nutrient Sample Values Below the Lower Limit of Quantification for DP23211 Maize Grain

Analyte	Number of Samples Below the LLOQ	
	Control Maize (n=32)	DP23211 Maize (n=32)
Furfural	32	32
Raffinose[a]	8	12

[a] This analyte had <50% below-LLOQ sample values in both maize lines and was subjected to the mixed model analyses.

Conclusions on the Food and Feed Safety Assessment of DP23211 Maize

An assessment was conducted of the compositional equivalence DP23211 maize compared to that of a conventional non-GM comparator with a history of safe use in food and feed. The results demonstrated that nutrient composition of forage and grain derived from DP23211 maize was comparable to that of conventional maize represented by non-GM near-isoline maize and non-GM commercial maize.

C. Information related to the nutritional impact of the food

As seen in above Section B5, the compositional analysis did not indicate any biologically relevant changes to the levels of nutrients in the forage and grain derived from DP23211 maize compared to the non-GM counterpart. The results demonstrated that nutrient composition of forage and grain derived from DP23211 maize was comparable to that of conventional maize represented by non-GM near-isoline maize and non-GM commercial maize.

D. Other Information

Overall Risk Assessment Conclusions for DP23211 Maize

This application presents information supporting the safety and nutritional comparability of DP23211 maize. The molecular characterisation analyses conducted on DP23211 maize demonstrated that the introduced genes are integrated at a single locus, stably inherited across multiple generations, and segregate according to Mendel's law of genetics. The toxicity and allergenicity potential of DvSSJ1 dsRNA and the IPD072Aa, PAT, and PMI proteins were evaluated and found unlikely to be toxic or allergenic to humans or animals. Based on the weight of evidence, consumption of DvSSJ1 dsRNA and the IPD072Aa, PAT, and PMI proteins is unlikely to cause an adverse effect on humans or animals. A compositional equivalence assessment demonstrated that the nutrient composition of DP23211 maize forage and grain is comparable to that of conventional maize, represented by non-genetically modified (non-GM) near-isoline maize and non-GM commercial maize.

Overall, data and information contained herein support the conclusion that DP23211 maize containing DvSSJ1 dsRNA and the IPD072Aa, PAT, and PMI proteins is as safe and nutritious as non-GM maize for food and feed uses.

References

Abendroth LJ, Elmore RW, Boyer MJ, Marlay SK (2011) Corn Growth and Development. Iowa State University Extension, PMR 1009

Ambros V (2004) The functions of animal microRNAs. Nature 431: 350-355

An G, Mitra A, Choi HK, Costa MA, An K, Thornburg RW, Ryan CA (1989) Functional Analysis of the 3' Control Region of the Potato Wound-Inducible Proteinase Inhibitor II Gene. The Plant Cell 1: 115-122

Anderson JA, Staley J, Challender M, Heuton J (2018) Safety of *Pseudomonas chlororaphis* as a gene source for genetically modified crops. Transgenic Research 27: 103-113

Andersson MS, de Vicente MC (2010) Maize, Corn (*Zea mays* L.). In Gene Flow between Crops and Their Wild Relatives. The Johns Hopkins University Press, Baltimore, pp 255-291

[redacted] 2019) Characterization of DP-Ø23211-2 Maize for Insertion Stability in Five Generations Using Southern Blot Analysis. Pioneer Hi-Bred International, Inc., Study No. PHI-2019-033

Auerbach A, Vyas G, Li A, Halushka M, Witwer K (2016) Uptake of dietary milk miRNAs by adult humans: a validation study. F1000Research 5: 721

Baier SR, Nguyen C, Xie F, Wood JR, Zempleni J (2014) MicroRNAs Are Absorbed in Biologically Meaningful Amounts from Nutritionally Relevant Doses of Cow Milk and Affect Gene Expression in Peripheral Blood Mononuclear Cells, HEK-293 Kidney Cell Cultures, and Mouse Livers. The Journal of Nutrition 144: 1495-1500

[redacted] (2016) Characterization of IPD072Aa Protein Derived from a Microbial Expression System. Pioneer Hi-Bred International, Inc., Study No. PHI-2015-096

[redacted] (2017) Characterization of IPD072Aa Protein Derived from a Microbial Expression System. Pioneer Hi-Bred International, Inc., Study No. PHI-2017-010

Baum JA, Bogaert T, Clinton W, Heck GR, Feldmann P, Ilagan O, Johnson S, Plaetinck G, Munyikwa T, Pleau M, Vaughn T, Roberts J (2007) Control of coleopteran insect pests through RNA interference. Nature Biotechnology 25: 1322-1326

Baum JA, Roberts JK (2014) Progress Towards RNAi-Mediated Insect Pest Management. In TS Dhadialla, SS Gill, eds, Advances in Insect Physiology, Vol 47. Academic Press, pp 249-295

[redacted] (2019a) Phosphomannose Isomerase: Assessment of Amino Acid Sequence Similarity to Known or Putative Allergens. Syngenta Crop Protection, LLC, Report No. SSB-152-19

[redacted] (2019b) Phosphomannose Isomerase: Assessment of Amino Acid Sequence Similarity to Known or Putative Toxins. Syngenta Crop Protection, LLC, Report No. SSB-153-19

Benjamini Y, Hochberg Y (1995) Controlling the False Discovery Rate: a Practical and Powerful Approach to Multiple Testing. Journal of the Royal Statistical Society B 57: 289-300

Boeckman C (2019) Characterizing the spectrum of activity of DvSSJ1: a double stranded RNA target for smooth septate junctions in Western corn rootworm (Diabrotica virgifera virgifera LeConte). Journal of Economic Entomology Article in preparation

[redacted] (2019) Southern-by-Sequencing Analysis of the T1 Generation of DP-Ø23211-2 Maize. Pioneer Hi-Bred International, Inc., Study No. PHI-2018-219

[redacted] (2000) PAT Microbial protein (FL): Acute Oral-Toxicity Study in CD-1 Mice. Dow AgroSciences LLC, Study No. 991249

Buhr T, Sato S, Ebrahim F, Xing A, Zhou Y, Mathiesen M, Schweiger B, Kinney A, Staswick P, Tom C (2002) Ribozyme termination of RNA transcripts down-regulate seed fatty acid genes in transgenic soybean. The Plant Journal 30: 155-163

Callis J, Carpenter T, Sun CW, Vierstra RD (1995) Structure and Evolution of Genes Encoding Polyubiquitin and Ubiquitin-Like Proteins in *Arabidopsis thaliana* Ecotype Columbia. Genetics 139: 921-939

Carlson AB, Mathesius CA, Ballou S, Boeckman CJ, Gunderson TA, Mirsky HP, Mukerji P, Roe JC, Schmidt JM, Zhang J, Delaney B (2019) Safety assessment of coleopteran active IPD072Aa protein from *Psuedomonas chlororaphis*. Food and Chemical Toxicology 129: 376-381

CERA - ILSI Research Foundation (2016) A Review of the Food and Feed Safety of the PAT Protein. International Life Sciences Institute, Center for Environmental Risk Assessment, http://ilsirf.org/publication/a-review-of-the-food-and-feed-safety-of-the-pat-protein/

CERA (2011) A Review of the Environmental Safety of the PAT Protein. International Life Sciences Institute, Center for Environmental Risk Assessment, http://www.cera-gmc.org/static/htmfiles/glufosinate.htm

CFIA (1994) The Biology of *Zea mays* (L.) (Maize). Canadian Food Inspection Agency, BIO1994-11

Chan SY, Snow JW (2017) Formidable challenges to the notion of biologically important roles for dietary small RNAs in ingesting mammals. Genes & Nutrition 12: 13

Chassy B, Hlywka JJ, Kleter GA, Kok EJ, Kuiper HA, McGloughlin M, Munro IC, Phipps RH, Reid JE (2004) Nutritional and Safety Assessments of Foods and Feeds Nutritionally Improved through Biotechnology. Comprehensive Reviews in Food Science and Food Safety 3: 38-104

Chen X, Dai G-h, Ren Z-m, Tong Y-l, Yang F, Zhu Y-q (2016) Identification of Dietetically Absorbed Rapeseed (*Brassica campestris* L.) Bee Pollen MicroRNAs in Serum of Mice. BioMed Research International 5413849: 5 pp

Cheo DL, Titus SA, Byrd DRN, Hartley JL, Temple GF, Brasch MA (2004) Concerted Assembly and Cloning of Multiple DNA Segments Using In Vitro Site-Specific Recombination: Functional Analysis of Multi-Segment Expression Clones. Genome Research 14: 2111-2120

Christensen AH, Sharrock RA, Quail PH (1992) Maize polyubiquitin genes: structure, thermal perturbation of expression and transcript splicing, and promoter activity following transfer to protoplasts by electroporation. Plant Molecular Biology 18: 675-689

Codex Alimentarius Commission (2003) Alinorm 03/34: Appendix III: Draft guideline for the conduct of food safety assessment of foods derived from recombinant-DNA plants, and Appendix IV: Proposed Draft Annex of the Assessment of Possible Allergenicity. Food and Agriculture Organization of the United Nations, World Health Organization, Rome, pp 47-60

Codex Alimentarius Commission (2008) Guideline for the Conduct of Food Safety Assessment of Foods Derived from Recombinant-DNA Plants. Codex Alimentarius, CAC/GL 45-2003

Codex Alimentarius Commission (2013) Codex Standard for Named Vegetable Oils. Codex Alimentarius, STAN-210-1999

Cong B, Maxwell C, Luck S, Vespestad D, Richard K, Mickelson J, Zhong C (2015) Genotypic and Environmental Impact on Natural Variation of Nutrient Composition in 50 Non Genetically Modified Commercial Maize Hybrids in North America. Journal of Agricultural and Food Chemistry 63: 5321-5334

Cullen EM, Gray ME, Gassmann AJ, Hibbard BE (2013) Resistance to Bt Corn by Western Corn Rootworm (Coleoptera: Chrysomelidae) in the U.S. Corn Belt. Journal of Integrated Pest Management 4: D1-D6

Daboussi F, Stoddard TJ, Zhang F (2015) Engineering Meganuclease for Precise Plant Genome Modification. In F Zhang, H Puchta, JG Thomson, eds, Advances in New Technology for Targeted Modification of Plant Genomes. Springer, New York, pp 21-38

Dale EC, Ow DW (1990) Intra- and intramolecular site-specific recombination in plant cells mediated by bacteriophage P1 recombinase. Gene 91: 79-85

Das OP, Ward K, Ray S, Messing J (1991) Sequence Variation between Alleles Reveals Two Types of Copy Correction at the 27-kDa Zein Locus of Maize. Genomics 11: 849-856

de Freitas FA, Yunes JA, da Silva MJ, Arruda P, Leite A (1994) Structural characterization and promoter activity analysis of the γ-kafirin gene from sorghum. Molecular and General Genetics 245: 177-186

DEEM/FCID (2018) Dietary Exposure Evaluation Model – Food Commodity Intake Database, Version 4.02, Durango Software, LLC. United States Environmental Protection Agency, https://www.epa.gov/pesticide-science-and-assessing-pesticide-risks/deem-fcidcalendex-software-installer

Delaney B, Goodman RE, Ladics GS (2018) Food and Feed Safety of Genetically Engineered Food Crops. Toxicological Sciences 162: 361-371

Della Vedova CB, Lorbiecke R, Kirsch H, Schulte MB, Scheets K, Borchert LM, Scheffler BE, Wienand U, Cone KC, Birchler JA (2005) The Dominant Inhibitory Chalcone Synthase Allele *C2-Idf (Inhibitor diffuse)* From *Zea mays* (L.) Acts via an Endogenous RNA Silencing Mechanism. Genetics 170: 1989-2002

Dennis ES, Gerlach WL, Pryor AJ, Bennetzen JL, Inglis A, Llewllyn D, Sachs MM, Ferl RJ, Peacock WJ (1984) Molecular analysis of the alcohol dehydrogenase (*Adhl*) gene of maize. Nucleic Acids Research 12: 3983-4000

Depicker A, Stachel S, Dhaese P, Zambryski P, Goodman HM (1982) Nopaline Synthase: Transcript Mapping and DNA Sequence. Journal of Molecular and Applied Genetics 1: 561-573

Dever JT, Kemp MQ, Thompson AL, Keller HGK, Waksmonski JC, Scholl CD, Barnes DM (2015) Survival and Diversity of Human Homologous Dietary MicroRNAs in Conventionally Cooked Top Sirloin and Dried Bovine Tissue Extracts. PLoS One 10: e0138275

Devos Y, Reheul D, De Schrijver A (2005) The co-existence between transgenic and non-transgenic maize in the European Union: a focus on pollen flow and cross-fertilization. Environmental Biosafety Research 4: 71-87

Dickinson B, Zhang Y, Petrick JS, Heck G, Ivashuta S, Marshall WS (2013) Lack of detectable oral bioavailability of plant microRNAs after feeding in mice. Nature Biotechnology 31: 965-967

Dong J, Feng Y, Kumar D, Zhang W, Zhu T, Luo M-C, Messing J (2016) Analysis of tandem gene copies in maize chromosomal regions reconstructed from long sequence reads. Proceedings of the National Academy of Sciences 113: 7949-7956

Dummitt B, Micka WS, Chang Y-H (2003) N-Terminal Methionine Removal and Methionine Metabolism in *Saccharomyces cerevisiae*. Journal of Cellular Biochemistry 89: 964-974

Dymecki SM (1996) A modular set of *Flp*, FRT and *lacZ* fusion vectors for manipulating genes by site-specific recombination. Gene 171: 197-201

Eckes P, Rosahl S, Schell J, Willmitzer L (1986) Isolation and characterization of a light-inducible, organ-specific gene from potato and analysis of its expression after tagging and transfer into tobacco and potato shoots. Molecular and General Genetics 205: 14-22

EFSA (2011) Guidance for risk assessment of food and feed from genetically modified plants. The EFSA Journal 9: 2150

EFSA Scientific Committee, More SJ, Bampidis V, Benford D, Bragard C, Halldorsson TI, Hernández-Jerez AF, Hougaard Bennekou S, Koutsoumanis KP, Machera K, Naegeli H, Nielsen SS, Schlatter JR, Schrenk D, Silano V, Turck D, Younes M, Gundert-Remy U, Kass GEN, Kleiner J, Rossi AM, Serafimova R, Reilly L, Wallace HM (2019) Guidance on the use of the Threshold of Toxicological Concern approach in food safety assessment. EFSA Journal 17: 5708

Ewing B, Green P (1998) Base-Calling of Automated Sequencer Traces Using *Phred*. II. Error Probabilities. Genome Research 8: 186-194

Ewing B, Hillier L, Wendl MC, Green P (1998) Base-Calling of Automated Sequencer Traces Using *Phred*. I. Accuracy Assessment. Genome Research 8: 175-185

FAO/WHO (1996) Biotechnology and food safety. Report of a Joint FAO/WHO Consultation, Rome, Italy, 30 September - 4 October 1996, Paper No. 61

FAO/WHO (2000) Safety aspects of genetically modified foods of plant origin: Report of a Joint FAO/WHO Expert Consultation on Foods Derived from Biotechnology, 29 May – 2 June 2000. World Health Organization, Geneva

FAO/WHO (2001a) Evaluation of Allergencity of Genetically Modified Foods: Report of a Joint FAO/WHO Expert Consultation on Allergenicity of Foods Derived from Biotechnology, 22 - 25 January 2001. Food and Agriculture Organization of the United Nations, Rome

FAO/WHO (2001b) Safety assessment of foods derived from genetically modified microorganisms, Report of a Joint FAO/WHO Expert Consultation on Foods Derived from Biotechnology. Food & Agriculture Organization of the United Nations, World Health Organization

Flachowsky G, Reuter T (2017) Future challenges feeding transgenic plants. Animal Frontiers 7: 15-23

Fling ME, Kopf J, Richards C (1985) Nucleotide sequence of the transposon Tn7 gene encoding an aminoglycoside-modifying enzyme, 3" (9)-*O*-nucleotidyltransferase. Nucleic Acids Research 13: 7095-7106

Forbes DC, Peppas NA (2012) Oral delivery of small RNA and DNA. Journal of Controlled Release 162: 438-445

Franck A, Guilley H, Jonard G, Richards K, Hirth L (1980) Nucleotide sequence of cauliflower mosaic virus DNA. Cell 21: 285-294

Frizzi A, Huang S (2010) Tapping RNA silencing pathways for plant biotechnology. Plant Biotechnology Journal 8: 655-677

FSANZ (2013) Response to Heinemann et al on the regulation of GM crops and foods developed using gene silencing. Food Standards Australia New Zealand, http://www.foodstandards.gov.au/consumer/gmfood/Documents/Heinemann%20Response%20210513.pdf

Furuse M, Izumi Y (2017) Molecular dissection of smooth septate junctions: understanding their roles in arthropod physiology. Annals of the New York Academy of Sciences 1397: 17-24

Galinat WC (1988) The Origin of Corn. In GF Sprague, JW Dudley, eds, Corn and Corn Improvement, Ed 3. ASA-CSSA-SSSA, Madison, pp 1-31

Gassmann AJ, Shrestha RB, Jakka SR, Dunbar MW, Clifton EH, Paolino AR, Ingber DA, French BW, Masloski KE, Dounda JW, St Clair CR (2016) Evidence of Resistance to Cry34/35Ab1 Corn by Western Corn Rootworm (Coleoptera: Chrysomelidae): Root Injury in the Field and Larval Survival in Plant-Based Bioassays. Journal of Economic Entomology 109: 1872-1880

Geary RS, Baker BF, Crooke ST (2015) Clinical and Preclinical Pharmacokinetics and Pharmacodynamics of Mipomersen (Kynamro®): A Second-Generation Antisense Oligonucleotide Inhibitor of Apolipoprotein B. Clinical Pharmacokinetics 54: 133-146

Gordon-Kamm WJ, Helentjaris TG, Lowe KS, Shen B, Tarczynski MC, Zheng P, inventors. Apr. 16, 2013. AP2 domain transcription factor ODP2 (ovule development protein 2) and methods of use. US Patent, Application No. US 8,420,893 B2

Guilley H, Dudley RK, Jonard G, Balàzs E, Richards KE (1982) Transcription of cauliflower mosaic virus DNA: detection of promoter sequences, and characterization of transcripts. Cell 30: 763-773

[redacted] (2019a) Characterization of IPD072Aa Protein Derived from DP-Ø23211-2 Maize. Pioneer Hi-Bred International, Inc., Study No. PHI-2019-049

[redacted] (2019b) Characterization of PAT Protein Derived from DP-Ø23211-2 Maize. Pioneer Hi-Bred International, Inc., Study No. PHI-2019-048

[redacted](2018) Determination of the Biological Activity of Heat-Treated IPD072Aa Protein Incorporated in an Artificial Diet and Fed to *Diabrotica virgifera virgifera*. Pioneer Hi-Bred International, Inc., Study No. PHI-2018-046

Han L, Luan Y-S (2015) Horizontal Transfer of Small RNAs to and from Plants. Frontiers in Plant Science 6: 1113

[redacted] (2019) Sequence Characterization of Insert and Flanking Genomic Regions of DP-Ø23211-2 Maize. Pioneer Hi-Bred International, Inc., Study No. PHI-2019-099

Hartley JL, Temple GF, Brasch MA (2000) DNA Cloning Using In Vitro Site-Specific Recombination. Genome Research 10: 1788-1795

Hérouet C, Esdaile DJ, Mallyon BA, Debruyne E, Schulz A, Currier T, Hendrickx K, van der Klis R-J, Rouan D (2005) Safety evaluation of the phosphinothricin acetyltransferase proteins encoded by the *pat* and *bar* sequences that confer tolerance to glufosinate-ammonium herbicide in transgenic plants. Regulatory Toxicology and Pharmacology 41: 134-149

Hershey HP, Stoner TD (1991) Isolation and characterization of cDNA clones for RNA species induced by substituted benzenesulfonamides in corn. Plant Molecular Biology 17: 679-690

Hong B, Fisher TL, Sult TS, Maxwell CA, Mickelson JA, Kishino H, Locke MEH (2014) Model-Based Tolerance Intervals Derived from Cumulative Historical Composition Data: Application for

Substantial Equivalence Assessment of a Genetically Modified Crop. Journal of Agricultural and Food Chemistry 62: 9916-9926

Hou Y-H, Jeyaraj A, Zhang X, Wei C-L (2017) Absolute quantification of microRNAs in green tea (*Camellia sinensis*) by stem-loop quantitative real-time PCR. Journal of the Science of Food and Agriculture 97: 2975-2981

[redacted] 2019) *In silico* analysis assess how conserved the *ssj1* gene sequence is across different organisms with varied evolutionary distance from Western Corn Rootworm (*Diabrotica virgifera virgifera*). Pioneer Hi-Bred International, Inc., Study No. PHI-R050-Y19

Hu X, Richtman NM, Zhao J-Z, Duncan KE, Niu X, Procyk LA, Oneal MA, Kernodle BM, Steimel JP, Crane VC, Sandahl G, Ritland JL, Howard RJ, Presnail JK, Lu AL, Wu G (2016) Discovery of midgut genes for the RNA interference control of corn rootworm. Scientific Reports 6: 30542

Hu X, Steimel JP, Kapka-Kitzman DM, Davis-Vogel C, Richtman NM, Mathis JP, Nelson ME, Lu AL, Wu G (2019) Molecular characterization of the insecticidal activity of double-stranded RNA targeting the smooth septate junction of western corn rootworm (*Diabrotica virgifera virgifera*). PLoS One 14: e0210491

ILSI (2016) ILSI Crop Composition Database, Version 6.0. International Life Sciences Institute, www.cropcomposition.org

ILSI (2019) ILSI Crop Composition Database, Version 7.0. International Life Sciences Institute, www.cropcomposition.org

ISAAA (2019) GM Crop Events List (519 Events). International Service for the Acquisition of Agri-Biotech Applications, https://www.isaaa.org/gmapprovaldatabase/eventslist/default.asp

Ivashuta SI, Petrick JS, Heisel SE, Zhang Y, Guo L, Reynolds TL, Rice JF, Allen E, Roberts JK (2009) Endogenous small RNAs in grain: Semi-quantification and sequence homology to human and animal genes. Food and Chemical Toxicology 47: 353-360

Jakka SRK, Shrestha RB, Gassmann AJ (2016) Broad-spectrum resistance to *Bacillus thuringiensis* toxins by western corn rootworm (*Diabrotica virgifera virgifera*). Scientific Reports 6: 27860

Jensen PD, Zhang Y, Wiggins BE, Petrick JS, Zhu J, Kerstetter RA, Heck GR, Ivashuta SI (2013) Computational sequence analysis of predicted long dsRNA transcriptomes of major crops reveals sequence complementarity with human genes. GM Crops and Food: Biotechnology in Agriculture and the Food Chain 4: 90-97

Jonas DA, Antignac E, Antoine JM, Classen HG, Huggett A, Knudsen I, Mahler J, Ockhuizen T, Smith M, Teuber M, Walker R, De Vogel P (1996) The Safety Assessment of Novel Foods: Guidelines prepared by ILSI Europe Novel Food Task Force. Food and Chemical Toxicology 34: 931-940

Kalla R, Shimamoto K, Potter R, Nielsen PS, Linnestad C, Olsen O-A (1994) The promoter of the barley aleurone-specific gene encoding a putative 7 kDa lipid transfer protein confers aleurone cell-specific expression in transgenic rice. The Plant Journal 6: 849-860

[redacted] (2018) Segregation Analysis and Tissue Production of Multiple Maize Generations Containing Event DP-Ø23211-2. Pioneer Hi-Bred International, Inc., Study No. PHI-2017-073 (Amended 2019)

Kang W, Bang-Berthelsen CH, Holm A, Houben AJS, Holt Müller A, Thymann T, Pociot F, Estivill X, Friedländer MR (2017) Survey of 800+ data sets from human tissue and body fluid reveals xenomiRs are likely artifacts. RNA 23: 433-445

Katzen F (2007) Gateway® recombinational cloning: a biological operating system. Expert Opinion on Drug Discovery 2: 571-589

Kay R, Chan A, Daly M, McPherson J (1987) Duplication of CaMV 35S Promoter Sequences Creates a Strong Enhancer for Plant Genes. Science 236: 1299-1302

Keil M, Sanchez-Serrano J, Schell J, Willmitzer L (1986) Primary structure of a proteinase inhibitor II gene from potato (*Solanum tuberosum*). Nucleic Acids Research 14: 5641-5650

Kenward MG, Roger JH (2009) An improved approximation to the precision of fixed effects from restricted maximum likelihood. Computational Statistics & Data Analysis 53: 2583-2595

Komari T, Hiei Y, Saito Y, Murai N, Kumashiro T (1996) Vectors carrying two separate T-DNAs for co-transformation of higher plants mediated by *Agrobacterium tumefaciens* and segregation of transformants free from selection markers. The Plant Journal 10: 165-174

Krieger EK, Allen E, Gilbertson LA, Roberts JK, Hiatt W, Sanders RA (2008) The Flavr Savr Tomato, an Early Example of RNAi Technology. HortScience 43: 962-964

Kroes R, Kleiner J, Renwick A (2005) The Threshold of Toxicological Concern Concept in Risk Assessment. Toxicological Sciences 86: 226-230

Kusaba M (2004) RNA interference in crop plants. Current Opinion in Biotechnology 15: 139-143

La Paz JL, Pla M, Papazova N, Puigdomenech P, Vicient CM (2010) Stability of the MON 810 transgene in maize. Plant Molecular Biology 74: 563-571

Langmead B, Trapnell C, Pop M, Salzberg SL (2009) Ultrafast and memory-efficient alignment of short DNA sequences to the human genome. Genome Biology 10: R25

Li H, Durbin R (2010) Fast and accurate long-read alignment with Burrows–Wheeler transform. Bioinformatics 26: 589-595

Link J, Thon C, Schanze D, Steponaitiene R, Kupcinskas J, Zenker M, Canbay A, Malfertheiner P, Link A (2019) Food-Derived Xeno-microRNAs: Influence of Diet and Detectability in Gastrointestinal Tract—Proof-of-Principle Study. Molecular Nutrition & Food Research 63: 1800076

Liu H, Shi J, Sun C, Gong H, Fan X, Qiu F, Huang X, Feng Q, Zheng X, Yuan N, Li C, Zhang Z, Deng Y, Wang J, Pan G, Han B, Lai J, Wu Y (2016) Gene duplication confers enhanced expression of 27-kDa γ-zein for endosperm modification in quality protein maize. Proceedings of the National Academy of Sciences 113: 4964-4969

Liu R, Mu L-M, Bai J, Du Y-F, Xie Y, Lu W-L (2019) Development of double strand RNA mPEI nanoparticles and application in treating invasive breast cancer. RSC Advances 9: 13186-13200

Lorenzer C, Dirin M, Winkler A-M, Baumann V, Winkler J (2015) Going beyond the liver: Progress and challenges of targeted delivery of siRNA therapeutics. Journal of Controlled Release 203: 1-15

Loretz B, Föger F, Werle M, Bernkop-schnürch A (2006) Oral gene delivery: Strategies to improve stability of pDNA towards intestinal digestion. Journal of Drug Targeting 14: 311-319

Lowe K, Wu E, Wang N, Hoerster G, Hastings C, Cho M-J, Scelonge C, Lenderts B, Chamberlin M, Cushatt J, Wang L, Ryan L, Khan T, Chow-Yiu J, Hua W, Yu M, Banh J, Bao Z, Brink K, Igo E, Rudrappa B, Shamseer P, Bruce W, Newman L, Shen B, Zheng P, Bidney D, Falco C, Register J, Zhao Z-Y, Xu D, Jones T, Gordan-Kamm W (2016) Morphogenic Regulators *Baby boom* and *Wuschel* Improve Monocot Transformation. The Plant Cell 28: 1998-2015

Luna VS, Figueroa MJ, Baltazar MB, Gomez LR, Townsend R, Schoper JB (2001) Maize Pollen Longevity and Distance Isolation Requirements for Effective Pollen Control. Crop Science 41: 1551-1557

Lundry DR, Burns JA, Nemeth MA, Riordan SG (2013) Composition of Grain and Forage from Insect-Protected and Herbicide-Tolerant Corn, MON 89034 x TC1507 x MON 88017 x DAS-59122-7 (SmartStax), Is Equivalent to That of Conventional Corn (*Zea mays* L.). Journal of Agricultural and Food Chemistry 61: 1991-1998

Lusk RW (2014) Diverse and Widespread Contamination Evident in the Unmapped Depths of High Throughput Sequencing Data. PLoS One 9: e110808

Marçais G, Kingsford C (2011) A fast, lock-free approach for efficient parallel counting of occurrences of *k*-mers. Bioinformatics 27: 764-770

Mayer KFX, Schoof H, Haecker A, Lenhard M, Jürgens G, Laux T (1998) Role of *WUSCHEL* in Regulating Stem Cell Fate in the *Arabidopsis* Shoot Meristem. Cell 95: 805-815

McLoughlin AG, Walker PL, Wytinck N, Sullivan DS, Whyard S, Belmonte MF (2018) Developing new RNA interference technologies to control fungal pathogens. Canadian Journal of Plant Pathology 40: 325-335

Messeguer J, Peñas G, Ballester J, Bas M, Serra J, Salvia J, Palaudelmàs M, Melé E (2006) Pollen-mediated gene flow in maize in real situations of coexistence. Plant Biotechnology Journal 4: 633-645

Metcalf RL (1986) Foreward. In JL Krysan, TA Miller, eds, Methods for the Study of Pest *Diabrotica*. Springer-Verlag, New York, pp vii-xv

Micó V, Martín R, Lasunción MA, Ordovás JM, Daimiel L (2016) Unsuccessful Detection of Plant MicroRNAs in Beer, Extra Virgin Olive Oil and Human Plasma After an Acute Ingestion of Extra Virgin Olive Oil. Plant Foods for Human Nutrition 71: 102-108

[redacted] (2018) Comparison of the DvSSJ1 Fragment to the Human Transcriptome. Pioneer Hi-Bred International, Inc., Study No. PHI-R056-Y18

[redacted] (2019a) Comparison of the DvSSJ1 Fragment to a Variety of Farm and Companion Animal Transcriptomes. Pioneer Hi-Bred International, Inc., Study No. PHI-R046-Y19

[redacted] (2019b) Reading Frame Analysis at the Insertion Site of Maize Event DP-Ø23211-2. Pioneer Hi-Bred International, Inc., Study No. PHI-2019-196/222

[redacted] (2019a) Comparison of the Amino Acid Sequence of the IPD072Aa Protein to the Amino Acid Sequences of Known and Putative Protein Allergens. Pioneer Hi-Bred International, Inc., Study No. PHI-2019-067/201

[redacted]2019b) Comparison of the Amino Acid Sequence of the PAT Protein to the Amino Acid Sequences of Known and Putative Protein Allergens. Pioneer Hi-Bred International, Inc., Study No. PHI-2019-069/201

[redacted] (2019c) Comparison of the IPD072Aa Protein Sequence to the Protein Sequences in the DuPont Pioneer Toxin Database. Pioneer Hi-Bred International, Inc., Study No. PHI-2019-039/211

[redacted] (2019) Comparison of the PAT Protein Sequence to the Protein Sequences in the DuPont Pioneer Toxin Database. Pioneer Hi-Bred International, Inc., Study No. PHI-2019-041/211

Mirsky HP, Cressman Jr RF, Ladics GS (2013) Comparative assessment of multiple criteria for the in silico prediction of cross-reactivity of proteins to known allergens. Regulatory Toxicology and Pharmacology 67: 232-239

Mlotshwa S, Pruss GJ, MacArthur JL, Endres MW, Davis C, Hofseth LJ, Peña MM, Vance V (2015) A novel chemopreventive strategy based on therapeutic microRNAs produced in plants. Cell Research 25: 521-524

[redacted] 2019a) Expressed Trait Protein Concentrations of a Maize Line Containing Event DP-Ø23211-2: US and Canada Test Sites. Pioneer Hi-Bred International, Inc., Study No. PHI-2018-010/010

[redacted] (2019b) Nutrient Composition of a Maize Line Containing the Event DP-Ø23211-2: U.S. and Canada Test Sites. Pioneer Hi-Bred International, Inc., Study No. PHI-2018-009/020

[redacted] (2019) Expressed Trait Protein and RNA Concentrations of a Maize Line Containing Event DP-Ø23211-2: US and Canada Test Sites. Pioneer Hi-Bred International, Inc., Study No. PHI-2018-010

[redacted] (2019c) DvSSJ1 double-stranded RNA Concentration of a Maize Line Containing Event DP-Ø23211-2: US and Canada Test Sites. Pioneer Hi-Bred International, Inc., Study No. PHI-2018-010/011

Moroz E, Lee SH, Yamada K, Halloy F, Martínez-Montero S, Jahns H, Hall J, Damha MJ, Castagner B, Leroux J-C (2016a) Carrier-free Gene Silencing by Amphiphilic Nucleic Acid Conjugates in Differentiated Intestinal Cells. Molecular Therapy - Nucleic Acids 5: e364

Moroz E, Matoori S, Leroux J-C (2016b) Oral delivery of macromolecular drugs: Where we are after almost 100 years of attempts. Advanced Drug Delivery Reviews 101: 108-121

[redacted] (2016) IPD072Aa Protein: Acute Oral Toxicity Study in Mice. Pioneer Hi-Bred International, Inc., Study No. PHI-2015-091

Negrotto D, Jolley M, Beer S, Wenck AR, Hansen G (2000) The use of phosphomannose-isomerase as a selectable marker to recover transgenic maize plants (*Zea mays* L.) via *Agrobacterium* transformation. Plant Cell Reports 19: 798-803

Niu X, Kassa A, Hu X, Robeson J, McMahon M, Richtman NM, Steimel JP, Kernodle BM, Crane VC, Sandahl G, Ritland JL, Presnail JK, Lu AL, Wu G (2017) Control of Western Corn Rootworm (*Diabrotica virgifera virgifera*) Reproduction through Plant-Mediated RNA Interference. Scientific Reports 7: 12591

O'Neill MJ, Bourre L, Melgar S, O'Driscoll CM (2011) Intestinal delivery of non-viral gene therapeutics: physiological barriers and preclinical models. Drug Discovery Today 16: 203-218

OECD (1993) Safety Evaluation of Foods Derived by Modern Biotechnology: Concepts and Principles. Organisation for Economic Cooperation and Development

OECD (1999) Consensus document on general information concerning the genes and their enzymes that confer tolerance to phosphinothricin herbicide. Organisation for Economic Co-operation and Development, ENV/JM/MONO(99)13

OECD (2002) Consensus Document on Compositional Considerations for New Varieties of Maize (*Zea Mays*): Key Food and Feed Nutrients, Anti-Nutrients and Secondary Plant Metabolites. Organisation for Economic Co-operation and Development, ENV/JM/MONO(2002)25

OECD (2003) Consensus Document on the Biology of *Zea mays* subsp. *mays* (Maize). Organisation for Economic Co-operation and Development, ENV/JM/MONO(2003)11

Parrott W, Chassy B, Ligon J, Meyer L, Petrick J, Zhou J, Herman R, Delaney B, Levine M (2010) Application of food and feed safety assessment principles to evaluate transgenic approaches to gene modulation in crops. Food and Chemical Toxicology 48: 1773-1790

Pawitan Y, Michiels S, Koscielny S, Gusnanto A, Ploner A (2005) False discovery rate, sensitivity and sample size for microarray studies. Bioinformatics 21: 3017-3024

Pearson WR, Lipman DJ (1988) Improved tools for biological sequence comparison. Proceedings of the National Academy of Sciences 85: 2444-2448

Pence M, Spence R, Rood T, Habig J, Collinge S (2016) Petition for Extension of Nonregulated Status for X17 Ranger Russet and Y9 Atlantic Potatoes with Late Blight Resistance, Low Acrylamide Potential, Lowered Reducing Sugars, and Reduced Black Spot. United States Department of Agriculture, Animal and Plant Health Inspection Service, USDA APHIS Petition No. 16-064-01P

Perkins DN, Pappin DJC, Creasy DM, Cottrell JS (1999) Probability-based protein identification by searching sequence databases using mass spectrometry data. Electrophoresis 20: 3551-3567

Petrick JS, Brower-Toland B, Jackson AL, Kier LD (2013) Safety assessment of food and feed from biotechnology-derived crops employing RNA-mediated gene regulation to achieve desired traits: A scientific review. Regulatory Toxicology and Pharmacology 66: 167-176

Petrick JS, Moore WM, Heydens WF, Koch MS, Sherman JH, Lemke SL (2015) A 28-day oral toxicity evaluation of small interfering RNAs and a long double-stranded RNA targeting vacuolar ATPase in mice. Regulatory Toxicology and Pharmacology 71: 8-23

PHI (2010) CropFocus: Corn Rootworm. Pioneer Hi-Bred International, Inc, https://www.pioneer.com/CMRoot/Pioneer/US/Non_Searchable/agronomy/cropfocus_pdf/corn_rootworm.pdf

Pickford AS, Cogoni C (2003) RNA-mediated gene silencing. Cellular and Molecular Life Sciences 60: 871-882

[redacted] (2018) Description and Sequence of the T-DNA Region from Plasmid PHP74643. Pioneer Hi-Bred International, Inc., Study No. PHI-2017-085

Privalle LS (2002) Phosphomannose Isomerase, a Novel Plant Selection System. Annals of the New York Academy of Sciences 964: 129-138

Proteau G, Sidenberg D, Sadowski P (1986) The minimal duplex DNA sequence required for site-specific recombination promoted by the FLP protein of yeast *in vitro*. Nucleic Acids Research 14: 4787-4802

Rabanel JM, Aoun V, Elkin I, Mokhtar M, Hildgen P (2012) Drug-Loaded Nanocarriers: Passive Targeting and Crossing of Biological Barriers. Current Medicinal Chemistry 19: 3070-3102

Raybould A, Higgins LS, Horak MJ, Layton RJ, Storer NP, De La Fuente JM, Herman RA (2012) Assessing the ecological risks from the persistence and spread of feral populations of insect-resistant transgenic maize. Transgenic Research 21: 655-664

Raybould A, Wilkinson MJ (2005) Assessing the environmental risks of gene flow from GM crops to wild relatives. In GM Poppy, MJ Wilkinson, eds, Gene flow from GM plants. Blackwell Publishing, Oxford, pp 169-185

Raynor GS, Ogden EC, Hayes JV (1972) Dispersion and Deposition of Corn Pollen from Experimental Sources. Agronomy Journal 64: 420-427

Reed J, Privalle L, Powell ML, Meghji M, Dawson J, Dunder E, Sutthe J, Wenck A, Launis K, Kramer C, Chang Y-F, Hansen G, Wright M (2001) Phosphomannose isomerase: An efficient selectable marker for plant transformation. In Vitro Cellular & Developmental Biology - Plant 37: 127-132

[redacted] (2018a) Characterization of the In Vitro Pancreatin Resistance of IPD072Aa Using SDS-PAGE and Western Blot Analysis. Pioneer Hi-Bred International, Inc., Study No. PHI-2016-053

[redacted] (2018b) Characterization of the In Vitro Pepsin Resistance of IPD072Aa Using SDS-PAGE and Western Blot Analysis. Pioneer Hi-Bred International, Inc., Study No. PHI-2016-051

[redacted] (2019) Safety Assessment of the DvSSJ1 Double-Stranded RNA (dsRNA) Expressed in Insect-Resistant and Herbicide-Tolerant DP-Ø23211-2 Maize. Pioneer Hi-Bred International, Inc., Study No. PHI-R054-Y19

[redacted] (2019) Development and Validation of an Event-Specific Quantitative Real-Time PCR (qPCR) Detection Method for Maize Event DP-Ø23211-2. Pioneer Hi-Bred International, Inc., Study No. PHI-2019-046 (Amended 2020)

Russell WA, Hallauer AR (1980) Corn. In Hybridization of Crop Plants. American Society of Agronomy-Crop Science Society of America, Madison, pp 299-312

Salanoubat M, Lemcke K, Rieger M, Ansorge W, Unseld M, Fartmann B, Valle G, Blöcker H, Perez-Alonso M, Obermaier B, Delseny M, Boutry M, Grivell LA, Mache R, Puigdomènech P, De Simone V, Choisne N, Artiguenave F, Robert C, Brottier P, Wincker P, Cattolico L, Weissenbach J, Saurin W, Quétier F, Schäfer M, Müller-Auer S, Gabel C, Fuchs M, Benes V, Wurmbach E, Drzonek H, Erfle H, Jordan N, Bangert S, Wiedelmann R, Kranz H, Voss H, Holland R, Brandt P, Nyakatura G, Vezzi A, D'Angelo M, Pallavicini A, Toppo S, Simionati B, Conrad A, Hornischer K, Kauer G, Löhnert TH, Nordsiek G, Reichelt J, Scharfe M, Schön O, Bargues M, Terol J, Climent J, Navarro P, Collado C, Perez-Perez A, Ottenwälder B, Duchemin D, Cooke R, Laudie M, Berger-Llauro C, Purnelle B, Masuy D, de Haan M, Maarse AC, Alcaraz JP, Cottet A, Casacuberta E, Monfort A, Argiriou A, Flores M, Liguori R, Vitale D, Mannhaupt G, Haase D, Schoof H, Rudd S, Zaccaria P, Mewes HW, Mayer KF, Kaul S, Town CD, Koo HL, Tallon LJ, Jenkins J, Rooney T, Rizzo M, Walts A, Utterback T, Fujii CY, Shea TP, Creasy TH, Haas B, Maiti R, Wu D, Peterson J, VanAken S, Pai G, Militscher J, Sellers P, Gill JE, Feldblyum TV, Preuss D, Lin X, Nierman WC, Salzberg SL, White O, Venter JC, Fraser CM, Kaneko T, Nakamura Y, Sato S, Kato T, Asamizu E, Sasamoto S, Kimura T, Idesawa K, Kawashima K, Kishida Y, Kiyokawa C, Kohara M, Matsumoto M, Matsuno A, Muraki A, Nakayama S, Nakazaki N, Shinpo S, Takeuchi C, Wada T, Watanabe A, Yamada M, Yasuda M, Tabata S (2000) Sequence and analysis of chromosome 3 of the plant *Arabidopsis thaliana*. Nature 408: 820-822

Sánchez-Navarro M, Garcia J, Giralt E, Teixidó M (2016) Using peptides to increase transport across the intestinal barrier. Advanced Drug Delivery Reviews 106: 355-366

Sánchez MA, Parrott WA (2017) Characterization of scientific studies usually cited as evidence of adverse effects of GM food/feed. Plant Biotechnology Journal 15: 1227-1234

Schellenberger U, Oral J, Rosen BA, Wei J-Z, Zhu G, Xie W, McDonald MJ, Cerf DC, Diehn SH, Crane VC, Sandahl GA, Zhao J-Z, Nowatzki TM, Sethi A, Liu L, Pan Z, Wang Y, Lu AL, Wu G, Liu L (2016) A selective insecticidal protein from *Pseudomonas* for controlling corn rootworms. Science 354: 634-637

Senda M, Kurauchi T, Kasai A, Ohnishi S (2012) Suppressive mechanism of seed coat pigmentation in yellow soybean. Breeding Science 61: 523-530

Shaw RH (1988) Climate Requirement. In GF Sprague, ed, Corn and Corn Improvement, Ed 3. ASA-CSSA-SSSA, Madison, pp 609-638

Sheehy RE, Kramer M, Hiatt WR (1988) Reduction of polygalacturonase activity in tomato fruit by antisense RNA. Proceedings of the National Academy of Sciences 85: 8805-8809

Sherman F, Stewart JW, Tsunasawa S (1985) Methionine or Not Methionine at the Beginning of a Protein. BioEssays 3: 27-31

Sherman JH, Munyikwa T, Chan SY, Petrick JS, Witwer KW, Choudhuri S (2015) RNAi technologies in agricultural biotechnology: The Toxicology Forum 40th Annual Summer Meeting. Regulatory Toxicology and Pharmacology 73: 671-680

Shrestha RB, Dunbar MW, French BW, Gassmann AJ (2018) Effects of field history on resistance to Bt maize by western corn rootworm, *Diabrotica virgifera virgifera* LeConte (Coleoptera: Chrysomelidae). PLoS One 13: e0200156

Shukla S, Sumaria CS, Pradeepkumar PI (2010) Exploring Chemical Modifications for siRNA Therapeutics: A Structural and Functional Outlook. ChemMedChem 5: 328-349

Slein MW (1950) Phosphomannose Isomerase. Journal of Biological Chemistry 186: 753-761

Sleper DA, Poehlman JM (2006) Breeding Corn (Maize). In Breeding Field Crops, Ed 5. Blackwell Publishing, pp 277-296

Snow JW, Hale AE, Isaacs SK, Baggish AL, Chan SY (2013) Ineffective delivery of diet-derived microRNAs to recipient animal organisms. RNA Biology 10: 1107-1116

Spelman RJ, Bovenhuis H (1998) Moving from QTL experimental results to the utilization of QTL in breeding programmes. Animal Genetics 29: 77-84

[redacted] (2019) Description of Transformation Method and Familiarity of PAT and PMI Proteins for Maize Event DP-Ø23211-2. Pioneer Hi-Bred International, Inc., Study No. PHI-2019-191

Stoutjesdijk PA, Singh SP, Liu Q, Hurlstone CJ, Waterhouse PA, Green AG (2002) hpRNA-Mediated Targeting of the Arabidopsis *FAD2* Gene Gives Highly Efficient and Stable Silencing. Plant Physiology 129: 1723-1731

Tao Y, Bidney D, Gordon-Kamm W, Lyznik L, inventors. January 25, 2007. Modified FRT Recombination Sites and Methods of Use. World Intellectual Property Organziation, Application No. PCT/US2006/027380

Tomizawa J-I, Ohmori H, Bird RE (1977) Origin of replication of colicin E1 plasmid DNA. Proceedings of the National Academy of Sciences 74: 1865-1869

Tran NL, Barraj LM, Collinge S (2017) Reduction in Dietary Acrylamide Exposure—Impact of Potatoes with Low Acrylamide Potential. Risk Analysis 37: 1754-1767

Tuteja JH, Clough SJ, Chan W-C, Vodkin LO (2004) Tissue-Specific Gene Silencing Mediated by a Naturally Occurring Chalcone Synthase Gene Cluster in *Glycine max*. The Plant Cell 16: 819-835

US-EPA (1997) Escherichia coli K-12 Derivatives Final Risk Assessment. United States Environmental Protection Agency, http://epa.gov/biotech_rule/pubs/fra/fra004.htm

US-EPA (2001) Environmental Protection Agency, 40 CFR Part 174, Exemption From the Requirement of a Tolerance Under the Federal Food, Drug and Cosmetic Act for Residues of Nucleic Acids that are Part of Plant-Incorporated Protectants (Formerly Plant-Pesticides). Federal Register 66: 37817-37830

US-EPA (2004) Phosphomannose Isomerase and the Genetic Material Necessary for Its Production in All Plants; Exemption from the Requirement of a Tolerance. Federal Register 69: 26770-26775

US-EPA (2016) A set of Scientific Issued Being Considered by the Environmental Protection Agency Regarding: RNAi Technology: Human Health and Ecological Risk Assessments for SmartStax PRO. In FIRFRA Scientific Advisory Panel Meeting, Arlington, VA, United States Environmental Protection Agency

US-FDA (1992) Statement of Policy: Foods Derived From New Plant Varieties. Federal Register 57: 22984-23005

US-FDA (2006) Guidance for Industry: Questions and Answers Regarding Food Allergens, including the Food Allergen Labeling and Consumer Protection Act of 2004 (Edition 4); Final Guidance. United States Food and Drug Administration, http://www.fda.gov/downloads/Food/GuidanceComplianceRegulatoryInformation/GuidanceDocuments/FoodLabelingNutrition/UCM301394.pdf

USDA-APHIS (2001) Approval of Mycogen Seeds c/o Dow AgroSciences LLC and Pioneer Hi-Bred International, Inc., Request (00-136-01p) Seeking a Determination of Non-regulated Status for Bt Cry1F Insect Resistant, Glufosinate Tolerant Corn Line 1507: Environmental Assessment and Finding of No Significant Impact. United States Department of Agriculture, Animal and Plant Health Inspection Service

USDA-APHIS (2005) Mycogen Seeds/Dow AgroSciences LLC and Pioneer Hi-Bred International Inc.; Availability of Determination of Nonregulated Status for Genetically Engineered Corn: Environmental Assessment and Finding of No Significant Impact. United States Department of Agriculture, Animal and Plant Health Inspection Service

USDA-APHIS (2011) Plant Pest Risk Assessment for Event 5307 Corn. United States Department of Agriculture, Animal and Plant Health Inspection Service, https://www.aphis.usda.gov/brs/aphisdocs/10_33601p_dpra.pdf

USDA-APHIS (2013) Determination of nonregulated status for Pioneer Event DP-ØØ4114-3 corn. United States Department of Agriculture, Animal and Plant Health Inspection Service, https://www.aphis.usda.gov/brs/aphisdocs/11_24401p_det.pdf

USDA-NASS (2018) Corn Acres - United States. United States Department of Agriculture, National Agricultural Statistics Service, https://www.nass.usda.gov/Charts_and_Maps/graphics/cornac.pdf

[redacted] (2019) Characterization of PMI Protein Derived from DP-Ø23211-2 Maize. Pioneer Hi-Bred International, Inc., Study No. PHI-2019-043

Van Eenennaam AL, Young AE (2014) Prevalence and impacts of genetically engineered feedstuffs on livestock populations. Journal of Animal Science 92: 4255-4278

Wagner AE, Piegholdt S, Ferraro M, Pallauf K, Rimbach G (2015) Food derived microRNAs. Food & Function 6: 714-718

Waigmann E, Gomes A, Lanzoni A, Perry JN (2013) Editorial: New Commission Implementing Regulation on Risk Assessment of GM plant applications: novel elements and challenges. The EFSA Journal 11: e11121

Waltz E (2015) Nonbrowning GM apple cleared for market. Nature Biotechnology 33: 326-327

Wang W, Hang C, Zhang Y, Chen M, Meng X, Cao Q, Song N, Itkow J, Shen F, Yu D (2017) Dietary miR-451 protects erythroid cells from oxidative stress via increasing the activity of Foxo3 pathway. Oncotarget 8: 107109-107124

Wasson-Blader T (2001) Living Colors™ DsRed2: Improved red fluorescent protein for use in living cells. Clontechniques 16: 2-3

Watson SA (1982) Corn: Amazing Maize. General Properties. In IA Wolff, ed, CRC Handbook of Processing and Utilization in Agriculture, Vol 2. CRC Press, Boca Raton, pp 3-29

Weber N, Halpin C, Hannah LC, Jez JM, Kough J, Parrott W (2012) Editor's Choice: Crop Genome Plasticity and Its Relevance to Food and Feed Safety of Genetically Engineered Breeding Stacks. Plant Physiology 160: 1842-1853

Wehrmann A, Van Vliet A, Opsomer C, Botterman J, Schulz A (1996) The similarities of *bar* and *pat* gene products make them equally applicable for plant engineers. Nature Biotechnology 14: 1274-1278

Weisser P, Krämer R, Sprenger GA (1996) Expression of the *Escherichia coli pmi* gene, encoding phosphomannose-isomerase in *Zymomonas mobilis*, leads to utilization of mannose as a novel growth substrate, which can be used as a selective marker. Applied and Environmental Microbiology 62: 4155-4161

Westfall PH, Tobias RD, Rom D, Wolfinger RD, Hochberg Y (1999) Concepts and Basic Methods for Multiple Comparisons and Tests. In Multiple Comparisons and Multiple Tests: Using SAS. SAS Institute Inc., Cary, NC, pp 13-40

WHO-GEMS (2019) Food Contamination Monitoring and Assessment Programme. Template for the evaluation of chronic exposure. World Health Organization/Global Environment Monitoring System, https://www.who.int/foodsafety/areas_work/chemical-risks/gems-food/en/

WHO (1995) Application of the Principles of Substantial Equivalence to the Safety Evaluation of Foods or Food Components from Plants Derived by Modern Biotechnology. World Health Organization, WHO/FNU/FOS/95.1

Witwer KW (2015) Contamination or artifacts may explain reports of plant miRNAs in humans. Journal of Nutritional Biochemistry 26: 1685

Witwer KW, Halushka MK (2016) Toward the promise of microRNAs – Enhancing reproducibility and rigor in microRNA research. RNA Biology 13: 1103-1116

Witwer KW, McAlexander MA, Queen SE, Adams RJ (2013) Real-time quantitative PCR and droplet digital PCR for plant miRNAs in mammalian blood provide little evidence for general uptake of dietary miRNAs. RNA Biology 10: 1080-1086

Witwer KW, Zhang C-Y (2017) Diet-derived microRNAs: unicorn or silver bullet? Genes & Nutrition 12: 15

Wohlleben W, Arnold W, Broer I, Hillemann D, Strauch E, Punier A (1988) Nucleotide sequence of the phosphinothricin *N*-acetyltransferase gene from *Streptomyces viridochromogenes* Tü494 and its expression in *Nicotiana tabacum*. Gene 70: 25-37

Yanagihashi Y, Usui T, Izumi Y, Yonemura S, Sumida M, Tsukita S, Uemura T, Furuse M (2012) Snakeskin, a membrane protein associated with smooth septate junctions, is required for intestinal barrier function in *Drosophila*. Journal of Cell Science 125: 1980-1990

Zastrow-Hayes GM, Lin H, Sigmund AL, Hoffman JL, Alarcon CM, Hayes KR, Richmond TA, Jeddeloh JA, May GD, Beatty MK (2015) Southern-by-Sequencing: A Robust Screening Approach for Molecular Characterization of Genetically Modified Crops. The Plant Genome 8: 1-15

Zhang L, Hou D, Chen X, Li D, Zhu L, Zhang Y, Li J, Bian Z, Liang X, Cai X, Yin Y, Wang C, Zhang T, Zhu D, Zhang D, Xu J, Chen Q, Ba Y, Liu J, Wang Q, Chen J, Wang J, Wang M, Zhang Q, Zhang J, Zen K, Zhang C-Y (2012) Exogenous plant MIR168a specifically targets mammalian LDLRAP1: evidence of cross-kingdom regulation by microRNA. Cell Research 22: 107-126

Zhuang J, Wang J-h, Zhang X, Liu Z-x (2011) Molecular Characterization of *Banana streak virus* Isolate from *Musa Acuminata* in China. Virologica Sinica 26: 393-402

Appendix A. Methods for Southern-by-Sequencing Analysis [redacted] 2019)

Test, Control and Reference Substances

The test substances in the study were defined as seeds from the T1 generation of DP23211 maize. The control substance was defined as seed from a maize line (PHR03) that was not transformed. PHR03 maize has a similar genetic background to the test substance; however, it does not contain the DP23211 maize insertion.

Plant Growth and Sample Collection

Test and control substance (DP23211 maize and control maize) seeds were planted and grown. The leaf tissues samples were collected and used for DNA extraction were maintained frozen (≤ -50 °C) until processing.

DNA Extraction and Quantitation

Genomic DNA was extracted from leaf tissue of DP23211 and control maize plants. The tissue was pulverized in tubes containing grinding beads using a Geno/Grinder™ (SPEX CertiPrep) and the genomic DNA was isolated using a standard Urea Extraction Buffer procedure. Following extraction, the DNA was quantified on a spectrofluorometer using the Quant-iT™ PicoGreen® dsDNA Assay Kit (Molecular Probes, Inc.) and visualized on an agarose gel to determine the DNA quality.

Southern-by-Sequencing

SbS was performed by Corteva Agriscience Genomics Technologies. SbS analysis utilizes probe-based sequence capture, Next Generation Sequencing (NGS) techniques, and bioinformatics procedures to capture, sequence, and identify inserted DNA within the maize genome (Zastrow-Hayes et al., 2015). By compiling a large number of unique sequencing reads and mapping them against the linearized transformation plasmid map and control maize genome, unique junctions due to inserted DNA are identified in the bioinformatics analysis. This information is used to determine the number of insertions within the plant genome, verify insertion intactness, and confirm the absence of plasmid backbone sequences. Genomic DNA isolated from the T1 generation of DP23211 maize was analyzed by SbS to determine the insertion copy number and intactness. SbS was also performed on control maize DNA and positive control samples (control maize DNA spiked with PHP74643, PHP56614, PHP21139, or PHP31729 plasmid DNA at a level corresponding to one copy of plasmid per copy of the maize genome) to confirm that the assay could reliably detect plasmid fragments within the genomic DNA.

The following processes were performed by Corteva Agriscience. Genomics Technologies using standard methods and were based on the procedures described in Zastrow-Hayes et al. (2015).

Capture Probe Design and Synthesis

Biotinylated capture probes used to select plasmid sequences were designed and synthesized by Roche NimbleGen, Inc. The probe set was designed to target all sequences within the PHP74643, PHP56614, PHP21139, and PHP31729 plasmids (**Figure 10**, Step 2).

Sequencing Library Construction

NGS libraries were constructed for DNA samples from individual maize plants, including DP23211 maize plants, a control maize plant, and the positive control samples. Genomic DNA purified as described above was sheared to an average fragment size of 400 bp using an ultrasonicator. Sheared DNA was end-repaired, A-tailed, and ligated to NEXTflex-HT™ Barcode adaptors (Bio Scientific Corp.) following the kit protocol so that samples would be

indexed to enable identification after sequencing. The DNA fragment libraries were amplified by PCR for eight cycles prior to the capture process. Amplified libraries were analyzed using a fragment analyzer and diluted to 5 ng/µl with nuclease-free water (**Figure 10**, Step 3).

Probe Hybridization and Sequence Enrichment

A double capture procedure was used to capture and enrich DNA fragments that contained sequences homologous to the capture probes. The genomic DNA libraries described above were mixed with hybridization buffer and blocking oligonucleotides corresponding to the adapter sequences and denatured. Following denaturation, the biotinylated probes were added to the genomic DNA library and incubated at 47 °C for 16 hours. Streptavidin beads were added to the hybridization mix to bind DNA fragments that were associated with the probes. Bound fragments were washed and eluted, PCR-amplified for five cycles, and purified using spin columns. The enriched DNA libraries underwent a second capture reaction using the same conditions to further enrich the sequences targeted by the probes. This was followed by PCR amplification for 16 cycles and purification as described above. The final double-enriched libraries were quantified and diluted to 2 nM for sequencing (**Figure 10**, Step 4).

Next Generation Sequencing on Illumina Platform

Following sequence capture, the libraries were submitted for NGS to a depth of 100x for the captured sequences. The sequence reads were trimmed for quality below Q20 (Ewing and Green, 1998; Ewing et al., 1998) and assigned to the corresponding individual plant based on the indexing adapters. A complete sequence set from each plant is referred to as "AllReads" for bioinformatics analysis of that plant (**Figure 10**, Step 5).

Quality Assurance of Sequencing Reads

The adapter sequences were trimmed from the NGS sequence reads with custom scripts. Further analysis to eliminate sequencing errors used JELLYFISH, version 1.1.4 (Marçais and Kingsford, 2011), to exclude any 31 bp sequence that occurred less than twice within "AllReads" as described in Zastrow-Hayes et al. (2015). This set of sequences was used for further bioinformatics analysis and is referred to as "CleanReads". Identical sequence reads were combined into non-redundant read groups while retaining abundance information for each group. The read group sequences from the most abundant 60% of the non-redundant groups (referred to as "Non-redundantReads") were used for further analysis, as described in Zastrow-Hayes et al. (2015) (**Figure 10**, Step 6).

Filtering Reads

Each set of "Non-redundantReads" was aligned to the maize reference genome using Bowtie, version 1.0.0 (Langmead et al., 2009) with up to two mismatches allowed. The "Non-redundantReads" not matching the maize reference genome were then compared to the plasmid sequences using Bowtie with zero mismatches allowed. Any "Non-redundantReads" that were not wholly derived from either maize or plasmid sequences were aligned to the plasmid backbone sequences with Bowtie 2, version 2.1.0, allowing zero mismatches. The ubiquitous presence of environmental bacteria, such as *Serratia marcescens,* provides an opportunity for their plasmid DNA to be sequenced along with plant genomic DNA. This resulted in low level detection of plasmid backbone sequences in the genomic DNA samples due to similarity with the plasmid backbone regions. The "Non-redundantReads" that aligned to the plasmid backbone sequence, but at a coverage depth below 35x across 50 bp, were deemed to be due to environmental bacteria (**Figure 10**, Step 7). Due to the detection of these bacterial sequences, coverage levels of 35x or below were considered to be the background level of sequencing.

Junction Detection

Following removal of "Non-redundantReads" with alignments wholly to the maize reference genome or plasmid sequence identified during the quality assurance phase, the remaining "Non-redundantReads" were aligned to the full plasmid sequence using BWA, version 0.5.9-r16, with the soft-trimming feature enabled (Li and Durbin, 2010). Chimeric reads contain sequence that is non-contiguous with the plasmid sequence from the alignment, such as genome-plasmid junctions or rearrangements of the plasmid. These chimeric reads are referred to as junction reads or junctions. The individual reads defining a junction were condensed to a unique identifier to represent the junction. This identifier (referred to as a 30_20 mer) includes 20 bp of sequence from PHP74643, PHP56614, PHP21139, or PHP31729, and 30 bp of sequence adjacent to the 20 bp from the plasmid. The adjacent 30 bp did not align to the plasmid contiguously to the known 20 bp. When the 20 bp from the plasmid and the adjacent 30 bp are combined into a 30_20 mer, they indicate the junction shown by the chimeric read. Junction reads were condensed into a unique junction if their 30_20 mers were identical, or if the 30_20 mer junctions were within 2 bp. The total number of sequence reads (referred to as "TotalSupportingReads") for each unique junction was retained for filtering. Junctions with fewer than five unique supporting reads, or if the "TotalSupportingReads" value was equal to or below 10% of the median sequencing depth for positions aligned to the plasmid, were filtered and removed from further analysis (**Figure 10**, Step 8).

Junction Identification

Variations between the maize reference genome used in the SbS analysis and the control maize genome may result in identification of junctions that are due to these differences in the endogenous maize sequences. In order to detect these endogenous junctions, control maize genomic DNA libraries were captured and sequenced in the same manner. These libraries were sequenced to an average depth approximately five times the depth for the DP23211 maize plant samples. This increased the probability that the endogenous junctions captured by the plasmid probes would be detected in the control maize samples, so that they could be identified and removed from the DP23211 maize sample. The 30_20 mers of the endogenous junctions detected in this analysis were used to filter the same endogenous junctions in the DP23211 maize samples (**Figure** 10, Step 8), so that the only junctions remaining in the DP23211 samples are due to actual insertions derived from PHP74643, PHP56614, PHP21139, or PHP31729 (**Figure 10**, Step 9).

SbS Results

Results for the control maize, positive control, and one DP23211 maize plant (Plant ID 343210845) are presented in the main body (Section 4a) of this document.

Remaining plant results from SbS analysis are presented in **Figures A1** to **A9** below:

A. Alignment to Intended Insertion

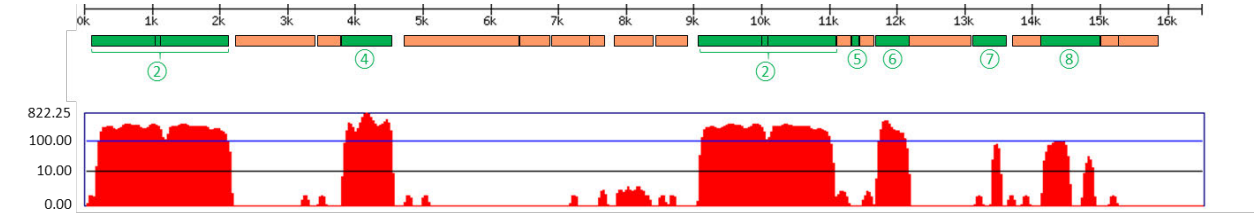

B. Alignment to PHP74643

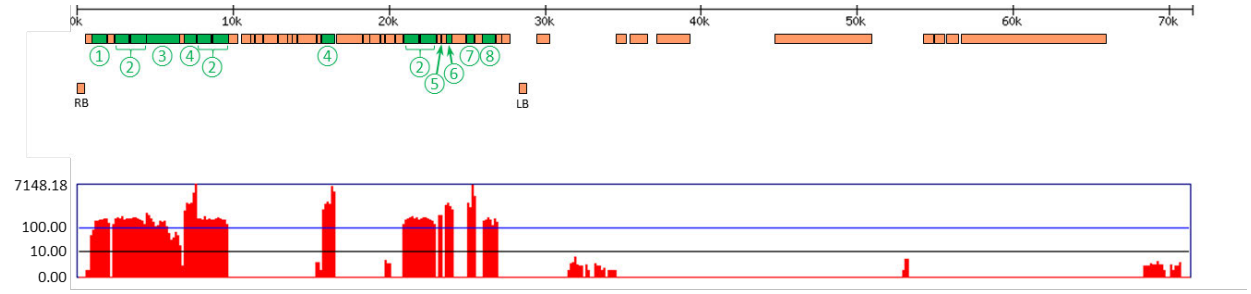

C. Alignment to PHP56614

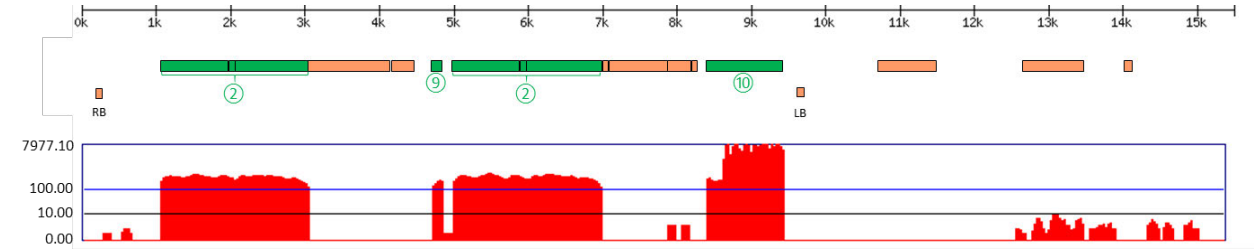

D. Alignment to PHP21139

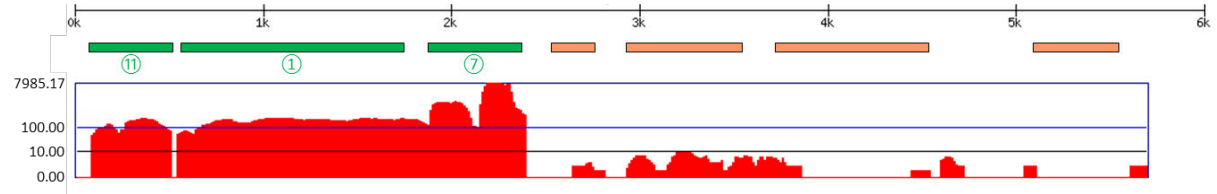

E. Alignment to PHP31729

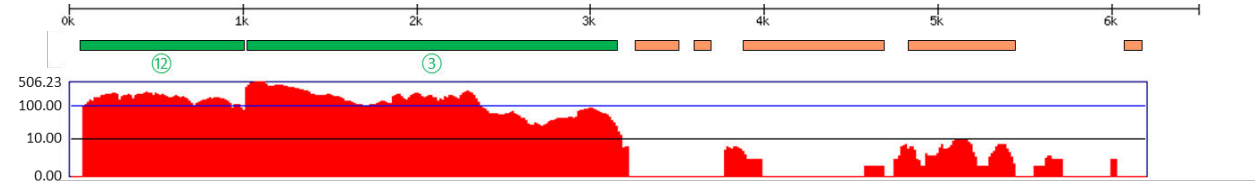

Figure A1. SbS Results for DP23211 Maize (Plant ID 343210846)

The red coverage graph shows the number of individual NGS reads aligned at each point on the intended insertion or construct using a logarithmic scale. Green bars above the coverage graph indicate endogenous genetic elements in each plasmid derived from the maize genome (identified by numbers, **Table 6**), while tan bars indicate genetic elements derived from other sources. **A)** SbS results aligned against the intended insertion (16,176 bp; **Figure**7), indicating that this plant does not contain the intended insertion. Coverage above background level (35x) was obtained only for regions derived from maize endogenous elements. Variation in coverage of the endogenous elements is due to some sequence variation between the control maize and the source of the corresponding genetic elements. As no junctions were detected between plasmid sequences and the maize genome, there are no DNA insertions identified in this plant, and the sequence reads are solely due to the endogenous elements present

in the maize genome. **B)** SbS results aligned against the plasmid PHP74643 sequence (71,116 bp; **Figure** 5). Coverage was obtained only for the endogenous elements. **C)** SbS results aligned against the plasmid PHP56614 sequence (15,339 bp; **Figure** 1). Coverage was obtained only for the endogenous elements. **D)** SbS results aligned against the plasmid PHP21139 sequence (5,687 bp; **Figure** 3). Coverage was obtained only for the endogenous elements. **E)** SbS results aligned against the plasmid PHP31729 sequence (6,181 bp; **Figure** 4). Coverage was obtained only for the endogenous elements. The absence of any junctions between plasmid and genomic sequences indicates that there are no insertions or backbone sequence present in this plant from the T1 generation of DP23211 maize.

A. Alignment to Intended Insertion

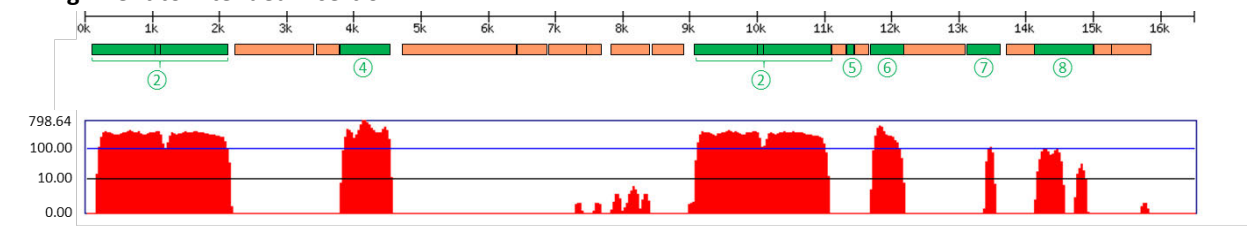

B. Alignment to PHP74643

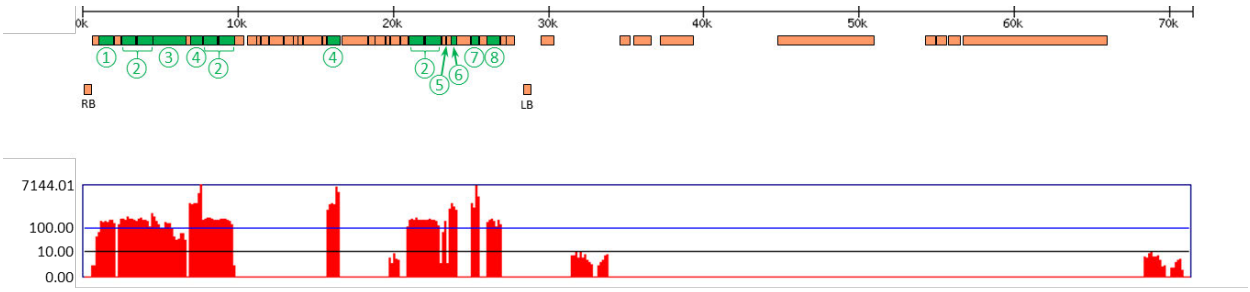

C. Alignment to PHP56614

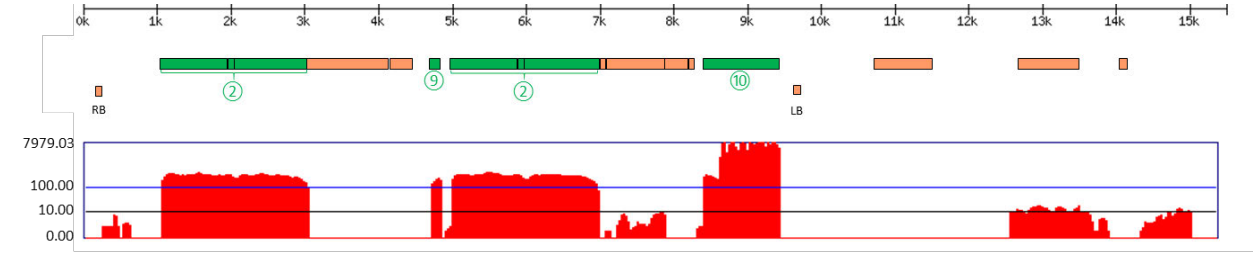

D. Alignment to PHP21139

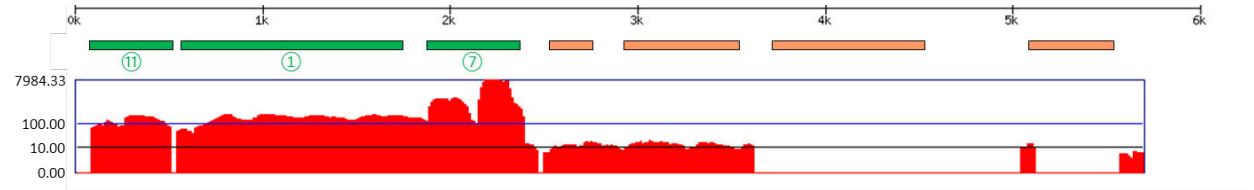

E. Alignment to PHP31729

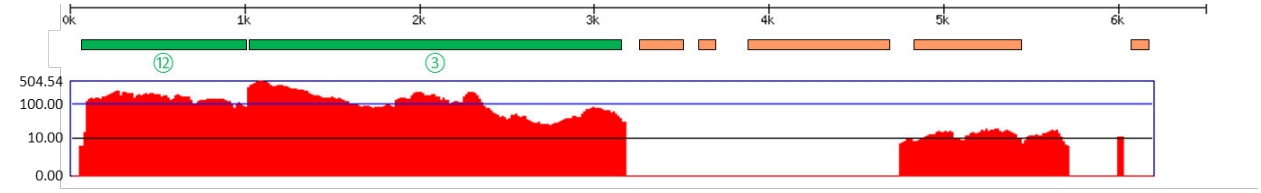

Figure A2. SbS Results for DP23211 Maize (Plant ID 343210847)

The red coverage graph shows the number of individual NGS reads aligned at each point on the intended insertion or construct using a logarithmic scale. Green bars above the coverage graph indicate endogenous genetic elements in each plasmid derived from the maize genome (identified by numbers, **Table 6**), while tan bars indicate genetic elements derived from other sources. **A)** SbS results aligned against the intended insertion (16,176 bp; **Figure** 7), indicating that this plant does not contain the intended insertion. Coverage above background level

(35x) was obtained only for regions derived from maize endogenous elements. Variation in coverage of the endogenous elements is due to some sequence variation between the control maize and the source of the corresponding genetic elements. As no junctions were detected between plasmid sequences and the maize genome, there are no DNA insertions identified in this plant, and the sequence reads are solely due to the endogenous elements present in the maize genome. **B)** SbS results aligned against the plasmid PHP74643 sequence (71,116 bp; **Figure** 5). Coverage was obtained only for the endogenous elements. **C)** SbS results aligned against the plasmid PHP56614 sequence (15,339 bp; **Figure** 1). Coverage was obtained only for the endogenous elements. **D)** SbS results aligned against the plasmid PHP21139 sequence (5,687 bp; **Figure** 3). Coverage was obtained only for the endogenous elements. **E)** SbS results aligned against the plasmid PHP31729 sequence (6,181 bp; **Figure** 4). Coverage was obtained only for the endogenous elements. The absence of any junctions between plasmid and genomic sequences indicates that there are no insertions or backbone sequence present in this plant from the T1 generation of DP23211 maize.

A. Alignment to Intended Insertion

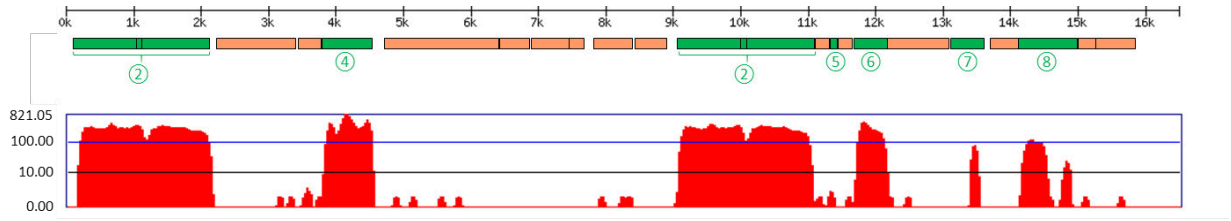

B. Alignment to PHP74643

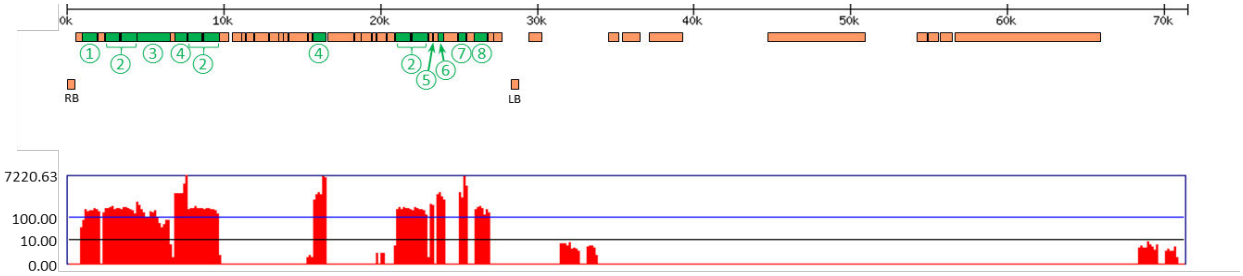

C. Alignment to PHP56614

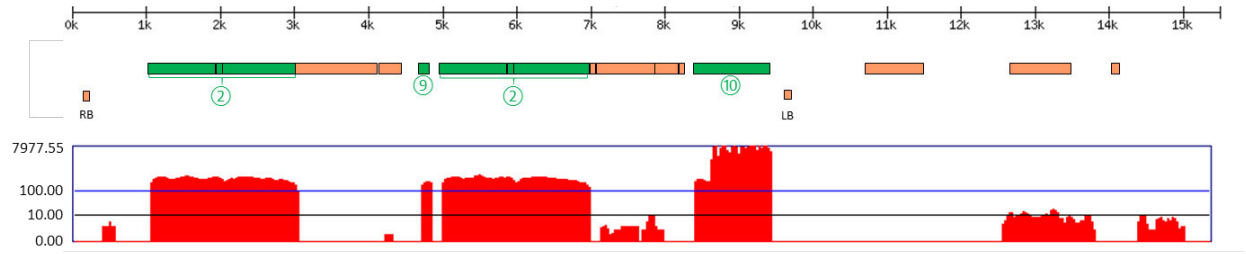

D. Alignment to PHP21139

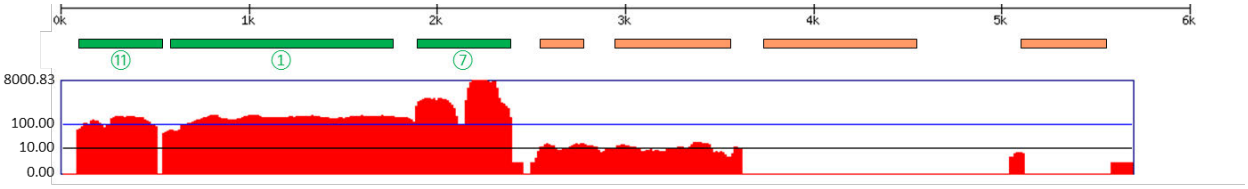

E. Alignment to PHP31729

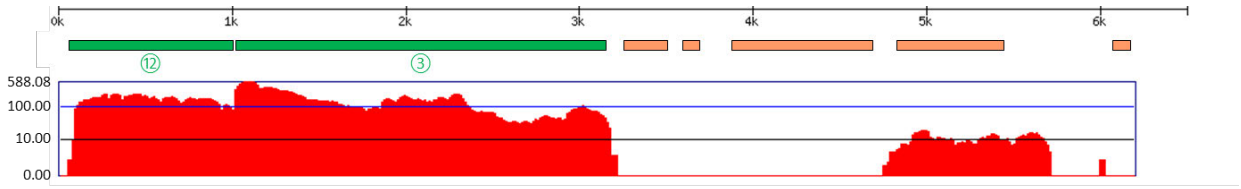

Figure A3. SbS Results for DP23211 Maize (Plant ID 343210848)

The red coverage graph shows the number of individual NGS reads aligned at each point on the intended insertion or construct using a logarithmic scale. Green bars above the coverage graph indicate endogenous genetic elements in each plasmid derived from the maize genome (identified by numbers, **Table 6**), while tan bars indicate genetic elements derived from other sources. **A)** SbS results aligned against the intended insertion (16,176 bp;

Figure 7), indicating that this plant does not contain the intended insertion. Coverage above background level (35x) was obtained only for regions derived from maize endogenous elements. Variation in coverage of the endogenous elements is due to some sequence variation between the control maize and the source of the corresponding genetic elements. As no junctions were detected between plasmid sequences and the maize genome, there are no DNA insertions identified in this plant, and the sequence reads are solely due to the endogenous elements present in the maize genome. **B)** SbS results aligned against the plasmid PHP74643 sequence (71,116 bp; **Figure** 5). Coverage was obtained only for the endogenous elements. **C)** SbS results aligned against the plasmid PHP56614 sequence (15,339 bp; **Figure** 1). Coverage was obtained only for the endogenous elements. **D)** SbS results aligned against the plasmid PHP21139 sequence (5,687 bp; **Figure** 3). Coverage was obtained only for the endogenous elements. **E)** SbS results aligned against the plasmid PHP31729 sequence (6,181 bp; **Figure** 4). Coverage was obtained only for the endogenous elements. The absence of any junctions between plasmid and genomic sequences indicates that there are no insertions or backbone sequence present in this plant from the T1 generation of DP23211 maize.

A. Alignment to Intended Insertion

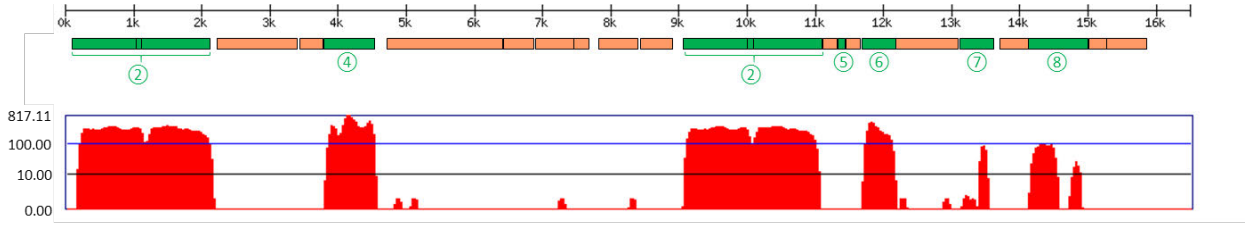

B. Alignment to PHP74643

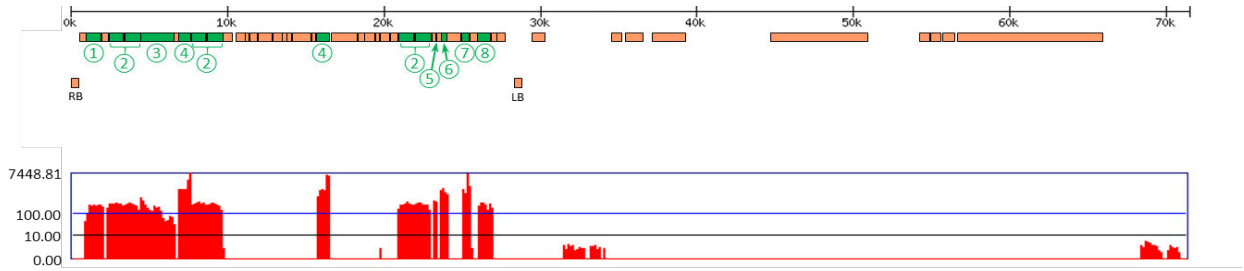

C. Alignment to PHP56614

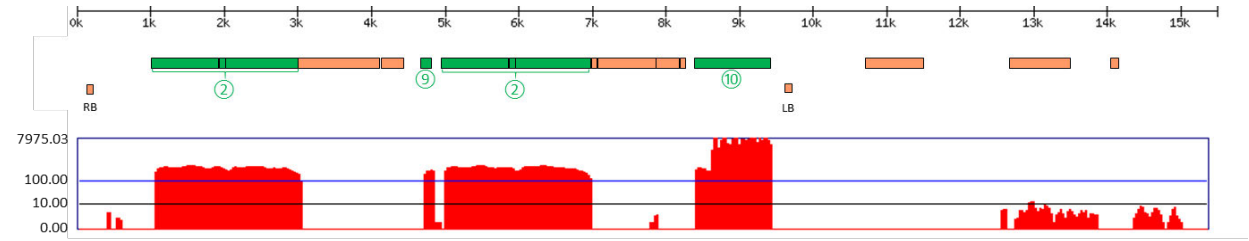

D. Alignment to PHP21139

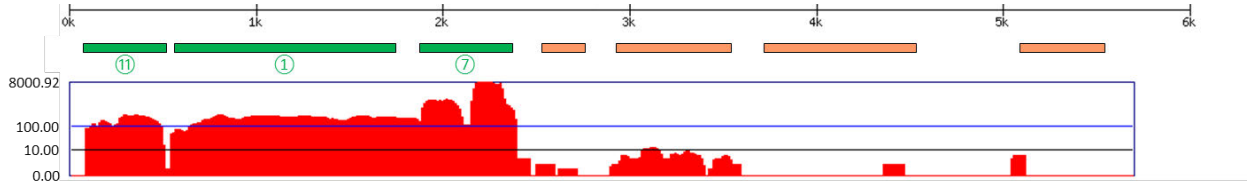

E. Alignment to PHP31729

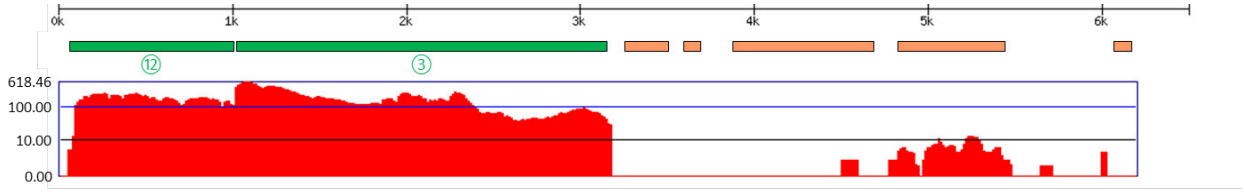

Figure A4. SbS Results for DP23211 Maize (Plant ID 343210849)

The red coverage graph shows the number of individual NGS reads aligned at each point on the intended insertion or construct using a logarithmic scale. Green bars above the coverage graph indicate endogenous genetic elements in each plasmid derived from the maize genome (identified by numbers, **Table 6**), while tan bars indicate genetic elements derived from other sources. **A)** SbS results aligned against the intended insertion (16,176 bp;

Figure 7), indicating that this plant does not contain the intended insertion. Coverage above background level (35x) was obtained only for regions derived from maize endogenous elements. Variation in coverage of the endogenous elements is due to some sequence variation between the control maize and the source of the corresponding genetic elements. As no junctions were detected between plasmid sequences and the maize genome, there are no DNA insertions identified in this plant, and the sequence reads are solely due to the endogenous elements present in the maize genome. **B)** SbS results aligned against the plasmid PHP74643 sequence (71,116 bp; **Figure 5**). Coverage was obtained only for the endogenous elements. **C)** SbS results aligned against the plasmid PHP56614 sequence (15,339 bp; **Figure 1**). Coverage was obtained only for the endogenous elements. **D)** SbS results aligned against the plasmid PHP21139 sequence (5,687 bp; **Figure 3**). Coverage was obtained only for the endogenous elements. **E)** SbS results aligned against the plasmid PHP31729 sequence (6,181 bp; **Figure 4**). Coverage was obtained only for the endogenous elements. The absence of any junctions between plasmid and genomic sequences indicates that there are no insertions or backbone sequence present in this plant from the T1 generation of DP23211 maize.

A. Alignment to Intended Insertion

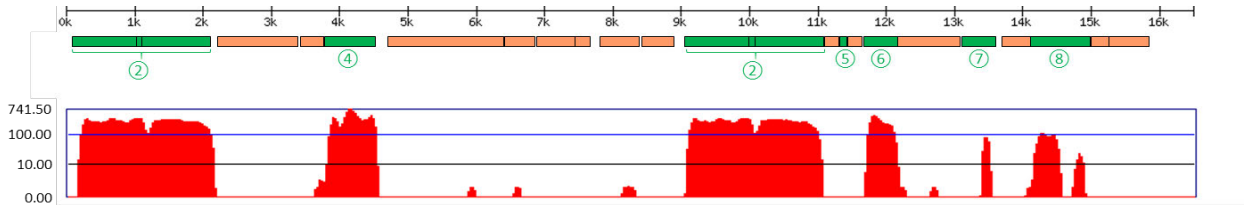

B. Alignment to PHP74643

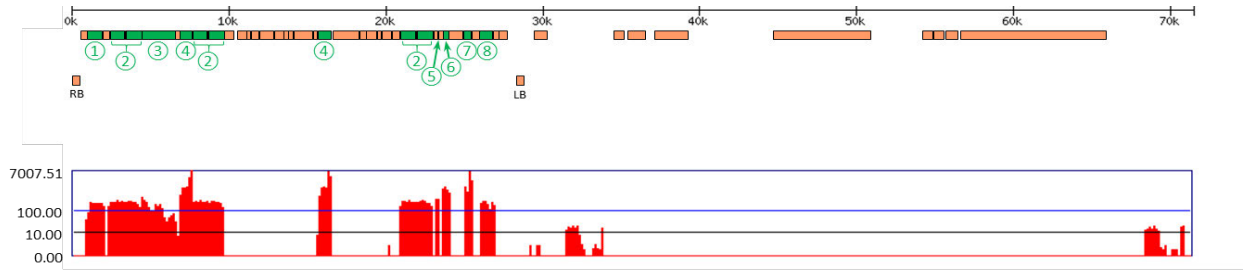

C. Alignment to PHP56614

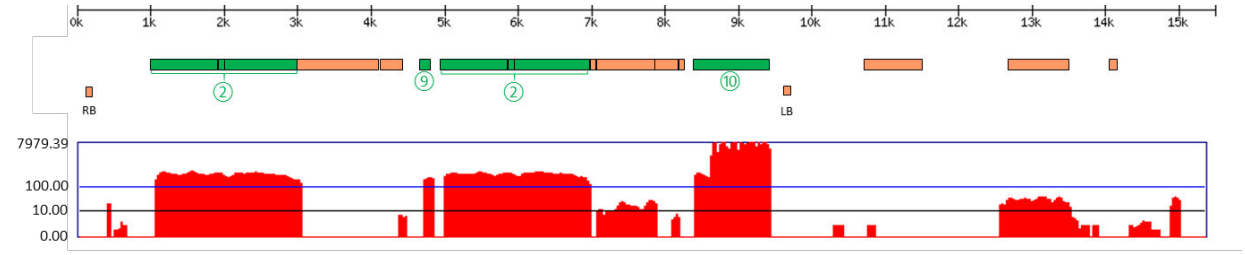

D. Alignment to PHP21139

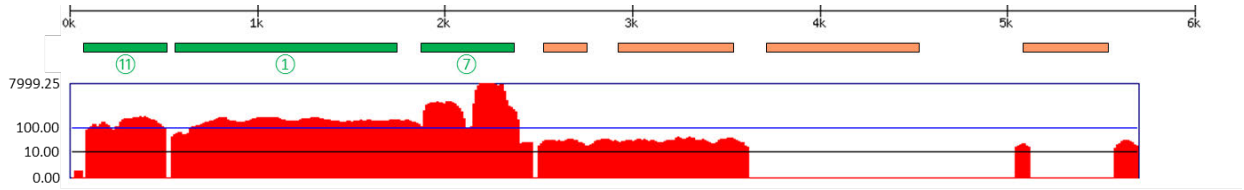

E. Alignment to PHP31729

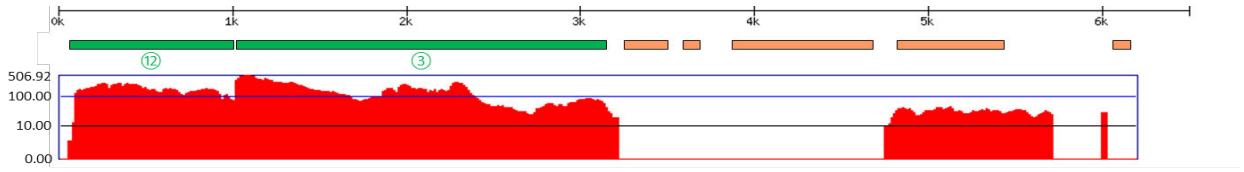

Figure A5. SbS Results for DP23211 Maize (Plant ID 343210850)

The red coverage graph shows the number of individual NGS reads aligned at each point on the intended insertion or construct using a logarithmic scale. Green bars above the coverage graph indicate endogenous genetic elements in each plasmid derived from the maize genome (identified by numbers, **Table 6**), while tan bars indicate genetic elements derived from other sources. **A)** SbS results aligned against the intended insertion (16,176 bp; **Figure 7**), indicating that this plant does not contain the intended insertion. Coverage above background level

(35x) was obtained only for regions derived from maize endogenous elements. Variation in coverage of the endogenous elements is due to some sequence variation between the control maize and the source of the corresponding genetic elements. As no junctions were detected between plasmid sequences and the maize genome, there are no DNA insertions identified in this plant, and the sequence reads are solely due to the endogenous elements present in the maize genome. **B)** SbS results aligned against the plasmid PHP74643 sequence (71,116 bp; **Figure 5**). Coverage was obtained only for the endogenous elements. **C)** SbS results aligned against the plasmid PHP56614 sequence (15,339 bp; **Figure 1**). Coverage was obtained only for the endogenous elements. **D)** SbS results aligned against the plasmid PHP21139 sequence (5,687 bp; **Figure 3**). Coverage was obtained only for the endogenous elements. **E)** SbS results aligned against the plasmid PHP31729 sequence (6,181 bp; **Figure 4**). Coverage was obtained only for the endogenous elements. The absence of any junctions between plasmid and genomic sequences indicates that there are no insertions or backbone sequence present in this plant from the T1 generation of DP23211 maize.

A. Alignment to Intended Insertion

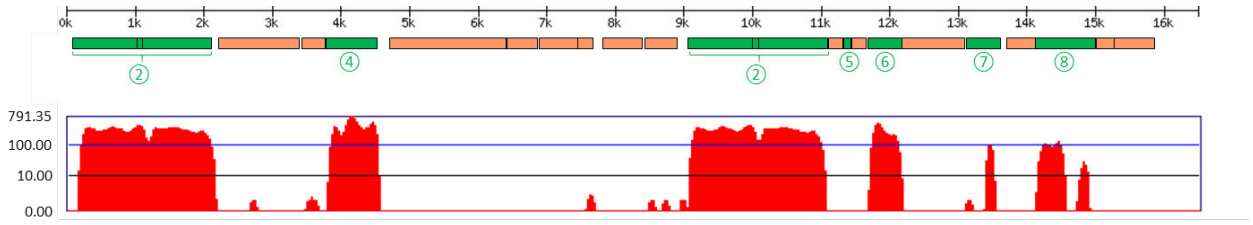

B. Alignment to PHP74643

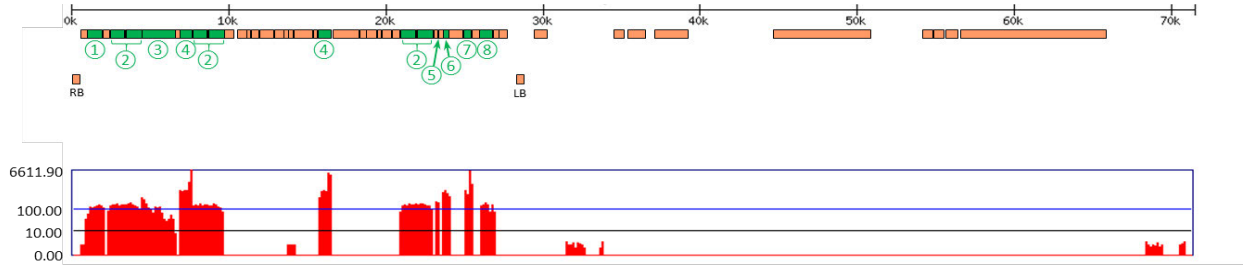

C. Alignment to PHP56614

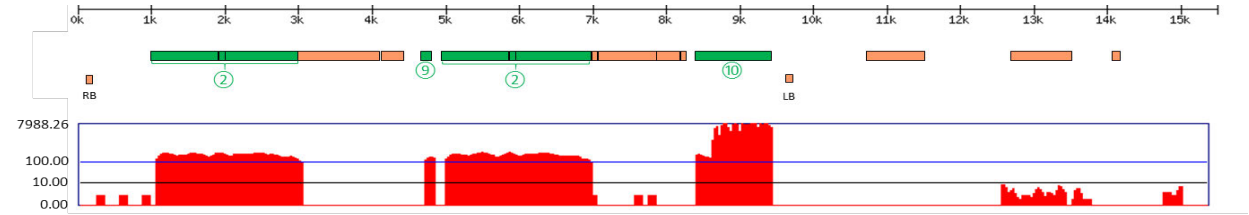

D. Alignment to PHP21139

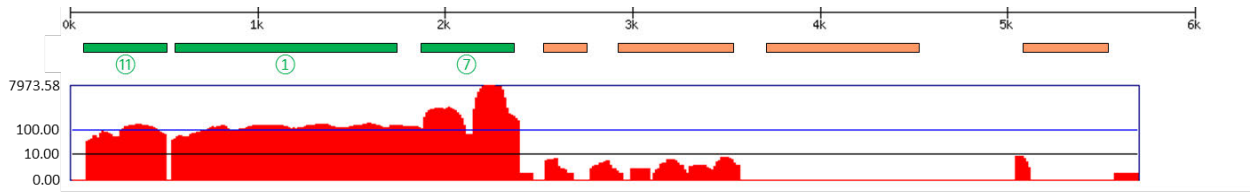

E. Alignment to PHP31729

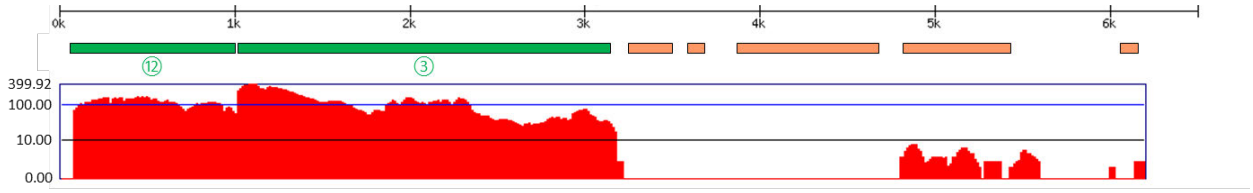

Figure A6. SbS Results for DP23211 Maize (Plant ID 343210851)

The red coverage graph shows the number of individual NGS reads aligned at each point on the intended insertion or construct using a logarithmic scale. Green bars above the coverage graph indicate endogenous genetic elements in each plasmid derived from the maize genome (identified by numbers, **Table 6**), while tan bars indicate genetic elements derived from other sources. **A)** SbS results aligned against the intended insertion (16,176 bp; **Figure 7**), indicating that this plant does not contain the intended insertion. Coverage above background level (35x) was obtained only for regions derived from maize endogenous elements. Variation in coverage of the

endogenous elements is due to some sequence variation between the control maize and the source of the corresponding genetic elements. As no junctions were detected between plasmid sequences and the maize genome, there are no DNA insertions identified in this plant, and the sequence reads are solely due to the endogenous elements present in the maize genome. **B)** SbS results aligned against the plasmid PHP74643 sequence (71,116 bp; **Figure 5**). Coverage was obtained only for the endogenous elements. **C)** SbS results aligned against the plasmid PHP56614 sequence (15,339 bp; **Figure 1**). Coverage was obtained only for the endogenous elements. **D)** SbS results aligned against the plasmid PHP21139 sequence (5,687 bp; **Figure 3**). Coverage was obtained only for the endogenous elements. **E)** SbS results aligned against the plasmid PHP31729 sequence (6,181 bp; **Figure 4**). Coverage was obtained only for the endogenous elements. The absence of any junctions between plasmid and genomic sequences indicates that there are no insertions or backbone sequence present in this plant from the T1 generation of DP23211 maize.

A. Alignment to Intended Insertion

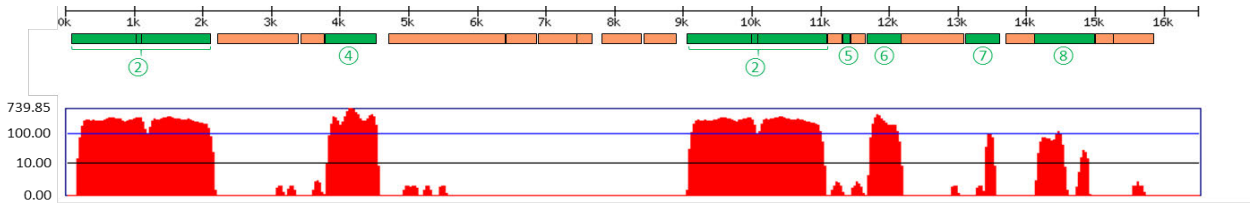

B. Alignment to PHP74643

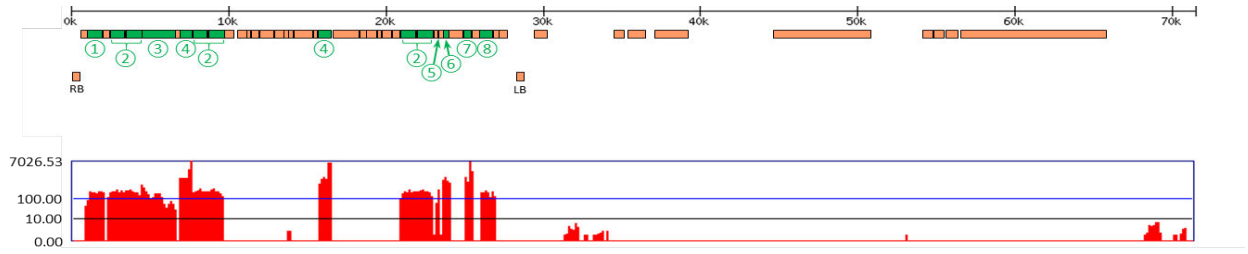

C. Alignment to PHP56614

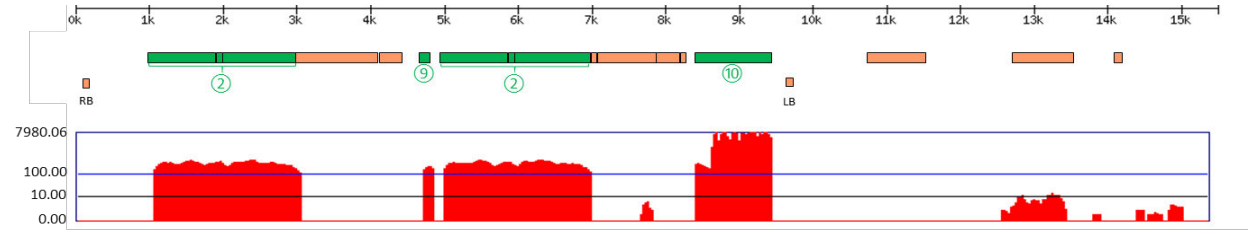

D. Alignment to PHP21139

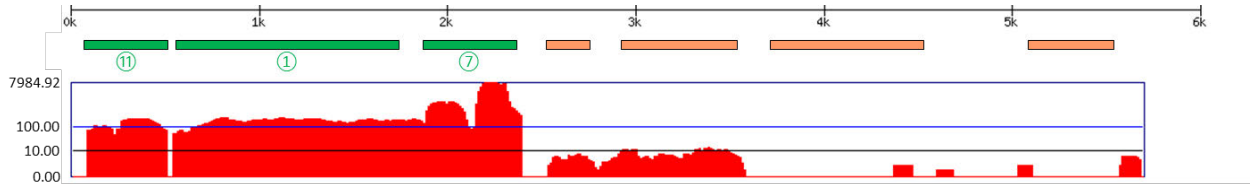

E. Alignment to PHP31729

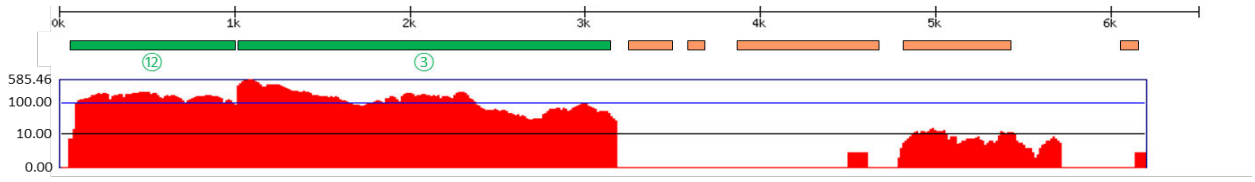

Figure A7. SbS Results for DP23211 Maize (Plant ID 343210852)

The red coverage graph shows the number of individual NGS reads aligned at each point on the intended insertion or construct using a logarithmic scale. Green bars above the coverage graph indicate endogenous genetic elements in each plasmid derived from the maize genome (identified by numbers, **Table 6**), while tan bars indicate genetic elements derived from other sources. **A)** SbS results aligned against the intended insertion (16,176 bp; **Figure 7**), indicating that this plant does not contain the intended insertion. Coverage above background level

(35x) was obtained only for regions derived from maize endogenous elements. Variation in coverage of the endogenous elements is due to some sequence variation between the control maize and the source of the corresponding genetic elements. As no junctions were detected between plasmid sequences and the maize genome, there are no DNA insertions identified in this plant, and the sequence reads are solely due to the endogenous elements present in the maize genome. **B)** SbS results aligned against the plasmid PHP74643 sequence (71,116 bp; **Figure 5**). Coverage was obtained only for the endogenous elements. **C)** SbS results aligned against the plasmid PHP56614 sequence (15,339 bp; **Figure 1**). Coverage was obtained only for the endogenous elements. **D)** SbS results aligned against the plasmid PHP21139 sequence (5,687 bp; **Figure 3**). Coverage was obtained only for the endogenous elements. **E)** SbS results aligned against the plasmid PHP31729 sequence (6,181 bp; **Figure 4**). Coverage was obtained only for the endogenous elements. The absence of any junctions between plasmid and genomic sequences indicates that there are no insertions or backbone sequence present in this plant from the T1 generation of DP23211 maize.

A. Alignment to Intended Insertion

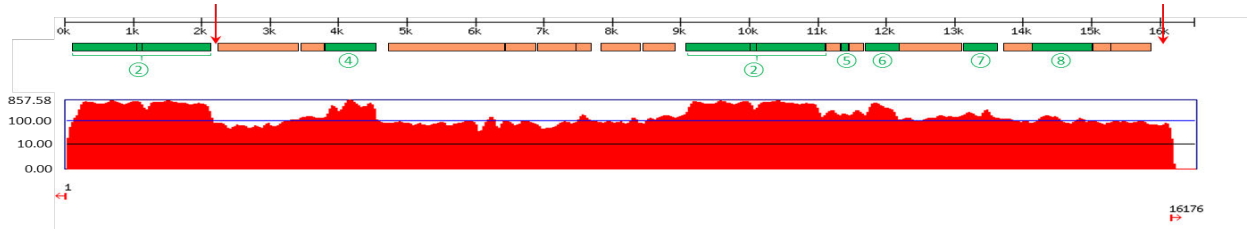

B. Alignment to PHP74643

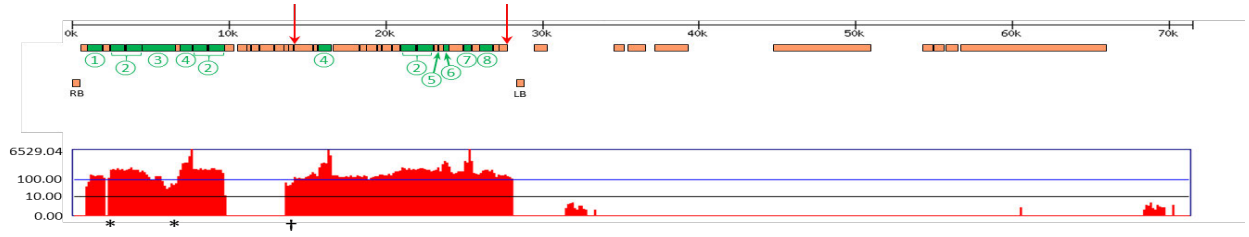

C. Alignment to PHP56614

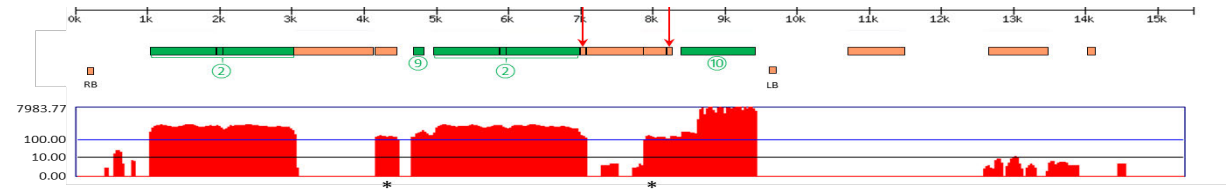

D. Alignment to PHP21139

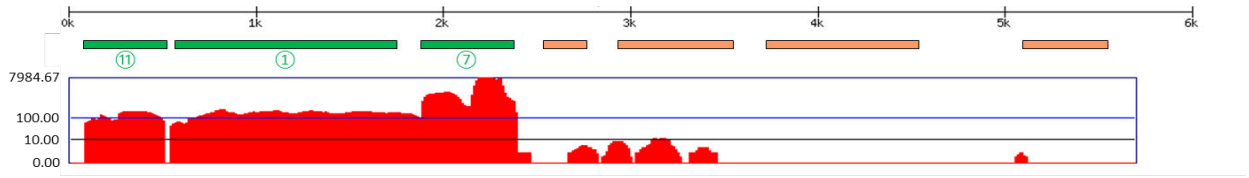

E. Alignment to PHP31729

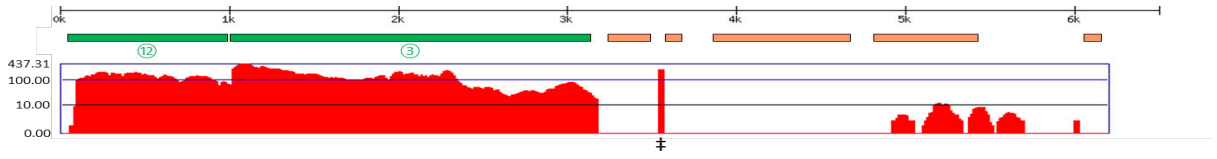

Figure A8. SbS Results for DP23211 Maize (Plant ID 343210853)

The red coverage graph shows the number of individual NGS reads aligned at each point on the intended insertion or construct using a logarithmic scale. Green bars above the coverage graph indicate endogenous genetic elements in each plasmid derived from the maize genome (identified by numbers, **Table 6**), while tan bars indicate genetic elements derived from other sources. FRT sites are indicated by red arrows. **A)** SbS results aligned against the intended insertion (16,176 bp; **Figure 7**), indicating that this plant contains the intended insertion. Arrows below the graph indicate the two plasmid-to-genome sequence junctions identified by SbS; the numbers above the arrows refer to the bp location of the junction relative to the intended insertion (**Figure 7**). The presence of only two junctions demonstrates the presence of a single insertion in the DP23211 maize genome. **B)** SbS results

aligned against the plasmid PHP74643 sequence (71,116 bp; **Figure 5**). Coverage was obtained for the elements between FRT1 and FRT87 transferred into DP23211 maize (region between the red arrows at top of graph). Coverage was also obtained for the endogenous elements in the region from approximately 1k to 10k that were not transferred into the DP23211 maize genome, and to the *pin*II terminator (*) and CaMV35S terminator (†) elements outside of the FRT sites due to alignment of reads derived from identical elements in the final insertion to all copies of these elements in PHP74643. **C)** SbS results aligned against the plasmid PHP56614 sequence (15,339 bp; **Figure 1**). Coverage was obtained for *zm*-SEQ9, *zm*-SEQ8, the elements found in the intended insertion (between *zm*-SEQ9 to FRT1 and between FRT87 to *zm*-SEQ8), and for the endogenous elements not in the intended insertion (the *ubi*ZM1 promoter, 5' UTR, and intron in the I-*Cre*I cassette), along with the *pin*II terminator elements (*) in PHP56614 due to alignment of reads derived from the *pin*II terminator in the *pmi* cassette of the intended insertion to the two copies of this element in PHP56614. **D)** SbS results aligned against the plasmid PHP21139 sequence (5,687 bp; **Figure 3**). Coverage was obtained only for the endogenous elements. **E)** SbS results aligned against the plasmid PHP31729 sequence (6,181 bp; **Figure 4**). Coverage was obtained for the endogenous elements and for a small segment of an *att* recombination site that matches an *att* site found in the intended insertion (‡). The absence of any junctions other than to the intended insertion indicates that there are no additional insertions or backbone sequence present in DP23211 maize.

A. Alignment to Intended Insertion

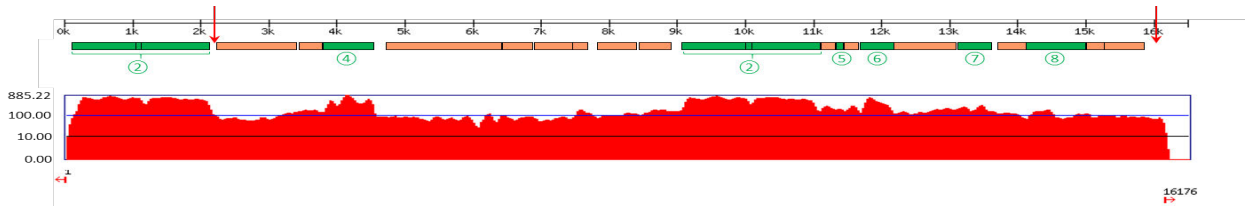

B. Alignment to PHP74643

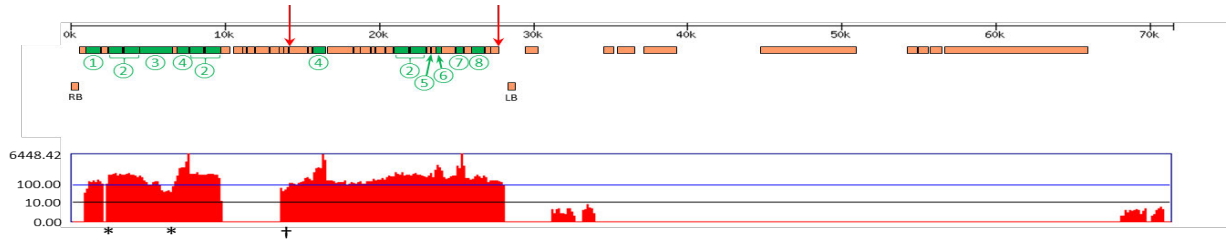

C. Alignment to PHP56614

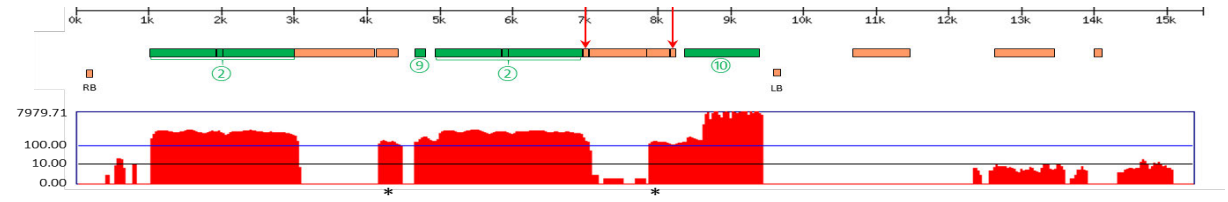

D. Alignment to PHP21139

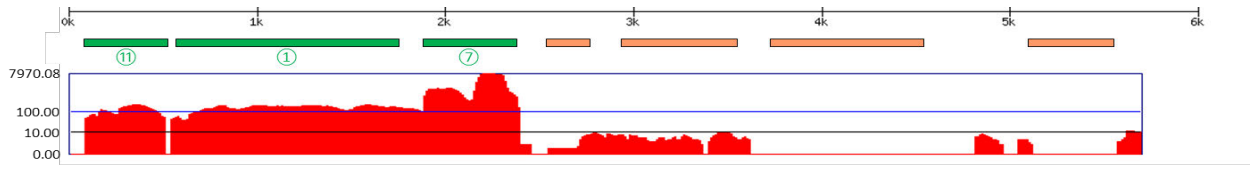

E. Alignment to PHP31729

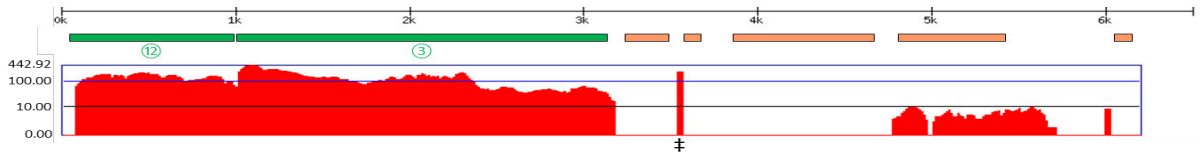

Figure A9. SbS Results for DP23211 Maize (Plant ID 343210854)

The red coverage graph shows the number of individual NGS reads aligned at each point on the intended insertion or construct using a logarithmic scale. Green bars above the coverage graph indicate endogenous genetic elements in each plasmid derived from the maize genome (identified by numbers, Table 6), while tan bars indicate genetic elements derived from other sources. FRT sites are indicated by red arrows. **A)** SbS results aligned against the intended insertion (16,176 bp; **Figure 7**), indicating that this plant contains the intended insertion. Arrows below the graph indicate the two plasmid-to-genome sequence junctions identified by SbS; the numbers above the arrows refer to the bp location of the junction relative to the intended insertion (**Figure 7**). The presence of only

two junctions demonstrates the presence of a single insertion in the DP23211 maize genome. **B)** SbS results aligned against the plasmid PHP74643 sequence (71,116 bp; **Figure 5**). Coverage was obtained for the elements between FRT1 and FRT87 transferred into DP23211 maize (region between the red arrows at top of graph). Coverage was also obtained for the endogenous elements in the region from approximately 1k to 10k that were not transferred into the DP23211 maize genome, and to the *pin*II terminator (*) and CaMV35S terminator (†) elements outside of the FRT sites due to alignment of reads derived from identical elements in the final insertion to all copies of these elements in PHP74643. **C)** SbS results aligned against the plasmid PHP56614 sequence (15,339 bp; **Figure 1**). Coverage was obtained for *zm*-SEQ9, *zm*-SEQ8, the elements found in the intended insertion (between *zm*-SEQ9 to FRT1 and between FRT87 to *zm*-SEQ8), and for the endogenous elements not in the intended insertion (the *ubi*ZM1 promoter, 5' UTR, and intron in the I-*Cre*I cassette), along with the *pin*II terminator elements (*) in PHP56614 due to alignment of reads derived from the *pin*II terminator in the *pmi* cassette of the intended insertion to the two copies of this element in PHP56614. **D)** SbS results aligned against the plasmid PHP21139 sequence (5,687 bp; **Figure 3**). Coverage was obtained only for the endogenous elements. **E)** SbS results aligned against the plasmid PHP31729 sequence (6,181 bp; **Figure** 4). Coverage was obtained for the endogenous elements and for a small segment of an *att* recombination site that matches an *att* site found in the intended insertion (‡). The absence of any junctions other than to the intended insertion indicates that there are no additional insertions or backbone sequence present in DP23211 maize.

Appendix B. Methods for Southern Blot Analysis [redacted] 2019)

Test, Control and Reference Substances

The test substances in the study were defined as seeds from DP23211 maize of the T1, T2, T3, T4, and T5 generations. The control substance was defined as seed from a maize line (PHR03) that was not transformed. PHR03 maize has a similar genetic background to the test substance; however, it does not contain the DP23211 maize insertion.

Plasmid DNA of PHP74643 that was used for *Agrobacterium*-mediated transformation to produce DP23211 maize was defined as a reference substance. This plasmid was used as a positive control for Southern analysis to verify probe hybridization. The *pmi, mo-pat* and *ipd072Aa* gene and DvSSJ1 fragment probes used in this analysis were derived from plasmid PHP74643.

DNA molecular weight markers for gel electrophoresis and Southern blot analysis were obtained from commercial vendors and were used as a reference to determine approximate molecular weights of DNA fragments. For Southern analysis, DNA Molecular Weight Marker III and VII, Digoxigenin (DIG)-labeled (Roche, Indianapolis, IN), were used as size standards for hybridizing fragments.

Sample Collection, Handling, Identification and Storage

Seed from each of the five generations of DP23211 maize and the control maize were planted in a controlled environment at Corteva Agriscience International, Inc., Johnston, Iowa, USA. Fresh leaf tissue samples from test and control maize were harvested and then lyophilized. Lyophilized tissue samples were shipped to Regulatory Sciences, Multi Crop Research Center, Corteva Agriscience Private Limited at Hyderabad, at ambient temperature. Upon arrival, samples were stored frozen (< -50°C freezer unit) until processing.

DNA Extraction and Quantification

Genomic DNA was isolated and analyzed from one plant for each of the T1, T2, T3, T4, and T5 generations of DP23211 maize and one plant from the PHR03 control maize.

The lyophilized leaf samples were pulverized with steel beads in tubes using a paint shaker (AGS Transact Technology Ltd., Mumbai, India). Care was taken to ensure leaf samples were ground sufficiently for DNA isolation. Genomic DNA was isolated using a high salt extraction buffer (2.0 M Sodium chloride, 100 mM Tris-Hydrochloride pH-8.0, 50 mM Sodium salt of EDTA, 3% β-mercaptoethanol (v/v) and 100 mM Sodium metabisulphite) and sequentially precipitated using potassium acetate and isopropyl alcohol. DNA was treated with Ribonuclease A, purified and precipitated using sodium acetate and chilled ethanol. Following the extraction, DNA was quantified using PicoGreen® reagent (Molecular Probes, Invitrogen) and visualized on a 1% agarose gel to check the quality of the isolated DNA.

Digestion of DNA and Electrophoretic Separation

Genomic DNA isolated from both test and control maize leaves was digested with the restriction enzyme *Kpn* I (Thermo Fisher Scientific., Waltham, MA, USA). PHP74643 plasmid DNA was added to the control maize DNA samples at a level equivalent to one plasmid copy per genomic copy and digested in the same manner. Following digestion with the restriction enzyme, the fragments produced were electrophoretically separated according to their sizes using an agarose gel and documented by photographing the gel under UV illumination (BioRad Gel doc XR^+ System., Hercules, CA, USA).

Southern Transfer

The DNA fragments separated on the agarose gel were denatured *in situ*, transferred to a nylon membrane (GE Healthcare, LC, Buckinghamshire, UK) and fixed to the membrane by UV crosslinking (UV Stratalinker, UVP, Cambridge, UK).

Probe Labeling and Southern Blot Hybridization

The DNA fragments bound to the nylon membrane were detected as discrete bands when hybridized to a labeled probe. DNA probes specific to the *pmi, mo-pat* and *ipd072Aa* gene and DvSSJ1 fragment elements were labeled by incorporation of Digoxigenin (DIG) labeled nucleotide DIG-11-dUTP into the fragments.

Labeled probes were hybridized to the DNA on the nylon membrane for detection of the specific genomic DNA fragments. DNA Molecular Weight Marker III and VII, Digoxigenin (DIG) labeled (Roche, Indianapolis, IN, USA) were used for visualization as the fragment size standards on the blot.

Detection of Hybridized Probes

After stringent washes, DIG-labeled DNA standards and single stranded DIG-labeled probes hybridized to DNA bound to the nylon membrane were visualized using CDP-Star Chemiluminescent Nucleic Acid Detection System with DIG Wash and Block Buffer Set (Roche, Indianapolis, IN, USA). Blots were exposed for one or more time points to detect hybridizing fragments and to visualize molecular weight standards. Images were captured by detection with the Syngene G-Box Chemi XT16 and XX6 (Syngene, Inc., Cambridge, UK). Detected bands were documented for each probe.

Stripping of Probes and Subsequent Hybridization

Following hybridization and detection, membranes were stripped of DIG-labeled probe to prepare blot for subsequent re-hybridization to a different probe. Membranes were rinsed briefly in distilled and de-ionized water and then stripped in a solution of 0.2N NaOH and 0.1% SDS at 37°C with constant shaking. The membranes were then rinsed in 2x SSC and either used directly for subsequent hybridizations or stored for later use. The alkali-based stripping procedure effectively removed probes labeled with alkali-labile DIG used in these experiments.

Appendix C. Methods for Multi-Generation Segregation Analysis ([redacted] 2018)

Five generations of DP23211 maize were evaluated using polymerase chain reaction (PCR) analyses and herbicide-tolerance testing to confirm Mendelian inheritance of genotype and phenotype.

Greenhouse Experimental Design

Five separate generations (BC1F1 in genetic background PH1V5T, BC2F1, T1, T5, and BC1F1 in genetic background PH2SRH) of DP23211 maize were planted and grown in a greenhouse under standard environmental conditions for maize production. Leaf samples were collected from each generation and analyzed using PCR amplification methods specific for event DP-Ø23211-2, DvSSJ1 fragments, and *ipd072Aa* gene*, mo-pat* gene*,* and *pmi* gene. After sample collection, all plants were treated with a broadcast application of glufosinate and then visually evaluated for herbicide tolerance.

Planting and Leaf Sample Collection

Maize seeds, more than 100 for each generation, were planted in separate 4-inch pots contained in flats of 15 pots each and grown in a controlled environment under conditions for producing maize plants. Fourteen to seventeen days after planting, each generation was thinned to a final population of 100 plants.

When plants were at the V3 growth stage (the growth stage when the collar of the third leaf is visible) and prior to herbicide application, leaf samples were collected from each plant. Each sample consisted of three leaf punches collected into one bullet tube and placed on dry ice until transferred to a freezer for storage. Individual plant and corresponding leaf samples were uniquely labeled to allow a given sample to be tracked back to the originating plant.

Genotypic Analysis

Leaf samples were analyzed using a qPCR assay to confirm the presence or absence of the event DP-Ø23211-2 and to confirm the presence or absence of the DvSSJ1 fragments, and *ipd072Aa* gene*, mo-pat* gene*,* and *pmi* gene. Leaf samples were also analyzed using endpoint PCR for the following genes or genetic elements; *STOPS2-UBI1, AT-T9-STOPS3,* and *ATTB2-S2-BSV*.

Phenotypic Analysis

Glufosinate herbicide was applied after PCR leaf punch sample collection. At the time of herbicide application, the maize plants were at the V4-V5 growth stages (occurs when the leaflets on the fifth or six leaf node, respectively, have unrolled). The spray mixture consisted of Ignite 280 SL containing 24.5% glufosinate-ammonium and ammonium sulfate at a rate of approximately 3.0 lb/A (3.4 kg/ha). No other adjuvants or additives were included in the spray mixture. Ignite 280 SL was applied at a target rate of 22 fl oz/A (1.66 L/ha) with a total spray volume of approximately 33 gal/A (312.4 L/ha), using a spray chamber to simulate a broadcast (over-the-top) application. Actual application rates were within 90-110% of the target herbicide application rate.

Four to five days after herbicide application, each plant was visually evaluated for herbicide tolerance in which presence of herbicide injury corresponded to an herbicide-susceptible phenotype and absence of herbicide injury corresponded to an herbicide-tolerant phenotype.

Statistical Analysis

A chi-square analysis was performed at the 0.05 significance level on the segregation results of each DP23211 maize generation to compare the observed segregation ratio to the expected segregation ratio (1:1 for the two BC1F1 generations, BC2F1, and T1). This analysis tested the hypothesis that the introduced traits segregated according to the Mendelian rules of inheritance. The critical value to reject the hypothesis at the 5% level is 3.84. Chi-square test was not performed for the T5 generation because all plants were identified as positive (*i.e.*, not segregating) as expected for a homozygous generation.

Appendix D. Methods for Characterisation and Safety Assessment of IPD072Aa Protein

Test Materials [redacted] 2016; [redacted] 2017; [redacted] 2019a)

IPD072Aa protein was isolated from DP23211 maize whole plant tissue. The tissue samples were collected at the V9 growth stage (the stage when the collar of the ninth leaf becomes visible; Abendroth *et al.*, 2011) of development from plants grown at a field location in Johnston, IA, USA. The tissue was lyophilized, homogenized and stored at ≤ -50 °C. The IPD072Aa protein was extracted from lyophilized maize tissue by homogenization with a Waring blender using chilled phosphate-buffered saline containing polysorbate 20 (PBST) extraction buffer (25 ml buffer per g tissue). The sample extract was then filtered through cheesecloth and clarified by centrifugation. Ammonium sulfate (AS) precipitation was used to further purify and concentrate the sample extract. Beginning at 0% AS saturation, AS was slowly added to the sample extract while stirring until 60% AS saturation was reached. The sample was centrifuged, and the AS process was repeated with the supernatant, this time beginning at 60% AS saturation and progressing to 80%. The sample was centrifuged again, and the fractionated pellet was solubilized in phosphate-buffered saline prior to running the sample through a desalting column. The eluted fraction was further purified by immunoaffinity chromatography. The immunoaffinity column was prepared by coupling an IPD072Aa protein mouse monoclonal antibody (21F1.E5) to AminoLink Plus Coupling Gel. Elutions 2-5 from the immunoaffinity purification were concentrated into one sample using a centrifugal concentrator (10K; Sartorius) and buffer exchanged to a volume of approximately 150 µl. Following extraction, purification, and concentration, the final volume in the concentrator was estimated and 25% 4X NuPAGE LDS and 10% 10X NuPAGE Sample Reducing Agent was added to the concentrated sample. The sample in the concentrator was heated for 2-5 minutes at 70-100 °C and then transferred to a microcentrifuge tube. The sample was then heat treated at 90-100 °C for 5 (±1) minutes and stored frozen at ≤ -10 °C.

IPD072Aa protein was produced at Pioneer Hi-Bred International, Inc. using a microbial expression system. The protein was expressed in an *E. coli* protein expression system as a fusion protein with an N-terminal His tag. The tagged protein was purified using Ni-NTA affinity chromatography. The fusion tag was cleaved by immobilized trypsin and then removed by Ni-NTA affinity chromatography. Following purification and His tag removal, tangential flow filtration was used to change the buffer to 50 mM ammonium bicarbonate. The protein in solution was then lyophilized and stored in a -80 °C freezer unit.

Further purification was conducted after lyophilization and mixing, by resuspension of the lyophilized powder in 25 mM Tris pH 8.0 followed by anion exchange chromatography. The buffer of the protein was then exchanged into 50 mM ammonium bicarbonate. The protein in solution was then lyophilized and stored in a -80 °C freezer unit.

SDS-PAGE Analysis [redacted] 2016; [redacted] 2017; [redacted] 2019a)

Maize-derived prepared IPD072Aa protein samples were re-heated for 5 minutes at 90-100 °C and then loaded into 4-12% Bis-Tris gels. Prestained protein molecular weight markers (Precision Plus Protein Dual Xtra Standards) were loaded into each gel to provide a visual verification that migration was within the range of the predicted molecular weight. Electrophoresis was conducted using a pre-cast gel electrophoresis system with MES SDS running buffer and NuPAGE Antioxidant at a constant 200 volts (V) for 35 minutes. Upon completion of electrophoresis, the gels were removed from the gel cassettes and used for Coomassie staining, western blot analysis, protein glycosylation analysis, or sample preparation for N-terminal amino acid sequencing and peptide mapping.

Microbially derived lyophilized IPD072Aa protein samples were solubilized in 1X LDS sample buffer (25% 4X NuPAGE LDS Sample Buffer, 10% 10X NuPAGE Sample Reducing Agent containing DTT, and 65% water) and heated at 90-100 °C for 5 minutes prior to SDS-PAGE analysis. The prepared protein samples were analyzed using 4-12% Bis-Tris gels. For Coomassie staining and glycosylation staining, 1 µg of IPD072Aa protein was loaded. For western blot analysis, 5 ng of IPD072Aa protein was loaded. For mass spectrometry analyses, 4 µg of IPD072Aa protein was loaded. Pre-stained protein molecular weight markers (Precision Plus Protein Dual Xtra Standards) were also loaded into the gels to provide a visual verification that migration was within the expected range of the predicted molecular weight. Electrophoresis was conducted using a Mini-Cell Electrophoresis System with 1X MES running buffer at a constant 200 volts (V) for 35 minutes. Upon completion of electrophoresis, the gels were removed from the gel cassettes and used for Coomassie staining, western blot analysis, protein glycosylation analysis, or sample preparation for peptide mapping.

For Coomassie staining, gels were washed with water three times for a minimum of 5 minutes each and stained with GelCode Blue Stain Reagent for approximately 60 minutes. Following staining, the gel was de-stained with water four times for a minimum of 5 minutes each or until the gel background was clear. Proteins were detected as blue-colored bands on the gels. The gel image was captured electronically using an imaging system.

Western Blot Analysis [redacted], 2016; [redacted] 2017; [redacted] 2019a)

Following SDS-PAGE, the resulting gel was assembled into a mini nitrocellulose iBlot Gel Transfer Stack. An iBlot Gel Transfer Device was used to transfer proteins from the gel to the nitrocellulose membrane for 7 minutes with a pre-set program (P3).

Following protein transfer, the membrane was blocked in phosphate buffered saline containing polysorbate 20 (PBST) containing 5% weight/volume (w/v) non-fat dry milk for approximately 60 minutes at ambient temperature. Before and after the blocking step, the membrane was washed with PBST three times for 1-5 minutes each to reduce the background. The blocked membrane was incubated in an IPD072Aa polyclonal antibody R2409 (Corteva Agriscience) diluted either 1:5,000 or 1:10,000 in PBST containing 1% w/v non-fat dry milk for 60 minutes at ambient temperature. Following primary antibody incubation, the membrane was washed with PBST three or four times for 5 minutes each. The membrane was incubated in a secondary antibody (anti-rabbit IgG horseradish peroxidase conjugate, Promega Corporation) diluted 1:10,000 in PBST containing 1% w/v non-fat dry milk for 60 minutes at ambient temperature. The membrane was then washed with PBST three or four times for 5 minutes each. The blot remained in PBST prior to incubating with a chemiluminescent substrate for 5 minutes. The chemiluminescent signal and the pre-stained markers were detected and captured using an imaging system.

Peptide Mapping by Mass Spectrometry ([redacted], 2016; [redacted], 2017; [redacted] 2019a)

Following SDS-PAGE, Coomassie staining, and imaging of the gels, the IPD072Aa protein band was excised from each sample lane and prepared for peptide mapping analysis.

Maize-derived IPD072Aa protein samples were reduced with DTT, alkylated with iodoacetamide, and then subsequently digested with trypsin or chymotrypsin. The digested samples were separated on an ACQUITY UPLC (Waters Corporation) fitted with a Cortecs UPLC C18 1.6 µm Column (2.1 x 100 mm) (Waters Corporation) by gradient elution. Eluent from the column was directed into an electrospray source, operating in positive mode, on a TripleTOF 5600+ hybrid quadrupole-TOF mass spectrometer (AB Sciex). The resulting MS data were processed using MS Data Converter (Beta 1.3) to produce a peak list. The peak list was used to perform an MS/MS ion search (Mascot Software version 2.6.1) and match peptides from the expected IPD072Aa protein sequence (Perkins et al., 1999). The following search parameters were used: peptide and fragment mass tolerance, ± 0.1 Da; fixed modifications, cysteine carbamidomethyl; variable modifications, methionine oxidation; maximum missed cleavages, 1 for trypsin and 2 for chymotrypsin. The Mascot-generated peptide ion score threshold was >13 which indicates identity or extensive homology ($p<0.05$). The combined sequence coverage was calculated with GPMAW version 9.2.

Microbially derived IPD072Aa protein samples were sent to Alphalyse for peptide sequencing. The protein samples were reduced and alkylated with iodoacetamide (i.e., carbamidomethylated), and subsequently digested in chymotrypsin which cleaves after leucine, phenylalanine, tryptophan, and tyrosine residues. For all samples, the resulting peptides were analyzed on a Bruker Autoflex Speed MALDI TOF/TOF instrument in positive reflector mode for accurate peptide mass determination. MALDI MS/MS was performed on some peptides for peptide fragmentation analysis, i.e., partial sequencing. The MS and MS/MS spectra were combined and used for database searching using the Mascot software.

N-Terminal Amino Acid Sequencing Analysis ([redacted] 2016; [redacted] 2017; [redacted] 2019a)

For maize-derived IPD072Aa protein samples, SDS-PAGE was conducted, and the resulting gel was incubated in cathode buffer (60 mM Tris, 40 mM CAPS, 0.075% SDS, pH 9.6) for 10-20 minutes. An Immobilon-P PVDF membrane was wetted in 100% methanol for 1 minute, followed by immersion in anode buffer (60 mM Tris, 40 mM CAPS, 15% methanol, pH 9.6) for 10-15 minutes. A Trans-Blot SD Semi-Dry Electrophoretic Transfer Cell system was used to transfer proteins from the gel to the membrane at 12 V for 45 minutes. Following protein transfer, the membrane was then stained with GelCode Blue stain reagent for 10 minutes and then destained with water and 50% methanol to visualize the IPD072Aa protein band. Two bands containing the maize-derived IPD072Aa protein were excised and stored frozen at ≤ -10 °C. Both bands were analyzed as a single sample using a Shimadzu PPSQ-51A sequencer. Ten cycles of Edman sequencing were performed. During each cycle, the N-terminal amino acid was sequentially derivatized with phenylisothiocyanate (PITC), cleaved with trifluoracetic acid, and converted to PTH-amino acid which was identified through chromatography. LabSolutions Software was used to automatically identify the N-terminal sequence.

For the microbially derived IPD072Aa protein samples, the lyophilized samples were solubilized in a solution of 0.5 mM ammonium acetate and 3% methanol and sent to Alphalyse for Edman N-terminal amino acid sequencing using an ABI Procise 494 sequencer (Applied Biosystems, Inc.) equipped with an online high-performance liquid chromatography system.

Glycoprotein Analysis [redacted], 2016; [redacted] 2017; [redacted] 2019a)

A Pierce Glycoprotein Staining Kit was used to determine whether the IPD072Aa protein was glycosylated. The IPD072Aa protein, a positive control protein (horseradish peroxidase), and a negative control protein (soybean trypsin inhibitor) were run by SDS-PAGE as described above.

Following electrophoresis, the gel was washed with water twice for 5 minutes each wash, fixed with 50% methanol for 30-35 minutes, and washed twice with 3% acetic acid for 10-15 minutes each wash. The gel was then incubated with oxidizing solution for 15-20 minutes and washed three times with 3% acetic acid for 5-7 minutes each wash. The gel was incubated with glycoprotein staining reagent for 15-20 minutes and then incubated in a reducing reagent for 5-7 minutes. The gel was then washed one to three times with 3% acetic acid for 5-7 minutes each wash and then rinsed in water once for 5 minutes. Glycoproteins were detected as magenta-colored bands on the gel.

Following glycoprotein detection, the image of the gel was captured electronically. The same gel was then stained with GelCode Blue stain reagent for approximately 60 minutes followed by three washes with water (minimum 5 minutes each wash) to visualize all protein bands. The image of the GelCode stained gel was then captured electronically.

Thermolability Analysis ([redacted]

Diet treatments were prepared for the bioassay as follows: Bulk bioassay control and test dosing solutions were prepared on Day 0 of the *D. virgifera* bioassay. To generate the test dosing solution, an aliquot of the test substance was thawed under chilled conditions and diluted in ultrapure water to an IPD072Aa protein concentration of 0.070 mg/ml. The bulk test dosing solution was divided into the following six aliquots: unheated, incubated for 30-35 minutes at 25 °C, 50 °C, 60 °C, or 95 °C, or autoclaved for approximately 30 minutes at 121 °C; and used to generate the test dosing solutions for Treatments 2-7, respectively. The bioassay control dosing solution used to generate Treatment 1 consisted of ultrapure water. Dosing solutions were maintained chilled (in a 4 °C refrigerator unit or on wet ice) until use.

On each day of diet preparation, the bioassay control dosing solution and test dosing solution aliquots were mixed with carrier in a 2.51:1 ratio (i.e., 2.51 ml of dosing solution to 1 g of carrier), generating Treatments 1-7. Each test diet contained a targeted concentration of 50 ng IPD072Aa protein per mg diet wet weight. The presence or absence of immunodetectable IPD072Aa protein in Treatment 1 and stability of the IPD072Aa protein test dosing solution used to prepare Treatment 2 were assessed, and western blot analysis was used to visually confirm the dose, stability under bioassay conditions, and homogeneity of the IPD072Aa protein in Treatment 2.

Treatments were arranged in a generalized randomized block design with a total of 10 blocks. Each block consisted of a 24-well bioassay plate and contained 3 replicates from each treatment. Each treatment was provided to a target of 30 *D. virgifera* individuals. *D. virgifera* eggs were incubated in an environmental chamber until the eggs hatched. *D. virgifera* neonates were used in the bioassay within 24 hours of hatching. On Day 0, approximately 300 µl (i.e., 1 g of wet diet equated to 1 ml of wet diet) of freshly prepared diets were dispensed into individual wells of 24-well bioassay plates. One *D. virgifera* neonate was placed in each well containing diet, each bioassay plate was sealed with heat-sealing film, and two small holes were poked over each well to allow for ventilation. The bioassay was conducted in an environmental chamber set at 21 °C, 65% relative humidity, and continuous dark for 7 days. On Day 4, new bioassay plates were prepared with fresh diet as described for Day 0,

living *D. virgifera* larvae were transferred to the new plates, missing or dead larvae were recorded, and the freshly prepared plates were placed in the environmental chamber. After 7 days, the bioassay was complete, mortality was assessed, and surviving larvae were individually weighed. Only wells that contained one organism were included in the total number of observed individuals; organisms recorded as missing from a well, or wells containing more than one organism, were excluded from statistical analysis.

Statistical analyses of mortality data were conducted using SAS software, Version 9.4. Weight data were not statistically compared due to high mortality. Fisher's exact test was conducted to compare the mortality rate of D. virgifera in Treatments 3-7 which were provided diet containing IPD072Aa protein (m_T) and the mortality rate of those in Treatment 2 which were provided the unheated test diet (m_C). The corresponding hypothesis test was

$$H_0 : m_T = m_c \quad vs. \quad H_a : m_T \neq m_c \ .$$

A significant difference was identified if the P-value was < 0.05. SAS PROC MULTTEST was utilized to conduct the Fisher's exact test.

Digestibility in Simulated Gastric Fluid (SGF) ([redacted], 2018b)

Test and control solutions were prepared as follows:

- The gastric control solution was comprised of 0.2% weight per volume (w/v) NaCl in 0.7% volume per volume (v/v) HCl with a pH of ~1.2.
- The pepsin digestion solution, referred to as simulated gastric fluid (SGF), was prepared fresh on the day of use by dissolving high-purity pepsin into gastric control solution with a target ratio of pepsin to test or control protein of 10 units pepsin per microgram protein in the final digestion mixture.
- The IPD072Aa protein stock solution was prepared by re-solubilizing a sub-sample of the lyophilized IPD072Aa powder in deionized water (ultrapure ASTM Type 1 water, referred to as water) to a target protein concentration of 5 mg/ml. The tube containing solubilized IPD072Aa protein was vortexed and centrifuged and the resulting supernatant was transferred to a new tube.
- To prepare the stock solutions for each of the control proteins (BSA and β-lactoglobulin), a sub-sample of 5.0 mg powder was weighed into an individual tube and solubilized by adding 1 ml of water (for a final protein concentration of 5 mg/ml) and then vortexed.
- Each test or control protein stock solution (5 mg/ml) was added to the SGF solution at a 1:20 dilution (e.g., 100 µl protein to 1900 µl SGF). The final concentration of the protein and pepsin in the SGF reaction mixture was 0.25 mg/ml IPD072Aa protein or control protein and 2500 units/ml pepsin.

An IPD072Aa protein pepsin digestion time-course was conducted. SGF solution (1900 µl) was dispensed into a 7-ml glass vial and placed in a 37 °C water bath for 2-5 minutes prior to the addition of 100 µl of IPD072Aa protein

solution at time 0. A circulating water bath was used to maintain the temperature of the digestion solution at 37 °C (± 1 °C). The IPD072Aa protein pepsin digestion reaction mixture was mixed constantly using a stir bar and a submersible magnetic stirrer. A 120-µl sub-sample of the IPD072Aa protein pepsin digestion reaction mixture was removed from the vial at the following analytical time points (± 10 seconds): 0.5, 1, 2, 5, 10, 20, 30, and 60 minutes. Each sub-sample was neutralized by adding it to a pre-labeled tube containing 139 µl of a pre-mixed sample solution (containing 34.5% stop solution, 46.8% 4X LDS sample buffer, and 18.7% 10X sample reducing agent). The neutralized samples were heated at 90-100 °C for 5 minutes. After heat inactivation, all digestion samples were kept on ice on the day of reaction and stored frozen (-20 °C freezer unit) prior to further analysis.

Bioassay control samples included in the SGF assay are provided in **Table D.1**.

Table D.1. Control Samples for Simulated Gastric Fluid (SGF) Digestibility Analysis

Protein	Digestion Solution	Digestion Time(s)
None (Water) - SGF Control	SGF	0 min, 60 min
BSA	SGF	0 min, 1 min, 60 min
β-Lactoglobulin	SGF	0 min, 1 min, 60 min
IPD072Aa	SGF	0 min
IPD072Aa	Water	0 min, 60 min
IPD072Aa	Gastric Control Solution (No Pepsin)	60 min

Control digestion samples at time zero were prepared by first neutralizing 114 µl of the designated digestion solution with 139 µl of a pre-mixed sample solution. Then, 6 µl of IPD072Aa, BSA, β-lactoglobulin protein stock solution, or water was added and mixed. All samples were then heated at 90-100 °C for 5 minutes. After heat inactivation, all digestion samples were kept on ice on the day of reaction and stored frozen (-20 °C freezer unit) prior to further analysis.

Control digestion samples at 1 or 60 minutes were pre-warmed in a 37 °C water bath for 2-5 minutes prior to adding 6 µl of the respective protein stock solution or water. The tubes were then incubated in the water bath for the allotted time. The 120-µl sample of each control reaction mixture was inactivated at each respective time point (± 10 seconds) by mixing with 139 µl of a pre-mixed sample solution. All samples were then heated at 90-100 °C for 5 minutes. After heat inactivation, all digestion samples were kept on ice on the day of reaction and stored frozen (-20 °C freezer unit) prior to further analysis.

SDS-PAGE analysis was conducted. The IPD072Aa protein pepsin digestion time-course samples and control samples were heated at 90-100 °C for 5 minutes, and loaded (20 µl/well) into 4-12% Bis-Tris gels for SDS-PAGE analysis. Pre-stained protein molecular weight markers were loaded into the gels to provide a visual estimate of molecular weight. Electrophoresis was conducted using a pre-cast gel electrophoresis system with MES running buffer at a constant 200 volts for 30-34 minutes. Upon completion of electrophoresis, the gels were removed from the gel cassettes for use in Coomassie staining or western blot analysis. For protein staining, the gels were washed with water three times for 5 minutes each, and stained with GelCode Blue Stain Reagent for 60 minutes at ambient laboratory temperature. Following staining, gels were destained by washing with water four times for at least 5 minutes each until the gel background was clear. Proteins were detected as blue-colored bands on the gels and the gel images were captured electronically.

The IPD072Aa protein pepsin digestion time-course samples were also analyzed by western blot. Following SDS-PAGE, the gel was assembled into an iBlot dry-blotting system. Proteins were transferred to a nitrocellulose membrane for 7 minutes. Following protein transfer, the nitrocellulose membrane was removed from the stack

and washed in phosphate-buffered saline containing polysorbate 20 (PBST) three times for 1 minute each. The washed membrane was blocked by incubation in PBST containing 5% (w/v) non-fat dry milk for 60 minutes at ambient laboratory temperature. The blocked membrane was washed in PBST three times for a minimum of 1 minute each and incubated for 60 minutes at ambient laboratory temperature with IPD072Aa polyclonal antibody R2409 (Pioneer Hi-Bred International, Inc.) diluted 1:150,000 in PBST containing 1% (w/v) non-fat dry milk. The blocked membrane was washed in PBST three times for 5 minutes each to remove unbound primary antibody and incubated for 60 minutes at ambient laboratory temperature with a secondary antibody (anti-rabbit IgG conjugated to horseradish peroxidase) diluted 1:150,000 in PBST containing 1% (w/v) non-fat dry milk. The membrane was then washed in PBST three times for 5 minutes each and incubated with a chemiluminescent substrate. The signal was detected and captured using an image analyzing system.

Digestibility in Simulated Intestinal Fluid (SIF) ([redacted] 2018a)

Test and control solutions were prepared as follows:

- The intestinal control solution was prepared as a stock solution containing 52.6 mM KH_2PO_4, pH ~7.5.
- The pancreatin digestion solution, referred to as simulated intestinal fluid (SIF), was prepared fresh on the day of use by dissolving pancreatin into intestinal control solution. The final SIF reaction mixture (SIF plus protein) contained 1% weight per volume (w/v) pancreatin and 50 mM KH_2PO_4.
- The IPD072Aa protein stock solution was prepared by re-solubilizing a sub-sample of the lyophilized IPD072Aa powder in deionized water (ultrapure ASTM Type 1 water, referred to as water) to a target protein concentration of 5 mg/ml. The tube containing solubilized IPD072Aa protein was vortexed and centrifuged and the resulting supernatant was transferred to a new tube.
- To prepare the stock solutions for each of the control proteins (BSA and β-lactoglobulin), a sub-sample of 5.0 mg powder was weighed into an individual tube and solubilized by adding 1 ml of water (for a final protein concentration of 5 mg/ml) and then vortexed.
- Each test or control protein stock solution (5 mg/ml) was added to the SIF solution at a 1:20 dilution (e.g., 100 µl protein to 1900 µl SIF). The final concentration of the test or control proteins in the SIF reaction mixture was 0.25 mg/ml and the final pancreatin concentration was 1% w/v.

An IPD072Aa protein pancreatin digestion time-course was conducted. SIF solution (1900 µl) was dispensed into a 7-ml glass vial and placed in a 37 °C water bath for 2-5 minutes prior to the addition of 100 µl of IPD072Aa protein solution at time 0. A circulating water bath was used to maintain the temperature of the digestion solution at 37 °C (± 1 °C). The IPD072Aa protein pancreatin digestion reaction mixture was mixed constantly using a stir bar and a submersible magnetic stirrer. A 120-µl sub-sample of the IPD072Aa protein pancreatin digestion reaction mixture was removed from the vial at the following analytical time points (± 10 seconds): 0.5, 1, 2, 5, 10, 20, 30, and 60 minutes. Each sub-sample was neutralized by adding it to a pre-labeled tube containing 64 µl of a pre-mixed sample solution (containing 71.9% 4X LDS sample buffer and 28.1% 10X sample reducing agent). The neutralized samples were heated at 90-100 °C for 5 minutes. After heat inactivation, all digestion samples were kept on ice on the day of reaction and stored frozen (-20 °C freezer unit) prior to further analysis.

Bioassay control samples included in the SIF assay are provided in **Table D.2**.

Table D.2. Control Samples for Simulated Intestinal Fluid (SIF) Digestibility Analysis

Protein	Digestion Solution	Digestion Time(s)
None (Water) - SIF Control	SIF	0 min, 60 min
BSA	SIF	0 min, 1 min, 60 min
β-Lactoglobulin	SIF	0 min, 1 min, 60 min
IPD072Aa	SIF	0 min
IPD072Aa	Water	0 min, 60 min
IPD072Aa	Intestinal Control Solution (No Pancreatin)	60 min

Control digestion samples at time zero were prepared by first neutralizing 114 µl of the designated digestion solution with 64 µl of a pre-mixed sample solution, and then inactivated by heating at 90-100 °C for 5 (± 1) minutes. Then, 6 µl of IPD072Aa, BSA, β-lactoglobulin protein stock solution, or water was added and mixed. All samples were then heated again at 90-100 °C for 5 (± 1) minutes. After heat inactivation, all digestion samples were kept on ice on the day of reaction and stored frozen (-20 °C freezer unit) prior to further analysis.

Control digestion samples at 1 or 60 minutes were pre-warmed in a 37 °C water bath for 2-5 minutes prior to adding 6 µl of the respective protein stock solution or water. The tubes were then incubated in the water bath for the allotted time. The 120-µl sample of each control reaction mixture was inactivated at each respective time point (± 10 seconds) by mixing with 64 µl of a pre-mixed sample solution. All samples were then heated at 90-100 °C for 5 minutes. After heat inactivation, all digestion samples were kept on ice on the day of reaction and stored frozen (-20 °C freezer unit) prior to further analysis.

SDS-PAGE analysis was conducted. The IPD072Aa protein pancreatin digestion time-course samples and control samples were heated at 90-100 °C for 5 minutes, and loaded (20 µl/well) into 4-12% Bis-Tris gels for SDS-PAGE analysis. Pre-stained protein molecular weight markers were loaded into the gels to provide a visual estimate of molecular weight. Electrophoresis was conducted using a pre-cast gel electrophoresis system with MES running buffer at a constant 200 volts for 30-34 minutes. Upon completion of electrophoresis, the gels were removed from the gel cassettes for use in Coomassie staining or western blot analysis. For protein staining, the gels were washed with water three times for at least 5 minutes each, and stained with GelCode Blue Stain Reagent for 60 minutes at ambient laboratory temperature. Following staining, gels were destained by washing with water four times for at least 5 minutes each until the gel background was clear. Proteins were detected as blue-colored bands on the gels and the gel images were captured electronically.

The IPD072Aa protein pancreatin digestion time-course samples were also analyzed by western blot. Following SDS-PAGE, the gel was assembled into an iBlot dry-blotting system. Proteins were transferred to a nitrocellulose membrane for 7 minutes. Following protein transfer, the nitrocellulose membrane was removed from the stack and washed in phosphate-buffered saline containing polysorbate 20 (PBST) three times for a minimum of 1 minute each. The washed membrane was blocked by incubation in PBST containing 5% (w/v) non-fat dry milk for 60 minutes at ambient laboratory temperature. The blocked membrane was washed in PBST three times for a minimum of 1 minute each and incubated for 60 minutes at ambient laboratory temperature with IPD072Aa polyclonal antibody R2409 (Pioneer Hi-Bred International, Inc.) diluted 1:150,000 in PBST containing 1% (w/v) non-fat dry milk. The blocked membrane was washed in PBST three times for 5 minutes each to remove unbound primary antibody and incubated for 60 minutes at ambient laboratory temperature with a secondary antibody (anti-rabbit IgG conjugated to horseradish peroxidase) diluted 1:150,000 in PBST containing 1% (w/v) non-fat dry

milk. The membrane was then washed in PBST three times for 5 minutes each and incubated with a chemiluminescent substrate. The signal was detected and captured using an image analyzing system.

Appendix E. Methods for Characterisation of PAT Protein [redacted] 2019b)

Test Substance

The test substance consisted of PAT protein isolated from tissue derived from DP23211 maize. The whole plant tissue was collected at the V9 growth stage (the stage when the collar of the ninth leaf becomes visible; Abendroth *et al.*, 2011) of development from plants grown at a field location in Johnston, IA, USA. The tissue was lyophilized, homogenized and stored at ≤ -50 °C, under study number PHI-2018-099.

Protein Extraction, Purification, and Concentration

The PAT protein was extracted from lyophilized maize tissue by homogenization with a Waring blender using chilled phosphate-buffered saline containing polysorbate 20 (PBST) extraction buffer (25 ml buffer per g tissue). The sample extract was then filtered through cheesecloth and clarified by centrifugation. Ammonium sulfate (AS) precipitation was used to further purify and concentrate the sample extract. Beginning at 0% AS saturation, AS was slowly added to the sample extract while stirring until 45% AS saturation was reached. The sample was centrifuged and the AS process was repeated with the supernatant, this time beginning at 45% AS saturation and progressing to 60%. The sample was centrifuged again and the fractionated pellets were solubilized in phosphate-buffered saline prior to running the samples through desalting columns. The eluted fractions were pooled and further purified by immunoaffinity chromatography. The immunoaffinity column was prepared by coupling a PAT protein mouse monoclonal antibody (2C10.D5.G8) to AminoLink Plus Coupling Gel. Elutions 2-5 from the immunoaffinity purification were pooled into one sample for further purification by ion exchange. The pooled sample was diluted 1:2 using 50 mM Tris pH 8 then added to the column containing Q Sepharose ion exchange resin. Eluted fractions were captured separately and then concentrated into one sample using a centrifugal concentrator (10K; Sartorius) and buffer exchanged to a volume of approximately 100 µl for the first purification run and 70 µl for the second purification run.

Following each purification, the final volume in the concentrator was estimated and 25% 4X NuPAGE LDS sample buffer and 10% 10X NuPAGE Sample Reducing Agent was added to the concentrated sample. The sample in the concentrator was heated for 2-5 minutes at 70-100 °C and then transferred to a microcentrifuge tube. The sample was then heat treated at 90-100 °C for 5 (±1) minutes and stored frozen at ≤ -10 °C.

Sodium Dodecyl Sulfate Polyacrylamide Gel Electrophoresis (SDS-PAGE)

The LDS-treated sample stored at ≤ -10 °C was re-heated for 5 minutes at 90-100 °C and then loaded into 4-12% Bis-Tris gels. Pre-stained protein molecular weight markers (Precision Plus Protein Dual Xtra Standards) were loaded into each gel to provide a visual verification that migration was within the range of the predicted molecular weight. Electrophoresis was conducted using a pre-cast gel electrophoresis system with MES SDS running buffer and NuPAGE Antioxidant at a constant 200 volts (V) for 35 minutes.

Upon completion of electrophoresis, the gels were removed from the gel cassettes and used for Coomassie staining, western blot analysis, protein glycosylation analysis, or sample preparation for N-terminal amino acid sequencing and peptide mapping.

For Coomassie staining, the gel was washed with ultrapure (American Society for Testing and Materials [ASTM] Type 1) water (referred to as water) 3 times for 5 minutes each and stained with GelCode Blue Stain Reagent for 60 minutes. Following staining, the gel was de-stained with water 4 times for at least 5 minutes each until the gel background was clear. Proteins were stained as blue-colored bands on the gel. The gel image was captured electronically using an imaging system (Bio-Rad ChemiDoc MP).

Western Blot Analysis

Following SDS-PAGE, the resulting gel was assembled into a nitrocellulose (NC) iBlot Gel Transfer Stack. An iBlot Gel Transfer Device was used to transfer proteins from the gel to the NC membrane for 7 minutes with a pre-set program (P3).

Following protein transfer, the membrane was blocked in PBST containing 5% weight/volume (w/v) non-fat dry milk for 60 minutes at ambient laboratory temperature. Before and after the blocking step, the membrane was washed with PBST 3 times for 1 minute each to reduce the background. The blocked membrane was incubated for 60 minutes at ambient laboratory temperature with a PAT monoclonal antibody 22H2.G4 (Corteva Agriscience) diluted 1:5000 in PBST containing 1% w/v non-fat dry milk. Following primary antibody incubation, the membrane was washed 4 times in PBST for 5 minutes each. The membrane was incubated for 60 minutes at ambient laboratory temperature with a secondary antibody (anti-mouse IgG, horseradish peroxidase conjugate; Promega Corporation) diluted 1:10,000 in PBST containing 1% non-fat dry milk. The membrane was washed 4 times with PBST for 5 minutes each. The blot remained in PBST prior to incubating with a chemiluminescent substrate for 5 minutes. The chemiluminescent signal and the pre-stained markers were detected and captured using an imaging system (Bio-Rad ChemiDoc MP).

Peptide Mapping and Sequencing Analysis by LC-MS Analysis

Following protein extraction, purification, and concentration as described above, and SDS-PAGE, Coomassie staining, and gel imaging using the methods as described above, four PAT protein bands were excised from a gel and stored frozen at ≤ -10 °C. The protein in two of the gel slices was reduced with DTT, alkylated with iodoacetamide, and then subsequently digested with trypsin or chymotrypsin. The digested samples were separated on an ACQUITY UPLC (Waters Corporation) fitted with a Cortecs UPLC C18 1.6 µm Column (2.1 x 100 mm) (Waters Corporation) by gradient elution. Eluent from the column was directed into an electrospray source, operating in positive mode, on a TripleTOF 5600+ hybrid quadrupole-TOF mass spectrometer (AB Sciex). The resulting MS data were processed using MS Data Converter (Beta 1.3) to produce a peak list. The peak list was used to perform an MS/MS ion search (Mascot Software version 2.6.1) and match peptides from the expected PAT protein sequence (Perkins et al., 1999). The following search parameters were used: peptide and fragment mass tolerance, ± 0.1 Da; fixed modifications, cysteine carbamidomethyl; variable modifications, methionine oxidation; maximum missed cleavages, 1 for trypsin and 2 for chymotrypsin. The Mascot-generated peptide ion score threshold was >13 which indicates identity or extensive homology ($p<0.05$). The combined sequence coverage was calculated with GPMAW version 9.2.

N-Terminal Amino Acid Sequence Analysis

Following SDS-PAGE as described above, the resulting gel was incubated in cathode buffer (60 mM Tris, 40 mM CAPS, 0.075% SDS, pH 9.6) for 10-20 minutes. An Immobilon-P PVDF membrane was wetted in 100% methanol for 1 minute, followed by immersion in anode buffer (60 mM Tris, 40 mM CAPS, 15% methanol, pH 9.6) for 10-15 minutes. A Trans-Blot SD Semi-Dry Electrophoretic Transfer Cell system was used to transfer proteins from the gel to the membrane at 12 V for 45 minutes. Following protein transfer, the membrane was then stained with GelCode Blue stain reagent for 8 minutes and then destained with water and 50% methanol to visualize the PAT protein band. A band containing the maize-derived PAT protein was excised and stored frozen at ≤ -10 °C. The band was analyzed using a Shimadzu PPSQ-51A sequencer. Ten cycles of Edman sequencing were performed. During each cycle, the N-terminal amino acid was sequentially derivatized with phenylisothiocyanate (PITC), cleaved with trifluoracetic acid, and converted to PTH-amino acid which was identified through chromatography. LabSolutions Software was used to automatically identify the N-terminal sequence with applicable adjustments.

Protein Glycosylation Analysis

The Pierce Glycoprotein Staining Kit was used to determine whether the PAT protein was glycosylated. The PAT protein, a positive control protein (horseradish peroxidase), and a negative control protein (soybean trypsin inhibitor), were run by SDS-PAGE as described above.

Following electrophoresis, the gel was washed with water twice for 5 minutes each wash, fixed with 50% methanol for 30-35 minutes, and washed twice with 3% acetic acid for 10-15 minutes each wash. The gel was then incubated with oxidizing solution for 15-20 minutes and washed three times with 3% acetic acid for 5-7 minutes each wash. The gel was incubated with glycoprotein staining reagent for 15-20 minutes and then incubated in a reducing reagent for 5-7 minutes. The gel was then washed with 3% acetic acid for 5 minutes and then rinsed in water for 5 minutes. Glycoproteins were detected as magenta colored bands on the gel.

Following glycoprotein detection, the image of the gel was captured electronically. The same gel was then stained with GelCode Blue stain reagent for 60 minutes followed by 3 washes with water (at least 10 minutes each) to visualize all protein bands. The image of the GelCode stained gel was then captured electronically.

Appendix F. Methods for Characterisation of PMI Protein ([redacted] 2019)

Test Substance

The test substance consisted of PMI protein isolated from tissue derived from DP23211 maize. The whole plant tissue was collected at the V9 growth stage (the stage when the collar of the ninth leaf becomes visible; Abendroth *et al.*, 2011) of development from plants grown at a field location in Johnston, IA, USA. The tissue was lyophilized, homogenized and stored at ≤-50 °C, under study number PHI-2018-099.

Protein Extraction, Purification, and Concentration

The PMI protein was extracted from lyophilized maize tissue by homogenization with a Waring blender using chilled phosphate-buffered saline containing polysorbate 20 (PBST) extraction buffer with EDTA-free Complete Protease Inhibitors (20 ml buffer per g tissue). The sample extract was then filtered through cheesecloth, clarified by centrifugation, filtered through a 0.45 µm PES vacuum filter unit, and fractionated using ammonium sulfate (AS) precipitation. Beginning at 0% AS saturation, AS was slowly added to the sample extract while stirring until 45% AS saturation was reached. The sample was centrifuged and the AS process was repeated with the supernatant, this time beginning at 45% AS saturation and progressing to 60%. The sample was centrifuged again and the fractionated pellet was solubilized in phosphate-buffered saline prior to running the sample through a desalting column. The eluted fraction was further purified by immunoaffinity chromatography. The immunoaffinity column was prepared by coupling rabbit polyclonal antibody (R164) anti-PMI to AminoLink Plus Coupling Gel. Elutions 2-4 from the immunoaffinity purification were concentrated into one sample using a centrifugal concentrator (Microsep 30K; Pall Life Sciences) and buffer exchanged to a volume of approximately 100 µl.

Following extraction, purification, and concentration, the final volume in the concentrator was estimated and an equal volume of 2X NuPAGE LDS sample buffer with Reducing Agent was added to the concentrated sample. The sample in the concentrator was heated for 2-5 minutes at 70-100 °C and then transferred to a microcentrifuge tube. The sample was then heat treated at 90-100 °C for 5 (±1) minutes and stored frozen at < -10 °C.

Sodium Dodecyl Sulfate Polyacrylamide Gel Electrophoresis (SDS-PAGE)

The LDS treated sample stored at ≤ -10 °C was re-heated for 5 minutes at 90-100 °C and then loaded into 4-12% Bis-Tris gels. Prestained protein molecular weight markers (Precision Plus Protein Dual Xtra Standards) were loaded into each gel to provide a visual verification that migration was within the range of the predicted molecular weight. Electrophoresis was conducted using a pre-cast gel electrophoresis system with MES SDS running buffer and NuPAGE Antioxidant at a constant 200 volts (V) for 35 minutes.

Upon completion of electrophoresis, the gels were removed from the gel cassettes and used for Coomassie staining, western blot analysis, protein glycosylation analysis, or sample preparation for peptide mapping.

For Coomassie staining, the gel was washed with ultrapure (American Society for Testing and Materials [ASTM] Type 1) water (referred to as water) 3 times for 5 minutes each and stained with GelCode Blue Stain Reagent for 60 minutes. Following staining, the gel was de-stained with water 4 times for at least 5 minutes each until the gel background was clear. Proteins were stained as blue-colored bands on the gel. The gel image was captured electronically using an imaging system (Bio-Rad ChemiDoc MP).

Western Blot Analysis

Following SDS-PAGE, the resulting gel was assembled into a nitrocellulose (NC) iBlot Gel Transfer Stack. An iBlot Gel Transfer Device was used to transfer proteins from the gel to the NC membrane for 7 minutes with a pre-set program (P3).

Following protein transfer, the membrane was blocked in PBST containing 5% weight/volume (w/v) non-fat dry milk for 60 minutes at ambient laboratory temperature. Before and after the blocking step, the membrane was washed with PBST for 1 minute to reduce the background. The blocked membrane was incubated for 60 minutes at ambient laboratory temperature with a PMI monoclonal antibody (13D11.F11.C12) conjugated to horseradish peroxidase diluted 1:10,000 in PBST containing 1% w/v non-fat dry milk. Following primary antibody incubation, the membrane was washed 3 times in PBST for 5 minutes each. The blot remained in PBST prior to incubating with a chemiluminescent substrate for 5 minutes. The chemiluminescent signal and the pre-stained markers were detected and captured using an imaging system.

Peptide Mapping and N-Terminal Amino Acid Sequence Analysis by LC/MS

Following SDS-PAGE, Coomassie staining, and gel imaging using the methods as described above, two PMI protein bands were excised from a gel and stored frozen at ≤ -5 °C. The protein in each gel slice was reduced with DTT, alkylated with iodoacetamide, and then subsequently digested with trypsin or chymotrypsin. The digested samples were separated on an ACQUITY UPLC (Waters Corporation) fitted with a Cortecs UPLC C18 1.6 µm Column (2.1 x 100 mm) (Waters Corporation) by gradient elution. Eluent from the column was directed into an electrospray source, operating in positive mode, on a TripleTOF 5600+ hybrid quadrupole-TOF mass spectrometer (AB Sciex). The resulting MS data were processed using MS Data Converter (Beta 1.3) to produce a peak list. The peak list was used to perform an MS/MS ion search (Mascot Software version 2.6.1) and match peptides from the expected PMI protein sequence (Perkins et al., 1999). The following search parameters were used: peptide and fragment mass tolerance, ± 0.1 Da; fixed modifications, cysteine carbamidomethyl; variable modifications, methionine oxidation and acetylation of the protein N-terminal amino acid; maximum missed cleavages, 1 for trypsin and 2 for chymotrypsin. The Mascot-generated peptide ion score threshold was >13 which indicates identity or extensive homology ($p<0.05$). The combined sequence coverage was calculated with GPMAW version 9.2.

Protein Glycosylation Analysis

The Pierce Glycoprotein Staining Kit was used to determine whether the PMI protein was glycosylated. The PMI protein, a positive control protein (horseradish peroxidase), and a negative control protein (soybean trypsin inhibitor), were run by SDS-PAGE as described above.

Following electrophoresis, the gel was washed with water twice for 10 minutes each wash, fixed with 50% methanol for 30-35 minutes, and washed twice with 3% acetic acid for 10-15 minutes each wash. The gel was then incubated with oxidizing solution for 15-20 minutes and washed three times with 3% acetic acid for 5-7 minutes each wash. The gel was incubated with glycoprotein staining reagent for 15-20 minutes and then incubated in a reducing reagent for 5-7 minutes. The gel was then washed with 3% acetic acid three times for 5 minutes each and then rinsed in water for 5 minutes. Glycoproteins were detected as magenta colored bands on the gel.

Following glycoprotein detection, the image of the gel was captured electronically. The same gel was then stained with GelCode Blue stain reagent for 65 minutes followed by 3 washes with water (at least 5 minutes each) to visualize all protein bands. The image of the GelCode stained gel was then captured electronically.

Appendix G. Methods for Expressed Trait dsRNA and Protein Analyses [redacted] 2019a; [redacted] 2019c)

Field Trial Experimental Design

A multi-site field trial was conducted during the 2018 growing season at six sites in commercial maize-growing regions of the United States (one site in each of Iowa, Illinois, Indianan, Minnesota, and Pennsylvania) and Canada (one site in Ontario). A randomized complete block design with four blocks was utilized at each site. Procedures employed to control the introduction of experimental bias included the use of non-systematic selection of trial and plot areas within each site, randomization of maize entries within each block, and uniform maintenance treatments across each plot area.

Sample Collection

The following tissue samples were collected: Root (V6, V9, R1, R4, and R6 growth stage), leaf (V9, R1, R4, and R6 growth stages), pollen (R1 growth stage), forage (R4 growth stage at five sites and R4-R5 growth stage at remaining site), whole plant (R1 and R6 growth stages), and grain (R6 growth stage). Growth stages are described in **Table G.1**. One sample per plot was collected for each tissue set. All samples were collected from impartially selected, healthy, representative plants to minimize potential bias.

Table G.1. Maize Growth Stage Descriptions

Growth Stage	Description
V6	The stage when the collar of the sixth leaf becomes visible.
V9	The stage when the collar of the ninth leaf becomes visible.
R1	The stage when silks become visible.
R4	The stage when the material within the kernel produces a doughy consistency.
R5	The stage when all or nearly all the kernels are dented or denting.
R6	Typical grain harvest would occur. This stage is regarded as physiological maturity.

Note: Growth stages (Abendroth et al. 2011).

Samples were collected as follows:

- Each root sample was obtained by cutting a circle 10-15 in. (25-38 cm) in diameter around the base of the plant to a depth of 7-9 in. (18-23 cm). The roots were thoroughly cleaned with water and removed from the plant. No above ground brace roots were included in the sample. The root tissue was cut into sections of 1 in. (2.5 cm) or less in length and collected to fill no more than 50% of a pre-labeled, 50-ml vial.
- Each leaf sample was obtained by pruning the youngest, healthy leaf that had emerged at least 8 in. (20 cm) from the whorl of the plant. The tissue was cut into sections of 1 in. (2.5 cm) or less in length and collected into a pre-labeled, 50-ml vial.
- Each pollen sample was obtained by bagging and shaking a selected tassel to dislodge the pollen. The tassel selected for sampling had one-half to three-quarters of the tassel's main spike shedding pollen. For

some plots, pollen may have been pooled from multiple plants within the same plot in order to collect the appropriate amount. The pollen was screened for anthers and foreign material, and then collected in a pre-labeled, 35-ml vial.

- Each whole plant sample was obtained by cutting the plants approximately 4-6 in. (10-15 cm) above the soil surface line. The stalks and ears (R1), or husks and cobs (R6) were chopped into sections of 3 in. (7.6 cm) or less in length and the leaves were cut into sections of 12 in. (30 cm) or less in length and collected into a pre-labeled, plastic-lined, cloth bag. The plants selected for sampling at the R1 growth stage contained ears that were covered prior to silking. The plants selected for sampling at the R6 growth stage contained self-pollinated ears. Any secondary or tertiary ears with exposed silks were removed from the plants selected for sampling. The R6 whole plant sample did not contain grain; kernels were removed from the cob and collected for grain sampling.
- Each forage sample was obtained by cutting one plant approximately 4-6 in. (10-15 cm) above the soil surface line. The stalk and ear were chopped into sections of 3 in. (7.6 cm) or less in length and the leaves were cut into sections of 12 in. (30 cm) or less in length and collected into a pre-labeled, plastic-lined, cloth bag. The plants selected for forage sampling contained self-pollinated ears.
- Each grain sample was obtained by husking and shelling the grain from one selected ear. Each ear selected for sampling was a primary ear that had previously been self-pollinated. For each sample, a representative sub-sample of 15 kernels was collected into an individual pre-labeled vial.

Sample Processing, Shipping, and Storage

Each sample was uniquely labeled with a sample identification number and barcode for sample tracking by site, entry, block, tissue, and growth stage. Samples were placed on dry ice immediately after collection in the field and stored on dry ice until shipment. Samples were then shipped frozen on dry ice to Corteva Agriscience for processing and analysis. Upon arrival, samples were stored frozen (-80 °C freezer unit).

For the samples for DvSSJ1 dsRNA analysis, pollen samples were stored frozen (-80 °C freezer unit) until analysis and root, leaf, forage, whole plant, and grain samples were finely homogenized and stored frozen (-80 °C freezer unit) until analysis.

For the samples for IPD072Aa, PAT, and PMI protein analysis, forage and whole plant samples were coarsely homogenized on dry ice prior to lyophilization. All samples were lyophilized under vacuum until dry. Following lyophilization, pollen samples were stored frozen (-20 °C freezer unit) until analysis and root, leaf, forage, whole plant, and grain samples were finely homogenized and stored frozen (-20 °C freezer unit) until analysis.

DvSSJ1 dsRNA Concentration Determination

Sample Weighing

Tissue sub-samples were weighed at the following target fresh weight ranges: 9-12 mg for pollen; 15-20 mg for leaf; 28-35 mg for grain, 24-30 mg for forage, and 40-50 mg for root and whole plant. Minor fluctuations outside of the weight ranges were allowed, as results were calculated per gram of fresh tissue.

Total RNA Extraction

Total RNA was extracted by adding 500 µl of RNA lysis buffer (50 mM sodium citrate pH 4.5, 25 mM EDTA, 75 mM sodium chloride, 1% sodium dodecyl sulfate, and 1% β-mercaptoethanol [freshly added]) to pre-weighed tissue samples. An equal volume (500 µl) of acid-phenol:chloroform mixture (1:1) was added to the slurry and samples were ground with 1.0 mm zirconium oxide beads. After grinding, samples were incubated for 5 minutes at approximately 65 °C then centrifuged in Phase Lock Gel-Heavy tubes to separate the phases. The aqueous phase was removed, transferred to fresh tubes, and 1.5 ml TRI-reagent and 2 ml 200-Proof Ethanol were added. The total RNA was purified using Zymo Direct-zol RNA Miniprep Plus Kit and eluted from the column in 100 µl of RNase-free water. The concentration of total RNA was determined using a NanoDrop 2000 UV-Vis Spectrophotometer. Representative samples were checked for RNA quality and integrity by gel electrophoresis. Samples that showed poor RNA quality were excluded from DvSSJ1 dsRNA concentration analysis. Total RNA was stored frozen (-80 °C freezer unit) until QuantiGene analysis.

Total RNA yield was calculated as follows:

$$Total\ RNA\ Concentration\ \frac{ng}{\mu l}\ x\ 100\ \mu l = Total\ RNA\ Yield\ (ng)$$

QuantiGene Analysis

QuantiGene analysis was used to determine the concentration of DvSSJ1 dsRNA in tissues derived from DP23211 maize. The QuantiGene method was internally validated to demonstrate method suitability.

The DvSSJ1 QuantiGene Plex Assay method utilized magnetic beads specific to the target to measure the amount of DvSSJ1 dsRNA in samples. Prior to analysis, total RNA was diluted to 10-30 ng total RNA/µl (equal to 200 – 600 ng total RNA/well) in QuantiGene Homogenizing Solution (QHS). Standards and samples (both typically analyzed in triplicate wells) were first denatured (95 °C for five minutes) and annealed (55 °C) in a 96-well PCR plate with a sequence-specific probe set designed by Affymetrix that included Capture Extenders (CE), Label Extenders (LE), and Blocking Probes. The mixture of sample and probe set was transferred to a hybridization plate containing bead mix (100 µl total volume) for overnight hybridization at approximately 54 °C. Following hybridization, a magnetic separation device was used to wash unbound substances from the plate. Signal was amplified on the LE probes by sequential incubations (each 1 – 2 hours at approximately 50 °C) with pre-amplifier, amplifier, and label probes, with each incubation followed by a wash step to remove unbound substances. Each well was then incubated with the fluorescent protein streptavidin phycoerythrin (SAPE; 30 minutes at room temperature) and then washed. The SAPE generated a signal that was proportional to the amount of DvSSJ1 dsRNA present in the reaction. The median fluorescence intensity (MFI) of each well was then determined using a MAGPIX Multiplex Reader running xPonent v4.2 software.

Calculations for Determining DvSSJ1 dsRNA Concentration (Fresh Weight)

SoftMax Pro GxP (Molecular Devices) microplate data software was used to perform the calculations required to convert the MFI values obtained for each set of sample wells to a DvSSJ1 dsRNA concentration value.

A seven-point standard curve was included on each plate (2.45×10^{-6} – 6.00×10^{-4} µg/ml). The standard curve was prepared by diluting the reference substance in 20 ng total RNA/µl (equal to 400 ng total RNA/well) extracted from conventional maize leaf tissue that did not contain DvSSJ1 (diluted in QHS). The standard curve diluent (referred to as blank) was also loaded to each plate and the average of the blank was subtracted from all wells on the plate.

The Log-Log fit was used to generate the standard curve and was applied as follows:

$$Log(y) = A + B * Log(x)$$

where x = known standard concentration (pg/well) and y = respective MFI value

Interpolation of the sample concentration (pg/well) was performed by solving for x in the above equation using the values for A and B that were determined for the standard curve.

The QuantiGene result (pg DvSSJ1 dsRNA/well) was divided by the amount of total RNA loaded to each well, for example:

$$\frac{pg\ DvSSJ1\ dsRNA}{well}\ x\frac{well}{400\ ng\ Total\ RNA} = \frac{pg\ DvSSJ1\ dsRNA}{ng\ Total\ RNA}$$

To calculate the concentration of DvSSJ1 dsRNA per gram tissue fresh weight for each sample, the amount of DvSSJ1 dsRNA per ng total RNA was multiplied by the total RNA yield from that sample, and divided by the sample fresh weight:

$$\frac{pg\ DvSSJ1\ dsRNA}{ng\ Total\ RNA}x\frac{Total\ RNA\ Yield\ (ng)}{Sample\ Weight\ (mg)}x\frac{1}{1000} = \frac{\mu g\ DvSSJ1\ dsRNA}{g\ tissue}$$

The reportable assay lower limit of quantification (LLOQ) was equal to the lowest standard concentration, as follows:

$$Reportable\ Assay\ LLOQ\ = 0.049\frac{pg}{well}\ x\frac{well}{20\ \mu l}\ x\frac{1}{1000} = 2.45x10^{-6}\frac{\mu g}{ml}$$

An average dilution factor to reach 400 ng total RNA/well was calculated for each tissue type (determined during the method validation). The dilution factor, sample volume, and average tissue fresh weight were used to calculate tissue-specific LLOQ as follows:

$$LLOQ = Reportable\ Assay\ LLOQ\ \left(\frac{\mu g}{ml}\right) x\ Dilution\ Factor\ x\ \frac{Sample\ Volume\ (ml)}{Tissue\ Fresh\ weight\ (mg)}\ x\frac{1000\ mg}{1\ g}$$

Due to sample to sample differences used to calculate tissue-specific LLOQ (e.g., total RNA yield), some variability around each LLOQ is expected.

Calculations for Determining DvSSJ1 dsRNA Concentrations (Dry Weight)

A sub-sample was collected from each tissue sample and lyophilized. Weights were recorded before and after lyophilization in order to calculate fresh weight to dry weight ratio (FW:DW) for each sample. The FW:DW ratio was then multiplied by the DvSSJ1 dsRNA fresh weight expression value to generate DvSSJ1 dsRNA expression values on a dry weight basis.

Protein Concentration Determination

The concentrations of IPD072Aa, PAT, and PMI proteins were determined using quantitative enzyme-linked immunosorbent assay (ELISA) methods that have been internally validated to demonstrate method suitability.

Processed tissue sub-samples were weighed at the following target weights: 5 mg for pollen; 10 mg for leaf; 20 mg for grain and root; and 30 mg for forage. IPD072Aa protein leaf, pollen, whole plant, forage, and grain samples were extracted with 0.60 ml of chilled 25% StabilZyme Select in phosphate-buffered saline containing polysorbate 20 (PBST), and root samples were extracted in chilled H5 buffer (comprised of 90 mM HEPES, 140 mM sodium chloride, 1.0% polyethylene glycol, 1.0% PVP-40, 1.0% bovine serum albumin, 0.007% thimerosal, and 0.3% polysorbate 20). PAT and PMI protein samples were extracted with 0.60 ml of chilled phosphate-buffered saline containing polysorbate 20 (PBST). All extracted samples were centrifuged, and then supernatants were removed and prepared for analysis.

ELISA Methods

ELISA methods were performed as follows:

- IPD072Aa Protein ELISA Method: Prior to analysis, samples were diluted as applicable with 25% StabilZyme Select in PBST. Standards (typically analyzed in triplicate wells) and diluted samples (typically analyzed in duplicate wells) were incubated in a plate pre-coated with an IPD072Aa specific antibody. Following incubation, unbound substances were washed from the plate and the bound IPD072Aa protein was incubated with a different IPD072Aa specific antibody conjugated to the enzyme horseradish peroxidase (HRP). Unbound substances were washed from the plate. Detection of the bound IPD072Aa antibody complex was accomplished by the addition of substrate, which generated a colored product in the presence of HRP. The reaction was stopped with an acid solution and the optical density (OD) of each well was determined using a plate reader.
- PAT Protein ELISA Method: Prior to analysis, samples were diluted as applicable in PBST. Standards (typically analyzed in triplicate wells) and diluted samples (typically analyzed in duplicate wells) were co-incubated with a PAT specific antibody conjugated to the enzyme HRP in a plate pre-coated with a different PAT specific antibody. Following incubation, unbound substances were washed from the plate. Detection of the bound PAT antibody complex was accomplished by the addition of substrate, which generated a colored product in the presence of HRP. The reaction was stopped with an acid solution and the OD of each well was determined using a plate reader.

- PMI ELISA Method: Prior to analysis, samples were diluted as applicable in PBST. Standards (typically analyzed in triplicate wells) and diluted samples (typically analyzed in duplicate wells) were incubated in plate pre-coated with a PMI-specific antibody. Following incubation, unbound substances were washed from the plate and the bound PMI protein was incubated with a different PMI-specific antibody conjugated to the enzyme HRP. Unbound substances were washed from the plate. Detection of the bound PMI-antibody complex was accomplished by the addition of substrate, which generated a colored product in the presence of HRP. The reaction was stopped with an acid solution and the OD of each well was determined using a plate reader.

Calculations for Determining IPD072Aa, PAT, and PMI Protein Concentrations

SoftMax Pro GxP (Molecular Devices) microplate data software was used to perform the calculations required to convert the OD values obtained for each set of sample wells to a protein concentration value.

A standard curve was included on each ELISA plate. The equation for the standard curve was derived by the software, which used a quadratic fit to relate the OD values obtained for each set of standard wells to the respective standard concentration (ng/ml).

The quadratic regression equation was applied as follows: $y = Cx^2 + Bx + A$

where x = known standard concentration and y = respective absorbance value (OD)

Interpolation of the sample concentration (ng/ml) was performed by solving for x in the above equation using the values for A, B, and C that were determined for the standard curve.

Sample Concentration (ng/ml) = $$\frac{-B + \sqrt{B^2 - 4C(A - \text{sample OD})}}{2C}$$

For example, given curve parameters of A = 0.0476, B = 0.4556, C= -0.01910, and a sample OD = 1.438

Sample Concentration = $$\frac{-0.4556 + \sqrt{0.4556^2 - 4(-0.01910)(0.0476 - 1.438)}}{2(-0.01910)}$$ = 3.6 ng/ml

The sample concentration values were adjusted for a dilution factor expressed as 1:N by multiplying the interpolated concentration by N.

Adjusted Concentration = Interpolated Sample Concentration x Dilution Factor

For example, given an interpolated concentration of 3.6 ng/ml and a dilution factor of 1:20

Adjusted Concentration = 3.6 ng/ml x 20 = 72 ng/ml

Adjusted sample concentration values obtained from SoftMax Pro GxP software were converted from ng/ml to ng/mg sample weight as follows:

$$\text{Sample Concentration} = \text{Sample} \times \frac{\text{Extraction Buffer Volume (ml)}}{\quad}$$

$$\text{(ng protein/mg sample weight)} = \frac{\text{Concentration (ng/ml)}}{\text{Sample Target Weight (mg)}}$$

For example, sample concentration = 72 ng/ml, extraction buffer volume = 0.60 ml, and sample target weight = 10 mg

$$\text{Sample Concentration (ng protein/mg sample weight)} = 72 \text{ ng/ml} \times \frac{0.60 \text{ ml}}{10 \text{ mg}} = 4.3 \text{ ng/mg}$$

The reportable assay lower limit of quantification (LLOQ) in ng/ml was calculated as follows:

Reportable Assay LLOQ (ng/ml) = (lowest standard concentration - 10%) x minimum dilution

For example, lowest standard concentration = 0.50 ng/ml and minimum dilution = 10

Reportable Assay LLOQ (ng/ml) = (0.50 ng/ml - (0.50 x 0.10)) x 10 = 4.5 ng/ml

The LLOQ, in ng/mg sample weight, was calculated as follows:

$$\text{LLOQ} = \text{Reportable Assay LLOQ (ng/ml)} \times \frac{\text{Extraction Buffer Volume (ml)}}{\text{Sample Target Weight (mg)}}$$

For example, reportable assay LLOQ = 4.5 ng/ml, extraction buffer volume = 0.60 ml, and sample target weight = 10 mg

$$\text{LLOQ} = 4.5 \text{ ng/ml} \times \frac{0.60 \text{ ml}}{10 \text{ mg}} = 0.27 \text{ ng/mg sample weight}$$

Statistical Analysis

Statistical analysis of the DvSSJ1 dsRNA concentration results consisted of the calculations of means, ranges, and standard deviations on fresh weight and dry weight basis.

Statistical analysis of the IPD072Aa, PAT, and PMI protein concentration results consisted of the calculations of means, ranges, and standard deviations. Individual sample results below the LLOQ were assigned a value equal to half of the LLOQ for calculation purposes.

Appendix H. Methods for Nutrient Composition Analysis ([redacted] 2019b)

Field Trial Experimental Design

A multi-site field trial was conducted during the 2018 growing season at eight sites in commercial maize-growing regions of the United States (two sites in Illinois and one site in each of Iowa, Indiana, Minnesota, Pennsylvania, and Texas) and Canada (one site in Ontario). Each site included DP23211 maize, control maize, and four of the following non-GM commercial maize lines: P0604, 2R602, 35A52, P0760, BK5883, XL5939, P0928, P0993, XL5828, BK6076, XL6158, P1105, P1151, and P1197 (referred to as reference maize). A randomized complete block design with four blocks was utilized at each site. Procedures employed to control the introduction of experimental bias included the use of non-systematic selection of trial and plot areas within each site, randomization of maize entries within each block, and uniform maintenance treatments across each plot area.

Sample Collection

One forage sample (R4 growth stage) and one grain sample (R6 growth stage) were collected from each plot. Each forage sample (combination of three plants) was obtained by cutting the aerial portion of the plants from the root system approximately 4-6 in. (10-15 cm) above the soil surface line; the plants were chopped into sections of 3 in. (7.6 cm) or less in length, pooled, and approximately one-third of the chopped material was collected in a pre-labeled, plastic-lined, cloth bag. Each grain sample was obtained from five ears at typical harvest maturity from self-pollinated plants; the ears were husked and shelled, and the pooled grain was collected into a large, plastic, resealable bag and then placed into a pre-labeled, plastic-lined, cloth bag.

All samples were collected from impartially selected, healthy, representative plants to minimize potential bias. Reference maize and control maize samples were collected prior to the collection of DP23211 maize samples to minimize the potential for contamination. Each sample was uniquely labeled with a sample identification number and barcode for sample tracking, and is traceable by site, entry, block, tissue, and growth stage. Samples were placed into chilled storage (e.g., coolers with wet ice, artificial ice, or dry ice) after collection and transferred to a freezer (≤ -10 °C). Samples were shipped frozen from each site to EPL Bio Analytical Services (EPL BAS; Niantic, IL, USA) for nutrient composition analyses.

Nutrient Composition Analyses

The forage and grain samples were analyzed at EPL BAS for the following nutrient composition analytes:

- *Forage proximates, fiber, and minerals composition*: moisture*, crude protein, crude fat, crude fiber, acid detergent fiber (ADF), neutral detergent fiber (NDF), ash, carbohydrates, calcium, and phosphorus
    - *moisture data were used to convert corresponding analyte values for a given sample to a dry weight basis, and were not included in subsequent statistical analysis and reporting of results.
- *Grain proximates and fiber composition*: moisture*, crude protein, crude fat, total dietary fiber (TDF), crude fiber, acid detergent fiber (ADF), neutral detergent fiber (NDF), ash, and carbohydrates
    - *moisture data were used to convert corresponding analyte values for a given sample to a dry weight basis, and were not included in subsequent statistical analysis and reporting of results.

- *Grain fatty acids composition*: lauric acid (C12:0), myristic acid (C14:0), palmitic acid (C16:0), palmitoleic acid (C16:1), heptadecanoic acid (C17:0), heptadecenoic acid (C17:1), stearic acid (C18:0), oleic acid (C18:1), linoleic acid (C18:2), α-linolenoic acid (C18:3), arachidic acid (C20:0), eicosenoic acid (C20:1), eicosadienoic acid (C20:2), behenic acid (C22:0), erucic acid (C22:1), and lignoceric acid (C24:0)
- *Grain amino acids composition*: alanine, arginine, aspartic acid, cysteine, glutamic acid, glycine, histidine, isoleucine, leucine, lysine, methionine, phenylalanine, proline, serine, threonine, tryptophan, tyrosine, and valine
- *Grain minerals composition*: calcium, copper, iron, magnesium, manganese, phosphorus, potassium, sodium, and zinc
- *Grain vitamins composition*: β-carotene, vitamin B1 (thiamine), vitamin B2 (riboflavin), vitamin B3 (niacin), vitamin B5 (pantothenic acid), vitamin B6 (pyridoxine), vitamin B9 (folic acid), α-tocopherol, β-tocopherol, γ-tocopherol, and δ-tocopherol
    - Note: an additional analyte (total tocopherols) was subsequently calculated as the sum of the α-, β-, γ-, and δ-tocopherol values for each sample for use in statistical analysis and reporting of results
- *Grain secondary metabolites and anti-nutrients composition*: *p*-coumaric acid, ferulic acid, furfural, inositol, phytic acid, raffinose, and trypsin inhibitor

Nutrient composition analytical methods and procedures are summarized in **Table H1**.

Table H.1. Methods for Compositional Analysis

Nutritional Analyte	Method
Moisture Forage and Grain	The analytical procedure for moisture determination was based on a method published by AOAC International. Samples were assayed to determine the percentage of moisture by gravimetric measurement of weight loss after drying in a forced air oven (forage) and a vacuum oven (grain).
Ash Forage and Grain	The analytical procedure for ash determination was based on a method published by AOAC International. Samples were analyzed to determine the percentage of ash by gravimetric measurement of the weight loss after ignition in a muffle furnace.
Crude Protein Forage and Grain	The analytical procedure for crude protein determination utilized an automated Kjeldahl technique based on a method provided by the manufacturer of the titrator unit (Foss-Tecator) and AOAC International. Ground samples were digested in the presence of a catalyst. The digestate was then distilled and titrated with a Foss-Tecator Kjeltec Analyzer unit.
Crude Fat Forage and Grain	The analytical procedure for crude fat determination was based on methods provided by the American Oil Chemists' Society (AOCS) and the manufacturer of the hydrolysis and extraction apparatus (Ankom Technology). Samples were hydrolyzed with 3N hydrochloric acid at 90 °C for 80 minutes for forage and 60 minutes for grain. The hydrolysates were extracted with a petroleum ether/ethyl ether/ethyl alcohol solution at 90 °C for 60 minutes. The ether extracts were evaporated and the fat residue remaining determined gravimetrically.
Carbohydrates Forage and Grain	The carbohydrate content in maize forage and grain on a dry weight basis was calculated using a formula obtained from the United States Department of Agriculture "*Energy Value of Foods,*" in which the percent dry weight of crude protein, crude fat, and ash was subtracted from 100%.
Crude Fiber Forage and Grain	The analytical procedure for crude fiber determination was based on methods provided by the manufacturer of the extraction apparatus (Ankom Technology), AOAC International, and the AOCS. Samples were analyzed to determine the percentage of crude fiber by digestion and solubilization of other materials present.
Neutral Detergent Fiber	The analytical procedure for neutral detergent fiber (NDF) determination was based on a method provided by the manufacturer of the extraction apparatus (Ankom Technology), AOAC International, and the *Journal of AOAC International*. Samples were analyzed to determine the percentage of NDF by digesting with a neutral detergent solution, sodium sulfite, and alpha amylase. The remaining residue was dried and weighed to determine the NDF content.
Acid Detergent Fiber Forage and Grain	The analytical procedure for acid detergent fiber (ADF) determination was based on a method provided by the manufacturer of the extraction apparatus (Ankom Technology) and AOAC International. Samples were analyzed to determine the percentage of ADF by digesting with an acid detergent solution and washing with reverse osmosis water. The remaining residue was dried and weighed to determine the ADF content.
Total Dietary Fiber	The analytical procedure for the determination of total dietary fiber in grain was based on methods provided by the manufacturer of the extraction apparatus (Ankom Technology), AOAC International, and the manufacturer of the protein titrator unit (Foss-Tecator). Duplicate samples were gelatinized with heat stable α-amylase, enzymatically digested with protease and amyloglucosidase to remove protein and starch, respectively, and then soluble dietary fiber precipitated with ethanol. The percipitate (residue) was quantified gravimetrically. Protein analysis was performed on one of the duplicate samples while the other duplicate sample was analyzed for ash. The weight of the protein and ash was subtracted from the weight of the residue divided by sample dry weight.
Minerals	The analytical procedure for the determination of minerals is based on methods published by AOAC International and CEM Corporation. The maize forage minerals determined were calcium and phosphorus. Additional grain minerals determined were copper, iron, magnesium, manganese, potassium, sodium, and zinc. The samples were digested in a microwave-based digestion system and the digestate was diluted using deionized water. Samples were analyzed by inductively coupled plasma optical emission spectroscopy (ICP-OES).
Tryptophan	The analytical procedure for tryptophan determination was based on an established lithium hydroxide hydrolysis procedure with reverse phase ultra-performance liquid chromatography (UPLC) with ultraviolet (UV) detection published by the *Journal of Micronutrient Analysis*.
Cystine and Methionine	The analytical procedure for cystine and methionine determination was based on methods obtained from Waters Corporation, AOAC International, and *Journal of Chromatography A*. The procedure converts cystine to cysteic acid and methionine to methionine sulfone, after acid oxidation and hydrolysis, to the 6-

	aminoquinolyl-N-hydroxysuccinimidyl carbamate derivatives which are then analyzed by reverse phase UPLC with UV detection.
Additional Amino Acids	Along with tryptophan, cystine, and methionine, 15 additional amino acids were determined. The analytical procedure for analysis of these amino acids was based on methods obtained from Waters Corporation and the *Journal of Chromatography A*. The procedure converts the free acids, after acid hydrolysis, to the 6-aminoquinolyl-N-hydroxysuccinimidyl carbamate derivatives, which are analyzed by reverse phase UPLC with UV detection.
Fatty Acids	The analytical procedure for determination of fatty acids was based on methods published by AOAC International and AOCS. The procedure converts the free acids, after ether extraction and base hydrolysis, to the fatty acid methyl ester (FAME) derivatives, which are analyzed by gas chromatography with flame ionization detection (GC/FID). Results are reported as percent total fatty acids but presented in the raw data as percent fresh weight.
Thiamine (Vitamin B1) and Riboflavin (Vitamin B2)	The analytical procedure for the determination of thiamine (vitamin B1) and riboflavin (vitamin B2) was based on a method published by the American Association of Cereal Chemists (AACC). The samples were extracted with 10% acetic acid/4.3% trichloroacetic acid solution. A 50-fold dilution was performed and then the samples were analyzed by reverse phase high pressure liquid chromatography (HPLC) tandem mass spectrometry (MS/MS).
Niacin (Vitamin B3)	The analytical procedure for the determination of niacin (vitamin B3) was based on a method published by the AACC. Niacin (vitamin B3) was extracted from the sample by adding deionized (DI) water and autoclaving. A tube array was prepared using three different dilutions of the samples. This tube array was inoculated with *Lactobacillus plantarum* and allowed to incubate for approximately 18 to 22 hours. After incubation, the bacterial growth was determined using a spectrophotometer at an absorbance of 660 nm. The absorbance readings were compared to a standard curve generated using known concentrations of nicotinic acid.
Pantothenic Acid (Vitamin B5)	The analytical procedure for the determination of pantothenic acid (vitamin B5) was based on a method from AOAC International. Pantothenic acid (vitamin B5) was determined using a microbiological assay. Pantothenic acid (vitamin B5) was extracted from the sample by adding an acetic acid buffer solution and autoclaving. The pH was adjusted and a tube array was prepared using three different dilutions of the samples. This tube array was inoculated with *Lactobacillus plantarum* and allowed to incubate for approximately 18-22 hours. After incubation, the microbial growth was determined using a spectrophotometer at an absorbance of 660 nm. The absorbance readings were compared to a standard curve generated using known concentrations of D-pantothenic acid hemicalcium salt.
Pyridoxine (Vitamin B6)	The analytical procedure for the determination of pyridoxine (vitamin B6) was based on a method from the AACC. Pyridoxine (vitamin B6) was determined using a microbiological assay. Pyridoxine (vitamin B6) was extracted from the sample by adding sulfuric acid and autoclaving. The pH was adjusted and a tube array was prepared using four different dilutions of the samples. This tube array was inoculated with *Saccharomyces cerevisiae* and allowed to incubate for approximately 18-22 hours. After incubation, the microbial growth was determined using a spectrophotometer at an absorbance of 600 nm. The absorbance readings were compared to a standard curve generated using known concentrations of pyridoxine hydrochloride.

Total Folate as Folic Acid (Vitamin B9)	The analytical procedure for determination of total folate as folic acid was based on a microbiological assay published by the AACC. Samples were hydrolyzed and digested by protease and amylase enzymes to release the folate from the grain. A conjugase enzyme was used to convert the naturally occurring folypolyglutamates. An aliquot of the extracted folates was mixed with a folate and folic acid free microbiological growth medium. The mixture was inoculated with *Lactobacillus casei*. The total folate content was determined by measuring the turbidity of the *Lactobacillus casei* growth response in the sample and comparing it to the turbidity of the growth response with folic acid standards using a spectrophotometer at 600 nm.
Total Tocopherols	The analytical procedure for determination of tocopherols was based on methods from the *Journal of the American Oil Chemists' Society* and *Analytical Sciences*. Alpha, beta, gamma, and delta tocopherols were extracted with hot hexane and the extracts were analyzed by normal phase UPLC with fluorescence detection.
β-Carotene	The analytical procedure for determination of beta-carotene was based on a method published by AOAC International. Samples were extracted using a 40:60 acetone:hexane with tert-butylhydroquinone (TBHQ) solution then analyzed by HPLC-UV.
Trypsin Inhibitor	The analytical procedure for the determination of trypsin inhibitor was based on a method published by the AOCS. Trypsin inhibitor was extracted with sodium hydroxide. Trypsin was added to the extracts to react with trypsin inhibitor. The residual trypsin activity was measured with a spectrophotometer using the chromogenic trypsin substrate Benzoyl-DL-arginine-p-nitroanilide hydrochloride (BAPNA). The amount of trypsin inhibitor was calculated based on the inhibition of trypsin activity.
Inositol and Raffinose	The analytical procedure for the determination of inositol and raffinose was based on a gas chromatography (GC) method published in the *Handbook of Analytical Derivatization Reactions*, an AACC method, and a method from the *Journal of Agricultural and Food Chemistry*. Extracted inositol and raffinose were analyzed by reverse phase HPLC with refractive index detection.
Furfural	The analytical procedure for the determination of furfural was based on methods published in the *Journal of Agricultural and Food Chemistry*. Ground maize grain was analyzed for furfural content by reverse phase HPLC with UV detection.
p-Coumaric and Ferulic Acid	The analytical procedure for the determination of *p*-coumaric and ferulic acids was developed based on methods published in *Journal of Agricultural and Food Chemistry* and *The Journal of Chemical Ecology*. Ground maize grain was analyzed to determine the amounts of *p*-coumaric acid and ferulic acid by separating the total content of phenolic acids using reverse phase HPLC and UV detection.
Phytic Acid	The analytical procedure for the determination of phytic acid was based on a method published by AOAC International. The samples were analyzed to determine the amount of phytic acid by extracting the phytic acid with dilute hydrochloric acid (HCl) and isolating it using an aminopropyl silica solid phase extraction column. Once isolated and eluted, the phytic acid was analyzed for elemental phosphorus by ICP-OES.

Statistical Analysis of Nutrient Composition Data

Prior to statistical analysis, the data were processed as follows:

- *LLOQ Sample Values*: For statistical analysis, nutrient composition values reported as below the assay lower limit of quantification (LLOQ) were each assigned a value equal to half the LLOQ.
- *Conversion of fatty acid assay values*: The raw data for all fatty acid analytes were provided by EPL BAS in units of percent fresh weight (%FW). Any fatty acid values below the %FW LLOQ were set to half the LLOQ value, and then all assay values were converted to units of % total fatty acids for statistical analyses. For a given sample, the conversion to units of % total fatty acids was performed by dividing each fatty acid analyte value (%FW) by the total fresh weight of all fatty acids for that sample; for analyte values below the LLOQ, the half LLOQ value was used as the analyte value. Half LLOQ values were also included in the

total fresh weight summations. After the conversion, a fixed LLOQ value was not available for a given individual fatty acid analyte on the % total fatty acids basis. One fatty acid, erucic acid (C22:1), was excluded from the conversion and from statistical analyses because all sample values in the current study and in historical commercial reference maize lies were below the LLOQ.

- *Calculation of additional analytes*: One additional analyte (total tocopherol) was calculated for statistical analyses. The total amount of tocopherol for each sample was obtained by summing the assay values of α-tocopherol, β-tocopherol, γ-tocopherol, and δ-tocopherol in the sample. If the assay value of an individual analyte was below the LLOQ for a given sample, half of the LLOQ value was used in computing the total. The total was considered below the LLOQ only when all the individual analytes contributing to its calculation were below the LLOQ.

Statistical analyses were conducted using SAS software, Version 9.4 (SAS Institute, Inc.). The following rules were implemented for each analyte:

- If both DP23211 maize and the control maize had < 50% of samples below the LLOQ, then an across-site mixed model analysis would be conducted.
- If, either DP23211 maize or the control maize had ≥ 50% samples below the LLOQ, but not both entries had 100% of samples below the LLOQ across sites, then Fisher's exact test would be conducted. The Fisher's exact test assessed whether there was a significant difference (P-value < 0.05) in the proportion of samples below the LLOQ between these two maize lines across sites.
- If, both DP23211 maize and the control maize had 100% of samples below the LLOQ, then statistical analyses would not be performed.

Statistical Model for Across-Site Analysis

For a given analyte, data were analyzed using the following linear mixed model:

$$y_{ijk} = \mu_i + \ell_j + r_{k(j)} + (\mu\ell)_{ij} + \varepsilon_{ijk} \qquad \text{Model 1}$$

$$\ell_j \sim iid\ N(0, \sigma^2_{Site}),\ r_{k(j)} \sim iid\ N(0, \sigma^2_{Rep}),\ (\mu\ell)_{ij} \sim iid\ N(0, \sigma^2_{Ent\times Site}),\ \text{and}\ \varepsilon_{ijk} \sim iid\ N(0, \sigma^2_{Error})$$

where μ_i denotes the mean of the i^{th} entry (fixed effect), ℓ_j denotes the effect of the j^{th} site (random effect), $r_{k(j)}$ denotes the effect of the k^{th} block within the j^{th} site (random effect), $(\mu\ell)_{ij}$ denotes the interaction between the entries and sites (random effect), and ε_{ijk} denotes the effect of the plot assigned the i^{th} entry in the k^{th} block of the j^{th} site (random effect or residual). Notation $\sim iid\ N(0, \sigma^2_a)$ indicates random variables that are identically independently distributed (*iid*) as normal with zero mean and variance σ^2_a. Subscript a represents the corresponding source of variation.

The residual maximum likelihood estimation procedure was utilized to generate estimates of variance components and entry means across sites. The estimated means are known as empirical best linear unbiased estimators (hereafter referred to as LS-Means). The statistical comparison was conducted by testing for a difference in LS-

Means between DP23211 maize and the control maize. The approximated degrees of freedom for the statistical test were derived using the Kenward-Roger method (Kenward and Roger, 2009). A significant difference was identified if a P-value was < 0.05.

For each analyte, goodness-of-fit of the model was assessed in terms of meeting distributional assumptions of normally, independently distributed errors with homogeneous variance. Deviations from assumptions were addressed using an appropriate transformation or a heterogeneous error variance structure. The statistical results for transformed data were back transformed to the original data scale for reporting purposes.

False Discovery Rate Adjustment

The false discovery rate (FDR) method of Benjamini and Hochberg (Benjamini and Hochberg, 1995; Westfall et al., 1999) was applied as a post-hoc procedure to control for false positive outcomes across all analytes analyzed using linear mixed models. A false positive outcome occurs if the difference in means between two entries is declared significant, when in fact the two means are not different. Since its introduction in the mid-1990s, the FDR approach has been widely employed across a number of scientific disciplines, including genomics, ecology, medicine, plant breeding, epidemiology, dairy science, and signal/image processing (e.g., Pawitan et al., 2005; Spelman and Bovenhuis, 1998). In the FDR method, the false discovery rate is held at 5% across comparisons of multiple analytes via an adjustment to the P-value and is not inflated by the number of analytes in the comparison.

Interpretation of Statistical Results

For a given analyte, when a statistically significant difference (P-value from mixed model analysis < 0.05, or Fisher's exact test P-value < 0.05) was identified in the across-site analysis, the respective range of individual values from DP23211 maize was compared to a tolerance interval. Tolerance intervals are expected to contain at least 99% of the values for corresponding analytes of the conventional maize population with a 95% confidence level (Hong et al., 2014). The tolerance intervals were derived from proprietary accumulated data from 28 multi-site field studies between 2003 and 2017. These studies consisted of a total of 144 non-GM commercial reference maize lines and 148 unique environments representative of commercial maize-growing regions in the United States, Canada, Chile, Brazil and Argentina. The selected commercial maize lines represent the non-GM maize population with a history of safe use, and the selected environments (site and year combinations) represent maize growth under a wide range of environmental conditions (i.e. soil texture, temperature, precipitation, and irrigation) and maize maturity group zones.

If the range of DP23211 maize contained individual values outside the tolerance interval, it was then compared to the respective literature range. Literature ranges were generated from relevant crop composition data obtained from published literature (Codex Alimentarius Commission, 2013; Cong et al., 2015; ILSI, 2019; Lundry et al., 2013; OECD, 2002; Watson, 1982). Literature ranges compliment tolerance intervals and in-study reference ranges in that they are composed of non-proprietary data from additional non-GM commercial maize lines and growing environments, which are not included in Corteva Agriscience' s proprietary database.

If the range of DP23211 maize contained individual values outside the literature range, it was then compared to the respective in-study reference range. In-study reference ranges were comprised of all individual values across-sites from all non-GM reference maize lines grown in this study. In-study reference data ranges compliment tolerance intervals and literature ranges in that they provide additional context of natural variation specific to the current study.

In cases when a raw P-value indicated a significant difference but the FDR adjusted P-value was >0.05, it was concluded that the difference was likely a false positive.